

A VARIABLE TEMPERATURE NUCLEAR  
MAGNETIC DOUBLE RESONANCE STUDY OF  
AQUEOUS ALKYLAMMONIUM IONS

By

Bruce Erickson Wenzel

A THESIS

Submitted to  
Michigan State University  
in partial fulfillment of the requirements  
for the degree of

DOCTOR OF PHILOSOPHY

Department of Chemistry

1969



© Copyright by

BRUCE ERICKSON WENZEL

1970



To my parents, who taught me the importance of an education and a profession, to my sisters, who encouraged me and showed me the way, to my wife, who stood by me and advised me, and to my progeny, who made everything worthwhile and necessary, I dedicate this thesis.



## ACKNOWLEDGMENTS

It is with sincere appreciation that I acknowledge the counsel of Professor Max T. Rogers, under whose direction these investigations were conducted.

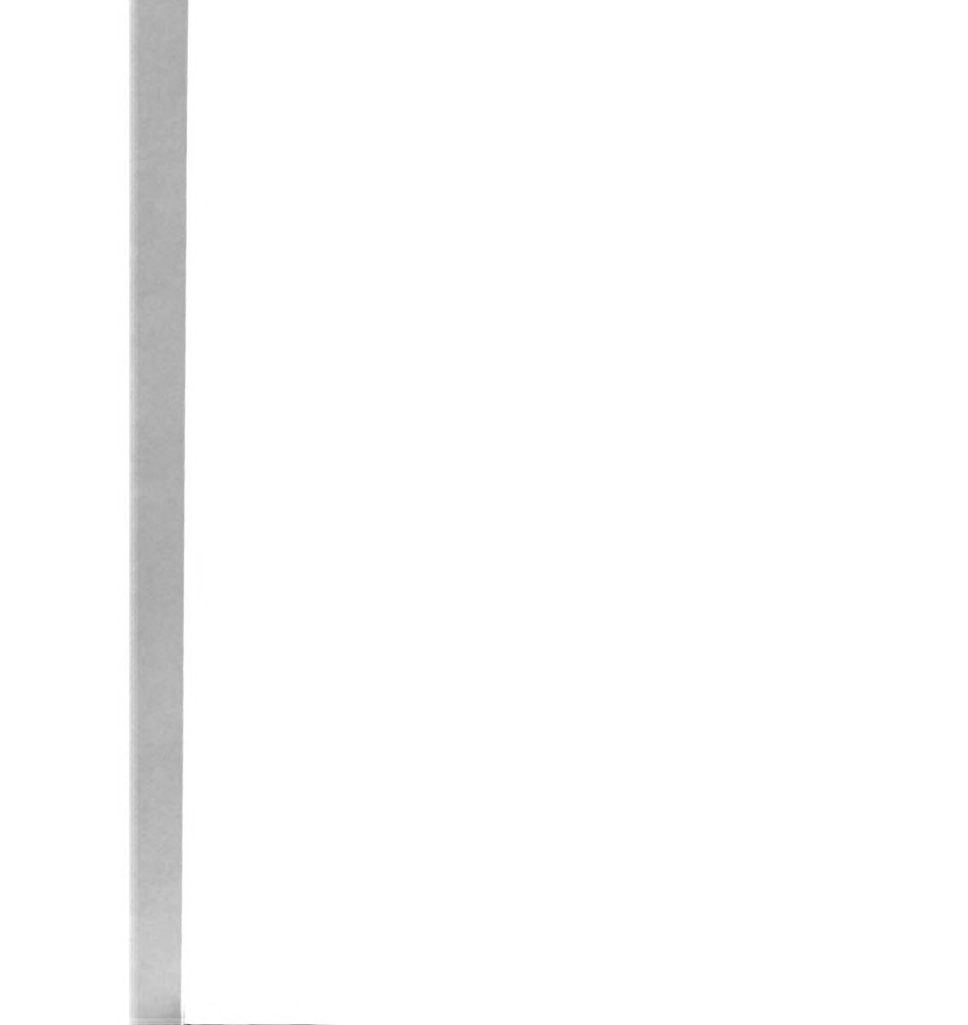
Thanks are expressed to Dr. Ruth R. Benerito, Dr. Joseph H. Boyer, Dr. John J. Eisch, and Dr. Irving Siegel for encouragement, inspiration, and advice.

## TABLE OF CONTENTS

Chapter	Page
I. INTRODUCTION . . . . .	1
II. HISTORICAL REVIEW . . . . .	4
A. NMR Studies of Proton Exchange Involving Substituted Ammonium Ions . . . . .	4
Ammonia . . . . .	4
Ammonium Salts . . . . .	10
Methylammonium Salts . . . . .	13
Dimethylammonium Salts . . . . .	19
Trimethylammonium Salts . . . . .	21
Other Alkylammonium Salts . . . . .	27
Other Nitrogen Compounds . . . . .	29
B. Nuclear Relaxation and Quadrupolar Effects . . . . .	31
General Theory of Nuclear Relaxation . . . . .	31
Relaxation for Nuclei with a Quadrupole Moment . . . . .	39
Nuclear Relaxation Times of Nitrogen Compounds . . . . .	43
Viscosity and Temperature Effects on $T_1$ of Quadrupolar Nuclei . . . . .	50
Activation Energies for the Relaxation Process . . . . .	58
Solvent Effects . . . . .	60
C. Nitrogen Chemical Shifts . . . . .	72
D. Nuclear Spin-Spin Coupling . . . . .	81
General Observations . . . . .	81
Mechanism of Spin-Spin Coupling . . . . .	86
Spin Coupling in Nitrogen Compounds . . . . .	88
Proton-Proton Coupling Constants . . . . .	89
$^{14}\text{N}$ -Proton Coupling Constants . . . . .	98
$^{15}\text{N}$ Proton Coupling Constants . . . . .	107

Chapter	Page
E. Nuclear Magnetic Double Resonance Spectroscopy . . . . .	114
III. EXPERIMENTAL . . . . .	137
A. Purification of Compounds . . . . .	137
B. NMR Spectrometers . . . . .	141
C. Homonuclear Decoupling-Variable Temperature Experiments . . . . .	143
D. Heteronuclear Decoupling Experiments . . . . .	150
E. Viscosity Measurements . . . . .	165
IV. RESULTS . . . . .	167
A. Spectra and Plots of Data . . . . .	167
B. Data Analysis by Digital Computer . . . . .	186
C. Data . . . . .	190
V. DISCUSSION . . . . .	216
A. N-H Lineshapes in the Proton Spectra of Substituted Ammonium Ions . . . . .	216
Contributions to Linewidths from Proton Exchange . . . . .	216
Contributions from $^{14}\text{N}$ Spin-Lattice Relaxation and Viscosity . . . . .	222
Spin-Spin Coupling Constants . . . . .	233
B. Heteronuclear Decoupling . . . . .	236
NH Proton Lineshapes . . . . .	237
Long-range $^1\text{H}$ - $^{14}\text{N}$ Spin-Spin Coupling . . . . .	239
Nitrogen Chemical Shifts . . . . .	240

Chapter	Page
C. Solvent Effect on Proton NMR Spectra of Ammonium Salts . . . . .	251
Changes of $1J(^1\text{H}-^{14}\text{N})$ with Solvent and Temperature . . . . .	251
General Effects on NH Lineshapes . . . . .	255
Ammonium Ion in Acidic (protic) Solvents . . . . .	256
Ammonium Ion in Non-Acid (aprotic) Solvents . . . . .	260
VI. SUMMARY . . . . .	269
VII. RECOMMENDATIONS . . . . .	273
BIBLIOGRAPHY . . . . .	276
APPENDICES . . . . .	291
A. Program QUADRELX . . . . .	292
B. Program NMR FIT8 . . . . .	297



# LIST OF TABLES

Table	Page
1. Reported nitrogen chemical shifts (ppm) . . .	73
2. Three-bond proton-proton coupling through nitrogen of the type $^3J(R-\underline{N}H-\underline{C}H_3)$ . . . . .	90
3. Three-bond proton-proton coupling through nitrogen of the type $^3J(\underline{H}C-\underline{N}H^+)$ . . . . .	93
4. Proton-proton coupling constants for the ethyl group. . . . .	96
5. $^1H$ - $^{14}N$ coupling constants across one bond. .	100
6. $^1H$ - $^{14}N$ coupling constants across two bonds .	103
7. $^1H$ - $^{14}N$ coupling constants across three bonds	105
8. $^1H$ - $^{15}N$ coupling constants. . . . .	109
9. Concentrations and pH values for solutions of substituted ammonium salts used in this work . . . . .	138
10. $^{14}N$ relaxation times for various J values. .	187
11. Results of computer least-squares fitting of ammonium proton lineshapes . . . . .	190
12. Variation of $^{14}N$ relaxation time with tem- perature for substituted ammonium ions . .	192
13. Results of least-squares fitting of relax- ation time-temperature data. . . . .	195
14. Results of least-squares fitting of viscos- ity-temperature data . . . . .	196

	Page
measured solution viscosities. . . . .	197
spin-lattice relaxation rates and calculated solution viscosities . . . . .	198
results of least-squares fitting of data to the equation $1/T_1(^{14}\text{N})$ vs. $\eta/T$ . . . . .	200
relaxation rates calculated for three selected values of viscosity/temperature. . . . .	200
proton coupling constants and chemical shifts for alkylammonium ions . . . . .	201
measured nitrogen and proton NH chemical shifts . . . . .	204
nitrogen chemical shifts for substituted amines . . . . .	205
nitrogen chemical shifts for substituted ammo- nium ions. . . . .	206
nitrogen chemical shifts for nitriles and isonitriles. . . . .	207
nitrogen chemical shifts for amides. . . . .	208
nitrogen chemical shifts for nitro compounds .	209
measured viscosities for ammonium salts in various solvents . . . . .	209
summary of NMR results for ammonium salts in various solvents and at various temperatures	210
physical properties of solvents. . . . .	214
calculated linewidths for central NH proton of aqueous monomethylammonium ion . . . . .	218
$J(^1\text{H}-^{14}\text{N})$ for ammonium salts in various sol- vents. . . . .	253
change of NH proton chemical shift with tem- perature . . . . .	266

## LIST OF FIGURES

Figure	Page
1. Detail of Dewar jacket, 60 MHz receiver coil insert, and 4.33 MHz transmitter coil for $^1\text{H}$ - $^{14}\text{N}$ decoupling experiments. . . . .	156
2. Detail of modified probe for variable temperature decoupling experiments showing relative position of supporting accessories . . .	157
3. Photograph of the experimental heteronuclear double resonance system of Figure 2. . . . .	158
4. Block diagram of electronic configuration for heteronuclear double resonance experiments .	160
5. Complete proton resonance spectra of a few alkylammonium chlorides in aqueous solution.	168
6. NH proton spectra for a series of alkylammonium salts. . . . .	169
7. NH lineshapes calculated for various values of $\eta = 10\pi\text{JT}_1$ from Pople's Equation (Ref. 9). .	170
8. Effect of temperature on the NH resonance of monomethylammonium and monoethylammonium ions . . . . .	171
9. NH resonance of monomethylammonium ion showing (A) single resonance spectrum (B) methyl proton decoupling and (C) nitrogen decoupling .	172
10. NH resonance of monomethylammonium ion showing variation with the frequency used to decouple the alkyl protons. . . . .	173

	Page
resonance of monomethylammonium ion showing variation with the frequency used to decouple nitrogen. . . . .	174
variable temperature study of NH proton resonance of monoethylammonium ion while decoupling nitrogen. . . . .	175
tail of the methylene proton spectrum of the series of ethylammonium ions showing the line broadening. . . . .	176
$^1\text{H}$ spin-lattice relaxation times <u>vs.</u> reciprocal of absolute temperature for the alkylammonium salts . . . . .	177
$^1\text{H}$ relaxation rates <u>vs.</u> viscosity/temperature for the alkylammonium salts. . . . .	178
calculated and experimental nitrogen chemical shifts for the alkylammonium salts . . . . .	179
proton chemical shifts for the alkylammonium salts. . . . .	180
nitrogen chemical shifts <u>vs.</u> $\sigma^{\text{P}}$ values (Grim) for amines and substituted ammonium ions. The chemical shifts are relative within each series . . . . .	181
relative nitrogen chemical shifts and $\sigma^{\text{P}}$ values for nitriles and nitro-compounds . . . . .	182
relative nitrogen chemical shifts and $\sigma^{\text{P}}$ values for amides . . . . .	183
proton NMR lineshapes for ammonium salts in various solvents at selected temperatures. . . . .	184
range of NH proton chemical shift with temperature for ammonium salts in several different solvents. . . . .	185



## I. INTRODUCTION

The proton magnetic resonance spectra of the majority of organic compounds containing nitrogen yield only broadened signals for hydrogens attached directly to nitrogen or removed two and three bond lengths from it. In a few exceptional compounds, however, triplet structure is observed due to spin-spin interactions between the protons ( $I = 1/2$ ) and the nitrogen ( $^{14}\text{N}$ ,  $I = 1$ ).

The broadening of proton signals for the majority of nitrogen-containing compounds may be a result of hydrogen bonding with nitrogen through the lone-pair electrons or of intermediate rates of exchange of protons between the nitrogen and the solvent. Another cause of broadening is the nitrogen nucleus itself which possesses an electric quadrupole moment that may interact with surrounding electric fields.

Where exchange is slow a symmetrical electric field leads to relatively slow spin-lattice relaxation and a symmetrical (1:1:1) triplet in the N-H proton spectrum from coupling with  $^{14}\text{N}$  ( $I=1$ ); an unsymmetrical



electric field, on the other hand, leads to rapid spin-lattice relaxation which collapses the triplet to a broad or sharp single line. This thesis is primarily concerned with effects of the nitrogen nucleus on the proton resonance spectra of nitrogen compounds and with nitrogen NMR spectra themselves. The effects of symmetry around nitrogen and of temperature on the nitrogen spin-lattice relaxation process have been studied. A set of compounds with gradually increasing asymmetry of the electric field at the nitrogen atom have been chosen for study; these are the mono-, di- and trialkyl ammonium chlorides.

Increasing temperature has two possible effects on the proton N-H lineshapes depending on whether exchange or quadrupolar spin-lattice relaxation processes predominate. The effect of increased proton exchange rate between nitrogen and solvent is to cause a collapse of multiplet structure in the nuclear magnetic resonance spectrum, e.g. a triplet would broaden and in the limit collapse to a single broad line which would then become narrower at very high exchange rates. Conversely, for quadrupolar nuclei in nonspherically symmetric electric environments, increasing temperature causes relaxation times to increase and relaxation rates to decrease. One purpose of this

75

76

77

78

79

80

81

82

83

84

thesis is to determine which process governs the proton NH lineshapes in NMR spectra of the mono-, di-, and tri-alkyl ammonium chlorides in aqueous solution at low pH.

Another method of studying the NH lineshapes in order to determine the effect of the nitrogen is by means of heteronuclear decoupling, i.e., observing the proton resonance spectrum while irradiating nitrogen at its resonance frequency with high RF power. An additional result of the double resonance study is to show the existence of nitrogen spin coupling with protons two and three bonds distant.

## II. HISTORICAL REVIEW

### A. NMR Studies of Proton Exchange Involving Substituted Ammonium Ions

#### Ammonia

The earliest nuclear magnetic resonance (NMR) work on amines was the kinetic study of proton exchange between methylamine and water performed by observing changes in the hydrogen resonance spectrum produced by changes in hydrogen ion and amine concentration. (1,2) This work was predated by that of Ogg (3,4), who reported the effect of proton exchange rates on the liquid ammonia spectrum. It is appropriate to begin any discussion of the kinetics of proton exchange in amines with a brief review of the NMR work on ammonia and the ammonia ion.

In their study of the effects of electrolytes on the proton chemical shift of the solvent water, Gutowsky and Saika (5) mentioned that solutions of ammonium hydroxide and ammonium chloride gave single lines whose shifts were concentration dependent as a result of proton exchange.



Gutowsky and Fujiwara (6) then showed from the change of proton chemical shift that there is significant association of ammonia with water in dynamic equilibrium and that the structure can neither be adequately represented as free ammonia mixed with water nor as ammonium ion and hydroxide ion. Ogg showed (3) that, first, there is a marked chemical shift on going from gaseous to liquid ammonia which he attributed to hydrogen bonding in the liquid phase. Secondly, he showed that a trace of water causes rapid proton exchange which collapses the triplet resulting from spin-spin interaction with the  $^{14}\text{N}$  nucleus ( $I=1$ ). (It should be pointed out here that there is some dispute as to the trace quantity of water and conditions necessary for proton exchange in liquid ammonia to occur. Nevertheless, these questions are deferred for the present).

In conclusion then, although the systems observed were similar, the approaches and results were quite different. Whereas Gutowsky et al. (5,6) observed chemical shift changes for the composite single proton line ( $\text{NH}_3$ ,  $\text{NH}_4^+$ ,  $\text{OH}^-$ ,  $\text{H}_2\text{O}$ ) by quantitatively varying the concentration of ammonia or ammonium salts, Ogg (4) noted the gradual collapse of the proton triplet by quantitatively varying the species present either in dry liquid ammonia ( $\text{NH}_2^-$  or  $\text{NH}_4^+$ ) or in aqueous ammonia ( $\text{H}_3\text{O}^+$  thus  $\text{NH}_4^+$ ).



Whereas Gutowsky et al., on the one hand, only speculated that dynamic processes were occurring, Ogg (4) was the first to show what species contributed and that it was possible to use NMR for obtaining kinetic data on ammonia and amines.

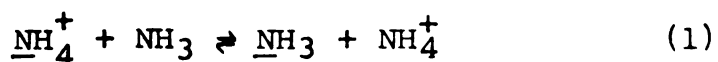
Considering all reports on amines and aqueous ammonium salts since the first work of Ogg and Gutowsky et al., there have been only developments of the basic ideas outlined above. The developments have followed three paths, first, improvements in chemical techniques have permitted more accurate values for the concentrations of various species in the systems observed. Secondly, improvement in magnetic resonance spectrometers has yielded more accurate values of the NMR parameters - chemical shifts, spin-spin splittings, half-height widths and spin relaxation times, as well as more accurate representations of line shapes. The third path has been the development of models for the system and mathematical treatment of the measurable quantities to yield reaction rate constants.

Ogg and Ray (7) were the first to clearly demonstrate that the unequal line widths and line heights for the proton triplet of pure dry liquid ammonia was a result of relaxation from quadrupolar interaction with the  $^{14}\text{N}$



A sample of pure dry ammonia enriched 99.8% with quadrupolar  $^{15}\text{N}$  nucleus was prepared in the same natural ammonia and yielded a proton spectrum consisting of a very sharp and narrow doublet. At about this time, Roberts (8) showed that this was generally true for a large number of amines and nitrogen compounds, *i.e.*, the broadening of proton resonances was due to  $^{14}\text{N}$  quadrupole relaxation rather than hydrogen bonding or rapid proton exchange. As a result of these reports, Pople (9) presented a theory based on nuclear quadrupole spin-lattice relaxation explaining the broadening of multiplet components, which very well reproduced the line shapes observed. However, a detailed discussion of relaxation effects is postponed until Section II B).

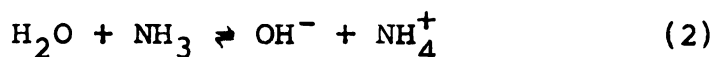
Archall and Jolly (10, 11) have used liquid ammonia as a solvent to measure the  $\text{pK}$  for weak acids such as malononitrile, cyclopentadiene and 2,4-dinitroaniline. They observed that the triplet in the proton spectrum of the solvent collapsed in solutions of the stronger acids ( $\text{pK} > 15$ ) and attributed this to increased concentration of ammonium ion resulting in the process:



Immediate concern here, they showed that Ogg's



position, that only a trace of water was necessary for rapid ammonia exchange and resultant triplet collapse is incorrect since the system consisting of water in liquid ammonia can easily be buffered with cyclopentadiene and cyclopentadienide ion to produce a partially collapsed ammonia triplet and a separate sharp water resonance. Water must then be a weaker acid than cyclopentadiene, and Ogg's suggested rate constant for the



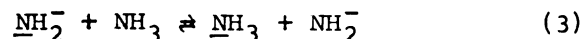
is affected by several orders of magnitude. This is further supported by Alei and Florin (12), who showed that the ammonia triplet is only partially collapsed with water present and that separate water and ammonia signals are possible even up to a concentration of 17 M water, so that special care is taken to remove any  $\text{NH}_4^+$

Alei and Florin suggest that  $\text{NH}_4^+$  may be formed by the reaction of ammonia with protons in the glass

They showed that ammonium ion concentrations from  $10^{-2}$  M are sufficient to cause rapid exchange so that an average broadened single line for the  $\text{H}_2\text{O}$  and ammonia resonances is produced.

J. Swift et al., using careful chemical

techniques and a more accurate mathematical method of determining proton line shapes, have reported a more precise value of the rate constant for amide-ammonia exchange (13):



as well as for the ammonium-ammonia exchange (14 and 15) given by Equation (1).

Perhaps it is worthwhile at this point to mention the suggestion of Powles and Strange (16) that pulsed radio frequency or spin-echo methods be used to study the proton exchange process. They have shown that for dry liquid ammonia a simple echo decay pattern, without modulation from spin-coupling with the  $^{14}\text{N}$  nucleus, is obtained for the protons. Thus, in a system containing amide or ammonium ion, the exchange effects on the echo pattern would be quite straightforward and tractable. Also, whereas in the steady-state method the experimenter has at his disposal only the line shape as a function of concentration and temperature, in the spin-echo method the experimenter has these and the advantage of another variable, the pulse spacing, plus freedom from heteronuclear coupling with the  $^{14}\text{N}$  nucleus which is a nuisance in the steady-state method. The reason for mentioning the spin-echo method is that although it has an obvious superiority over the



ate method for studying ammonia exchange, and  
it was mentioned in 1962, it has not yet been

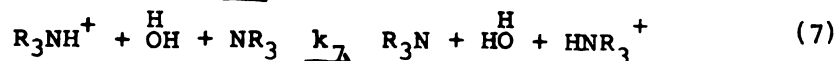
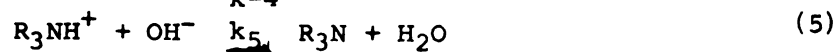
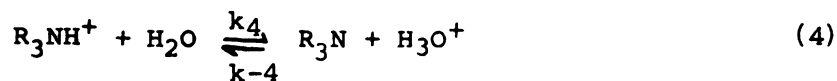
### Salts

was mentioned before, the first reported work on  
salts was by Gutowsky et al., (5,6) who observed  
ra of aqueous ammonia or ammonium salts at various  
tions, but with no regard to pH. Under these  
s only a single proton resonance is obtained  
a composite of those for several species and is  
ect to exchange averaging of the chemical shifts.  
and Saika (5) gave a theory to support their in-  
lon and made a rough estimate of the proton life-  
porting  $10^{-4}$  sec or less. Ogg (4) was the first  
that the exchange rates between  $\text{NH}_4^+$  and solvent  
be decreased by acidification so that separate  
sonances were observable for ammonium ion and  
ent water. McConnell and Thompson (17) gave a  
etchy theoretical justification for Ogg's obser-  
n the case of acidified aqueous ammonium ion, but  
sented all the details. The first detailed study  
um ion in aqueous solution was by Meiboom et al.  
by carefully changing concentrations and pH, were

able to obtain kinetic rate data from changes in the spectra.

They found that the kinetics could be accounted for by the

following mechanisms:



where, for the ammonium ion,  $\text{R}=\text{H}$ . Under their conditions,  $1.5 < \text{pH} < 2.5$ , Reaction (5) is negligible and  $k_4$  of (4) can only be estimated;  $k_6$  and  $k_7$  (of 6 and 7) were determined, but are not given here as the values have since been revised. Grunwald et al., (19 and 20) by extending the pH range and by controlling the ionic strength of the solutions were able to determine accurately  $k_4$ ,  $k_{-4}$  and  $k_6$  and establish that these were diffusion controlled. By means of deuterium exchange they were able to determine the mean lifetime of the ammonia-water hydrogen bond and estimate its rate of rupture by both diffusion and rotation. Finally, Connor and Loewenstein (21) obtained rate constants as functions of temperature, and thus obtained activation energies for Reactions (4) and (6). Most recently, Grunwald and Ku (22) report a new value for  $k_7$ .

Kinetics of ammonium-solvent proton exchange in a

aqueous solvents has also been investigated. The problem is that the exchange mechanisms are usually retarded by ion-association, which is promoted by solvents of low dielectric constant. Grunwald et al. (23) and (24) studied the proton exchange of ammonium acetate in glacial acetic acid and report that the proton is exchanged between the ion pair and the acetic acid carboxyl group. In order to calculate a rate constant, values of the nitrogen spin-spin coupling constant and the  $^{14}\text{N}$  spin-lattice relaxation time were required. It is important to point out that their values for these were obtained at  $0^\circ\text{C}$  or below and used in calculations of rate constants from Arrhenius plots. Perhaps it should be mentioned that the exchange of protons in the case of ammonium chloride in glacial acetic acid was too slow to measure.

The studies by Alei and Florin (12), and by Swift and Alei (13, 14 and 15) of the ammonium ion-ammonia proton exchange were mentioned above. As these studies were conducted in liquid ammonia or solutions composed chiefly of liquid ammonia they can be included with the studies of ammonium ion exchange in non-aqueous solvents. As mentioned before, Florin presented data for ammonium ion-water-proton exchange in liquid ammonia, which they compared

with the aqueous solution studies of Meiboom (18) and Grunwald (19 and 20). Swift and Clutter (14 and 15) studied the ammonium ion-ammonia exchange for ammonium halides added to liquid ammonia and also the ammonium ion-water-ammonia exchange. They showed that exchange is due to ammonium ion, which is generated from reaction with water, reacting with the solvent ammonia as given by Equation (2); thus they did not obtain specific rate constants for direct water-ammonia exchange.

#### Methylammonium Salts

Turning now to the alkylammonium studies, let us consider methylamine and aqueous methylammonium ion. Kinetic studies of this system by NMR (1,2) were the first on alkylammonium ions. Grunwald et al. (1,2) studied proton exchange in aqueous methylammonium chloride in a concentration range from 0.272 M to 4.47 M and pH range from 3 to 5. At low pH the exchange is slow and three sets of lines are apparent in the proton spectrum: the methyl hydrogens appear as a quartet from spin-spin coupling with the three ammonium ion protons, the solvent water hydrogens yield a single sharp line, and the ammonium ion protons produce a large triplet, from coupling with  $^{14}\text{N}$  ( $I=1$ ), each component being broadened by the  $^{14}\text{N}$  quadrupole

n. There is also a barely discernable coupling of methyl hydrogens. At high pH exchange between amine is rapid so that only two lines are observed from the methyl hydrogens (showing no spin because proton residence time on the nitrogen is ) and the other a composite of hydrogen signals from the protons, ammonium ions, water and hydrogen ions. It was calculated that the mechanism for exchange followed Reaction 4-7, with  $R_3 = CH_3H_2$ . Rate constants were determined from the change in shape of the methyl signal by comparing experimental spectra with theoretically calculated shapes. They showed that Reaction 4 is negligible and is very small. Thus, the total rate of exchange is assumed to follow the equation:

$$\frac{d[\text{CH}_3\text{NH}_3^+]}{dt} = k[\text{H}^+] = k_5 K_W + (k_6 + k_7) K_A [\text{CH}_3\text{NH}_3^+] \quad (8)$$

$$K_W = [\text{H}^+][\text{OH}^-]; K_A = [\text{H}^+][\text{CH}_3\text{NH}_3^+].$$

Plot of mean values of  $k_{11}$  vs.  $[\text{CH}_3\text{NH}_3^+]$  they obtained  $(k_6 + k_7)$  and found that  $k_5$  contributes only a small amount to the overall rate since it is small. From the broadening of the water signal, an estimate of  $k_7/(k_6 + k_7)$  was obtained. The broad ammonium ion triplet was used only as an order-of-magnitude check on the overall rate, since it is observable only up to pH = 4.0 and



at high methylammonium ion concentrations.

It is worth-while at this place to depart from the discussion of kinetics and mention something in detail about the broad ammonium ion triplet. Grunwald et al. (1,2) readily admitted that the chief cause of broadening of the triplet components was spin-lattice relaxation by the quadrupolar nitrogen nucleus and they made an estimate of the  $^{14}\text{N}$  spin-lattice relaxation time of 0.02 sec (25). That relaxation was the chief cause of broadening was very clearly demonstrated by Ogg and Ray (26), who presented the spectrum of acidified aqueous methylammonium chloride enriched 65% with the non-quadrupolar  $^{15}\text{N}$  isotope in which the  $-\text{NH}_3^+$  resonance was a very sharp quartet from spin-spin coupling with the methyl hydrogens. Unfortunately, Ogg and Ray did not report the concentrations used, nor did they study the collapse of the  $-\text{NH}_3^+$  peak with changing pH, so that no direct comparison with the work of Grunwald (2) could be made. In summary, then, although it was realized and substantiated very early that the line shape for the ammonium proton resonance was chiefly governed by nitrogen spin-lattice relaxation, no study of the relaxation process itself was undertaken.

Returning now to the discussion of exchange kinetics

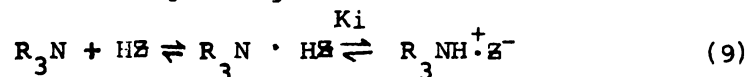
ylammonium salts, recent work has chiefly added  
 cation to the earlier studies (1 and 2) to obtain  
 nsight into the mechanisms. Grunwald and co-  
 (27) extended their earlier studies by obtaining  
 ct values for  $k_6$  and  $k_7$  of processes (6) and (7).  
 stants were obtained from the methyl group line  
 bserved over the range of concentrations of  
 monium chloride from 1.7 M to 8.1 M, and of pH  
 to 8.0. Using these data in conjunction with  
 ge in shape of the water line,  $k_6$  and  $k_7$  were  
 ed separately, and using viscosity data were extra-  
 to the viscosity of pure water. The ammonium ion  
 again was used only to confirm the mechanism in the  
 from 2.5 to 4.0. In another study (20) the mean  
 of the amine-water hydrogen bond was determined  
 dies of deuterated species in very strongly acidic  
 s.

changes in the line shapes of the methyl quartet  
 d to obtain exchange rates vs. temperature, while  
 monium ion and hydrogen ion concentrations were  
 stant. From plots of these rates vs. temperature,  
 nd Loewenstein (21) obtained the activation energy  
 combined process represented by  $k_6 + k_7$ ,  $k_4$  and  $k_5$   
 all and thus neglected. They noted that the value

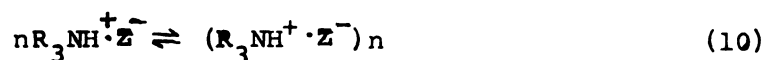
was surprisingly low ( $\Delta E \approx 16.0$  cal/mole) and that within experimental error the ratio  $k_6/k_7$  was temperature independent. They observed that the  $-\text{NH}_3^+$  triplet sharpens with increasing temperature, and attributed this to the change in correlation time ( $\tau_c$ ) of the nitrogen which affects  $T_1$  for the  $^{14}\text{N}$  nucleus.

Unlike ammonia and ammonium salts, discussed above, methylamine proton exchange was studied in a number of solvents. In general, the interaction of alkyl amines or alkyl-ammonium salts with solvents may be formulated as in the following reactions, which may occur concurrently or stepwise depending on the gegen ion and solvent properties:

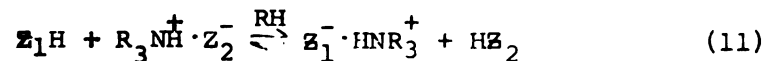
Ionization (ion-pairing):



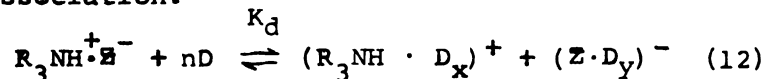
Homo-ion association:



Direct ion-pair solvent transfer:



Ion-dissociation:



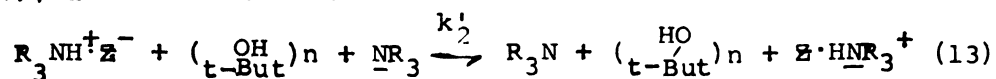
After dissociation all the usual proton exchange processes are possible [Equations (4) through (7)]. It has been pointed out by Bruckenstein (28) that base dissociation occurs in two major steps, Equations (9) and (12), especially

in the case of a weak base such as methylamine in a solvent of low dielectric constant. Equations (10) and (11) describe additional processes occurring.

Grunwald and Price (23 and 29) studied methylamine (0.02 M-0.5 M) in glacial acetic acid finding that it was largely converted to ion pairs, Equation (9), and that the exchange followed Equation (11). Kinetic rate data were obtained from the broadening of the carboxyl proton peaks, with which only the NH protons are exchanging, by means of spin-echo measurements. Quite interestingly, methylammonium chloride forms higher aggregates, Equation (10), in glacial acetic acid and proton exchange was too slow to measure. In addition, they noted that the line shape for the  $\text{NH}^+$  proton resonance, being governed by  $^{14}\text{N}$  spin-lattice relaxation, is concentration dependent. Thus, for glacial acetic acid solvent, the gegen ion determines which process controls the NH line shape.

Proton exchange rates for methylammonium salts in the solvents methanol and t-butanol, were obtained by Cocivera and Grunwald (24, 30, 31, and 32). Methanol, with a very high dielectric constant, behaves very much like water with exchange described by Equations (6) and (7) accounting in large part for the overall rate (30 and 31). On the other hand, t-butanol induced quite noticeably

different results. Owing to its low dielectric constant the salts exist largely in the form of ion pairs, as evidenced by the change in NH chemical shift with gegen ion. As a result of the close proximity of the gegen ion, an asymmetric electric field exists around the nitrogen nucleus producing rapid  $^{14}\text{N}$  spin-lattice relaxation and, consequently, the  $\text{NH}^+$  proton peak is not split into a triplet by  $^{14}\text{N}$  as it is in water and methanol solutions. Oddly enough, though, the NH proton peak is split into a quartet from spin-spin coupling with the methyl protons since exchange is slower than in water. The exchange process in t-butanol was found to follow a mechanism analogous to that in water and methanol (Equation 7), and formulated as:



(for methylamine  $\text{R}_3 = (\text{CH}_3)_2\text{H}$ )

$k_7$  for water was found to be about twenty-four times faster than  $k_2'$  for t-butanol.

#### Dimethylammonium Salts

Of the alkyl amines studied by NMR, the dimethyl is the one to which the least attention has been devoted. The most likely reason for this is that in aqueous solutions its exchange mechanisms and corresponding rate constants are very similar to those of methylamine and both

of these are very different from trimethylamine.

The kinetic analysis of protolysis of dimethylammonium ion in aqueous solution in the concentration range from 0.23 M to 4.68 M and the pH range between 3 and 5 was carried out by Loewenstein and Meiboom (33). They noted that  $k_6$  of Reaction (6) is measureably slower and  $k_7$  of Reaction (7) is measureably faster, although of the same order of magnitude, than for the methylammonium ion. Again  $k_4$  and  $k_5$  were found to be small with  $k_6$  and  $k_7$  being the major contributors to the overall exchange rate. In addition, they noted that the NH resonance is a broader triplet than observed for the monomethyl derivative and ascribed this to increased quadrupole relaxation from the  $^{14}\text{N}$  nucleus.

Exchange kinetics in non-aqueous solvents were studied only in alcohols. Although not stated specifically, it is implied by Cocivera and Grunwald (30 and 31) that in methanol the dimethylammonium ion behaves very much like the monomethylammonium ion, showing no measureable difference in exchange rates from water. *t*-Butanol was the only other solvent investigated (31 and 32), and there is definitely a measureable difference from the aqueous solution value. As mentioned before, *t*-butanol promotes ion pairing and the rate of proton exchange was found to vary with gegen ion. Studies with added tetraethylammonium

salts (32), gave a significant decrease in rate which was attributed to increased solution viscosity and to the formation of less reactive aggregates.

### Trimethylammonium Salts

There has been much more attention devoted to the proton exchange kinetics of trimethyl- and monomethylammonium salts than any others. Quite typically, trimethylammonium was studied first in aqueous solutions as reported by Loewenstein and Meiboom (33). Trimethylammonium chloride was studied in the concentration range from 0.26 to 2.3 M and aqueous pH range from 3 to 5. Exchange reactions given by Equations (4) through (7) were considered and, as before,  $k_5$  could not be measured experimentally, only an upper limit being assigned. The rate constants  $k_7$ ,  $k_6$ , and  $k_4$  were measured, as they had been for the mono- and dimethyl salts, and  $k_7$  was found to be lowest for the trimethyl compound. Unlike the mono- and dimethylammonium ions  $k_6$  proved almost unmeasurable for trimethylammonium ion, whereas  $k_4$  became measurable for the first time. No correlation of the  $pK_A$ 's was found with any of the rate constants for the mono-, di- and trimethylammonium series.

In a later study, Grunwald (34) obtained proton exchange rate data for aqueous trimethylammonium chloride

in dilute solution ( $0.15 \text{ M} \leq \text{conc.} \leq 0.65 \text{ M}$ ) and at low pH values (1.58–3.32). Activation parameters were obtained from rate data in the temperature range  $35^\circ$  to  $80^\circ$ . Over this temperature range  $k_6 \leq 0.1 k_7$  and  $k_4$  was shown to be diffusion controlled. In his most recent study Grunwald (22) has aimed at getting a better insight into the mechanism governing  $k_6$ , Equation (6). This was accomplished by varying the ammonium ion ( $\text{R}_3\text{NH}^+$ ,  $\text{R}=\text{CH}_3$  or H) and the amine ( $\text{R}_3\text{N}$ ,  $\text{R}=\text{CH}_3$  or H), and measuring the rate constants. From this study it was hypothesized that Reaction (6) can be broken up into three steps and that the rate constant  $k_6$  is governed by the number of methyl groups. Additional methyl groups reduce the speed at which the ammonium ion and the amine molecule become nearest neighbors.

Grunwald et al. (20), by studies of exchange rates of deuterated trimethylammonium ion in sulfuric acid–water solutions, determined the mean lifetime of the hydrogen bond between water and trimethylamine. This proves to be longer in the case of trimethylamine than for ammonia or monomethylamine. They presented two alternative hypotheses to explain this, but their data could support either. These rates depend on  $k_4$ , Reaction (4), and it was noted that at high acid concentrations,  $\text{pH} < 2$ , this rate constant decreases markedly. Thus, Grunwald (35) showed that  $k_4$

can be subdivided into a two-step mechanism in which the first step is the equilibrium described by  $K_A$ . Also, the acid dissociation in aqueous media proceeds in such a way that the connection to the previously covalent proton remains intact for a measurable period. In a recent and more detailed investigation (36), it was shown that the rate of breaking the trimethylamine-water hydrogen bond measures the rate of diffusion of the water molecule from the amine into bulk solvent.

Using the deuterated ammonium salt ( $0.44 \text{ M} \leq [(\text{CH}_3)_3\text{ND}^+] \leq 1.76 \text{ M}$ ) in  $\text{D}_2\text{O}$  with deuterium chloride ( $0.08 \text{ M} \leq [\text{D}^+] \leq 5 \times 10^{-5}$ ) Day and Reilley (37) determined rate constants for deuterium exchange by fitting the methyl line shapes. They found that transfer rates for deuterium between amine and ammonium ion fit the mechanisms advanced by Grunwald et al. for the corresponding proton transfer rates. On the other hand, Fraenkel and Asahi (38) measured exchange rates in strong acid solution (concentration of  $\text{D}_2\text{SO}_4$  from 31% to 81% in  $\text{D}_2\text{O}$ ) by mixing quantities of trimethylammonium nitrate ( $(\text{CH}_3)_3\text{NH}^+\text{NO}_3^-$ ) and integrating the methyl signals with time. Measuring the rates over the temperature range from  $40^\circ - 103^\circ\text{C}$  yielded values for the activation parameters. Their rates and mechanisms for strong acid solutions agree with those of Grunwald et al. (20, 34, and 35).

The order of the reaction with respect to water, Equation (7), was shown to be one from a proton spin-echo study of the water resonance line in buffered trimethylamine-trimethylammonium salt solutions using water enriched with  $^{17}\text{O}$  at various concentrations. Using the appropriate mathematical relationship to treat the data, Luz and Meiboom (39) showed that one water molecule is involved in Reaction (6).

Although the studies carried out in deuterium oxide and deuterated sulfuric acid which were just discussed might be categorized as being performed in a non-aqueous system proton exchange involving trimethylamine in more conventional non-aqueous solvents will now be considered.

A study of proton exchange in the system trimethylamine-glacial acetic acid has been reported by Grunwald and Price (23). In glacial acetic acid, trimethylamine was found to first react forming ion-pairs, Equation (9), and then to exchange by means of transfer of acetic acid between the amine, the solvent shell of the amine, and the bulk solvent, Equation (11). They found that exchange rates for trimethylammonium ion were slower than for ammonium ion but faster than for monomethylammonium ion. Concentrations of trimethylammonium acetate ranged from 0.0207 to 0.1520 M and a temperature interval from  $15^{\circ}$  to  $75^{\circ}$  was used.

Interestingly, they noted that the rate of exchange for trimethylammonium chloride in glacial acetic acid is negligibly slow, and because of this they obtained a "moderately precise" ( $\pm 30\%$ ) value for the  $^{14}\text{N}$  relaxation time  $T_1$ . From  $T_1$  for the chloride salt they estimated  $T_1$  for the acetate salt, since this value is necessary to describe the broadening of the carboxyl proton line shape, from which the exchange rates were determined.

Unlike monomethyl- and dimethylammonium salts, the trimethylammonium salt in methanol yielded proton exchange rates measurably different from those in water (24, 30 and 31). In a recent detailed report Grunwald (40) shows that the kinetics follow two mechanistic paths, the first being acid dissociation, an equilibrium analogous to Equation (4). The second path of exchange involves the solvent and is analogous to Equation (7). Concentrations of trimethylammonium salt ranged from 0.001 M to 0.55 M and HCl from zero (excess amine) to 0.51 M. The kinetic data indicate that in the buffered system (excess amine) the second path plays a major role in the overall rate, whereas in the presence of excess HCl the second path is not the dominant reaction, the acid dissociation being more important. He also noted that the  $^{14}\text{NH}$  spin-spin interaction is well resolved at  $50^\circ$ . *t*-Butanol, owing to

its low dielectric constant, causes trimethylammonium salts to exist predominantly as ion pairs, Equation (9). This is evidenced most obviously by the dependence of the NH proton chemical shift on gegen ion, a difference of 0.78 ppm between trifluoroacetate and tosylate being noted (31). Exchange rates were also dependent on the gegen ion and could be attributed to the process described by Equation (13) (24, 30 and 31). The exchange rate for the tosylate was seven times faster than that for the chloride in t-butanol, and comparing  $k_7$  for water (Equation 7) to  $k'_2$  for t-butanol, it was 560 times faster than the tosylate and 3500 faster than the chloride. Unlike mono- and dimethylammonium salts, addition of quaternary alkylammonium salts to the solutions of trimethylammonium salts caused no major change in the exchange rates because the formation of aggregates greater than pairs (i.e.  $n > 1$  in Equation 10) is not possible (32).

Cocivera noted (31) that the NH proton peaks for the trimethylammonium salts in t-butanol exhibit fine structure not observed in aqueous solutions. This is a result of ion pairing; the closeness of the gegen ion generates an electric field which causes rapid relaxation of the nitrogen nucleus and thus prevents any  $^{14}\text{N}$  coupling, while at the same time exchange is slow so that the alkyl protons can couple with the NH proton. It was pointed

out before that a similar effect was found for monomethylammonium salts in t-butanol.

### Other Alkylammonium Salts

The only other simple alkyl amine studied in detail is triethylamine, reported by Ralph and Grunwald (41). In the pH range 5-8 the kinetically significant reactions are given by Equations (5) and (7), whereas at  $\text{pH} < 1$  they are those given by (4) and (9). Although not stated specifically, direct transfer of protons to the base must be insignificant since no mention of anything similar to Process (6) is made. Comparing these rates to the methylamines,  $k_7$  for triethylamine is much smaller than expected and this is attributed to steric hindrance from the bulky ethyl groups. At low pH, where exchange is slow, the deuterated triethylammonium ion in water was studied to determine  $k_H$  of Reaction 11. Grunwald and Ralph (36) considered the series of amines (ammonia, monomethyl-, and trimethyl-, and triethylamine) but found no correlation between  $k_H$  and basicity,  $K_B$ , but a systematic decrease of  $k_H$  with number and size of alkyl substituents. Two additional points should be mentioned. First, exchange rates were determined by spin-echo measurements of the dominant solvent water line, i.e.

changing exchange rates causes broadening of the water resonance. The second point is that parameters necessary for treating the spin-echo data are the  $^{14}\text{N-H}$  spin-spin coupling value and the  $^{14}\text{N}$  spin-lattice relaxation time. The values used in the triethylammonium study (41) were not actually measured, but were estimated from those for trimethylammonium ion. This procedure was justified on the basis that the kinetic results are not sensitive to small errors in these parameters.

Reviewing the results of a number of workers over a period of more than a decade, Grunwald, in a recent publication (22), has pointed out some general relationships. The effects of alkyl substitution on the various rate constants in water are quite different. Thus,  $k_7$  for Equation 7 changes very little, being the same order of magnitude for all. Although  $k_7$  showed no correlation with  $\text{pK}_\text{a}$  (33), a measure of the proton donating capacity of the alkyl ammonium ion, there is a correlation with  $\text{K}_\text{B}$ , the base dissociation constant, and with the number of methyl substituents, the triethylamine being an exception (41). For both  $k_6$  (Equation 6) and  $k_\text{H}$  (Equation 11) there is a change of two orders of magnitude, and a progressive decrease in rate with increasing number and size of alkyl substituents, on going from ammonia to

triethylamine (22, 36). These kinetic results, then, lead to speculation as to the reason for lack of correlation. One explanation given by Brown (42), which seems very likely, is that the decrease of  $k_H$  and  $k_6$ , and the lack of correlation of  $k_7$  in all cases, is due to increased steric hindrance or strain with increasing number and size of alkyl groups.

#### Other Nitrogen Compounds

In concluding the review of kinetic work, it is appropriate to point out the work on alkylammonium salts by Swain and co-workers (43, 44, and 45), who used tracer techniques. Although they did not report actual values for the rate constants, they nevertheless did obtain relative rates for the ammonium ion, the series of ethyl-substituted ammonium ions, and aniline. They also pointed out the chief mechanisms for exchange, which are the same as those mentioned above. They also studied exchange in acetic acid and methanol, as well as a number of solvents which have not as yet been employed in the NMR method, including dimethylformamide, toluene, ethylene glycol, and formic acid. While Swain et al., did not obtain the detailed information that the NMR investigators did, their work predated (43) the first NMR reports (1



and 2) and pointed the way for that work as well as for the later studies in other solvents (23, 24, 29, 30, 31, and 32) because their reports showed that exchange rates were in the correct range to be observed by the NMR spectroscopic technique.

While it is true that the methylamine series discussed above has been studied most extensively, and in far greater detail than all other amines, one should not conclude that these are the only amines for which proton exchange between amine and solvent or between amine and ammonium ion have been studied by the NMR techniques. For example, proton exchange between glacial acetic acid and tris-(hydroxymethyl)methylammonium acetate has been studied (23). Steinblatt investigated sites and mechanisms of protonation for glycylglycine (46) and triglycine (47), reporting the rates of exchange in aqueous solutions. Grunwald and Cocivera (24) considered p-toluidinium ion in methanol solution, and Grunwald and Puar (48) reported exchange rates and mechanisms for N,N-dialkylanilinium tosylates (dialkyl = dimethyl, diethyl, and di-n-propyl) in acetic acid. The dissociation constant of the dibenzylmethylamine-water hydrogen bond has been found (36). Although not measuring specific rates, Alei and Florin (12) have observed that the

exchange of water with the amine protons of ethylenediamine is so rapid over the entire range of composition of water-ethylenediamine solutions that steady-state methods cannot be employed, but presumably one could use the spin-echo method (23, 29, and 48). Most recently, the steady-state method has been employed by Sudmeier and Occupati (49) to study proton exchange in aqueous  $N,N'$ -dimethylpiperazine hydrochloride. All the compounds and systems discussed above have been illustrative of the types of compounds, other than simple alkylamines, which have been studied by NMR. No attempt at a complete review of all proton exchange research has been made, for this would be placing undue emphasis on that aspect of the NMR work.

#### B. Nuclear Relaxation and Quadrupolar Effects

##### General Theory of Nuclear Relaxation

Nuclei possessing a magnetic moment, when placed in a static magnetic field ( $H_0$ ), tend to be aligned in specific orientations with respect to this field. The natural tendency is for the nuclei to be aligned parallel to the static field, for that is the condition of minimum potential energy. However, as a result of random molecular

translational and rotational motion (i.e. Brownian motion) at room temperature, each nucleus will experience a rapidly fluctuating magnetic field produced by neighboring nuclear magnetic moments. Since the energy produced by these fluctuations far exceeds the energy difference between parallel and antiparallel alignments, there is only a small excess of nuclei in the lowest energy state.

For simplicity, consider a set of nuclei with a spin quantum number of  $1/2$ . These nuclei have a symmetrical charge distribution which is spherical and possess a magnetic dipole moment. In the absence of a magnetic field there will be equal populations in the two spin states but if these nuclei are suddenly placed in a strong static magnetic field ( $H_0$ ), one is then concerned with how long it will take for the populations of these nuclear spin states to reach equilibrium as described above, that is, with a small excess number in the lower state. After equilibrium is reached, if a strong radiofrequency field of frequency  $\omega$  is applied in a direction perpendicular to the static field, transitions between the two levels will occur as energy is absorbed, provided that the Larmor precession condition (14) is met (i.e.  $\omega = \omega_0$ ):

$$\omega_0 = \gamma H_0 \quad (14)$$

where  $\gamma$  is the nuclear gyromagnetic ratio. If the

radiation field at the precession frequency is sufficiently strong, transitions to the upper state will occur until the two states have equal populations. One is then concerned with how much time must elapse before the equilibrium number in the lower level is re-established, once the strong radiation is removed. Both this latter situation and the former one involve the approach to equilibrium between the nuclear spins and the environment (or the "lattice") by means of energy exchange with thermally induced fluctuations, after a stress is either introduced or removed. This establishment of equilibrium, then, is termed relaxation and the characteristic time for all but  $1/e$  of the excess spins in the upper state to return to the lower energy level is called the spin-lattice, thermal or longitudinal relaxation time (50 and 51).

As Sillescu (52) has mentioned, the longitudinal or thermal relaxation time ( $T_1$ ) was first introduced by Bloch (53) as an empirical constant in his famous phenomenological equations. Bloembergen et al. (54 and 55) showed that a reasonably good value of the spin-lattice relaxation time could be obtained from a time-dependent perturbation treatment of a suitable set of fluctuation functions describing the Brownian motion. Unfortunately, this work was riddled with errors as pointed out by Kubo and Tomita (56). Andrew

(57) presents a clearer outline of the important features of Bloembergen's derivation. The best treatments of relaxation in general are presented by Abragam (58) and Slichter (60). These presentations give the most details, the clearest explanations and methods for the most general applications. Let us proceed, then, to consider the important features of the theoretical approach to spin-lattice relaxation time.

It should be re-emphasized that the following discussion is limited to the case of nuclei with a spin quantum number of  $1/2$ , and as a result of their spherical charge distribution only dipolar interactions are important. In addition, it is assumed that the dipolar coupling between nuclei is weaker than the coupling with the lattice. This is the characteristic condition of nuclei in the liquid state and thus the chief mechanism for relaxation is Brownian motion. The situation is different in solids since internuclear dipolar coupling is much stronger in the rigid lattice (51 and 60) than in liquids.

In any form of spectroscopy, the intensity of absorption or emission of electromagnetic radiation is related to the rate of transitions between energy levels, which is in turn related to the probability of these transitions occurring. For an emission process, the lifetime in an excited

state is then of concern (61). This is true also with NMR, the major distinction resulting from the relatively small differences in energy between nuclear spin states. Whereas with other forms of absorption spectroscopy, relative populations of upper levels are small, and emission is unimportant, with NMR emission is quite important because of the very small differences in energy between upper and lower levels and the nearly equal populations of these levels. Thus, for NMR the absorption spectrum is closely related to the lifetimes of the excited states and the time necessary to reach the equilibrium populations of upper and lower levels is of prime concern.

Pake (50), Andrew (51), and Slichter (60) have shown that the rate of change of the excess number of nuclei approaching thermal equilibrium with the lattice is an exponential function. The spin-lattice relaxation time ( $T_1$ ), then, is the time constant of this exponential function or the characteristic time in which the spin-system exponentially approaches the temperature of the lattice. It is shown that there is a simple relation between the spin-lattice relaxation time and  $W$ , the mean value of the two transition probabilities, from lower to upper and from upper to lower levels:

$$T_1 = 1/2 W \quad (15)$$

ore, the main problem of any nuclear magnetic relax-  
theory centers on a method of computing  $W$ .

The first attempt at calculating a value for the  
transition probability was made by Bloembergen et al.  
(55). Their final values of  $T_1$  were quite close to

measured experimentally, although their general  
on was in error having incorrect constant coeffi-

Kubo and Tomita (56) re-examined this work and  
some of the equations. The correct result, also  
by Andrew (57) is:

$$W = \frac{3}{4} \gamma^4 h^2 I (I + 1) [J_1 (\omega_0) + \frac{1}{2} J_2 (2\omega_0)] \quad (16)$$

,  $h$ , and  $I$  have their usual meaning and  $J (\omega)$  is the  
density of the random functions or the intensity of  
carrier spectrum of the fluctuation functions of the  
on co-ordinates (i.e., functions which describe the  
in motion).  $J (\omega)$  is obtained as the Fourier trans-  
of the correlation function and therefore is:

$$J (\omega) = \int_{-\infty}^{+\infty} G(\tau) \exp (i\omega\tau) d\tau \quad (17)$$

relation function,  $G(\tau)$ , of the fluctuation func-  
is so named because it tells how these functions at  
time  $t$  are correlated to their value at a later time  
( $t + \tau$ ). Finally, the functions in Equation (17) should

the same subscripts as those of Equation (16). These  
pts denote which of the three fluctuation functions,

2, are capable of inducing transitions in a neighboring nucleus; from Equation (16) function 1 at frequency 2 at  $2\omega_0$ , are able to do so, but function 0 is not. At the outset this discussion was limited to liquids nuclei of spin one-half, whereas Equation (16) has had restrictions placed on I. This seemingly contradictory conclusion does indeed have very major limitations when  $I > 1/2$ . First, the population distribution among adjacent levels must vary exponentially so that a spin temperature may be defined. Second, as will be given in more detail shortly, certain symmetry requirements must be fulfilled so that only nuclear dipolar interactions are operative.

Finally, in considering the case of nuclei with spin  $I > 1/2$  in the liquid state, one should examine another technique presented by Abragam (58) and Slichter (60). They present the technique of the density matrix which is more generally applicable. There are a number of advantages to this approach: it does not require the concept of a spin temperature, and thus is very useful when this concept is not applicable, and it is ideally suited for situations in which the resonance is narrowed by the motion of nuclei as in liquids. It also has the advantage that both  $T_1$  and

cesses are handled in a natural way.

The density matrix method of Wangness and Bloch (59)

more qualitative theory of Bloembergen, Purcell and

ield the same result, namely that the spin-lattice

ion time is related to the transition probability

alue is determined by the spectral density function,

Both methods give the same expression for the

$$J(\omega) \propto 2\tau_c / (1 + \omega_0^2 \tau_c^2) \quad (18)$$

most cases the constant of proportionality is one.

relation time,  $\tau_c$ , is determined by the random

n motion. It is of the order of the time necessary

molecule to turn through a radian or to move through

nce comparable with its dimensions so that the rela-

sitions of the nuclei with respect to the external

nd thus the fluctuation functions have changed

ably. There have been a number of suggestions as to

calculate this correlation time. From methods listed

Evans and Richards review (62), as well as from the

1 form proposed by Bloembergen et al. (54), one may

\* $T_2$  is the spin-spin or transverse relaxation time,  
re of the time necessary to destroy phase coherence  
precessing components of the transverse nuclear  
c moments.

the general equation:

$$\tau_c = c' \eta / kT \quad (19)$$

$\eta$  is the solution viscosity,  $k$  is the Boltzmann con-

stant and  $T$  is the absolute temperature. Alternatively,

we write  $c'/k = c$  so that

$$\tau_c = c \eta / T \quad (20)$$

is Equation 6 of the treatment given by Arnold and

(63).

#### Relaxation for Nuclei with a Quadrupole Moment

Now we turn to the more complex case, nuclei with a

spin quantum number greater than one-half ( $I > 1/2$ ), which

have an asymmetrical (non-spherical) nuclear charge dis-

tribution and possess an electric quadrupole moment. Spin-

lattice relaxation may result from this quadrupole moment

interacting with fluctuating electric field gradients pro-

ducing the nucleus by various molecular degrees of free-

dom motion. This additional mechanism contributes to spin-lattice

relaxation and consequent broadening of signals. When there

is no symmetric molecular electric field about the quad-

rupole nucleus, the quadrupole coupling may be quite

impor-

tant. For the special case of spin  $I = 1$  (e.g.  $^{14}\text{N}$ ) Abragam

has shown how the quadrupolar effect can be calculated

and added to a term in the expression for  $T_1$ , the spin-lattice

relaxation time:

$$1/T_1 = 3/80 (1+a^2/3) [(eQ/\pi) (\partial^2 V/\partial z^2)] [\tilde{J}(\omega_0) + 4 \tilde{J}(2\omega_0)] \quad (21)$$

where  $a$  is the asymmetry parameter,  $Q$  the scalar quadrupolar moment,  $\partial^2 V/\partial z^2$  is the electric field gradient at the nucleus, and  $\tilde{J}(\omega)$  is the Fourier transform of the reduced correlation function, its constant of proportionality is unity here and from Equation (18) we now have:

$$\tilde{J}(\omega) = 2\tau_C / (1 + \omega_0^2 \tau_C^2) \quad (22)$$

From the values of the nitrogen quadrupole coupling constants and the nitrogen relaxation times given by Kemp et al. (64), one finds values of the correlation time of  $3 \times 10^{-11}$  sec for both of the two extremes, methyl isocyanide with a symmetrical electric field gradient around nitrogen and methyl cyanide with an asymmetrical electric field gradient around nitrogen. This is clear experimental evidence that spin-lattice relaxation time for a quadrupolar nucleus is a major function of the field gradient since the correlation times for both extremes are the same and the  $T_1$  values differ only because the electric field gradients differ. This value for the correlation time used in conjunction with a value of  $3.5 \times 10^6$  rad sec<sup>-1</sup> for the nitrogen Larmor frequency leads to  $\omega_0 \tau_C \ll 1$  and consequently from (22):



$$\tilde{\gamma}(2\omega_0) = \tilde{\gamma}(\omega_0) = 2\tau_c$$

which is the condition for extreme narrowing (58). This condition has also been given by Kintzinger and Lehn (65) and by Moniz and Gutowsky (66) using slightly different approaches.

For the case of extreme narrowing, Equation (21) now reduces to:

$$1/T_1 = 3/8 (1+a^2/3) [(eQ/h) (\partial^2 V/\partial z^2)]^2 \tau_c \quad (23)$$

Values of the asymmetry parameter,  $a$ , are usually quite small for  $^{14}\text{N}$  so it is justifiable to neglect it, as has been shown by Moniz and Gutowsky (66) and:

$$1/T_1 = 3/8 [(eQ/h) (\partial^2 V/\partial z^2)]^2 \tau_c \quad (24)$$

Comments above regarding the correlation time should be recalled here as well as Equation (20).

Perhaps it is appropriate at this point to mention that Abragam has shown that a derivation of the spin-spin relaxation time,  $T_2$ , for nuclei with  $I = 1$  leads to the same result as given for the spin-lattice relaxation time. Equation (21) and finally Equation (24). This is pointed out because widths of resonance signals at half-maximum amplitude are generally used as a measure of  $T_2$ ; however, for the case of interest here ( $^{14}\text{N}$ ) they also measure  $T_1$ .

Attention is finally turned to the term in brackets in Equation (24),  $(eQ/h) (\partial^2 V/\partial z^2)$ , the quadrupole coupling constant. This term determines the interaction between the fluctuating electric field gradients and the nuclear quadrupole moment. Thus, Equation (24) shows how the



quadrupole coupling constant is related to the spin-lattice relaxation time. As was pointed out by Kemp et al. (64), the electric field gradient is a function of the electronic structure around the nitrogen nucleus and thus is the most important thing to take into account when explaining differences in relaxation times and line shapes. Both Pople (90) and Gordy (67) show that the field gradient is a function of  $1/r_i^3$ , the distance between the  $i$ th electron and the nucleus. Thus, as the distance  $r$  grows larger, there will be less influence on the quadrupolar nucleus and, hence, less influence on the relaxation time. This was shown experimentally by Ogg and Ray (68) who observed no difference in line widths in the  $^{14}\text{N}$  magnetic resonance spectra of tetramethylammonium and trimethylbenzylammonium salts.

The net effect of the field gradient and symmetry in the case of  $^{14}\text{N}$  compounds is to afford another mechanism for spin-lattice relaxation. For an asymmetric electric field around the quadrupolar nucleus, spin-lattice relaxation will be rapid and the quadrupolar nucleus will reside in each of its spin states for too short a time to allow spin-coupling interactions with other nuclei to occur. Thus, an additional result of the rapid spin-lattice relaxation of a quadrupolar nucleus is the loss of spin-spin coupling with other nuclei. For example, in the case of nitrogen

compounds a single, rather broad proton magnetic resonance signal is usually observed for the hydrogen ( $I = 1/2$ ) attached to nitrogen ( $I = 1$ ) in compounds with little or no symmetry around the nitrogen nucleus (8 and 69). On the other hand, for a completely symmetrical electric field around the quadrupolar nucleus, the spin-lattice relaxation time is longer since only magnetic dipolar processes operate. It is then often possible to observe spin-spin coupling not only over one bond, but even over two and three bonds (8, 65, 70-82).

The effects of fast, intermediate, and slow nitrogen relaxation rates on proton magnetic resonance signals have been treated theoretically by Pople (9). A similar treatment has been given by Bacon et al. (83) for the effect of a quadrupolar nucleus of spin  $3/2$  on the spectrum of a nucleus of spin one-half. Theoretical treatments for both these quadrupolar nuclei, and in addition for nuclei of spin  $I = 2, 5/2$ , and  $3$ , have been presented by Suzuki and Kubo (84). In all of these, line shapes of the low spin nuclear resonance ( $I = 1/2$ ) are presented for various relaxation times of the quadrupolar nucleus ( $I > 1/2$ ).

#### Nuclear Relaxation Times of Nitrogen Compounds

A review of some results which have been reported for nitrogen compounds will now be given. Considering

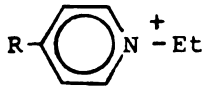
first molecules with symmetrical electrical fields, the quadrupolar nucleus will have a long spin-lattice relaxation time and consequently spin-spin coupling will be observed in the spectrum of the low spin nucleus ( $I = 1/2$ ). This review will be limited to proton ( $I = 1/2$ ) spectra of nitrogen ( $I = 1$ ) compounds since this thesis is concerned with alkyl amines.

A  $^{14}\text{N}$  spin-lattice relaxation time of greater than one second was estimated from the proton spectrum of aqueous tetramethylammonium ion by Grunwald et al. (25). Independently, the same observation of  $^1\text{H}$ - $^{14}\text{N}$  coupling for the tetramethyl- as well as the tetraethylammonium ions was made by Hertz and Spalthoff (70), although they gave no explanation for the conditions of its existence. Shortly thereafter, Anderson et al. (71) and Bullock et al. (72) reported the observation of  $^1\text{H}$ - $^{14}\text{N}$  coupling in the tetraethylammonium ion noting that it was independent of anion and solvent, but dependent on symmetry around nitrogen since the coupling was absent when one of the ethyls was replaced with some other alkyl group or when the quaternary structure was non-existent, as in the free amine. That the coupling was definitely with nitrogen was proved by the heteronuclear double resonance ( $^{14}\text{N}$ -decoupling) experiment of Anderson et al. (71). Neumann and Lehn (74) estimated the  $^{14}\text{N}$  spin-lattice

relaxation time for quaternary ammonium ions to be about 0.2 sec although they later (73) reported a lower limit of 34 milliseconds (msec) for  $^{14}\text{N}$  in aqueous tetraethylammonium bromide. In an interesting study (73) they estimated  $T_1(^{14}\text{N})$  for two symmetrical compounds of the series  $[\text{Et}_3\text{N}^+(\text{CH}_2)_n - \text{N}^+ - \text{Et}_3]2\text{Br}^-$ :

$T_1 (^{14}\text{N})$	n
31 msec	6
29	5

Although they did not estimate  $T_1 (^{14}\text{N})$ , Gassman and Heckert (75) made use of the fact that it is long for quaternary ammonium salts to measure  $^1\text{H}$ - $^{14}\text{N}$  coupling in ten alicyclic alkyl ammonium and seven alicyclic ammonium salts. Another type of quaternary salt having long  $^{14}\text{N}$  relaxation times is the 4-substituted ethylpyridinium salts reported by Biellmann and Callot (78). The  $^{14}\text{N}$  relaxation times estimated are:

$T_1 (^{14}\text{N})$	R	
0.21 sec	-CN	} 
0.22	-CF <sub>3</sub>	

A second class of compounds exhibiting long nitrogen spin-lattice relaxation times is the isonitriles or isocyanides. Kuntz *et al.* (85) estimated  $T_1 (^{14}\text{N}) = 0.3 \text{ sec}$

100

101

102

103

104

105

106

107

108

109

110

111

112

113

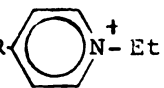
114

from the proton spectra of five compounds using Pople's (9) lineshapes, whereas Kemp et al. (64) report  $T_1 (^{14}\text{N}) = 0.35 \pm 0.1$  sec for  $\text{CH}_3\text{-NC}$  from spin-echo measurements.

Recently Lamberton et al. (86) reported yet another class of compounds for which the electric field gradient around nitrogen is symmetrical enough so that relaxation times are long and  $^1\text{H}\text{-}^{14}\text{N}$  coupling is observed. This class is the dialkylnitramines and the unusual feature is that the nitrogen with the long  $T_1$  is in the nitro group rather than the amino group. This was suggested by the magnitude of the proton-nitrogen coupling constant. It has been confirmed by heteronuclear decoupling (87), the optimum  $^{14}\text{N}$  decoupling frequency being in the chemical shift range of nitro groups rather than amino groups.

The second group of relaxation times includes the intermediate range where the rate of  $^{14}\text{N}$  spin-lattice relaxation is beginning to cause coalescence of the proton spectrum triplet arising from spin-coupling with  $^{14}\text{N}$ . For this intermediate range of relaxation times, from values of  $T_1$  where the components of the triplet are beginning to broaden to values where they are coalescing, the electric field gradient is much less symmetrical provided the correlation times are all about the same, as they should be for fluid liquids. The first report of a  $^{14}\text{N}$  relaxation time for

this category was by Grunwald et al. (25) who estimated  $T_1 = 20$  msec for aqueous methylammonium chloride. For dry liquid ammonia Pople (9) estimated  $^{14}\text{N } T_1 = 22.2$  msec from the line widths but noted that this might be slightly high. Indeed, Anderson and Baldeschwieler (88) report a value of 15.9 msec and the data reported by Swift et al. (13) essentially agree with this. Lehn and Neumann (73) show the spectra of several compounds in a homologous series and specifically the tetramethylene one,  $\text{Et}_3\text{N}^+(\text{CH}_2)_4\text{N}^+\text{Et}_3 2 \text{Br}^-$ , exhibits the characteristic lineshape for this category. They estimate a  $T_1$  value of 23 msec. Similarly Biellmann and Callot (78) estimate the following relaxation times for those 4-substituted ethylpyridinium ions which come in this intermediate range of  $T_1$  values:

$T_1$ ( $^{14}\text{N}$ )	R
.15 sec	-COOEt
.09	-CONH <sub>2</sub> } R- 
.08	-COOH

Moniz and Gutowsky (66) made an extensive study of  $^{14}\text{N}$ -spin-lattice relaxation by  $^{14}\text{N}$  spin-echo experiments, listing  $T_1$  values for some twenty-five liquid compounds. Although they obviously did not observe the proton spectra, and hence could not comment on proton line shapes, we can see from the  $T_1$  values listed below that some of their compounds

would fall into this intermediate category:

$T_1(^{14}\text{N})$	Compound
45.0 msec	$\text{C}_2\text{H}_5\text{-ONO}_2$
22.0	$\text{CH}_3\text{NO}_2$
15.8	$\text{C}_2\text{H}_5\text{NO}_2$
10.8	iso- $\text{C}_3\text{H}_7\text{NO}_2$
10.5	$\text{C}_3\text{H}_7\text{NO}_2$

The last group of  $^{14}\text{N}$  spin-lattice relaxation times includes those compounds for which the  $^1\text{H}\text{-}^{14}\text{N}$  multiplet collapses so that no  $^{14}\text{N}$  coupling is seen in the proton spectrum, but only broadening of the lines. This is the result of a highly asymmetrical electric field gradient at the  $^{14}\text{N}$  nucleus. From the NH line shapes, Grunwald and Price (29) estimated a  $T_1(^{14}\text{N})$  value of 2.5 msec for methylammonium acetate in glacial acetic acid, (with probable error  $\pm 25\%$ ). They estimated that the  $T_1$  value for methylammonium chloride in the same solvent was concentration dependent and for  $0.39 \text{ M} < \text{conc.} < 1.2 \text{ M}$  the range is  $4.35 \text{ msec} > T_1(^{14}\text{N}) > 2.78 \text{ msec}$  with a smaller error of  $\pm 10\%$ . For the same solvent, glacial acetic acid, they reported (23) the following values of  $T_1$ , noting that due to ion-pairing some are very concentration dependent:

$T_1$ ( $^{14}\text{N}$ )	Compound	Conditions	Conc. Dependence
9.5 msec	$\text{NH}_4\text{OAc}$	0.11 M < conc. < 0.74	indep.
1.1 ( $\pm 30\%$ )	$\text{Me}_3\text{NHC1}$	0.6 < conc. < 6 M	dep.
1.5	$\text{Me}_3\text{NHOAc}$	(estimated from the chloride)	-
0.14	$(\text{HOCH}_2)_3\text{CNH}_3\text{OAc}$	0.9 M	-

It should be noted that these values are estimated from the line shapes and that there may be sizable errors. Similarly, Ralph and Grunwald (41) reported an estimated value of 2.5 msec for triethylammonium chloride in water. For the remaining compounds in the series,  $\text{Et}_3\text{N}^+(\text{CH}_2)_n\text{NEt}_3^+$  Lehn and Neumann (73) report values of 12 ( $n = 3$ ) and 4.5 ( $n = 2$ ) msec. Similarly for the 4-substituted quaternary ethylpyridinium salts, Biellmann and Callot (78) estimated values of  $T_1$  ( $^{14}\text{N}$ ) ranging from 50 msec to < 10 msec. In view of other reported estimates and measurements of relaxation times for compounds with asymmetric field gradients, these values seem a little long. Indeed, Kawazoe *et al.* (79) estimate from proton line shapes that  $T_1 < 20$  msec for a number of quaternary alkylammonium salts. Kintzinger and Lehn (65) estimated  $T_1$  values of the same order of magnitude, 0.18 msec <  $T_1$  < 4.55 msec, from the  $^{14}\text{N}$  line widths of five heterocyclic compounds. Finally, for all the remaining compounds

reported by Moniz and Gutowsky (66) the values of  $T_1$  range from 0.8 msec to 5.8 msec, these being obtained from  $^{14}\text{N}$  spin-echo measurements. In addition to these, values of  $4.9 \pm 0.8$  msec for acetonitrile (64, 89 and 90) and  $1.24 \pm 0.07$  msec for 2-fluoropyridine (89 and 90) have been reported.

The various values can now be summarized. When  $^{14}\text{N}$  is in a symmetrical electric field, the  $^{14}\text{N}$  spin-lattice relaxation values range from 0.5 sec down to 0.2 sec, Grunwald's estimate (25) that  $T_1$  should be longer than a second being much too long. When  $^{14}\text{N}$  is in an asymmetric electric field the range is 12 msec to 0.2 msec and values for electric fields intermediate between these two extremes run from 90 msec down to about 15 or 10 msec. Implicit in all these speculations about the field gradients and relaxation times is the assumption that the correlation times are of the same order of magnitude throughout.

#### Viscosity and Temperature Effects on $T_1$ of Quadrupolar Nuclei

We shall now consider the factors influencing the correlation time and the effect of its variation on the nuclear relaxation times. As Equation (20) shows, the correlation time is directly proportional to the viscosity of the sample system and inversely proportional to the temperature. Thus, there are two possibilities; first, for isothermal



conditions increasing the viscosity raises the correlation time and according to Equation (24) this results in a faster relaxation rate and thus a shorter relaxation time. A plot of

$$1/T_1 \text{ vs. } \eta \quad (\text{Form I})$$

should yield a straight line with a positive slope of  $3/8[(eQ/h)(\partial^2 V/\partial z^2)]^2 C/T$ . A treatment of this type we shall call Form I. The second possibility is to increase the temperature holding viscosity constant which would lower the relaxation time since the correlation time, Equation (20), is inversely proportional to temperature. However, increasing temperature also lowers the viscosity which lowers the correlation time and, therefore, both will operate in conjunction. According to Equation (24), a lower correlation time means a slower relaxation rate and thus a longer relaxation time. A plot of

$$1/T_1 \text{ vs } \eta/T \quad (\text{Form II})$$

also yields a straight line with a positive slope of  $3/8[(eQ/h)(\partial^2 V/\partial z^2)]^2 C$ . This type of treatment we shall call Form II.

Evans and Richards (62) reported one of the first studies of the behavior of nitrogen relaxation times with viscosity, following Form I. They used the  $^{14}\text{N}$  magnetic resonance line widths as a measure of relaxation rates

and, indeed, the plots of these values versus solution viscosities yield the predicted straight lines. From the slopes, using an average value for the quadrupole coupling constant from microwave data, they were able to obtain values for C for three alkylcyanides. These agree very well with the calculated ones. In a study of the  $^{115}\text{In}$  resonance in indium perchlorate and sulfate solutions Cannon and Richards (91) showed that, despite the larger quadrupole moments, these still follow Form I.

Grunwald and Price showed that there was a viscosity effect of Form I on the  $^{14}\text{N}$  relaxation time for methylammonium chloride (29), ammonium acetate, trimethylammonium acetate, and trimethylammonium chloride (23) in glacial acetic acid. Recently, Kintzinger and Lehn (65), in a qualitative fashion, reported data following both Forms I and II for the nitrogen and hydrogen NMR spectra of five heterocyclic compounds.

Studying compounds of other quadrupolar nuclei, Massey et al. (81) report qualitatively effects of Form I for quaternary alkyl salts of  $^{75}\text{As}$  and  $^{121}\text{Sb}$ . They caution that solution viscosity should not be the only criterion of relaxation rate when considering electrolytes in a series of solvents, but that solute-solvent and ion-pairing are also very important because they may induce changes in the

electric field gradient about the quadrupolar nucleus (82).

Arnold and Packer (92) studied relaxation times as a function of viscosity for the hexafluoroarsenate salts of potassium and a few other cations.  $^{75}\text{As}$  relaxation times were obtained from changes in the  $^{19}\text{F}$  resonance line shapes, plots of Form I were linear for various solvents and concentrations. Although the results were not conclusive, they supported the contribution of ion-ion interactions in the relaxation process. In a more recent study (93) of solutions of potassium, silver, and tetra-n-butyl-hexafluoroarsenate salts in acetonitrile and acetone, a treatment of Form II was made. They found that the relaxation process was due to changes in the electric field gradient and was short ranged being a function of the cation. They noted that the plots, although linear, did not follow the predictions of Form II, since they intercepted the y-axis above the origin. They suggested that the slope is concentration dependent at lower concentrations, but did not speculate as to the cause.

Arnold and Packer (63) have looked into the basic assumption which so many have accepted, namely, that viscosity affects the correlation time and thereby the relaxation rate. Since most of their previous work dealt with aqueous electrolyte solutions, quite naturally these were

the focus of their attention. Deviations from the correlation time-viscosity proportionality had been noted by others and Arnold and Packer concluded that such deviations were found when ions have a marked effect on the "structural equilibrium" of the water. They conclude that the relationship holds, i.e. is linear as in Form I and Form II, when the viscosity reflects changes in the local mobility or diffusion of the relaxing nucleus.

Turning now to another series of studies, we shall consider those which deal with the temperature effect on the quadrupolar nuclear spin-lattice relaxation time or the effect this will have on the line shape of the resonance for the spin  $1/2$  nucleus, which is more easily observable. The first report of work along these lines was by Roberts (8), who pointed out that the broadening of a sharp proton singlet or the appearance of a triplet from a broad peak observed on increasing temperature in the case of ten nitrogen compounds was caused by an increase of  $^{14}\text{N}$  spin-lattice relaxation time with temperature. He emphasized that this was unlike the temperature effect on exchange, since increasing temperature then causes increased exchange rates which first collapse a triplet to a broad singlet and finally lead to narrowing of the single line. Since then, a number of others have observed this

temperature effect on nitrogen-containing compounds so that the connection is well established now. Anderson et al. (71) noted the effect of a 70° temperature change on  $(C_2H_5)_3N-(CH_2S\ CH_3)^+ I^-$  in water. At the high temperature, relaxation is sufficiently slow so that triplet structure arising from coupling between  $^{14}N$  and the  $CH_3$  protons of the ethyl groups is observed. Similarly, Lehn and Neumann (73) reported  $^{14}N$  triplet fine structure for the  $CH_3$  protons of the ethyl group of  $(C_2H_5)_3N-(CH_2)_4-N-(C_2H_5)_3^{+2} 2 Br^-$  about 60° above ambient temperature. The data on liquid ammonia presented by Swift et al. (13) clearly shows that the  $^{14}N$  relaxation time increases with increasing temperature. For a 65° increase in temperature, Biellmann and Callot (78) show that  $^{14}N$  triplet coupling of the  $CH_3$  for the ethyl becomes observable for N-ethylpyridinium ion and becomes much better resolved for N-ethyl-4-trifluoromethylpyridinium ion. Along these same lines, Kawazoe et al. (79) presented spectra showing more pronounced  $^{14}N$ -methyl proton coupling for tetraethylammonium bromide in chloroform and for cis-2,6,N,N-tetramethylpiperidinium iodide in water for a 60° temperature increase. Kintzinger and Lehn (65) studied the temperature induced change in the proton spectra of the hydrogen α to the nitrogen in five heterocyclic compounds observing only broadening of the



line, but noting that this followed the usual relaxation-time-temperature relationship. The nitramines of Stanton et al. (86) also follow this relationship. They noted that the  $\text{CH}_3$  signal of dimethylnitramine in tetramethane is a sharp singlet at  $-20^\circ$  and a sharp triplet at  $-100^\circ$ . In summary, an increase of spin-lattice relaxation time with increasing temperature has been observed for a variety of compounds but is limited to those which are in an asymmetric electrical environment (71).

It is important to point out that the spin-lattice relaxation time-temperature relationship is not limited to quadrupolar nuclei. It is general for all quadrupolar nuclei. To cite a few examples, it has been observed for  $^2\text{D}$  in  $\text{D}_2\text{O}$  solutions in acetone- $\text{d}_6$  and benzene- $\text{d}_6$  (95); for  $^{11}\text{B}$  in liquid boron trifluoride (83) and dimethoxy- $\text{d}_6$ -borane,  $(\text{CD}_3\text{O})_2\text{BH}$  (83); for  $^{35}\text{Cl}$  in perchloryl fluoride (83) and in chloroform (97); and for  $^{75}\text{As}$  in potassium hexafluoroarsenate (97).

For the quadrupolar nuclei studied so far, increasing temperature always causes slower relaxation rates or longer relaxation times.

The theory of the temperature effect will now be considered. From the basic Equation, (24), the relaxation time is a function of two variables, namely, the quadrupole coupling constant and the correlation time. The

lation time is inversely proportional to the temperature and directly proportional to the viscosity. Since increasing temperature lowers the viscosity this will also tend to decrease the correlation time. The question is whether the correlation time is the only thing affected by temperature change or whether the quadrupole coupling constant is also temperature dependent. Turning microwave and pure quadrupole resonance (NQR) spectroscopy by means of which one can measure the quadrupole coupling constant directly, the situation is not clarified. Microwave data, obtained from studies of gases at low pressures, give no support to temperature dependence, whereas NQR data, obtained from studies on crystalline solids, indicates there is a measurable temperature dependence of quadrupole coupling constant (98 and 99). The difference in the two may perhaps be due to the fact that microwave results refer to a single molecule, the field gradient being related to molecular axes, whereas NQR data refer to the entire crystal, the field gradient tensor being related to crystal axes. A change of quadrupole coupling with temperature in the latter case may represent solid-state effects. Thus, the question in the case of NQR studies of liquids and solutions is still unanswered. Results presented so far seem to indicate that

there is indeed a definite temperature effect on the quadrupole coupling constant for species in solution (63, 93, and 100).

### Activation Energies for the Relaxation Process

For any thermally dependent process it is possible to obtain an activation energy so one may assume, as did Moniz and Gutowsky (66), that the correlation time is described by an Arrhenius-type equation:

$$\tau_c = \tau_c^0 \exp (E_a/RT) \quad (25)$$

Combining this with Equation (24), taking logarithms of both sides and changing signs, one obtains:

$$\log T_1 = -(E_a/2.303 RT) - \log (3/8 (e^2 q Q / \hbar)^2 \tau_c^0) \quad (26)$$

A plot of  $\log T_1$  vs.  $1/T$  should be a straight line of slope  $-E_a/2.303 R$ . The assumption is that only the correlation time is temperature dependent and that it follows the Arrhenius equation. However, even if the nitrogen quadrupole coupling constant,  $Q_N$ , is also temperature dependent, one still obtains a straight line for a plot of  $\log T_1$  vs.  $1/T$  because it can be shown that:

$$\log T_1 = -(2E_a(Q) + E_a(C))/2.303 RT - \log(3/8(Q_N^0)^2 \tau_c^0) \quad (27)$$

When, in addition to (25), the quadrupole coupling is also considered to be temperature dependent according to the relationship:



$$(e^2 q Q / h) = Q_N = Q_N^0 \exp(E_a(Q) / RT). \quad (28)$$

The only differences between Equations (26) and (27) are that, first, the activation energy obtained from the slope is the sum of the activation energies for quadrupole coupling,  $E_a(Q)$ , and for correlation,  $E_a(C)$ , for the latter, whereas for the former it is simply the activation energy for the correlation process. The second difference between the two equations will be in the interpretation of the value obtained for the high temperature intercept. Thus, implicit in the assumption of Moniz and Gutowsky is the assumption that,  $E_a(C) \gg E_a(Q)$  which results in,  $E_a = E_a(C)$  and  $Q_N = Q_N^0$ . Nevertheless, it is possible to obtain a value for the activation energy of the relaxation process.

Based on the assumption outlined above, Moniz and Gutowsky (66) obtained activation energies for nine nitrogen compounds. The values range from 1.4 to 3.2 kcal/mole and both these and the differences among them were generally compatible with predictions based on the relative sizes and shapes of the molecules. Hertz and Zeidler (94), from spin-echo studies of deuterium compounds, obtained an activation energy of 3.5 kcal/mole for pure  $D_2O$  and a range from 3.7 to 5.6 kcal/mole for the solvent  $D_2O$  in six electrolyte solutions. Values of  $1.7 \pm 0.2$  kcal/mole for

$\text{CD}_3\text{COCD}_3$  and  $1.5 \pm 0.2$  kcal/mole for  $\text{C}_6\text{D}_6$  were reported by Bonera and Rigamonti (95), who obtained the deuterium  $T_1$  from the signal height after adiabatic rapid passage. Bacon et al., (83) report a  $^{35}\text{Cl}$  activation energy of 1.0 kcal/mole for perchloryl fluoride and 1.4 cal/mole for  $^{11}\text{B}$  in boron trifluoride. Also, for  $^{11}\text{B}$ , the value  $1.2 \pm 0.1$  kcal/mole has been reported by Boden et al. (96) for dimethoxy ( $d_6$ )-borane,  $(\text{CD}_3\text{O-})_2\text{BH}$ . Finally, Arnold and Packer (93) found a range of activation energies for  $^{75}\text{As}$  from 2.09 to 4.10 kcal/mole in potassium hexafluoroarsenate at five different concentrations in diethyleneglycol-dimethyl ether (diglyme). These reported values give some idea of the magnitude of the activation energy for the relaxation process regardless of the exact mechanism, which is not known at present.

### Solvent Effects

The last topic for consideration is the effect of variation of solvent on the spin-lattice relaxation of a quadrupolar nucleus. It may be again pointed out that changing solvent, and thus varying the viscosity, causes a change in  $\tau$  and, according to Equation (24), a change in the relaxation rate.

For a pure covalent compound, the major effect of

solvent is to change the correlation time and the relaxation rate as described before. The electric field gradient, being short ranged, is largely unaffected because it is intramolecular in origin. Examples of this type of behavior have been given by Kintzinger and Lehn (65) for nitrogen heterocycles in various aprotic solvents. For these solvents, the chief effect is to change viscosity and hence the correlation time. A similar situation is found for low concentrations of electrolytes in solvents of high dielectric constant, where solvation and ionization are complete. The only change is in viscosity, from solvent variation or from small concentration changes in a given solvent. Examples of this type have been given by Randall and colleagues (80, 81, and 82) for quaternary methyl and/or ethyl halides of boron, aluminum, nitrogen, arsenic and antimony in water ( $\epsilon = 80.4$  at  $20^\circ$ ); also by Kawazoe (79) for tetraethylammonium bromide in water, dimethylsulfoxide ( $\epsilon = 48.9$  at  $20^\circ$ ), and methanol ( $\epsilon = 32.4$  at  $20^\circ$ ). Similar behavior was observed for  $^{87}\text{Rb}$  for concentrations of  $\text{RbI}$  below  $10^{-2}$  M in dimethylsulfoxide (DMSO) by Crawford and Gasser (101). The set of conditions where only viscosity effects operate to change the correlation time, and hence the quadrupole relaxation rate, will be called Case I.

The warning of Massey, Randall and Shaw (81) is again emphasized here: solution viscosity should not be

the only criterion for relaxation rate variation. A detailed examination of the conditions, other than viscosity, which lead to solvent effects on the relaxation rate will now be made and will be designated in Case II.

The quadrupole coupling constant should be considered as another possible source of variation (Equation 24) which can be affected by changing solvents since the electric field gradient,  $(\partial^2 V / \partial z^2)$ , is dependent on the surrounding structure and hence has a very marked effect on the relaxation rate. This was pointed out earlier for those cases where the electric fields were intramolecular in origin. Now electric fields induced by the solvent are examined.

Consider an electrolyte, an ionic compound, in a solvent of low dielectric constant. Here there can be little doubt about the microstructure. The low dielectric constant of the solvent will not favor ionization, therefore the electrolyte will be present as ion pairs or higher aggregates and, as a result of the close proximity of the ions there will be a definite interaction.

Now consider an electrolyte, one of the ions of which contains a quadrupolar nucleus, in a solvent of high dielectric constant. The ions will be completely solvated and separated and the ion of the quadrupolar

nucleus, for the sake of simplicity chosen monatomic, e.g.  $^{79}\text{Br}^-$ , will be in a symmetric electrical environment, nuclear relaxation will be slow and a narrow resonance line will be observed. At extremely high concentrations in a solvent of high dielectric constant, or near saturation in a solvent of low dielectric constant, there will be significant ion-ion interaction such as ion pairing. As a result of the ion pairing, the gegen ion will set up an electric field near the quadrupolar nucleus. In the example of the  $^{79}\text{Br}^-$  ion the electric field caused by its gegen ion will be asymmetrical and faster relaxation with a wider resonance line will be the result.

The appearance or disappearance of spin coupling (from coupling with the quadrupolar nucleus) in the proton spectrum provides a method of determining whether or not ion pairing is important. Kawazoe and workers (79) investigated the solvent effect on quaternary ammonium halides. They noted that chloroform ( $\epsilon = 4.8$  at  $20^\circ$ ) caused a broadening or collapse of the  $^{14}\text{N}$  coupling for tetraethylammonium, 2,N,N-trimethylpiperidinium and cis-2,6,N,N-tetramethylpiperidinium halides compared to aqueous solutions. They pointed out, that there was little observable effect on changing the various halide gegen ions. Randall and co-workers, on the contrary, reported that there was no

solvent effect on tetramethyl- and tetraethylammonium halides (80 and 82) whereas there was a very definite effect on the tetramethyl- and tetraethylarsonium and antimonium halides (80, 81, and 82). This solvent effect, in which multiplet-structure is lost in solvents of low dielectric constant, they attributed to ion pairing. In addition to these, Crawford and Gasser (101) noted considerable broadening of the  $^{87}\text{Rb}$  resonance line with increased concentration of  $\text{RbI}$  in  $\text{DMSO}$  which they attributed to ion-pairing. Their conductivity measurements indicate that above  $10^{-2}$  M the salt exists as ion pairs in  $\text{DMSO}$ .

Next, consider the more complex situation in which some type of chemical reaction between solute and solvent occurs. The obvious case is the one we are most concerned about, namely, the protonation of the nitrogen lone pair electrons. Although they did not appreciate the complexity of the situation, Tiers and Bovey (69) were the first to report this type of effect. The emphasis of their paper was on the collapse of  $^1\text{H}$ - $^{14}\text{N}$  coupling owing to an asymmetric field at nitrogen caused by the molecular structure; however, the solvent they chose was trifluoroacetic acid. Obviously all the amines and amides were protonated to form the trifluoroacetate salts, but since the dielectric constant



( $\epsilon = 39.5$  at  $20^\circ$ ) is rather low ion pairing could be appreciable. As a result, the electric field at nitrogen could have been more or less symmetrical than they assumed but certainly was quite different. Along these same lines, Grunwald and Price (23 and 29) reported a very definite effect of anion on the NH line shape, and hence on  $^{14}\text{N}$  relaxation times, for monomethyl- and trimethyl-ammonium salts in glacial acetic acid ( $\epsilon = 6.22$  at  $25^\circ$ ). From freezing point data, they knew that the salts existed as ion pairs and from the change in NH line shape compared to aqueous solutions they reasoned that the close proximity of the anion caused a strong electric field gradient at the nitrogen. Similarly, Cocivera (31) reported the collapse of  $^1\text{H}$ - $^{14}\text{N}$  coupling and change in line shapes for salts of the same amines in t-butyl alcohol ( $\epsilon = 12.47$  at  $25^\circ$ ). This he explained as being caused by the anion being in intimate contact with the ammonium ion so that a strong electric field is created at the nitrogen nucleus causing rapid  $^{14}\text{N}$  relaxation. Another case in which the reaction of solute and solvent is quite clearcut is that of solutions of nitrogen heterocycles in sulfuric acid. Kintzinger and Lehn (65) pointed out that the protonation of nitrogen in any compound tends to make the electric field around nitrogen more symmetric. This will be true in any solvent



where protonation can occur; however, if the protic solvent has a low dielectric constant ion-pairing will occur, as was described for glacial acetic acid solution, and the gegen ion will again produce an asymmetric electric field at nitrogen. As was described in detail in Section IIA, an additional complicating feature of the particular solvents glacial acetic acid and t-butanol is that they are weak acids and so rapid proton exchange between the nitrogen and solvent occurs. These two complications are eliminated by using sulfuric acid since it is a strong acid and proton exchange between it and the nitrogen is very slow; also, since it has a very large dielectric constant ( $\epsilon = 100.0$  at  $25^\circ$ ) the electrolytes will be fully dissociated.

Finally, we come to the most complicated situation, one which is a composite of all the features previously discussed. The solute is a salt and ion-ion or ion-solvent interactions may occur. The ion-solvent interaction may be an induced field gradient near the ion from solvent dipoles, or unsymmetrical solvent co-ordination. This ion-solvent interaction is quite different from the exchange phenomena discussed already. This last case, then, is complicated because it is not clear in which manner the quadrupole coupling constant and the correlation time are

being affected.

So far we have always considered the correlation time to be a function of only the viscosity and temperature as given by Equation (20) and nothing has been said about the constant term  $C$ . This term may contain such things as the radius of the solute molecule, Boltzmann's constant, average distance apart between solute (or ion) and solvent, moments of inertia and masses of ion and various functions of these parameters. The manner in which the non-constant parameters in these expressions change is uncertain. All of these possible complications were discussed by Arnold and Packer (63) who concluded they were small and under certain conditions unimportant.

In their study of  $^{75}\text{As}$  relaxation in hexafluoroarsenate salts in various solvents, Arnold and Packer (92) concluded that ion-ion interaction was the major cause of variation in  $^{75}\text{As}$  relaxation time although their data on solvation studies did not completely rule out the possibility of hexafluoroarsenate-solvent interaction. In their second paper on hexafluoroarsenates (93), they again concluded that the cation has a much larger effect on the  $^{75}\text{As}$  relaxation rate than does coordination with solvent molecules.

For the solvent water it is probably better to consider a covalent solute first. Here again, we review the results

of Kintzinger and Lehn (65) who report the effect of dissolution in water on the  $^{14}\text{N}$  relaxation times for heterocyclic compounds. The obvious interaction is hydrogen bonding which has two opposite effects. It is similar to protonation, but weaker, so it leads to a more symmetric field gradient and to longer relaxation times. However, the re-orientation rates are slower in water than for the neat liquids so the correlation times are longer and relaxation times shorter. The second effect dominates since viscosities of the water solutions are greater than those of the neat liquids and the  $^{14}\text{N}$ -resonance line widths are therefore greater (quadrupolar line widths are proportional to reciprocal of the relaxation time). In addition to these results of Kintzinger and Lehn (65), several other references could be cited which show that either hydrogen bonding alone, or complete protonation, produces more symmetric field gradients which sharpen the lines (longer  $^{14}\text{N}$  relaxation time) relative to the neat liquids, although each component of the multiplet may still be somewhat broadened from other causes. Discounting proton exchange (cf. Section IIA) as a source of this residual broadening, i.e. working at low pH values, it seems likely that viscosity effects are responsible. For example, the proton spectra of pure liquid ammonia (13), or even wet ammonia (12),

have components which are much broader than the ammonium ion resonance (19). The  $^{14}\text{N}$  resonance spectra of Ogg and Ray (68) also show that the ammonium ion has sharper components (longer relaxation time) than pure liquid ammonia. There has been no comment on the origin of the component broadening of aqueous ammonium ion lines at low pH. This residual broadening could be a result of viscosity changing the reorientation rates, hence shortening the relaxation time and thereby causing a slight broadening of the individual components.

Having mentioned the ammonium ion, the discussion has shifted to electrolytes in aqueous media; consequently, let us now pursue this in more detail. A relatively recent review of magnetic resonance studies of aqueous electrolyte solutions has been published by Hertz (102). He covers mainly chemical shift changes for  $^1\text{H}$  and  $^{17}\text{O}$  resonances of the solvent water itself caused by various electrolytes but also treats the relaxation time measurements of these same nuclei for the study of reorientation and residence times of the water molecule at the ion. A review of the results from studies of the chemical shifts and relaxation times of the ions themselves is also given. Later, Hertz and Zeidler (94) reported the results of relaxation studies, by the spin-echo method, on the solvent water and on certain

solutes such as alkyl compounds and quaternary ammonium salts. They interpret the data as showing that molecules with small alkyl groups reorient relatively rapidly. The question of the effect of the dissolved species on the structure of the solvent was also considered. In a similar manner Eisenstadt and Friedman (103) obtained  $^{23}\text{Na}$  relaxation times from spin-echo studies and report values for salts of a variety of anions in water, interpreting the results as due either to ion-ion interaction or to the effect of the ions on the structure of water.

The studies of spin-lattice relaxation times of water and/or dissolved particles inevitably leads to the question of the structure of liquid water. For this reason, Hertz (104) gave a rather thorough review of the various physical measurements on aqueous solutions of alkyl compounds. The properties measured included viscosity, electrical conductivity, sonic absorption, nuclear resonance chemical shift, thermal conductivity, diamagnetic susceptibility, dielectric and nuclear magnetic relaxation. His aim was to define the phrases "structure making," "iceberg formation," and "structure-promoter" given by various authors to interpret the anomalous data from the various measurements. There is much confusion and contradiction as to the effect of the same salts on water structure as observed by different

techniques. Since the various techniques sense quite different ion-ion, salt-water, or water-water interactions it is understandable that each reports anomalies for different salts or different conditions and thus that the interpretations of salt-water interaction or water structure based on various experiments is often different and sometimes in contradiction.

The earlier review by Frank and Wen (105) of ion-solvent interactions and the structure of water is of interest. In their discussion of dielectric relaxation data, tetraethylammonium chloride and triethylammonium chloride along with ethylamine are considered structure makers whereas ethylammonium- and n-propylammonium chloride are less so and tetramethylammonium is in the transition region between structure-makers and breakers. The relevance of this to the topic of spin-lattice relaxation is simply that water structure promotion would decrease the molecular reorientation rate or lengthen the correlation time and it will be recalled that this is related to the spin-lattice relaxation rate, Equation (24).

In general, long-chain alkyl groups tend to increase the structure of water (104 and 105). As can be seen for the tetra-n-alkylammonium halides, apparently the only amines which have been studied to any great extent, anomalies are

observed for compounds with shorter alkyl chains. Bunzl (106), using near infrared measurements at various temperatures, indicates that the tetrabutyl- and tetrapropylammonium bromides are structure-makers while tetramethylammonium ion is a structure-breaker and tetraethylammonium ion is in the transition region between the two. From the lengthy discussion in the above paper, it can be seen that the question of salt interaction with water structure has not been resolved and continues to be an active area of research.

#### C. Nitrogen Chemical Shifts

Although nitrogen -14 was the nucleus which lead to one of the first discoveries of the dependence of resonance frequency on chemical structure (i.e. "chemical shift") (107 and 108), it has received relatively little attention in the past eighteen years due to the greater interest in other nuclei particularly protons, but also fluorine -19, carbon-13, and phosphorus-31, etc. Nevertheless, the utilization of  $^{14}\text{N}$ -magnetic resonance data is still an active area of investigation as shown by several recent publications (65 and 109-115).

The  $^{14}\text{N}$  chemical shifts of quaternary amines, the compounds we are specifically concerned with, show a discrepancy in the values reported as indicated in Table 1.

Table 1. Reported nitrogen chemical shifts (ppm).

Compound	Abbr.	Ref.116	Ref.117	Ref.118	Ref.119
$\text{NH}_4^+$	4H	0	0	$0 \pm 1$	0
$\text{CH}_3\text{NH}_3^+$	1Me3H		-9*	$-11 \pm 3^*$	-11
$(\text{CH}_3)_2\text{NH}_2^+$	2Me2H		-17*	$-17 \pm 5^*$	
$(\text{CH}_3)_3\text{NH}^+$	3Me1H		-2*	$-3 \pm 1^*$	
$(\text{CH}_3)_4\text{N}^+$	4Me	-50	-20	$-21 \pm 2$	
$(\text{CH}_3\text{CH}_2)_4\text{N}^+$	4Et			$-41 \pm 2$	

\*Obtained from the spectra of Ogg and Ray (68).

For the methyl series, the shift to lower field follows the order  $4\text{Me} > 2\text{Me2H} > 1\text{Me2H} > 3\text{Me1H} > 4\text{H}$  which seems unusual since it would be reasonable to expect increasing alkyl substitution to have an additive effect on the  $^{14}\text{N}$  shift. Details of the concept of substituent additivity effects on chemical shifts have been presented by Maslov (120). From the work of Schmidt et al. (117), Evans and Richards (118), and Bose et al. (119), one learns that these workers often did not observe the shift values they reported, but rather obtained them from the earlier published spectra of Ogg and Ray (68). Indeed, in reviewing the work of Ogg and Ray (68), one sees that only the spectra are presented; neither a listing of the chemical shift values are given,

nor are details as to how the spectra were calibrated given since the main point of their paper was to establish the  $^{14}\text{N}$  line shapes and the effects of quadrupolar relaxation. (Section IIB).

A review of some of the theories of chemical shifts in general will now be presented, after which nitrogen chemical shifts are treated specifically.

Magnetic coupling of the surrounding electrons to the observed nucleus arises from magnetic fields originating from the motion of the electrical charges. The fields at the nucleus caused by orbital motion of the surrounding electrons act either in conjunction with, or opposed to, the applied magnetic field  $H_0$ . Thus, the nucleus in a molecule will resonate at an applied field different from the resonance field necessary for a bare nucleus. Furthermore, as the field at the nucleus is a function of the electronic structure about it, there will be a shift in applied field with a change in chemical structure. This may conveniently be expressed as:

$$\omega = \gamma(H_0 - \sigma H_0) = \gamma H_0(1 - \sigma) \quad (29)$$

where  $\omega$  is the resonance frequency,  $\gamma$  is the gyromagnetic ratio, and  $\sigma$  is a parameter describing the shift in resonance with respect to the bare nucleus, i.e. the chemical shielding parameter (121). The shielding term may be broken up into

the sum of three other terms (122):

$$\sigma = \sigma_D + \sigma_p + \sigma_A \quad (30)$$

$\sigma_D$  is a diamagnetic effect from electrons in s-states, given by (121):

$$\sigma_D = (q^2/3mc^2) \overline{(1/r)} \quad (31)$$

where  $q$  is the charge of the electron,  $m$  its mass, and  $r$  is the distance from the electron to the nucleus.

$\sigma_p$  is a paramagnetic effect resulting from "unquenching" of p-states, given by (121):

$$\sigma_p = -(2/3\Delta E) (\hbar q/mc)^2 \overline{(1/r^3)} \quad (32)$$

where  $\Delta E$  is the mean excitation energy and the other terms are as defined above.  $\sigma_A$  includes long-range effects from other electrons in the molecule.  $\sigma_A$  is very difficult to evaluate since it depends on the orientation of the group producing the effect relative to the observed nucleus and the resultant contribution is often very small.

The diamagnetic term acts contrary to the applied field, causes shifts to higher field, and as Slichter (121) has pointed out, its range is small being only  $\sim 10$  ppm for the  $F_2$  molecule, whereas  $\sigma_p$  is two orders of magnitude larger for the same molecule. Since the diamagnetic shift is caused by  $\sigma$  bonds, it should be of little importance for nitrogen compounds since these bonds have considerable p character. The  $\sigma_p$  term generally makes

the largest contribution to the shielding in nuclei other than protons, both because its effects are two orders of magnitude larger than  $\sigma_D$  and because, in the case of nitrogen, bonds involving  $\pi$  electrons are important. It is difficult to obtain good wave functions for the molecules and difficult to evaluate the mean excitation energy,  $\Delta E$ , which is also necessary for the theoretical calculation. For these reasons,  $^{14}\text{N}$  chemical shifts have so far been calculated for only a few compounds. Lambert and Roberts (123) have calculated the diamagnetic contribution for seven nitrogen compounds and have shown that it accounts for only about 1/7 of the observed  $^{15}\text{N}$  chemical shifts. Kent and Wagner (124), on the other hand, considering only the paramagnetic contributions, have gotten quite good agreement between their calculated and experimental  $^{14}\text{N}$  chemical shifts for twelve linear triatomic molecules and ions.

In order to circumvent the difficulties in choosing a value for the mean excitation energy and calculating the paramagnetic shielding, Witanowski et al., have used  $\pi$ -bond orders and charge densities to explain  $^{14}\text{N}$  chemical shifts for m- and p-dinitrobenzene (113) and for nitriles and isonitriles (114). This approach is typical because, rather than face all the difficulties encountered in making a full calculation of the  $^{14}\text{N}$  shifts, the observed values

are usually rationalized in semi-quantitative or qualitative terms.

There are a few useful qualitative correlations, mostly stemming from the early work of Holder and Klein (116), of the observed  $^{14}\text{N}$  chemical shifts. (a) Since  $\text{NH}_3$  resonates at high field,  $\text{NO}_3^-$  and  $\text{NO}_2^-$  at lowest field, and various carbon-nitrogen compounds in between, they suggested that the electronegativity of the neighboring atoms or group plays a major role in the chemical shift value. Thus, the more electronegative the substituents attached to nitrogen, the greater will be the deshielding of nitrogen and the result will be a paramagnetic or low-field shift. Conversely, electropositive atoms or groups cause nitrogen to be shielded with upfield shifts resulting. (b) Their second general observation is that since  $\text{NH}_4^+$  has a more ionic bond and resonates at high field whereas the more covalent  $\text{NO}_3^-$  resonates at low field, bond character must also be of considerable importance. An atom with closed shell, i.e., a noble-gas configuration, possesses zero angular momentum, and as a result, would have no paramagnetic contribution. Thus, the ammonium ion, which fulfills this prerequisite of having nitrogen in an electronic environment most similar to the noble-gas structure, is dominated by the diamagnetic term and resonates at high field. Conversely, as asymmetries

in the electronic structure become manifest, orbital angular momentum will result, the paramagnetic term will not be negligible and resonance will occur at lower applied field. (c) For a series of structurally similar compounds, Witanowski et al. (111, 113, 114 and 125) have shown that the  $^{14}\text{N}$  chemical shifts for nitro-, compounds, -nitriles, and -isonitriles are governed by inductive effects, either electron-donating (+I) or electron-withdrawing (-I), which can be estimated by considering the  $\pi$ -bond polarity (114). All of these theories, in general, do agree with the experimentally observed  $^{14}\text{N}$  shifts and do give reasonable explanations why some resonances are at higher field than others. For specific cases, such as the alkyl ammonium salts we are dealing with here, however, all theories do not offer valid explanations since their predictions often fail to agree with what is observed.

The electronegativity of the group bonded to  $^{14}\text{N}$  seems to explain gross nitrogen shifts over the entire range observed, as was pointed out above. In the specific case of alkyl nitro compounds, Witanowski et al. (125) point out that their results are just the opposite of what is predicted on the basis of electronegativity. In addition, and also apropos to our observations, Evans and Richards (118) have indicated that electronegativity

fails to explain the shifts for the symmetric ammonium ions; the shifts to low field are found to be in the order:



whereas the opposite order should be observed if electronegativity is of major importance.

Ionic character of the bonds to nitrogen cannot be the only factor as shown by Schmidt et al. (117), who pointed out that in  $\text{NH}_4^+$  the NH bond has about 20% ionic character while the NO bond in  $\text{NO}_3$  has about 12% ionic character; thus, the theory relating  $^{14}\text{N}$  chemical shift to ionic character must account for a very large shift, approximately 350 ppm, for such a small change (ca. 8%) in ionic character. The theory would be even more hard-pressed for the alkyl ammonium salts (cf. Table 1); as the bonding is very similar for all, one would expect changes for ionic character in the third significant figure and this would have to account for shifts of up to 43 ppm. Nevertheless, it could possibly be argued that the quaternary alkyl ammonium ions (4Et and 4Me) have a more covalent carbon-nitrogen bond than the hydrogen-nitrogen bond of the ammonium ion (4H), hence, should show a paramagnetic shift as observed. This explanation

does not account for the ethylammonium ions consistently resonating at lower field than the corresponding methyl analogues, nor could a prediction for such alkyl substituted ions as butyl, cyclohexyl and neopentyl be made.

Witanowski et al. (113 and 114) have shown that inductive effects adequately explain the  $^{14}\text{N}$  shifts for nitro compounds, nitriles and isonitriles but bond orders and charge densities are not always easily obtained. An additional point is that their approach is based on  $\pi$ -bond orders, as paramagnetic shifts and paramagnetic shielding is dependent on the amount of  $\pi$ -bonding between nitrogen and the adjacent atoms. In the alkylammonium ions  $\pi$ -bonding is negligible so this approach is not helpful.

Finally, let us consider specifically ammonia and the alkyl amines, which are our chief concern. For these compounds, the nitrogen shifts result mainly from the diamagnetic shielding term, the paramagnetic shielding term having only a small second-order effect. The reason is that excited states for ammonia and the amines correspond to an  $n \rightarrow \sigma^*$  transition rather than to an  $n \rightarrow \pi^*$  transition as in nitrogen-heterocyclics, nitro and nitroso compounds, nitrates and nitrites. Since  $\sigma_p$  is inversely proportional to the excited state energy and since  $\Delta E$  for an  $n \rightarrow \sigma^*$  transition is greater than  $\Delta E$  for an  $n \rightarrow \pi^*$  transition,

it is easy to see that  $\sigma_p$  for ammonia and amines will be of less importance than it is for other nitrogen containing compounds (118, 119 and 123). As a result of the greater importance of the  $\sigma_p$  shielding term, ammonia and amines appear at the high field end of the nitrogen resonance spectrum.

#### D. Nuclear Spin-Spin Coupling

##### General Observations

Under high-resolution conditions (high degree of magnetic field homogeneity) fine structure is sometimes observed in the NMR spectrum. This fine structure is intramolecular in origin like chemical shifts but unlike chemical shifts, which are due to the electronic shielding of the nucleus, this fine structure results from the interaction of the nucleus with neighboring nuclei. Since the orientation of the neighboring nuclear spins may be parallel, antiparallel or inclined at various fixed angles to the applied magnetic field, the local field at the observed nucleus will have values greater than, less than or the same as the applied field. As a result, the resonance of the observed nucleus will be split into two or more lines with separation  $J$  depending on the number of allowed orientations of the spins of

neighboring nuclei. In turn, the resonances of the neighboring nuclei will themselves be split by the same value,  $J$ . Since one nucleus (or set of equivalent nuclei) has its spin(s) coupled with another set of chemically shifted nuclear spins, this interaction is called "spin-spin coupling" and the fine structure splitting value  $J$  is termed the "spin-spin coupling constant" or simply the "coupling constant" (126 and 127).

Throughout the years a large number of coupling constants for various molecules and nuclei have been measured and a number of generalizations can now be made (128 and 129). First, coupling is not observed between equivalent nuclei. For example, the hydrogens of a methyl group do not couple with one another nor do the hydrogens of benzene. Coupling is only observed when the nuclei are magnetically non-equivalent. For example, when there is a chemical shift difference between the nuclei they are obviously non-equivalent.

Secondly, when the chemical shifts (measured in units of frequency) are an order of magnitude or more greater than the coupling constant, the number of equally spaced resonance lines is given by:

$$\text{Number of resonance signals} = 2nI + 1 \quad (33)$$

where  $n$  is the number of equivalent neighboring nuclei and

$I$  is the nuclear spin number of the neighboring nuclei. In addition, for nuclei of spin  $1/2$  the relative intensities of the lines will be given by the binomial coefficients. For example, the resonance peak for a nucleus (or set) with one neighbor ( $I = 1/2$ ) will be split into an equal-intensity doublet and the peak for a nucleus with three equivalent neighbors ( $I = 1/2$ ) will be split into a quartet with intensity ratios  $1:3:3:1$ . If  $I > 1/2$  the relaxation time of the quadrupolar nucleus ( $I > 1/2$ ) must be sufficiently long so that coupling can be observed (cf. Section II B). Under these conditions the number of lines will be given by Equation (33); however, the intensities may not follow predictions and the separations may be less than the true coupling constant, both of these being a function of the relaxation time as shown by Pople (9), Bacon et al. (116), and Suzuki and Kubo (84). As an example of this situation consider the ammonium ion in aqueous solution. The proton spectrum consists of three lines of equal intensity resulting from coupling with one  $^{14}\text{N}$  nucleus ( $I = 1$ ) and the  $^{14}\text{N}$  spectrum consists of five lines with intensity ratios  $1:4:6:4:1$ . It is to be emphasized, that all of the foregoing description applies to the situation where  $\delta \geq 10 \text{ J}$  and such spectra are called first order because some of the

spin states are degenerate. The other situation is strong coupling where the degeneracy is removed and this occurs when the chemical shift approaches the same magnitude as the coupling constant. This condition leads to anomalous intensities, spacings, and number of lines. Now there are more lines than predicted by first-order theory (i.e. Equation 33), the intensities do not follow the binomial coefficients and there may be no spacing directly identifiable as a chemical shift or coupling constant. In this situation one must employ a complete quantum mechanical analysis of the spin system. A digital computer is then most conveniently used for analysis of the spectrum to determine coupling constants and chemical shifts.

A third generalization is that the magnitude of the coupling constant between two nuclei increases with increasing atomic number, e.g.  $^{19}\text{F}$ - $^{19}\text{F}$  coupling is greater than  $^1\text{H}$ - $^1\text{H}$  coupling and  $^{19}\text{F}$ - $^{13}\text{C}$  coupling is greater than  $^1\text{H}$ - $^{13}\text{C}$  coupling. In addition, for two isotopes (nuclei with the same atomic number) coupling with a common third nucleus, coupling is proportional to the gyromagnetic ratios of the isotopes so will be larger for the nucleus with the larger gyromagnetic ratio, e.g.,  
 $J(^1\text{H}-^{15}\text{N}) > J(^1\text{H}-^{14}\text{N})$  and  $J(^{19}\text{F}-^{11}\text{B}) > J(^{19}\text{F}-^{10}\text{B})$ .

Fourth, the magnitude of the coupling constant generally falls off with distance, that is, as the number of bonds intervening between two coupled nuclei increases, the coupling constant decreases. There are exceptions to this as will be pointed out later. There may also be an angular dependence of the coupling.

Fifth, the coupling constant is independent of the applied magnetic field and often also of temperature, whereas chemical shifts vary directly with the applied field and are often quite temperature dependent. This provides an experimental method for simplifying the interpretation of a spectrum. By obtaining spectra at two or more field strengths (preferably each 20-30% larger than the one previous), centers of multiplets which are chemically shifted will be spread further apart, whereas the spacings within the multiplets will be the same regardless of the increased field value, as these spacings are due to spin-spin coupling. This is one stimulus for achieving very high magnetic fields since most spectra will approach first-order structure and analysis will be simpler.

Finally, theoretical calculations (130) and experimental measurements agree that the coupling constant has a sign associated with it and signs for most J values

are now known.

### Mechanism of Spin-Spin Coupling

The mechanism involved in spin coupling should now be examined, to better understand these values. The original explanation proposed was interaction of electronic orbital currents with the nuclear spins; namely, one nucleus induces currents in the electron cloud of the bond, which then pass the information to the other nucleus. This model failed, however, because calculations based on it failed to agree with observed values by an order of magnitude or more (126 and 127). A mechanism was proposed later in which the nuclear spins interact with the electron spins, following the Hund rule that all spins remain antiparallel. Calculations based on this model yield values which have the correct order of magnitude.

Theoretical derivations based on the use of a Hamiltonian for the motion of the electrons in the fields produced by nuclei having magnetic moments yield a coupling constant which is the sum of three major terms. The first is from interaction between electron orbital and nuclear magnetic moments, the second arises from magnetic dipole interaction between electronic and nuclear spins and the third is the Fermi-contact term. The most significant term and the one which has the biggest effect is

the last one, the contact term, which is expressed (130):

$$J(AB)_{\text{Fermi}} = -K(\gamma_A \gamma_B / \Delta E) \sum_i^{\text{occ.}} \sum_j^{\text{unocc.}} (\phi_i \phi_j)_A (\phi_i \phi_j)_B \quad (34)$$

Where  $K$  is a constant,  $\gamma_A$  and  $\gamma_B$  are the gyromagnetic ratios of the two nuclei  $A$  and  $B$ , respectively, and  $\Delta E$  is the mean value of the excitation energies. The summations are over all occupied and unoccupied orbitals. Similarly, the other two terms involve the gyromagnetic ratios of the two coupled nuclei and an approximate excitation energy. The standard quantum mechanical approaches of molecular orbital theory or valence bond theory, combined with the variational method, have been employed for calculations of  $J$  values but a complete discussion of the theoretical calculation of coupling constants is beyond the scope of this review; further details may be found in discussions given by Pople, Schneider and Bernstein (128) and Emsley, Feeney and Sutcliffe (129).

For protons the main contribution to the coupling comes from the Fermi-contact term, Equation (34), with the other two terms making little or no contribution. The chief reason for this is that the hydrogen atoms use a  $1s$ -type atomic orbital in bond formation; the other coupling terms drop out unless other orbitals such as  $p$ ,  $d$  and

f are involved. For nuclei other than protons the other two terms, the electron-orbital and the electron-nuclear dipole terms, also enter into the calculation as p- and d- type atomic orbitals now must be considered. Because of the inclusion of these terms, and because more orbitals are contributing, it is easy to see why coupling involving nuclei other than protons is in general larger than proton-proton coupling. Since more orbitals must now be evaluated, it is understandable that the task is also considerably more difficult.

#### Spin Coupling in Nitrogen Compounds

A brief review of spin coupling in alkyl amines and ammonium salts will now be given. Alkyl ammonium salts contain the elements carbon, hydrogen, and nitrogen and there are many different pairs of nuclei which are capable of coupling but this discussion will be limited to H-H and N-H couplings as these are readily observable and the only ones of major concern to us here. Proton-proton couplings will be discussed first as these are the most obvious in the spectra since they always occur, whereas the proton-nitrogen couplings may not always be observed as discussed above (Section II B).

### Proton-Proton Coupling Constants

The first type of proton-proton coupling to be considered is that between an NH proton and the alkyl  $\alpha$ -hydrogens, i.e. proton-proton coupling across three bonds and through nitrogen. (Incidentally, all couplings are classified first as to the number of intervening bonds between the two spin-coupled nuclei, as we have mentioned above that the coupling decreases with distance; couplings with two and three intervening bonds are designated  $^2J$  and  $^3J$ , etc. A subscript is then added to identify the particular nuclei involved.) This particular coupling,  $^3J(\underline{H}-N-\underline{CH})$ , is present in all members of the series of alkylamines and alkylammonium salts, the simplest ones being methylamine and ammonium ion. The most extensive list of these is that given by Freifelder, Mattoon and Kriese (131), who reported values for N-monosubstituted methylamines. Their results, together with a few other similar couplings, are given in Table 2. From the values listed it can be seen that the NH proton coupling with the N-alkyl proton is about 5 Hz. Also, there is a measurable difference in  $^3J(\underline{H}N\underline{CH})$  depending on the R group on the nitrogen. Clearly we are seeing the effects of more than just the s electrons and contributions to J

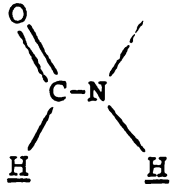
Table 2. Three bond proton-proton coupling through nitrogen of the type  $^3J(R-NH-CH_3)$ .

R-Group	$^3J(\underline{H}NCH)$	Reference
Amides (BCO--)*	4.5-5.0 Hz	131
Formamides (HCO--)	4.9-5.0	132
Ureas, Biurets ) (BNHCO--)	4.0-5.0	131
and Guanidines )		
Ethyl Carbamyl (EtOCO--)	4.9	97
Sulfonamides (B-SO <sub>2</sub> --)	5.0	131
Nitramines (NO <sub>2</sub> --)	4.0	86
Dinitro- trinitrophenyls	5.3-5.7	133

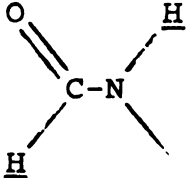
\*B represents a hydrocarbon group.

from terms other than the Fermi contact term. Unfortunately, Freifelder et al. (131) and Hedberg et al. (133) did not speculate in this regard only commenting that in some compounds no coupling was observed, probably because these were weak bases and proton exchange was occurring (cf. Section II A). Quite interestingly, if the three-bond proton-proton coupling through nitrogen involves something other than methyl or simple alkyl substituents

on nitrogen a wider range of values are found. For example, Freifelder et al. (134) report a value of 6 Hz for an acetylated amine of the structure  $-\underline{\text{CH}}_2-\underline{\text{NH}}-\text{COCH}_3$  (protons coupling are underlined). For substituted formamides, coupling of the NH proton with the formyl proton over three bonds exhibits a much wider range than the simple  $5.0 \pm 1.0$  Hz of Table 2. Sunners, Piette, and Schneider (135) report a range in various solvents of 1.7 to 2.1 Hz for formamide and Randall and Baldeschwieler (132) a range of 1.8-2.3 Hz for N-methylformamide; the pro-

tons being cis in both cases, i.e. . The values

are much larger, 12.9-13.6 Hz, for the trans coupling,

i.e. , of formamide (135). Thus, we can now see

how difficult it is to rationalize coupling constants as not only the number of intervening bonds but also the bond types and angles quite naturally causes differences. In addition, another complicating factor is the medium ("solvent effect") which is the reason for the range of values for the formamides mentioned (132 and 135).

Values of  $^3J$  (HNCH) for quaternary ammonium ions are summarized in Table 3, along with the concentrations and solvents, both of which may possibly be important. From the table we see that for the same concentration in water, there is a decrease in the magnitude of the coupling constant from monomethyl- to trimethylammonium ion. Although these values come from and were used in the kinetic studies (cf. Section II A), the authors of those articles never commented on the J values. One value in Table 3 that appears to be very much out of line with the others in its group is the 6.5 Hz reported by Emerson et al. (20) for trimethylammonium ion in sulfuric acid solution. Fraenkel and Asahi (38) noted that this coupling constant is a function of the sulfuric acid concentration but never found values as large as 6.5 Hz.

Table 3. Three-bond proton-proton coupling through nitrogen of the type  $3J(\text{HC-NH}^+)$ .

Compound	Conc., Solvent, etc.	$3J(\text{HNCH}^+)$	Reference
$\text{CH}_3\text{NH}_3^+\text{Cl}^-$	0.5-4.5 M, $\text{H}_2\text{O}$	$6.20 \pm 0.05$ Hz	2
$\text{CH}_3\text{NH}_3^+\text{Cl}^-$	1.7-7.9 M, $\text{H}_2\text{O}$	$6.30 \pm 0.10$	27
$\text{CH}_3\text{NH}_3^+\text{Cl}^-$	0.3-0.4 M, 34-58 wt% $\text{H}_2\text{SO}_4$	6.31	20
$\text{CH}_3\text{NH}_3^+\text{Cl}^-$	(?)	6.17	29
$(\text{CH}_3)_2\text{NH}_2^+\text{Cl}^-$	0.2-4.7 M, $\text{H}_2\text{O}$	5.7	33
$(\text{CH}_3)_3\text{NH}^+\text{Cl}^-$	0.3-2.3 M, $\text{H}_2\text{O}$	5.2	33
$(\text{CH}_3)_3\text{NH}^+\text{Cl}^-$	0.2-0.5 M, 25-54 wt% $\text{H}_2\text{SO}_4$	6.5	20
$(\text{CH}_3)_3\text{NH}^+\text{Cl}^-$	0.2-0.6 M, $\text{H}_2\text{O}$	5.15	34
$(\text{CH}_3)_3\text{NH}^+\text{Cl}^-$	0.6-6.0 M, acetic acid	5.14	23
$(\text{CH}_3)_3\text{NH}^+\text{NO}_3^-$	? M, 0-90 wt% $\text{D}_2\text{SO}_4$	4.8-5.4	38
Pyrrolidine	? M, dil. HCl	7.0	8

Table 3 (Continued)

Compound	Conc., Solvent, etc.	$^3J(\text{HNCH}^+)$	Reference
N,N-Dimethylaniline	0.3 M, 0.4 M HTos* in acetic acid	6.1	48
N,N'-Dimethyl- piperazine	? M, dil. HCl	5.0	49

\*HTos = p-toluenesulfonic acid

Other types of compounds have been included in Table 3 for general interest. The value for the N,N'-dimethylpiperazinium ion, a cyclic tertiary ammonium ion, is about the same as those for the acyclic tertiary trimethylammonium ion. The value for the other tertiary ammonium ion, N,N-dimethylanilinium ion, may or may not be significant. It would first have to be measured in dilute aqueous HCl for comparison with the others. Similarly, based on the values of  $J$  for dimethylpiperazinium and trimethylammonium ions one would expect the  $J$  value for the pyrrolidinium ion to be near that of the dimethylammonium ion; here the difference may be due to strain in the five-membered pyrrolidinium system.

The second type of proton-proton coupling to be reviewed is the coupling within the alkyl group itself and the only one which we are concerned with is the three bond coupling  $^3J(\underline{\text{H}}\text{C}\underline{\text{C}}\text{H})$  within the ethyl group, that is, the coupling between the methyl and the methylene protons. For convenience, a few of these values have been listed in Table 4 in order of increasing coupling constant. Examining Table 4 it can be seen that the values depend on the atom to which the ethyl group is attached. This seems to have escaped the attention of earlier workers,

Table 4. Proton-proton coupling constants for the ethyl group.

$^3 J(\overline{\text{HCCH}})$	Compound	Reference	$^3 J(\overline{\text{HCCH}})$	Compound, Solvent	Reference
6.8 Hz	$\text{NaBEt}_4$	80	7.2 Hz	$\text{Et}_4\text{NBr}/\text{H}_2\text{O}$	74
7.0	$\text{BEt}_3$	80	7.2	$\text{Et}_4\text{NBr}/\text{H}_2\text{O}$	71
7.0	$\text{HgEt}_2$	136, 137	7.4	$\text{Et}_4\text{NBr}/\text{H}_2\text{O}$	80
7.2	$\text{Et-C}\equiv\text{CH}$	138	7.48	$\text{Et}_4\text{NI}/\text{D}_2\text{O}$	72
7.2	$\text{EtSH}$	138	7.3	$\text{Et}_3\text{NMeI}/\text{H}_2\text{O}$	74
7.42	$\text{EtSH}$	139	7.3	$\text{OCH}_2\text{NEt}_3\text{Cl}/\text{H}_2\text{O}$	74
7.4	$\text{EtPMe}_3^+$	81	7.3	$\text{HOOC}(\text{CH}_2)_{10}\text{NEt}_3\text{OH}/\text{H}_2\text{O}$	74
7.5	$\text{Et}_2\text{PMe}_2^+$	81	7.3	$\text{Et}_3\text{N}(\text{CH}_2)_n\text{NEt}_3\text{Br}_2/\text{H}_2\text{O}$ (n = 4-6)	74
7.5	$\text{Et}_3\text{PMe}^+$	81			
7.8	$\text{Et}_4\text{P}^+$	81			
7.8	$\text{Et}_3\text{As}$	80			
7.8	$\text{Et}_4\text{AsBr}$	80			
7.8	$\text{Et}_3\text{MeAsBr}$	80			

Table 4 (Cont'd)

$^3J(\underline{\text{HCCH}})$	Compound	Reference	$^3J(\underline{\text{HCCH}})$	Compound, Solvent	Reference
7.8	$\text{Et}_4\text{Ge}$	140			
$7.9 \pm 0.2$	$\text{Et}_4\text{Si}$	139			
(8.0)	$\text{Et}_2\text{SiCl}_2$	140			
8.0	$\text{EtSiCl}_3$	140			
8.6	$\text{ZnEt}_2$	140			

probably because they were studying either the effect of the central element on internal chemical shift between methyl and methylene (80, 81 and 140) or its effect on the relative couplings between the central element and methylene and methyl hydrogens (80 and 81). The value of  $^3J(\underline{HCCH})$  for ethyl substituted quaternary ammonium ions seems to be affected little, if at all, by other substituents on nitrogen. Massey et al. (80) detected no difference on quaternization, reporting the same value, 7.4 Hz, for triethylamine and tetraethylammonium ion. Also, Freifelder, et al. (134) report  $^3J = 7.0$  Hz for several diethylamines.

#### $^{14}\text{N}$ -Proton Coupling Constants

Now we come to the third major type of spin-spin coupling, the proton-nitrogen coupling. Coupling between protons and nitrogen will not always be observed depending on the electric field gradient at nitrogen (Section II B). Nevertheless, there have been a number of reports of  $^1\text{H}$ - $^{14}\text{N}$  coupling constants so it is worthwhile reviewing them. Surprisingly enough, there are a sufficient number of wealthy chemists around so that a considerable number of  $^{15}\text{N}$  enriched compounds have been synthesized. The importance of this is that  $^{15}\text{N}$  ( $I = 1/2$ ) has no quadrupole

moment so will always exhibit coupling with protons. From the  $^1\text{H}$ - $^{15}\text{N}$  couplings one can calculate the corresponding  $^1\text{H}$ - $^{14}\text{N}$  values. We shall review both, considering the  $^{14}\text{N}$  values first. Here again they are grouped according to number of intervening bonds, those for coupling across one bond being listed in Table 5.

Some of the values are clearly inaccurate, the older ones being particularly suspect. Some general trends can be seen, however; first, protonation definitely increases the value as can be seen by comparing  $^1J(^1\text{H}-^{14}\text{N})$  for liquid ammonia and the ammonium ion, where an increase of 8 to 9 Hz is observed. Second, replacing ammonium hydrogens by alkyl groups causes a change in  $^1J(^1\text{H}-^{14}\text{N})$ . Third, if the nitrogen is part of a double bond system or a heteroaromatic ring there is an extremely large increase. Because the precision of these values is rather poor, further comment is reserved until the  $^1\text{H}$ - $^{15}\text{N}$  values are considered since there is no doubt about the accuracy of these. In addition, a number of workers who have reported  $^{15}\text{N}$  data have made suggestions to explain the various differences in the values. Muira and Saika (148) recalculated the coupling constant for liquid ammonia and showed that the Fermi contact term accounts for about 70% of the value; they agree with Pople and Santry (130) that this value is

Table 5.  $^1\text{H}$ - $^{14}\text{N}$  coupling constants across one bond.

$^1J(^1\text{H}-^{14}\text{N})$	Compound	Conditions	Reference
$40.0 \pm 1.0$ Hz	$\text{NH}_3$	Dry liquid	141
46.0	$\text{NH}_3$	Dry liquid	4
$46.0 \pm 2.0$	$\text{NH}_3$	Dry liquid	7
43.5	$\text{NH}_3$	Dry liquid	142
$43.8 \pm 0.3$	$\text{NH}_3$	Dry liquid	13
$43.9 \pm 0.4$	$\text{NH}_3$	Dry liquid	88
50.0	$\text{NH}_4^+$	$\text{H}_2\text{O}$ (pH < 1)	18
$50.0 \pm 1.0$	$\text{NH}_4\text{NO}_3$	2 N HCl	112
$51.0 \pm 2.0$	$\text{NH}_4\text{Cl}$	Saturated in 3 N HCl	143
$52.0 \pm 1.0$	$\text{NH}_4\text{Ac}$	Glacial acetic acid, $0^\circ\text{C}$	23, 29
$52.6 \pm 0.1$	$\text{NH}_4\text{NO}_3$	Water acidified with $\text{HNO}_3$	144
$53.5 \pm 0.2$	$\text{NH}_4\text{Br}$	50% $\text{H}_2\text{SO}_4$	145
54.3	$\text{NH}_4\text{Cl}$	$\text{H}_2\text{O}$ (pH < 1)	19

Table 5 (Cont'd)

$^1J(^{1}H-^{14}N)$	Compound	Conditions	Reference
49.0 $\pm$ 2.0	$CH_3NH_3Cl$	50% in acidified $H_2O$	8
54.0 $\pm$ 1.5	$CH_3NH_3Cl$	1.7-8.0 M in acidified $H_2O$	27
53.0 $\pm$ 3.0	$(CH_3)_2NH_2Cl$	50% in acidified $H_2O$	8
51.0	$(CH_3)_3NHCl$	Methanol at 50°C	40
50.0 $\pm$ 2.0	$CH_3CH_2NH_3Cl$	50% in acidified $H_2O$	8
55.0	$(CH_3CH_2)_3NHCl$	$H_2O$ , estimated value	41
52.0 $\pm$ 4.0	Pyrrolidine $\cdot$ $HCl$	50% in acidified $H_2O$ , 30°C	8
55.0 $\pm$ 5.0	Pyrrole	Neat, 70°C	8
56.0 $\pm$ 5.0	Acetamide	Neat, 185°C	8
60.0 $\pm$ 5.0	N-Methyl acetamide	Neat, 250°C	8
60.0 $\pm$ 4.0	Formamide	Neat, 60°C	8
60.0	Pyridine	20% in $H_2SO_4$	65
67.6 $\pm$ 0.5	Pyridinium	3 Mole% in formic acid	146
70.0	Pyridine	5 Mole% in trifluoroacetic acid	147

positive. They point out one of the major pitfalls of all theoretical calculations of coupling constants, namely, the difficulty of estimating a value for the mean excitation energy [cf. Equation (34)].

The two-bond nitrogen-proton couplings are listed in Table 6. Some generalizations can be made. First, the two-bond coupling  $^2J(\text{CH}_3\text{-N})$  is consistently greater for methyl than is  $^2J(\text{CH}_2\text{-N})$  for the methylenes of ethyl and other derivatives. This can be seen not only in the values for the quarternary alkylammonium ions, but also in those of the isonitriles and was pointed out by Massey, *et al.* (81) who noted that it is true also of alkyl groups on elements other than nitrogen. They gave no theory to explain this fact although it seems rather obvious that replacing a methyl hydrogen with a methylene (i.e. a carbon-hydrogen bond with a carbon-carbon bond) will cause a change in the hybridization and excitation energies, and hence, in the coupling constant. The problem is to come up with a theory to explain the direction of the change. The answer to this perhaps comes from the third point which isn't emphasized in Table 6, namely, the sign. McFarlane (149) has shown the two-bond NH coupling to be negative, as had been proposed by Bourn, *et al.* (154), in ethyl isonitrile where the nitrogen couples through an alkyl carbon. Bourn

Table 6.  $^1\text{H}$ - $^{14}\text{N}$  coupling constants across two bonds.

$2J(^1\text{H}-^{14}\text{N})$	Compound <sup>a</sup>	References
0.2 Hz	$(\text{CH}_3\text{CH}_2)_4\text{N}^+$	149
< 0.5	$(\text{CH}_3\text{CH}_2)_4\text{N}^+$	71, 72
~ 0	$(\text{CH}_3\text{CH}_2)_4\text{N}^+$	74, 150
- 0.4	$(\text{CH}_3)_4\text{N}^+$	149, 151
0.5	$(\text{CH}_3)_3\text{NCH} = \text{CHR}^+$	76, 152
$0.54 \pm 0.06$	$(\text{CH}_3)_4\text{N}^+$	25
$0.55 \pm 0.05$	$(\text{CH}_3)_4\text{N}^+$	81, 82
~1.0	$(\text{CH}_3)_4\text{N}^+$	70
$1.33 \pm 0.06$	$\text{CH}_3\text{-NCO}$	90
$1.30 \pm 0.2$	$\text{C}_6\text{H}_5\text{-CH}_2\text{NC}$	85
$1.80 \pm 0.2$	$(\text{CH}_3)_2\text{CHNC}$	85
- 1.9	$\text{CH}_3\text{CH}_2\text{NC}$	149
- 2.0	$\text{CH}_3\text{CH}_2\text{NC}$	150
2.0	$\text{CH}_3(\text{CH}_2)_2\text{CH}_2\text{NC}$	85
- 2.3	$\text{CH}_3\text{NC}$	149
2.35	$\text{CH}_3\text{NC}$	153
2.7	$\text{CH}_3\text{NC}$	85
2.5	$(\text{CH}_3)_3\text{NCH} = \text{CHCOOH}^+$	76
+ 2.9	$(\text{CH}_3)_3\text{NCH} = \text{CH-C}_6\text{H}_5^+$	152
+ 3.5	$(\text{CH}_3)_3\text{NCH} = \text{CH}_2^+$	152
3.6	$(\text{CH}_3)_3\text{NCH} = \text{CH}_2^+$	76

<sup>a</sup>Protons coupling with the nitrogen are underlined.

and co-workers (154) showed that this is also true for N-methyl amides, the coupling between the amide nitrogen and the methyl proton being negative. However, Ohtsuru and Tori (152) have shown that the two-bond coupling of nitrogen with the geminal proton of the vinyl group is positive, so that comparison of values in the table without knowledge of the signs is dangerous. They attribute this sign change to different hybridization of either the nitrogen or the carbon which sounds quite reasonable as Bourn et al. (154) show that for N-methylformamides coupling between nitrogen and the formyl proton is positive whereas coupling between nitrogen and the methyl protons is negative.

The number of compounds for which three-bond  $^1\text{H}$ - $^{14}\text{N}$  has been reported, is so large that a complete listing is impractical, so only a few are given in Table 7 for illustrative purposes. Some of the more interesting studies are now described in detail. The nitramines reported by Lamberton et al. (86) constitute a new class of compounds for which  $^1\text{H}$ - $^{14}\text{N}$  coupling can be directly observed. The somewhat unusual feature is that the coupling is with the nitro-group nitrogen as was shown by heteronuclear decoupling experiments (87). The work of Lehn and Seher (76), as well as that of Ohtsuru and Tori (152),

Table 7.  $^1\text{H}$ - $^{14}\text{N}$  coupling constants across three bonds.

$3J(^1\text{H}-^{14}\text{N})$	Compound	References
$1.38 \pm 0.08$ Hz	$\text{CH}_3\text{CN}$	89, 90
1.45	$\text{CH}_3\text{CH}_2\text{NCH}_3\text{NO}_2$	86
1.5	$(\text{CH}_3)_2\text{NNO}_2$	86
1.65	$\text{CH}_3\text{CH}_2\text{NCH}_3\text{NO}_2$	86
1.5	$(\text{CH}_3\text{CH}_2)_4\text{N}^+$	70
1.65	$(\text{CH}_3\text{CH}_2)_4\text{N}^+$	72
1.7	$(\text{CH}_3\text{CH}_2)_4\text{N}^+$	79, 82
+ 1.8	$(\text{CH}_3\text{CH}_2)_4\text{N}^+$	71, 74, 149
$1.8 \pm 0.03$	$(\text{CH}_3\text{CH}_2)_4\text{N}^+$	75
$1.77 \pm 0.03$	2,N,N-Trimethylpiperidinium	79
1.9	Several alkyl CH and $\text{CH}_2$ quaternary N	74
+2.0	$(\text{CH}_3)_3\text{CNC}$	149
$2.4 \pm 0.1$	$\text{R}-\text{C}_6\text{H}_4\text{N}-\text{CH}_2\text{CH}_3$	78
+2.5	$\text{CH}_3\text{CH}_2\text{NC}$	149, 150
2.6	$(\text{CH}_3)_2\text{CHNC}$	85
3.5	$(\text{CH}_3)_3\text{CNC}$	85
1.8	$(\text{CH}_3)_3\text{NCH} = \text{CHCOOH}^+$ ( <u>cis</u> ) <sup>a</sup>	76
2.2	$(\text{CH}_3)_3\text{NCH} = \text{CHC}_6\text{H}_5^+$ ( <u>cis</u> ) <sup>a</sup>	152
2.6	$(\text{CH}_3)_3\text{NCH} = \text{CH}_2^+$	76, 152
$3.0 \pm 0.2$	$\text{R}-\text{C}_6\text{H}_4\text{N}-\text{CH}_2\text{CH}_3$ (the $\text{C}_3$ and $\text{C}_5$ hydrogens)	78
3.5	$(\text{CH}_3)_3\text{NCX} = \text{CH}_2^+$ ( <u>trans</u> ) <sup>a</sup>	76
3.8	$(\text{CH}_3)_2\text{NC(OEt)} = \text{CH}_2$ ( <u>trans</u> ) <sup>a</sup>	76
$5.55 \pm 0.05$	$(\text{CH}_3)_3\text{NCH} = \text{CH}_2$	76, 152

<sup>a</sup>Hydrogen nuclei cis and trans to quaternary nitrogen.

merits special attention because in one simple type of compound, the trimethylvinylammonium salts, they have demonstrated a number of features. The first is that hybridization of the carbon and/or nitrogen has a very major effect on the coupling constant. Witness the fact that the couplings for the vinyl groups are at one end of Table 7 and couplings in simple alkyls are at the other end. The study of the effect of hybridization on the  $^3J(^1H-^{14}N)$  has also been the subject of a paper by Gassman and Heckert (75) who investigated seventeen alkyl, cycloalkyl and bicyclo-quaternary amines! The values they obtained ranged from 1.5 to 2.15 Hz. A second point made by Ohtsuru, Lehn, and their co-workers is that there is a strong angular dependence of the proton-nitrogen coupling; thus, the vinyl hydrogen trans to the quaternary nitrogen has a larger coupling than the cis. Biellmann and Callot (78) pointed out that the coupling for the nitrogen and the ring  $C_3$ - and  $C_5$ -hydrogens in 4-substituted ethylpyridinium ions is about 3 Hz for the transoid structure, which agrees well with the values for the trans vinyl derivatives. Terui, Aono, and Tori (155) have recently presented a very concise study showing the dependence of the proton-nitrogen coupling on dihedral angle in three bicyclo compounds, where the dihedral angles

are fixed. They point out that at  $0^\circ$  it is 1.4 - 2.7 Hz, decreases to almost zero at  $80^\circ$  then rises at  $120^\circ$  and they predict it could be 5-6 Hz at  $180^\circ$ .

Lehn and Seher (76), Maher (150), and Ohtsuru and Tori (152) all suggested that evidence pointed toward the  $^3J(^1H-^{14}N)$  being positive. Indeed, the heteronuclear decoupling experiments of McFarlane (149) and the report of Bourn et al. (154) show that the sign of the three-bond nitrogen-alkyl proton coupling for ethyl isonitrile is positive. At this time there have been no reports of negative three-bond couplings.

Considering the two-bond and three-bond nitrogen alkyl proton couplings, it seems that generally  $^3J$  is larger than  $^2J$ . This was pointed out by Massey et al. (80 and 81) who noted that this is true of a number of other elements than nitrogen. They point out that no satisfactory explanation has been given, probably because there are too many variables involved in the coupling constant.

### $^{15}N$ - Proton Coupling Constants

The proton -  $^{15}N$  couplings do not tell anything different from what has already been learned from  $^{14}N$  couplings except that data may be obtained for compounds

where the  $^1\text{H}$ - $^{14}\text{N}$  couplings are not observed. An additional feature of  $^{15}\text{N}$  couplings is that they are larger than the  $^1\text{H}$ - $^{14}\text{N}$  values because of the larger gyromagnetic ratio for  $^{15}\text{N}$ . For these reasons it is worthwhile considering the reported  $^{15}\text{N}$  values but since there are so many we shall only consider the ones relevant to the alkyl amines and ammonium ions; these are listed in Table 8.

For  $^{15}\text{NH}$  coupling across one bond, the values for amides, ureas, thioureas and the N-alkyl mono-substituted derivatives are all much higher than those listed, falling in the range 88 to 95 Hz (135, 157, 162, 163, and 164). It is important to compare these values with those for the  $^{14}\text{NH}$  couplings of Table 5 noting that the  $^1\text{H}$ - $^{15}\text{N}$  couplings established with certainty that in amides, etc., the coupling constants are larger than they are in ammonium salts. Some mention should be made of the Ogg and Ray (26) spectrum of 65%  $^{15}\text{N}$ -enriched methylammonium ion; unfortunately they did not report the values of any  $^1\text{H}$ - $^{15}\text{N}$  coupling constants. To calculate the values from their calibration markers would be committing the same error as others have done with the nitrogen chemical shifts and therefore it was not attempted.

For coupling across two bonds, we should add a few general ranges as the list of values is quite extensive.

Table 8.  $^1\text{H}$ - $^{15}\text{N}$  coupling constants.

$J(^1\text{H}-^{15}\text{N})$	$J(\gamma(14)/\gamma(15))$	Compound	Reference
<u>Across one bond</u>			
61.0 Hz	(+) 43.5 Hz	$\text{NH}_3$ (liq.)	142
$61.2 \pm 0.9$	43.6	$\text{NH}_3$ (liq.)	156
$64.0 \pm 2.0$	45.6	$\text{NH}_3$ (liq.)	7
$73.0 \pm 2.0$	52.0	$\text{NH}_4^+$	143
$73.2 \pm 0.2$	52.2	$\text{NH}_4^+$	157
$73.7 \pm 0.1$	52.5	$\text{NH}_4^+$	144
$75.6 \pm 0.2$	53.9	$\text{CH}_3\text{NH}_3^+$	157
$78.5 \pm 0.2$	55.9	$\text{C}_6\text{H}_5\text{-NH}_2$	158; 159
<u>Across two bonds</u>			
$0.0 \pm 0.2$	$\pm 0.14$	$\text{C}_6\text{H}_5\text{-N}(\text{CH}_2\text{CH}_3)_2$	157
$0.8 \pm 0.2$	(-) 0.6	$\text{CH}_3\text{NH}_3^+$	157
1.0	0.7	$\text{CH}_3\text{NH}_2$	157
<u>Across three bonds</u>			
0.7	(+) 0.5	$\text{C}_6\text{H}_5\text{-N}(\text{CH}_2\text{CH}_3)_2$	157
1.7	1.2	$\text{CH}_3\text{CN}$	157
1.8	1.3	$\text{CH}_3\text{CN}$	160
2.0	1.4	$\text{CH}_3\text{CH}_2\text{CN}$	161

For the proton-nitrogen coupling in the N-substituted amides and amines, the values are in the range  $< 1.0$  to 1.6 Hz (151, 162, 163, 165 and 166). All other values reported are much larger, perhaps due to a double bond or  $\pi$ -electron system being involved. For oximes, or in general any type of imino group, the values are 2.3 - 3.8 Hz for the syn isomer and 14.0 - 16.8 Hz for the anti isomer (164, 167, and 168). 7.5 - 8.4 Hz is the range for geminal coupling in olefins (164). The largest values are found for  $^{15}\text{N}$  coupling with the formyl proton of formamides, 14.1 - 19.0 Hz, (135, 151, 162 and 163) and for  $^{15}\text{N}$ -ring proton in aromatic heterocycles, 11.1 - 16.0 (65 and 166-170). Here again, as was pointed out with two-bond  $^1\text{H}$ - $^{14}\text{N}$  couplings there is also a difference in sign as well as magnitude, the signs of the couplings for heterocycles, formamides and anti-oximes being opposite to those for the syn-oximes and alkyl groups (154, 162, 168 and 170).

To the list of three-bond couplings we should add the following: acetamide-type, or coupling through a carbonyl group with alkyl hydrogens, 0.7 - 2.5 Hz (157, 166, and 171); coupling between the ring nitrogen and ring hydrogens in heteroaromatic systems, 0.6 to 1.7 Hz (65, 166 and 170; cis-olefinic couplings, 1.5 to 2.5 Hz (164,

165 and 172); geminal olefinic alkyl-- $^{15}\text{N}$  couplings, 2.2 to 2.7 Hz (165), somewhat higher than through the carbonyl; and, finally, trans-olefinic couplings are highest with 3.5 to 5.1 Hz being reported (164, 165, 166, 170 and 172), in agreement with the general observation that trans couplings are larger than cis. So far, three-bond couplings are unlike the two-bond couplings in that they are all of one sign (160 and 170), which is the same as the sign of single-bond couplings.

Perhaps this would be a good place to make a generalization about proton-nitrogen couplings since the  $^1\text{H}$ - $^{15}\text{N}$  couplings have been observed on a wider variety of structural types than have  $^1\text{H}$ - $^{14}\text{N}$  couplings. Considering all structures, nitrogen-proton coupling is largest across one bond, next largest over two bonds and smallest over three bonds, so the general rule of decreasing  $J$  with distance holds true. Second, the single-bond and three-bond couplings are all the same sign, positive for  $^{14}\text{N}$ , (note that since  $^{15}\text{N}$  has a negative gyromagnetic ratio the signs of  $^1\text{H}$ - $^{15}\text{N}$  couplings will be opposite to those of  $^1\text{H}$ - $^{14}\text{N}$  couplings; also, the magnitudes will be larger in the ratio  $\gamma(^{15}\text{N})/\gamma(^{14}\text{N})$  whereas two-bond couplings may be either positive or negative.)

In considering the effect of protonation of nitrogen

on various coupling constants, we shall only consider changes in magnitude of  $J$ . For hydrogen-nitrogen coupling across a single bond, the values increase, as can be seen by comparing values for ammonia and ammonium ion in Tables 5 and 8. For two- and three-bond couplings only results from  $^{15}\text{N}$ -enriched compounds can be considered since  $^1\text{H}$ - $^{14}\text{N}$  couplings are unobservable because of the asymmetric field gradient in most unprotonated  $^{14}\text{N}$  compounds. In Table 8 we see exactly the compound we are looking for, an alkyl amine. As reported by J.D. Roberts and co-workers (157), on protonation the two-bond coupling decreases for methylamine. Decreases in two-bond coupling on protonation or quaternization have also been noted for heteroaromatics (65, 168 and 170) and for the anti-form of oximes (167 and 168). The opposite effect, an increase on protonation, has been noted for the syn-form of oximes (167 and 168), and was attributed to the difference in coupling-constant sign and electron pair position for the syn- and anti-forms. Three-bond couplings generally show an increase on protonation, although the studies have so far been limited to heteroaromatic systems (65 and 170).

Roberts and co-workers, (157 and 173) and Bourn and

Randall (162) suggest that single-bond proton-nitrogen coupling arises principally from the Fermi contact term so that from the observed  $^1J(^1\text{H}-^{15}\text{N})$  values the percentages character of the bond may be estimated because the Fermi contact term is determined by the hybridization of the orbitals making up the bond. They then proceed to correlate measured coupling constants with known hybridization, obtaining a linear relationship. The next step, is to make use of the correlation to determine the percent s hybridization of unknowns from their measured coupling constants. Unfortunately, some values are as much as 30-50% off their linear plot (157, 158, 159, 162 and 173), and the amount of s character predicted is then unreasonable. They explain these differences as being due to a large orbital contribution. The theoretical calculation of Kato, Muira and Saika (148) on ammonia, one of the compounds used to establish the linear relationship between J and s character, shows at best only a 70% contribution of the Fermi-contact term to the coupling. A 30% contribution from orbital (and also dipole) interactions is no small amount so the linear relationship between  $J(\text{HN})$  and s character will not be expected to hold too well. On the other hand, a better value for the Fermi-contact contribution may yet be calculated. This is the

present status of theoretical discussion of proton-nitrogen couplings.

#### E. Nuclear Magnetic Double Resonance Spectroscopy

Up until now, nothing has been said about the spectroscopic method of obtaining all the experimental data described in Sections A through D. It has tacitly been assumed that the Larmor condition, Equation (14), was obtained by changing ("sweeping") either the frequency,  $\omega_1$ , or the magnetic field,  $H_0$ , until a resonance signal was detected. Since these nuclear magnetic resonance signals would have been obtained by one oscillatory (radio frequency) field  $H_1$  of frequency  $\omega_1$  and one magnetic field  $H_0$ , this is termed single resonance. Double (or more generally multiple) resonance refers to the NMR spectroscopic method of simultaneously irradiating the sample at two (or more) frequencies. Indeed, all of the data, with one exception, discussed in the preceding sections could have been obtained by single-resonance methods. The one exception is the determination of the relative signs of the coupling constants discussed in Section D-multiple resonance is the best experimental method of obtaining these.

The variables available to the NMR spectroscopist using the single-resonance methods are quite limited and,

therefore, also the possible experiments. One variable is the relative rate of sweep through the spectrum and another is the amplitude (or power level) of the radio frequency field,  $H_1$ . Both of these must be adjusted so that saturation does not occur:

$$(\gamma H_1)^2 T_1 T_2 < 1 \quad (35)$$

A third variable is the mode of sweeping in order to obtain the spectrum. One may scan be sweeping the magnetic field  $H_0$ , holding the observing frequency  $\omega_1$  constant; or alternatively, the frequency may be swept while the magnetic field is held constant. Although field-sweep is the most common mode used for obtaining single-resonance spectra, both methods yield equivalent results because the total field (or frequency) range for the spectrum is very small in comparison to the static field (or frequency) value.

The introduction of one or more irradiating frequencies provides the NMR spectroscopist with a whole new set of variables and thereby provides him with the ability to do experiments which were not possible before. Prior to reviewing the multiple-resonance experiments on nitrogen-containing compounds in general, and quaternary amines specifically, let us first set down the general methods and conditions.

The concepts of multiple resonance are not readily understood, so we shall simplify the discussion by limiting all of the following to nuclear magnetic double resonance (NMDR). Once the basic principles of NMDR are understood, it is relatively easy to extend them to triple and quadruple (i.e., multiple) resonance.

In the double resonance experiment, one set of nuclei, which we shall call A, is observed with an oscillatory field of amplitude  $H_1$  and angular frequency  $\omega_1$ , while a second group of spin coupled J(AX) nuclei, X, is irradiated with a field  $H_2$  and frequency  $\omega_2$ . Depending on the conditions of the double resonance experiment, certain modifications of the multiplet structure of set A will result. The important prerequisite here is that set A must be spin coupled to the irradiated set X for any changes to occur in the A multiplets. For example, irradiation by  $\omega_2$  of another set, L, say, spin coupled with X by J(LX) but not with A ( $J(AL) = 0$ ), will not produce any change in the A spectrum but will, of course, alter the X spectrum.

Homonuclear double resonance refers to the case where A and X nuclei are both of the same isotopic species, i.e. both are  $^1\text{H}$  or  $^{19}\text{F}$ , etc. Heteronuclear double resonance, on the other hand, refers to the case where nuclei A and X are of different isotopic species, i.e.  $^1\text{H}$  and  $^{13}\text{C}$ ,  $^{19}\text{F}$

and  $^1\text{H}$ ,  $^1\text{H}$  and  $^{15}\text{N}$ , etc.

NMDR experiments can be classified according to, first, method of introduction of the irradiating frequency and the sweep mode and, secondly, the amplitude of the irradiating field,  $H_2$ . All these classifications apply to either homonuclear or heteronuclear double resonance (174 and 175). There are three basic kinds of double resonance experiments which can be distinguished:

(a) Field-sweep double resonance maintains the frequencies constant ( $\omega_1 - \omega_2$ ) while varying the magnetic field  $H_0$ . Experimentally, this is the easiest to perform while the results are most difficult to interpret. The reason for the difficulty of interpretation is that one observes in the A spectrum the effects of a slowly varying perturbation in the X part because, while the observation frequency  $\omega_1$  scans through the A lines the irradiation frequency  $\omega_2$  is simultaneously scanning through the X lines. From another viewpoint, field-sweep double resonance may be considered as "pulling" the spectrum through two fixed, constant frequencies  $\omega_1$  and  $\omega_2$ . Hence, the various multiplet components of A (at  $\omega_1$ ) are recorded under different (varying) irradiation conditions ( $\omega_2$ ,  $H_2$ ) at X.

(b) Frequency-sweep double resonance maintains the irradiating frequency ( $\omega_2$ ) and the magnetic field ( $H_0$ )

constant while varying the observing frequency ( $\omega_1$ ). Experimentally this kind of double resonance is more difficult but the results are easier to interpret. The reason for the experimental difficulty is that it requires extraordinary stability of the field/frequency ratio ( $\gamma H_0/\omega_2$ ). The interpretation is simplified because the perturbation of the X system remains constant due to continuously irradiating the X multiplet at a fixed spectral position while sweeping through the A multiplet with  $\omega_1$ .

From the foregoing descriptions of these two kinds of NMDR experiments it can be seen that field-sweep and frequency-sweep modes as a rule are no longer equivalent as they were in the case of single resonance. Field-sweep and frequency-sweep double resonance become equivalent only when the width of the field swept over the observed part of the spectrum (A) is small compared to the irradiation amplitude  $H_2$  (174).

(c) There is yet a third kind of double resonance experiment which can be performed, namely, maintaining the observing frequency ( $\omega_1$ ) and the magnetic field ( $H_0$ ) constant while the irradiating frequency ( $\omega_2$ ) is swept.

In this kind of NMDR experiment, the observing frequency is set at a fixed spectral position of A (e.g. at the peak of a line) while the irradiating frequency  $\omega_2$  is swept through the X multiplets. The advantage of this approach is that only those nuclei spin coupled with A will be detected, that is sweeping  $\omega_2$  through L ( $J(AL) = 0$ ) will not be detected. Here again, the price one must pay for easily interpretable results is a very high degree of field-frequency stability ( $\gamma H_0/\omega_1$ ). This kind of frequency sweep double resonance is more commonly called inter-nuclear double resonance (INDOR) (175 176 and 177).

The second major classification, then, is according to the power or strength of the irradiating field,  $H_2$ . While the intensity of the observing field  $H_2$  is generally kept as small as possible to prevent saturation and as high as possible for a good signal to noise ratio, the intensity of the irradiating field,  $H_2$ , has three possible ranges:

(1) Low-power or weak irradiation such that:

$$(1/T_2)_X < \gamma_X H_2 \ll |2\pi J(AX)| \quad (36)$$

Since low-power irradiation generally only causes perturbations in the spin system, this is usually called "tickling." This is generally used in INDOR (175) and

transitory selective irradiation (TSI) (174 and 178) experiments.

(2) Strong perturbation of the multiplet structures:

$$\nu_X H_2 \gtrsim |2\pi J(AX)| \quad (37)$$

This is the condition necessary to completely collapse a multiplet and hence is called "decoupling." Its greatest application has been in the simplification of complex spectra by removing certain couplings (174 and 179).

(3) Saturation:

$$(\nu_X H_2)^2 T_1 T_2 > 1 \quad (38)$$

Application of  $H_2$  power at this level causes a redistribution of the energy level populations which results in intensity changes (either increase or decrease) of certain lines in the A multiplet, or if Condition (37) holds, of the collapsed multiplet (174, 178 and 179). If this Condition (38) is met while a double resonance experiment of Type (b) is performed, then this is termed a generalized nuclear Overhauser effect (NOE) (174, 175, and 178 - 181).

Before proceeding with more detailed descriptions of tickling, INDOR, TSI and NOE, the aspects of spin decoupling should be pointed out. It may be recalled that proton exchange (Section IIA) and quadrupolar relaxation effects (Section IIB) both cause collapse of spin multiplets which appears to be analogous to spin

decoupling, Condition (37). In actuality, these three phenomena have quite different origins. A clue to this difference is the rather complex spectra obtained from intermediate values of  $H_2$  and  $\omega_2$  in decoupling experiments, whereas intermediate exchange rates and relaxation rates produce very simple partially coalesced spectra (174 and 179). Another point to be emphasized is that spin decoupling does not arise from saturation of the X group resonance as can be seen by Conditions (37) and (38). The decoupling process involves the orientation of the magnetization vectors and saturation of the X group is only a side effect (179 and 182).

At this point, we shall quickly look at the important features of the NMDR experiments mentioned above. The common feature of them all is that they may be applied to either homonuclear or heteronuclear spin systems.

Spin tickling, Case (1), may be conducted in either field (a) or frequency sweep (b) modes, the latter being the best because the point of irradiation in the X multiplet may be controlled. The result of this, is that lines sharing a common energy level will be split into doublets. The amount of splitting depends on whether or not the transitions between energy levels giving rise to the line are progressive (in series) or regressive (in parallel).

There are a number of limitations to this technique. First, it works very well for first-order spectra and when  $\omega_2$  is applied to well separated non-degenerate lines. For spectra with many lines, it is a small task to see which are affected and which aren't; in addition, overlapping lines increase the difficulties and effects on lines broadened by a quadrupolar nucleus such as  $^{14}\text{N}$  may be undetected (174 and 175).

The TSI experiment is performed in field sweep mode (a), and at low power such as Case (1). This experiment is executed by applying  $H_2$  to a line in the X group after passing a line in the A multiplet and turning off  $H_2$  before reaching the next adjacent line in the A multiplet. Thus, for changes in the A spectrum to be observed, the sweep time from line  $A_n$  to  $A_{n+1}$  must be less than  $T_1(X)$ . The advantage of this over tickling NMDR is the ease of identifying the progressive and regressive transitions of non-degenerate lines. Progressive transitions show an intensity increase compared to the unperturbed spectrum, and a deflection above the baseline, whereas regressive transitions show an intensity decrease and a deflection below the baseline (174). The difference between TSI and NOE is that for TSI  $H_2$  is given by Case (1); also, TSI is usually conducted in field sweep (a),

and  $H_2$  is only transitory (174 and 178). The difficulty is that each non-degenerate line in the A group must be observed and interpretation for closely lying lines or second-order spectra will not be simple.

NOE experiments are performed in the frequency-sweep mode (b) and with  $H_2$  amplitude sufficient for saturation, Case (3). This is different from TSI both in the irradiating amplitude  $H_2$  and the fact that  $H_2$  is applied continuously to a line in the X multiplet (178). The major limitation in the use of NOE is that  $T_1(A)$  must be greater than  $T_1(X)$  (174, 178-181). The general characteristics of INDOR have been given, namely frequency sweep of a special kind (c) and the relatively low  $H_2$  power of Case (1). As for TSI, the time required to sweep from one line,  $X_n$ , to another,  $X_{n+1}$ , is shorter than the relaxation time  $T_1(A)$  (174). Again, as for TSI, regressive transitions show a decrease (deflection below the baseline) while progressive transitions show an increase (deflection above the baseline). This is an advantage over the tickling method. A major advantage over both spin tickling and TSI is that only those lines in the X group having a common energy level with the A line being observed are recorded (recall that in INDOR, Type (c),  $\omega_1$  is set on one line in the A multiplet). Thus, not only are multiplets not coupled with A undetected, e.g. L multiplets for which

$J(AL) = 0$ , but also lines in the X multiplet not connected with the particular A line being observed at  $\omega_1$  are also not detected (175 and 183). An additional application of INDOR is in the heteronuclear mode. Here one can make use of the strong inherent sensitivity of one nucleus while recording the spectrum of another of lower sensitivity. This was shown by Baker et al., who observed either  $^1\text{H}$  or  $^{19}\text{F}$  at  $\omega_1$  while sweeping  $\omega_2$  through spectrum of the desired nucleus, e.g.  $^{13}\text{C}$ ,  $^{14}\text{N}$ ,  $^{29}\text{Si}$  or  $^{31}\text{P}$  (176 and 177).

This then concludes the basic NMDR methods, techniques, and descriptions which will be necessary to discuss the applications of NMDR to nitrogen containing compounds. There are a number of other methods and techniques, such as pulsing (184 and 185) and modulating (186) the frequency, which were not discussed because their applications are quite limited. The theoretical background has also been neglected because the emphasis in the following will be on experimental results. Details of the theory can be found in the early and extensive review of Baldeschwieler and Randall (179) or the more up-to-date work of Hoffman and Forsen (174).

Throughout the following review, the notation of Baldeschwieler and Randall (179) will be used. This notation designates the observed nucleus first with the

irradiated nucleus second and in brackets,  $A-\{X\}$ ; e.g.  $^1\text{H}-\{^{14}\text{N}\}$  means that hydrogen was observed while  $^{14}\text{N}$  was irradiated.

The first  $^1\text{H}-\{^{14}\text{N}\}$  NMDR experiment performed was that by Piette, Ray and Ogg (187). It was of Type (a) Case (2) and the sole purpose was to remove partial  $^{14}\text{N}$  coupling which was broadening the hydrogen resonances as a result of an intermediate rate of  $^{14}\text{N}$  quadrupolar relaxation (cf. Section IIB). Thus, they were then able to measure all of the proton-proton coupling constants for pure formamide, and for various partially deuterated formamides in aqueous solution. As a result, they demonstrated the existence of a solvent effect on both chemical shifts and coupling constants and in addition proved the thesis of Roberts (8) that the broadening of NH proton peaks in pure amides arises from partially collapsed  $^1\text{H}-^{14}\text{N}$  coupling rather than from hydrogen-bonding, viscosity or intermediate proton exchange rates.

In a similar manner, Randall and Balderschwiler (132) used  $^{14}\text{N}$  decoupling to simplify the spectrum of N-methylformamide for complete analysis of proton chemical shifts and coupling constants. They obtained quantitative values for the solvent effects on the coupling constants and suggested an explanation of these effects. In addition

they performed  $^1\text{H}-\{^{14}\text{N}\}$  decoupling on *N,N*-dimethylformamide, acetamide and *N*-methylacetamide, but were unable to resolve all the proton-proton couplings. More recently Kamei (188) was able to completely decouple  $^{14}\text{N}$  and so measure the proton chemical shifts and coupling constants for formamide, acetamide and *N*-methylacetamide.

Another example is the  $^1\text{H}-\{^{14}\text{N}\}$  decoupling of pyridine and pyridinium ion, in order to obtain better resolved proton spectra so that computer fitting of the spectra would be easier. This was done by Merry and Goldstein (189), who were measuring changes in the proton coupling constants with protonation, and by Castellano et al., (190) who wanted a well resolved spectrum in order to obtain very accurate proton chemical shifts and coupling constants.

A more sophisticated use of decoupling is to prove that coupling exists between two sets of nuclei. Hetero-nuclear decoupling,  $^1\text{H}-\{^{14}\text{N}\}$ , was used by Anderson, Baldschwieler, et al. (71) to prove that the triplet fine structure of the methyl group of aqueous tetraethylammonium (4Et) bromide arises from large long range  $^1\text{H}-^{14}\text{N}$  coupling and was confirmed by Milner and Turner (185) and by McFarlane (149). Whereas Anderson and Baldeschwieler (71) could detect no effect of  $^{14}\text{N}$  decoupling on the methylene of

the tetraethylammonium ion, McFarlane (149) reported a 4% intensity increase on decoupling  $^{14}\text{N}$ . McFarlane thus proved that the slight broadening of the methylene peak in the single-resonance spectrum is due to unresolvable  $^1\text{H}$ - $^{14}\text{N}$  coupling. In addition, by decoupling  $^{14}\text{N}$ , McFarlane (149) definitely proved that the triplet structure of the proton peaks of tetramethylammonium ion (25) and of isonitriles (85) is due to  $^1\text{H}$ - $^{14}\text{N}$  coupling. In a similar manner, Lehn and Seher (76) both simplified the spectra and proved the presence of  $^1\text{H}$ - $^{14}\text{N}$  coupling in five trimethyl (substituted vinyl) ammonium salts by  $^1\text{H}$ - $\{^{14}\text{N}\}$ . Most recently, Hampson and Mathias (87) used  $^1\text{H}$ - $\{^{14}\text{N}\}$  decoupling to prove definitely that the fine structure of certain nitramines (86) arises from proton-nitrogen coupling.

The last example leads to a third use of NMDR. Since  $\omega_1$  and  $\omega_2$  are known very accurately and since  $\omega_2$  must be at the center of the X multiplet for optimum decoupling, the difference,  $\omega_1 - \omega_2$ , gives a very accurate value for the chemical shift between the A and X multiplets. This technique is extremely useful for two major reasons, first, the accuracy just mentioned and, second, it permits location of peaks which may be hidden, as in homonuclear decoupling, or unobserved, as in the case of heteronuclear decoupling. An example of homonuclear decoupling is given

by Kowalewski et al. (175), who performed  $^1\text{H}-\{^1\text{H}\}$  decoupling on 3-acetylpyridine. By means of homonuclear INDOR they were able to determine accurately all the frequencies of the doublets of the hydrogens at the 2 and 6 positions even though these were so broadened by the pyridine nitrogen as to be unresolvable in the single-resonance spectrum. Other examples are given in the reviews (174 and 179). For heteronuclear NMDR chemical shift determination, the A multiplet is observed while the X nuclei are not observed,  $\omega_2$  being at a very different radio frequency. Baldeschwieler and Randall (191) were the first to demonstrate this technique for obtaining nitrogen chemical shifts by  $^1\text{H}-\{^{14}\text{N}\}$ . They did field-sweep decoupling, NMDR Type (a) Case (2), on ammonia, ammonium ion, pyridine and pyridinium ion (incidentally, a printing error has been pointed out (182) in (191); the figures are mislabeled and incorrect values for the chemical shifts are given in (191) but appear correctly in the review (192).). Briefly, the method is to obtain the value of  $\omega_2$  for optimum  $^{14}\text{N}$  decoupling of some reference compound, such as  $\text{NH}_4^+$ , while observing the hydrogen spectrum, and then to scan the other nitrogen compounds again noting the value of  $\omega_2$  for optimum decoupling. The difference between

these latter  $\omega_2$  values and the  $\omega_2$  of the reference  $\text{NH}_4^+$  are the  $^{14}\text{N}$  chemical shifts with respect to the ammonium nitrogen. The chief advantage of this method is that it makes use of the inherently greater sensitivity of hydrogen NMR while obtaining the  $^{14}\text{N}$  "spectrum," hence gives a better signal-to-noise ratio. At about the same time as the work of Baldeschwieler and Randall (191), this method was independently proposed by Glasel, Jackman and Turner (193). This technique was used by Hampson and Mathias for obtaining the  $^{14}\text{N}$  chemical shifts of twenty-seven primary and secondary amides (194) and six thioamides (109), using a modified INDOR method, Type (c) Case (1). Thus, in concluding we come to the example which brought us on the subject of chemical shifts by NMDR, the  $^{14}\text{N}$  decoupling of nitramines by Hampson and Mathias (87). Nitramines have two nitrogen atoms in different chemical environments,  $\text{R}_2\text{NNO}_2$ . The  $\omega_2$  frequency necessary to decouple  $^{14}\text{N}$  from the R group fell in range of nitro group chemical shifts and was over 100 ppm different from amine chemical shift values. The NMDR experiment clearly shows that the alkyl group proton coupling is to the nitro group nitrogen rather than the amino nitrogen.

The most effective way of obtaining chemical shifts from NMDR, particularly of the heteronuclear variety, is by

2

3

4

1

2

t

c

1

0

0

a

t

w

n

f

n

1

c

e

A

B

b

br

INDOR. Baker et al. (176 and 177) have shown how the complete spectrum of the unobserved nucleus can be recorded by setting  $\omega_1$  on a line in the A spectrum which is spin coupled to X. For example, they obtained the  $^{13}\text{C}$  spectrum of trifluoroacetic acid by observing  $^{19}\text{F}$ , the  $^{29}\text{Si}$  spectrum of tetramethylsilane by  $^1\text{H}\{-^{29}\text{Si}\}$  decoupling, the  $^{31}\text{P}$  spectrum of trimethylphosphate by  $^1\text{H}\{-^{31}\text{P}\}$  decoupling and, of interest here, the  $^{14}\text{N}$  spectrum of the ammonium ion by  $^1\text{H}\{-^{14}\text{N}\}$  decoupling. The nature of the INDOR method permits coupling constants to be very accurately obtained.

Baldeschwieler and Anderson (88 and 144) showed that field-sweep double resonance, Type (a) Case (1), was a sensitive method of accurately determining the nitrogen resonance frequency provided that a theoretical fit of the observed partially decoupled spectrum could be made. Baldeschwieler (144) confirmed this by performing  $^1\text{H}\{-^{14}\text{N}\}$  decoupling on ammonium- $^{14}\text{N}$  ion and  $^1\text{H}\{-^{15}\text{N}\}$  decoupling on ammonium- $^{15}\text{N}$  ion. Actually the first NMDR experiments on  $^{14}\text{N}$  and  $^{15}\text{N}$  ammonium ion were done by Anderson, Pipkin and Baird (143). Later, Anderson and Baldeschwieler (88) applied the method to  $^{14}\text{N}$  ammonia but found that, since they did not take into account the broadening due to nitrogen relaxation, their accuracy was

limited to  $\pm 1$  Hz and that experimentally  $H_2$  was limited to low values, Case (1). The basic method has been outlined by Anderson (195), who pointed out that it only works for the field-sweep type of NMDR because values of  $\omega_2$  above and below optimum decoupling yield mirror-image spectra (thus "point" to the correct  $\omega_2$ ), whereas the frequency-sweep type of NMDR yields symmetric identical spectra for values of  $\omega_2$  above and below optimum decoupling.

As a consequence of being able to determine the optimum decoupling frequency in heteronuclear NMDR, one can very accurately measure the frequencies of both nuclei. Dividing one by the other, one is thus able to obtain a ratio of the gyromagnetic ratios with an accuracy of better than 1 part in  $10^8$ . This is a minor application of NMDR and the values of  $\gamma(^{14}\text{N}) / \gamma(^1\text{H})$  and  $\gamma(^{15}\text{N}) / \gamma(^1\text{H})$  obtained from the ammonium ion were reported by Anderson et al. (143). Baldeschwieler (144) later reported slightly more accurate values for these and Baker (176) reported a value for  $\gamma(^{14}\text{N}) / \gamma(^1\text{H})$  in agreement with that of Baldeschwieler.

Now we come to the most sophisticated application of NMDR, the determination of relative signs of coupling constants and, very closely related to it, the determination of the energy level arrangement of the spins.

S

:

A

A

P

S

S

I

C

A

C

S

A

S

M

A

A

A

B

I

A

A

A

A positive coupling constant is defined as resulting from an interaction which minimizes the spin coupling energy when the two nuclear spins are antiparallel and, conversely, a negative coupling constant results from an interaction minimizing the energy when the spins are parallel (174). First-order spectra remain invariant to sign reversal of coupling constants and, as a consequence, spectra calculated theoretically with various sets of relative signs will all have the same appearance. Second-order spectra, on the other hand, have a quite different appearance for each set of relative signs and so theoretically calculated spectra can be used to obtain relative signs. Now we see the real power and utility of NMDR, as it can be applied to obtain relative signs of both first- and second-order spectra and, thus, is the only method of obtaining relative signs for first-order spectra. Absolute signs are usually obtained from NMDR by relating all signs of the coupling constants to one which is known absolutely and the reference is  $^1J(^1H-^{13}C)$  which has been calculated theoretically by molecular orbital theory (130) to be positive.

The technique may be explained very briefly with an example. Consider the three-spin system ALX in which all three types of nuclei are spin coupled with each other

and all couplings are resolvable, also the chemical shifts are large so that no multiplets overlap. Irradiation with  $H_2$  (Case (2)) of the low field line of A can have two effects on the L multiplet. If the low field lines of LX multiplets change in intensity, then  $J(AX)$  and  $J(LX)$  have the same sign, as double irradiation affects those A and L nuclei connected with the same X spin state. On the other hand, if irradiation of the low field line of A had produced perturbations in the high field LX multiplets, then  $J(AX)$  and  $J(LX)$  are of opposite sign. Because lines appearing in the resonance spectrum are due to transitions between energy levels of the spin states, and as we have just seen here, resonance lines arising from spin states in common can be detected, the application of NMDR to the construction of an energy level diagram is straightforward. Recall also, that use of low  $H_2$  power, Case (1) with either spin tickling or INDOR, can distinguish whether the energy levels in common are progressive or regressive. More details on the methods of relative sign determination and energy level diagram construction can be found in the two reviews (174 and 179) and in a short note by Friedman and Gutowsky (196).

Kowalewski, de Kowalewski and Ferra (175) used

homonuclear INDOR,  $^1\text{H}-\{^1\text{H}\}$ , to construct the energy level diagram and prove the relative signs of the coupling constants in a substituted pyridine. Using the same technique, Baker (183) performed  $^{19}\text{F}-\{^{19}\text{F}\}$  decoupling experiments on the compound trans- $\text{CClFBrCFBrCF}=\text{CFCI}$  for the same two purposes. McFarlane (160) determined the absolute sign of  $^3\text{J}(^1\text{H}-^{15}\text{N})$  as negative by relating all signs to  $^1\text{J}(^1\text{H}-^{13}\text{C})$ , obtaining the relative signs by  $^1\text{H}-\{^{13}\text{C}\}$  and  $^1\text{H}-\{^{15}\text{N}\}$  NMDR experiments on acetonitrile with 96%  $^{15}\text{N}$  enrichment. In a similar manner, from  $^1\text{H}-\{^{13}\text{C}\}$  and  $^1\text{H}-\{^{14}\text{N}\}$  experiments, he (149) obtained the absolute signs of  $^2\text{J}(^1\text{H}-^{14}\text{N})$  and  $^3\text{J}(^1\text{H}-^{14}\text{N})$  in methyl-, ethyl-, and t-butylisocyanides and in tetraethylammonium hydroxide. By means of  $^1\text{H}-\{^{15}\text{N}\}$  decoupling, Bourn, Gillies and Randall (154) were able to obtain the relative signs of  $^2\text{J}(^1\text{H}-^{15}\text{N})$  and  $^4\text{J}(^1\text{H}-^1\text{H})$  for N,N-dimethylformamide- $^{15}\text{N}$ . From the relative signs of  $\text{J}(^1\text{H}-^{15}\text{N})$  and  $\text{J}(^1\text{H}-^1\text{H})$  in other formamides, and from the knowledge that  $^1\text{J}(^1\text{H}-^{15}\text{N})$  is absolutely negative, they were able to assign the absolute signs of all the other coupling constants.

The relative signs of several proton-nitrogen coupling constants were determined by  $^1\text{H}-\{^1\text{H}\}$  NMDR. Bourn and Randall obtained the relative signs of all the

$J(^1\text{H}-^{15}\text{N})$  values for formamide- $^{15}\text{N}$ , N-methylformamide- $^{15}\text{N}$  (162) and N,N-dimethylformamide- $^{15}\text{N}$  (151). Ohtsuru and Tori (152) found all the  $^{14}\text{N}$ -vinyl proton couplings to be of the same sign for trimethylvinylammonium bromide.  $^2J(^1\text{H}-^{14}\text{N})$  was demonstrated to be opposite in sign to  $^3J(^1\text{H}-^{14}\text{N})$  for ethylisonitrile and tetraethylammonium iodide by the frequency sweep NMDR, Type (b) Case (1), experiment of Maher (150). Recently Tori, Ohtsuru and colleagues (170) reported the absolute signs for  $^2J(^1\text{H}-^{15}\text{N})$  and  $^3J(^1\text{H}-^{15}\text{N})$  for quinoline- $^{15}\text{N}$ , its ethiodide and its N-oxide showing that complexing the nitrogen and solvents not only change the magnitude but also the sign of  $^1\text{H}-^{15}\text{N}$  couplings.

A summary of the applications of NMDR which were discussed above will now be given. First, a spectrum can be simplified by removing couplings obscuring lines which it is desired to measure. Second, definite proof of which nuclei are coupling and, hence, definite proof of structure can be obtained. Third, by completely decoupling and collapsing a multiplet, chemical shifts may be determined, since this is the irradiation frequency necessary for optimum decoupling. Fourth, the frequencies from heteronuclear decoupling provide very precise ratios of

gyromagnetic ratios, because electronic counters are available which can measure frequency to ten or twelve significant figures. The fifth and most sophisticated application is the determination of relative signs of coupling constants and construction of the energy level diagram.

### III. EXPERIMENTAL

#### A. Purification of Compounds

For the  $^{14}\text{N}$  spin-lattice relaxation time experiments alkylammonium chloride salts (1Me3H, 2Me2H, 3Me1H, EtMe2H, 1Et3H, 2Et2H, and 3Et1H where 1Me3H =  $\text{CH}_3\text{NH}_3^+$  etc.) were obtained as reagent grade chemicals from the Eastman Kodak Company. Although Heilbron (197) recommends recrystallizing these salts from ethanol or ethanol-ether mixtures, absolute ethanol-isopropyl alcohol was found to be a better solvent system. In most cases one recrystallization was found to be adequate but for a few compounds two or three recrystallizations were necessary. In one case recrystallization proved to be detrimental and attempts to purify the ethylmethylanmonium salt (EtMe2H) seemed to hasten decomposition since the material became very dark and an oil formed. Other methods of purifying this salt also proved futile and, because its purity was in doubt, a complete relaxation time study was not made on this substance. The recrystallized products were then

see

wee

see

see

see

see

see

see

see

see

see

see

see

see

was

see

see

see

in a 2

stored in an evacuated desiccator over  $P_2O_5$  for several weeks prior to making up the aqueous solutions and obtaining the spectra. Solutions were acidified with conc. HCl prior to final dilution and pH measurement. pH values were measured with a Sargent Model LS pH Meter after calibrating with a standard pH = 1.0 solution. The final concentrations and pH values are given in Table 9.

Table 9. Concentrations and pH values for solutions of substituted ammonium salts used in this work.

Compound	Conc.	pH	Compound	Conc.	pH
4H	5.04 M	0.2	EtMe <sub>2</sub> H	5.00 M	< 0.5
1Me <sub>3</sub> H	5.11	< 0.5	1Et <sub>3</sub> H	5.00	< 0.5
2Me <sub>2</sub> H	5.00	< 0.5	2Et <sub>2</sub> H	4.80	0.4
3Me <sub>1</sub> H	4.80	0.4	3Et <sub>1</sub> H	4.07	0.8
4Me	3.23	---	4Et	~3.00	---

2,2,2-Trifluoroethylamine hydrochloride (TFEA·HCl) was prepared essentially by the method of McKay and Vavasour (198) and Bissell and Finger (199). 5g of trifluoroethylamine (Pierce Chemical Co.) was dissolved in 30 ml of ether. Dry HCl gas was slowly bubbled through the solution in a 2 X 50 cm "test tube," which was cooled by an ice bath.

After an hour bubbling was stopped and the ether decanted from the white precipitate. The product was washed with fresh ether, recrystallized from absolute ethanol-ether and stored in vacuo over  $P_2O_5$  for several days. A 4.36 M aqueous solution was made up and acidified ( $pH < 0.0$ ), however, the  $TFEA \cdot HCl$  is such a strong acid,  $pK_a = 5.6$  (200), that rapid proton exchange is still occurring and no separate NMR signal for the  $NH^+$  group can be detected. Attempts to reduce proton exchange by dissolving  $TFEA \cdot HCl$  in conc.  $HCl$  proved unsuccessful as the  $TFEA \cdot HCl$  is much less soluble in conc.  $HCl$ .

Benzylamine hydrochloride was prepared from benzylamine (Eastman Kodak Co.) by the method outlined above. It also was recrystallized from absolute ethanol-ether and stored under vacuum over  $P_2O_5$ . Here again the solubility in water was so poor that the signal from the aromatic hydrogens could barely be seen.

The ammonium salts (chloride, iodide, nitrate, sulfate, acetate and formate) were high purity reagent grade chemicals and were used without further purification. As a precaution these materials were stored for a period of several days in a vacuum desiccator over  $P_2O_5$ , prior to use.

Ammonium trifluoroacetate was prepared by slowly bubbling gaseous ammonia through a 50% aqueous solution of trifluoroacetic acid in a test tube which was cooled by an ice bath. After several hours, the ammonia was stopped and the excess ammonia and water removed in vacuo. The salt was recrystallized from absolute ethanol-isopropyl alcohol, then stored over  $P_2O_5$  in a vacuum desiccator for a few days until ready to use.

Most solvents were used without special preparation as the reagent grade materials were pure enough for NMR purposes. Special care was taken in a few cases as listed below.

Glacial acetic acid and trifluoroacetic acid were dried by adding a few drops of the corresponding anhydrides just before preparing solutions in these solvents.

Dimethylsulfoxide (DMSO) was stored over Linde Molecular Sieve 5A for several days. It was shown to be quite dry by scanning the NMR spectrum at high gain when no proton signal from water protons could be seen. On adding one drop of water per 5 ml. of DMSO the OH resonance could just be detected.

Commercial nitromethane was purified by the procedure of Clarke and Sadler (201) followed by refluxing

for 24 hours over BaO under a nitrogen atmosphere. The nitromethane was then distilled from the reflux flask and the fraction boiling at 97-98°C/750 mm. was used.

All the solutions of the ammonium salts studied were saturated, as solubility was usually poor. Exceptions were 100% sulfuric acid, which was made 2.5 M with ammonium sulfate, and aqueous ammonium chloride which was made 5.0 M. A few drops of conc. HCl was added to the latter solution before dilution to the mark in a volumetric flask and the pH was measured and found to be 0.2 whereas an unacidified 4.99 M solution of ammonium chloride had a pH of 4.22.

#### B. NMR Spectrometers

The two NMR spectrometers used in the course of these investigations were the DA-60-IL and the HA-100, both manufactured by Varian Associates (202). Both of these instruments had the V-4354-Internal Reference Field-Frequency Stabilization Unit, which permits field or frequency sweep. In addition, homonuclear double resonance may be performed with this unit provided that an audio-frequency (for  $\omega_2$ ) is supplied from an external oscillator (either a Hewlett-Packard Model 200CD or Model 200ABR

Audio Oscillator was used for this purpose). Details of the operation of this unit were given by Freeman (203a) and systems similar to it have been described in the literature (203b-f). Both instruments were located in an air-conditioned room and the 110 VAC to each console was maintained constant with a Stabiline Voltage Regulator.

The HA-100 was a standard instrument. This particular one had an electromagnet with 12" diameter polepieces, the tapered pole caps allowing a magnet gap of only 0.75", a Varian V-2100 Power Supply provided regulated current and a V-3506 flux stabilizer gave further stabilization of the magnetic field. An audio frequency counter (202) was supplied with the instrument. A V-4343 Temperature Control Unit was used with the V-4333 NMR Probe for variable temperature experiments. The DA-60-IL instrument had been converted from a DP-60, which in turn had been converted from an HR-40 spectrometer, and both energizing coils on the V-4012A Electromagnet had been replaced. This system contained a V-3521 Integrator and Baseline Stabilizer Unit and as a result required an attenuator when using the V-4333 NMR Probe. For homonuclear decoupling and variable temperature work, the V-4333 NMR Probe (tuned for 60 MHz), which was designed to be used with the V-4354 "lock box,"

the V-4343 Temperature Controller, an external audio oscillator (either HP Model 200CD or 200ABR), and an external audio counter (either HP-Model 521A or 5245L electronic frequency counter) were used. For heteronuclear decoupling work, a specially modified V-4331A NMR Probe (containing two transmitter coils), an NMR Specialties SD-60/EC-60 unit, an audio oscillator (HP-200CD or 200ABR), an audio counter (HP-521A or 5245L), and an additional cathode ray oscilloscope (CRO) were used. Details on the operation of these follow (III C and III D).

A Varian C-1024 time averaging computer, was used to smooth out the noise on samples where the NH protons gave a broad signal which could be seen as a gradual and reproducible drift above the baseline (e.g. 3Me1H, 2Et2H and 3Et1H). For this situation, only 10 to 20 scans of the C-1024 were necessary.

#### C. Homonuclear Decoupling- Variable Temperature Experiments

The internal reference system operates by locking the magnetic field and the radio frequency with a signal obtained from some peak in the spectrum of the sample. For this purpose hexamethyldisiloxane was used. Since it is immiscible with the aqueous solutions under

investigation, it was contained within a sealed capillary tube which was held concentric to the NMR sample tube by means of two Teflon plugs. The capillary of disiloxane was sufficient to generate a strong lock signal; in addition, disiloxane had a boiling point well above the highest temperature used. It should be mentioned that other methods of generating a lock signal were attempted. For example, the water soluble sodium 3-(trimethylsilyl)-propyl sulfonate was tried but the lock signal was so weak that the system kept jumping lock to the alkyl or water peak in the spectrum. Locking on the solvent water peak was also tried, but its lock signal was so intense that noticeable sidebands fell on the peaks of interest.

Homonuclear decoupling was carried out in the frequency-sweep mode for the reason given in Section II E. Since the Varian system has some convenient features about it which make decoupling particularly easy, these will be pointed out.

The first step in the homonuclear decoupling-variable temperature experiment was setting the V-4343 at the approximate temperature and making a rough check of temperature with the appropriate calibration standard (ethylene glycol at high temperatures, methanol at low temperatures)

and the chart supplied with the V-4343. Next, the sample of interest was placed in the probe and allowed to reach thermal equilibrium for about 20 min.; since the acidified aqueous alkylammonium salts are conductors, leakage had to be adjusted with the probe paddles at this point. The third step was to scan the complete spectrum (sweep range 500 Hz or 10 Hz/cm, cf.-Figure 5, Section IV A). The recorder arm was mechanically linked to the sweeping frequency ( $\omega_1$ ), hence the recorder was positioned on one side of the alkyl multiplet and the selector set to D1, or difference one, position. This is the difference between sweeping frequency ( $\omega_1$ ) and locking frequency ( $\omega_3$ ), i.e.,  $D1 = \omega_1 - \omega_3$ , and its value was read on the audio frequency counter, and noted on the spectrum. The recorder was then moved to the other side of the multiplet and D1 again read, noting its value on the spectrum. Having done this, the spectrum was then spread out (i.e., a narrower sweep range, 250 Hz or 5 Hz/cm, was selected) and the  $\text{NH}^+$  peaks moved onto the chart paper (cf.-Figure 6, Section IV A). Since the alkyl multiplet could no longer be seen, the importance of the D1 values read previously is now apparent. The fourth step was the actual decoupling to remove the fine structure resulting from coupling with

alkyl protons which was present in the NH peaks. This was accomplished in the following manner. An audio frequency from an external oscillator ( $\omega_2$ ) was introduced by switching to SPIN DECOUPLE mode while simultaneously adding about 10db more RF power on the 60 MHz RF Unit in order to restore power to all sidebands now that an additional one had been added. Now the selector was set to D2, or difference two, position, which gave the difference between the external (or decoupling) frequency and the locking frequency, i.e.,  $D2 = \omega_2 - \omega_3$ . The external oscillator was varied to obtain a value of D2 corresponding to one of the values of D1 read before and the NH spectrum scanned. Next the external oscillator was changed, so that D2 approached the other value of D1, and the NH spectrum again scanned. Again the external oscillator was changed with D2 approaching the other D1 value, the NH spectrum scanned, and the whole process repeated until D2 reached the second D1 value. Thus, the irradiating oscillator ( $\omega_2$  read by D2) slowly marched through the alkyl multiplet and we detected this by observing the NH multiplets (cf. Figure 10, Section IV A). The NH multiplet patterns show sharpening as  $\omega_2$  approaches the center of the alkyl group, should be sharpest when  $\omega_2$  is at the center, and broaden out more as

$\omega_2$  approaches the other side of the alkyl multiplet. By looking for the sharpest NH group, the optimum frequency for decoupling could be determined. The external oscillator was then set to this value by reading D2. Now the amplitude of the external oscillator was varied, each time scanning the NH group. This was done until no further sharpening in the NH group could be detected on increasing the amplitude. The correct decoupling amplitude,  $H_2$ , had then been achieved, and the spectrum contained only the nitrogen single-bond proton couplings. The fifth and final step was to get an accurate measure of the temperature and this was done by putting the appropriate temperature calibration standard in the probe. After thermal equilibrium was reached, the peak was recorded and D1 values on each side measured. At a later time the position of this peak was calculated. The temperature was then calculated from the appropriate linear equation listed below since the calibration curves supplied with the V-4343 were found to be in error (204):

$$\text{TEMP} (^{\circ}\text{C}) = 191.7 - 1.076 (\text{AMEFRQ})$$

$$\text{TEMP} (^{\circ}\text{C}) = 191.9 - 1.017 (\text{ETGFRQ})$$

where AMEFRQ is the separation between the two methanol peaks in Hz and ETGFRQ is the separation between the two

ethylene glycol peaks in Hz. As these two equations were derived for a spectrometer frequency of 100 MHz, the corresponding values of peak separations obtained from the DA-60-IL had to be divided by 0.6 before using them in the appropriate equation to obtain the temperature. Corrections similar to this have been noted by others (205a) and other NMR "thermometers" have been used (205b and c).

A 36:1 gear reducer was installed on the external audio frequency oscillator, which was used to generate the irradiating frequency  $\omega_2$ . With this attachment  $\omega_2$  could be changed in 1Hz increments; thus, "marching" across the alkyl group was under much better control than using an unmodified oscillator.

From the foregoing description, it can be seen that a number of hours were consumed in obtaining one good decoupled spectrum. The spectrum then had to be analyzed or decomposed to yield the usable parameters, coupling constants, chemical shifts, and relaxation times. Proton-proton coupling constants were obtained directly from the spectra, utilizing calibration markers obtained from D1 readings. These coupling constants were obtained from spectra in which the peaks for the alkyl groups were spread out, e.g., a 50 Hz sweep width or 1 Hz/cm (cf.

Figure 13, Section IV A). Some proton-nitrogen coupling constants were read directly from the spectra whereas others were obtained from the computer output. This procedure together with that used for determination of the relaxation times, which also came from the computer fit is described separately (Section IV B).

In cases where the  $^{14}\text{N}$  relaxation time was short, i.e., the NH triplet in the proton spectrum was coalescing or was a single broad peak, decoupling of the alkyl protons had no observable effect. This is reasonable, because no multiplet from coupling of the alkyl group with the NH protons could be detected throughout the temperature range. This was found to be true for 3Me1H, 2Et2H and 3Et1H. However, what was saved in decoupling effort had to be spent in time averaging. Since there are fewer hydrogens on the nitrogen, and also the concentrations are lower, the signal/noise ratio for the  $\text{NH}^+$  group peak was poor. As a consequence, the intensities from spectra of this type would be of dubious value for comparison with computed spectra and it was necessary to use the Varian C-1024 to obtain smoother line shapes. The C-1024 was used for 3Me1H and 3Et1H when scanning on the DA-60-IL spectrometer and for 3Me1H, 2Et2H, and 3Et1H when scanning on the

HA-100 spectrometer, since the signal/noise ratio was poorer. Generally 15-20 accumulations in the C-1024 were sufficient to smooth the curves.

#### D. Heteronuclear Decoupling Experiments

For the purposes of heteronuclear decoupling,  $^1\text{H}$ - $\{^{14}\text{N}\}$ , a Spin Decoupler Unit, Model SD-60 (206) was employed. This unit operated at a nominal frequency of 4.33 MHz. Initial decoupling experiments were made by double tuning the V-4331A NMR Probe transmitter coil to oscillate both at 60 and 4.33 MHz. High 4.33 MHz power levels were required to decouple the ammonium protons, as can be seen from the magnitude of the coupling,  $1J(^1\text{H}-^{14}\text{N}) \approx 50\text{Hz}$ , and Equation (37). Consequently a large amount of heat was generated in the probe and this caused the leakage to vary, resulting in poor spectra. Another experiment with a second (4.33 MHz) transmitter coil and proper insulation, although not eliminating the problem completely, greatly improved the situation and showed the direction to move. Thus, it was decided to mount the second coil on a Dewar vessel concentric with, and in between, both the 60 MHz transmitter and receiver coils. Since care must be taken to insulate the system properly, it was decided to construct a complete variable temperature system and thereby be able

to carry out variable temperature-heteronuclear decoupling experiments.

A number of variable temperature systems have been described (207a-e). Two of these designs (207c and d) were abandoned because the fabrication was too involved and they were for wide-line rather than high-resolution work. Two others (207a and b) were rejected because the leads from the receiver coil are twisted when it is rotated and rotation is necessary to obtain minimum coupling to the surrounding transmitter coils. The design of Shafer (207e) was selected as most suitable because the receiver coil, leads, and female BNC connector are all attached to a tube and rotate together. The seal between this receiver coil insert and the Dewar vessel is made by a closely fitting Nylon bottom piece and gaskets (cf. detailed drawing in the upper right hand corner of Figure 1).

The 60 MHz receiver coil insert was made by mounting the coil on selected 8 mm O.D. quartz tubing cut 11 cm long. The tube was scratched on one end while three 2 mm dia. holes were burned through about 8 mm from the other end. The tube was then cleaned by washing successively with hot trisodium phosphate, water, aqua regia, water, concentrated aqueous ammonia, water and then oven dried. It was placed in a wooden jig which held it upright and

wrapped with uninsulated #30 copper wire (oxygen free, high conductivity) (three turns for a 60 MHz coil). One end of the wire was tied to a rubber band, which was then stretched around the back of the jig and tied with the other end of the wire so the wire was held under tension. Using Nylon thread as a spacer, the turns were moved close together and Craftsman epoxy cement (Sears, Roebuck & Co.) was applied and allowed to set for 4 hours, until the resin was tacky. The spacer thread was then removed and a very light coat of additional epoxy applied which was allowed to set overnight. The two ends of the coil were measured for proper length, cut, bent down, and one soldered to the outside "dimple" of a machined female BNC (UG-290/U). The tube and BNC were removed from the jig, carefully bending the lead over, and the other lead soldered to the center pin of the BNC. A Teflon "cup" bearing was inserted in the bottom end of the tube and epoxy smeared over the bottom of the BNC. The tube was put upright on the BNC and held in this position in the jig while the epoxy was allowed to cure overnight. It was then removed from the jig and placed in an oven at 70°C for an hour, after which the temperature was slowly (10°C per hour) raised to 120°C, in order to cure the epoxy cement.

The spacing between the windings is quite important. If the coil is wound tight without spacing, one can find two nulls on rotation but the paddles will have little or no effect on leakage adjustment. If the spacing is too wide, rotation nulling and paddle leakage control will be normal but such a coil has a poor  $Q$  and consequently the instrument will have poor signal-to-noise. After several failures, the best spacing was found to be the same as the diameter of the wire.

The 4.33 MHz transmitter coil attached to the outside of the Dewar vessel proved more of a challenge. After a few attempts to wind it with a continuous wire (insulated, #30 gauge copper) in the curved configuration, first on the Dewar vessel itself and afterward on a cardboard chart-paper center piece, a very simple method was used. First, the transmitter coil was wound, one-half section at a time. A jig, consisting of two pieces of plexiglass with a 2.0 cm by 3.0 cm rectangular brass spacer the thickness of the wire, was used for this purpose. One piece of plexiglass was notched so that epoxy cement could be applied in four places to the wound coil. The jig was held together by two bolts for easy dismantling after winding the coil, which had eight turns (211). After both half sections were made, they were bent (on the 2 cm sides)

to fit the curved contour of the Dewar jacket. The half sections were positioned on the Dewar jacket held in place by rubber bands and the epoxy cement applied. After the epoxy cement set, one lead from each half section was soldered together on the side while the other leads were brought around the back underneath the Dewar jacket sideneck.

Details about loop antennae (receiver coil), transmitter antennae, and characteristics of LC circuits are found in Terman's book (208). Another reference source for material of this general nature, as well as hints on construction techniques, is the "Radio Amateur's Handbook" (209). However, for details about coil construction and characteristics specific to NMR the best source is Sontif and Gabillard (210).

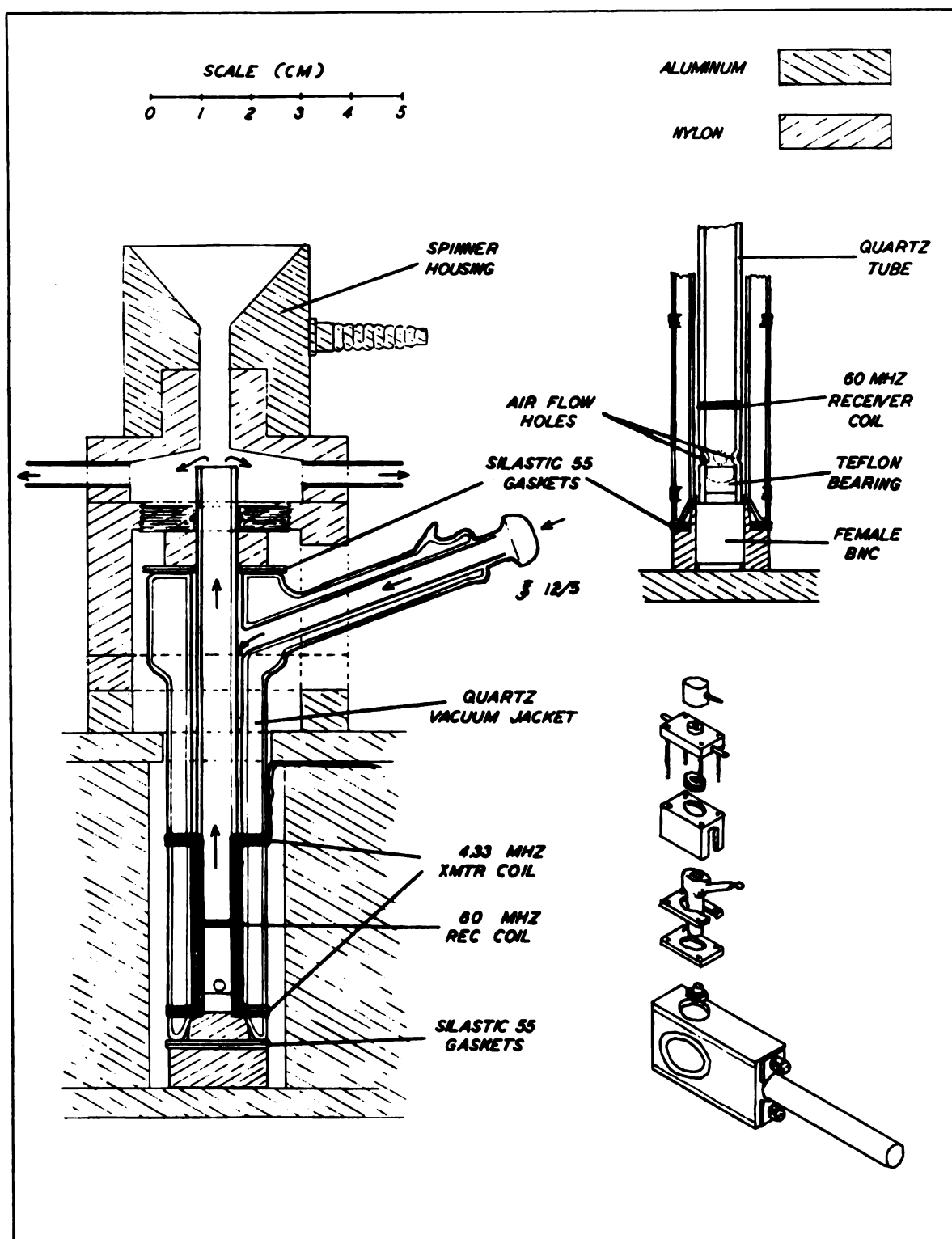
The Dewar jacket - 4.33 MHz transmitter coil was placed in the probe and one lead each from the 4.33 MHz and the 60 MHz transmitter coils were soldered to a ground lug inside the back of the probe. The other lead of the 4.33 MHz coil was soldered to one pin of the female Twinax connector at the rear of the probe body. To the second pin of this Twinax connector was soldered the other lead of the 60 MHz transmitter coil. The Dewar jacket was sealed to the top and bottom of the 60 MHz receiver coil by means of gaskets cut from Silastic 55 (Dow Corning, Midland, Michigan). The Dewar jacket and receiver coil were held in

place by a threaded piece at the top, which had an "O" ring to hold the receiver coil and provided pressure to lock the Dewar vessel in place. Details of this can be seen in Figure 1, left hand drawing.

A vacuum jacketed tube (Pyrex) was fabricated to hold the standard Varian heater sensor element. The V-4343 Temperature Controller Unit was used to regulate temperature. The superstructure for holding the Dewar jacket, receiver coil and spinner housing (see Figure 1) and the rig to hold the vacuum jacket and heater sensor (Figure 2) were machined according to blueprints kindly provided by Dr. Paul Shafer (207e).

The complete assembly can be seen in Figures 1, 2 and 3, however certain details should be pointed out. The rear connection of Tygon tubing to the heater-sensor jacket, as well as the ball-joint connection between the front of this and the receiver coil Dewar jacket, were insulated by wrapping with foam rubber (see Figure 3). The inside of the probe was cooled by passing air through a polyethylene tube in the receiver trimmer hole in the bottom of the probe (see Figure 3). This has a channel which goes into the receiver coil area (see detail, left-hand side of Figure 1). Tygon tubing was attached to the exit ports mounted above the receiver coil top and below the spinner housing bottom (see left-hand side of Figure 1). One of these can be seen in Figure 3. The purpose of this is to lead exit gas from the probe away from the magnet.

The  $^1\text{H}\{-^{14}\text{N}\}$  double resonance system consisted of an



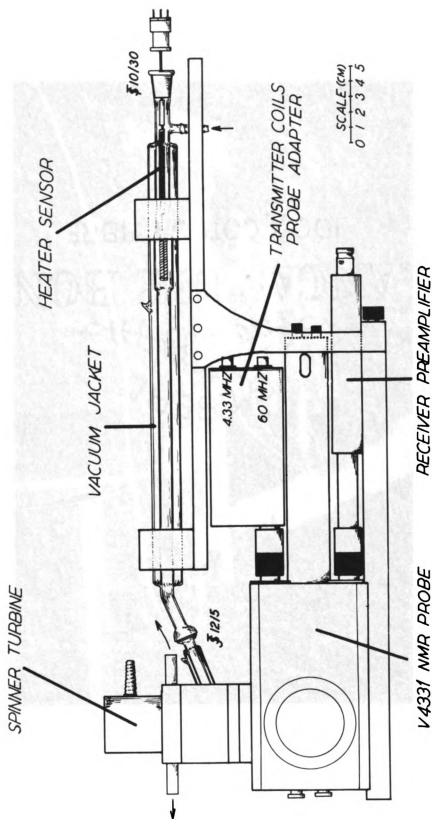


FIGURE 2. DETAIL OF MODIFIED PROBE FOR VARIABLE TEMPERATURE DECOUPLING EXPERIMENTS SHOWING RELATIVE POSITION OF SUPPORTING ACCESSORIES.

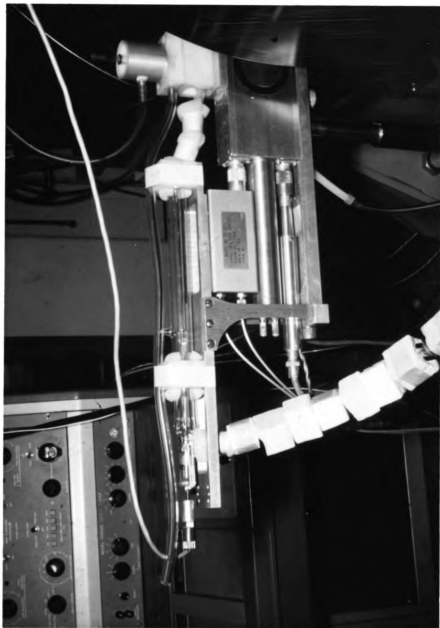


Figure 3. Photograph of the experimental heteronuclear double resonance system of Figure 2.

NMR Specialties, Model SD-60 RF oscillator, Model EC-60 heterodyne unit, an audio oscillator, an audio frequency counter, and a DuMont Model 274 Cathode Ray Oscilloscope (CRO). In addition, a probe adapter which allows adjustment of the LC ratio for each of the two transmitter coils was used. The connection of all of these units is shown in Figure 4.

The SD-60 generates a signal of about 4.33 MHz which could be varied continuously by means of the external audio oscillator. The 4.33 MHz frequency was generated by mixing the output from a variable frequency oscillator (VFO), about 5.38 MHz, with the output of a crystal oscillator at 9.71 MHz. The difference between the VFO frequency and the 5.37 MHz frequency the EC-60 was fed by a BNC "tee" connector both into the audio counter, for monitoring purposes, and into one side of a diode-varicap stabilization circuit (VFO control) in the SD-60 Unit. The output from the audio oscillator was fed into the other side of the stabilization circuit. Both sides of this stabilization circuit was monitored by means of the CRO, a lissajou pattern consisting of a distorted circle indicated stable RF oscillation. Since the stabilization circuit varicap was in parallel with the main tuning capacitor of the VFO section, a change in the audio

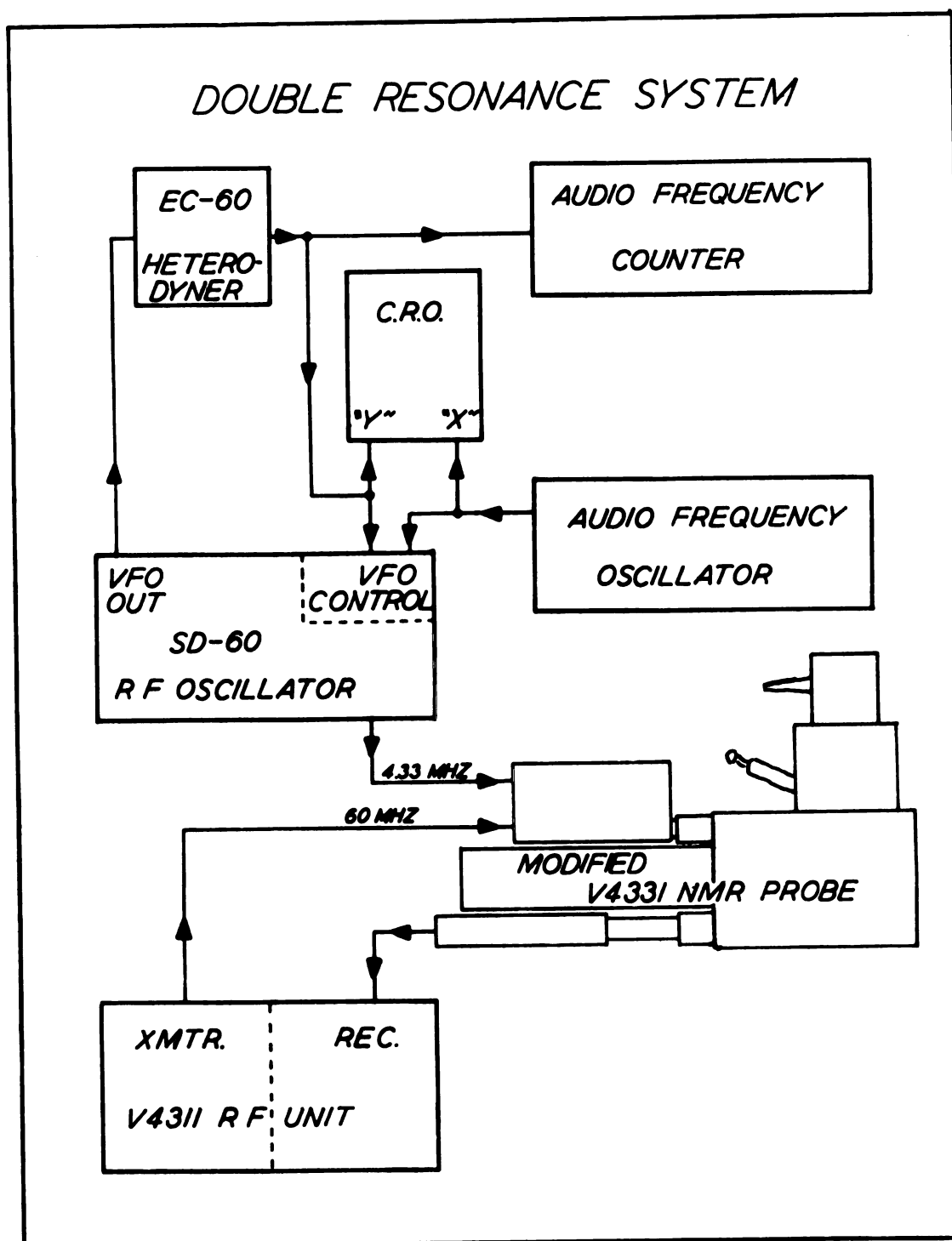


FIGURE 4. BLOCK DIAGRAM OF ELECTRONIC CONFIGURATION FOR HETERONUCLEAR DOUBLE RESONANCE EXPERIMENTS.

oscillator frequency caused a change in the VFO frequency and consequent RF output to the probe. For best stability of the system, the voltage of the EC-60 output ("Y" of CRO) should match that of the audio oscillator ("X" of CRO). Fine adjustment of the audio frequency was accomplished by means of a 36:1 gear reducer attached to the large frequency control of the audio oscillator.

This perhaps is a good place to mention something about the stability of the system. Heteronuclear decoupling with the system just described, in conjunction with the DA-60-IL system operating in frequency-sweep mode, requires the peak performance of a number of oscillators. There are three audio oscillators and five crystal-controlled radiofrequency oscillators in operation. At best a drift of 5 Hz (determined from variation in the  $^{14}\text{N}$  decoupling frequency for  $^1\text{H}-\{^{14}\text{N}\}$  decoupling of the ammonium ion) during a five-day period was measured and at worst 10 Hz over three days. When greater instabilities occurred, the trouble was traced to the HP-200CD oscillator and the HP-521A counter, both vintage models, in the 4.33 MHz system.

As a bonus from  $^{14}\text{N}$  decoupling studies,  $^{14}\text{N}$  chemical shifts were obtained by the method first suggested by Baldeschwieler and Randall (191) and used recently by Hampson and Mathias (109 and 194). This method was

described in Section IIE. As an example of the method, details of the  $^{14}\text{N}$  chemical shift measurement of  $1\text{Et}3\text{H}$  are presented. While observing the  $\text{NH}^+$  protons at a sweep width of 250 Hz (5 Hz/cm), the audio frequency of the 4.33 MHz system was changed from 12,649 Hz to 12,950 Hz, a total of 301 Hz in increments of about 33 Hz. The 249 Hz interval, from 12,651 Hz to 12,900 Hz, was then scanned at lower SD-60 RF power than before, incrementing the audio frequency every 10 Hz (e.g. for  $1\text{Me}3\text{H}$  see Figure 11, p.174 ). Comparing the decoupled spectra, the frequency of optimum decoupling for  $1\text{Et}3\text{H}$  is 12,805 Hz as noted by matching pairs on both sides of this value. Next, the  $\text{NH}^+$  proton spectrum of  $4\text{H}$  was scanned, while varying the audio frequency every 33 Hz from 12,301 Hz to 13,001 Hz for a total of 700 Hz. The SD-60 RF power was reduced and the audio frequency changed in 10 Hz from 12,610 to 12,900, the center of matched pairs being 12,740 Hz. The resulting chemical shift of the monoethylammonium ion from the reference ammonium ion is the difference of these two audio frequencies, 65 Hz or 15 ppm. The  $^{14}\text{N}$  chemical shifts of all the compounds were determined in this same manner, subtracting the audio frequency necessary for optimum decoupling of the ammonium ion from the optimum decoupling frequency of the alkyl ammonium ions, carefully noting the

sign. It was known from the  $^{14}\text{N}$  single resonance work of Evans and Richards (118), that 4Et and 4Me resonances occur at lower fields than that of the ammonium ion and thus their chemical shifts are negative. Consequently, all the  $^{14}\text{N}$  shifts found in this work conform to this convention. Another example of a similar use of the SD-60 is given by Stothers and Robinson (212), who performed  $^1\text{H}\{-^{31}\text{P}\}$  decoupling.

In the  $^{14}\text{N}$ -NMR spectrum of the ammonium ion, there are five lines, each with a 52 Hz interval (the  $^1\text{J}(^1\text{H}\text{-}^{14}\text{N})$  seen in the proton spectrum). Since it is possible to observe partial collapse of the proton spectrum when hitting any one of these five  $^{14}\text{N}$  peaks, a large frequency range (700 Hz) was tried first in order to insure hitting the correct position in the  $^{14}\text{N}$  spectrum for optimum decoupling, namely the center of the multiplet. Optimum decoupling can be noted since the proton peak will be most intense for this nitrogen decoupling frequency; also, equivalent nitrogen frequencies above and below this value will show exactly the same partially collapsed spectrum, as was shown theoretically by J.M. Anderson (195). In a similar fashion, and for the same reason, large ranges of frequencies were covered in all the alkylammonium ion spectra. Experiments decoupling  $^{14}\text{N}$  while observing the

alkyl group resonance of 1Et3H, 3Et1H and 1Me3H yielded the same  $^{14}\text{N}$  chemical shift as that found from decoupling the  $^{14}\text{N}$  resonances for the  $\text{NH}^+$  group while observing the proton resonance. This is significant since for the ammonium ion only  $\text{NH}^+$  can be observed, and for 4Et and 4Me only the alkyl group can be observed.

As was pointed out in Section IIB, lineshapes in both the proton and nitrogen spectra will be governed by the  $^{14}\text{N}$  spin-lattice relaxation time which is a function of the symmetry around nitrogen. Consequently, the quite symmetrical 4H, 1Me3H, 1Et3H, 4Me and 4Et compounds will have long relaxation times, allowing  $^1\text{H}$ - $^{14}\text{N}$  coupling to be seen in both the proton and nitrogen spectra. For the unsymmetrical cases, EtMe2H, 3Me1H, and 3Et1H, nitrogen relaxation times are short and one observes only collapse of the triplets in the proton spectrum; quite the opposite happens in the nitrogen spectrum where the single resonance line is extremely broad. Realizing this, it is easy to see that the optimum  $^{14}\text{N}$  decoupling frequency will be found more accurately ( $\pm 1$  Hz) for the symmetrical (long  $T_1$ ) cases while the  $^{14}\text{N}$  decoupling frequency has a greater error ( $\pm 10$  Hz) for the unsymmetrical cases.

Reported  $^{14}\text{N}$  chemical shifts (Table 20) were the results of at least three determinations. The shift

for 1Me3H was also determined at a 4 M concentration and found to fall within the experimental error of the value for 5.11 M. Therefore, if there is a concentration effect, it should not be important for our purposes since all solutions studied here were between 4 M to 5 M.

#### E. Viscosity Measurements

Viscosities were measured for the alkylammonium salt solutions, and a few ammonium salt solutions, by means of a calibrated Cannon-Ubbelohde Viscometer (213). The viscometer is calibrated in centistokes/sec, so only the efflux times of the solutions had to be measured. Relatively short efflux times were measured with an Elgin stop watch and relatively long ones were measured with a Standard Type S-1 Clock (214). The efflux times used to calculate the viscosities were an average of five measurements. Units of centistokes were converted to centipoise by multiplying by the solution density, obtained at the same temperature with a calibrated pycnometer.

Temperatures were obtained by immersing the viscometer and pycnometer in tanks containing five gallons of water. Measurements were made at three temperatures, and temperature control ( $\pm 0.001^\circ\text{C}$ ) was achieved by means of a

Sunic Type EA-3 Electronic Relay, a Micro-Set differential-range Mercurial Thermoregulator, and a knife-type immersion heater (250 W), (215). The low temperature was maintained by constant circulation of tap water thru a copper coil and the thermoregulator was set a few degrees above this value. All baths had propeller-type stirrers. The viscosity and density measurements were made on the same solutions from which the NMR spectra were obtained.

## IV. RESULTS

### A. Spectra and Plots of Data

The following spectra are meant to be illustrative in nature, rather than including all spectra for each and every type of experiment. The essential features which these spectra portray are described in Sections III and V. The plots are of data given in Part C, which follows, and is described in the DISCUSSION, Section V.

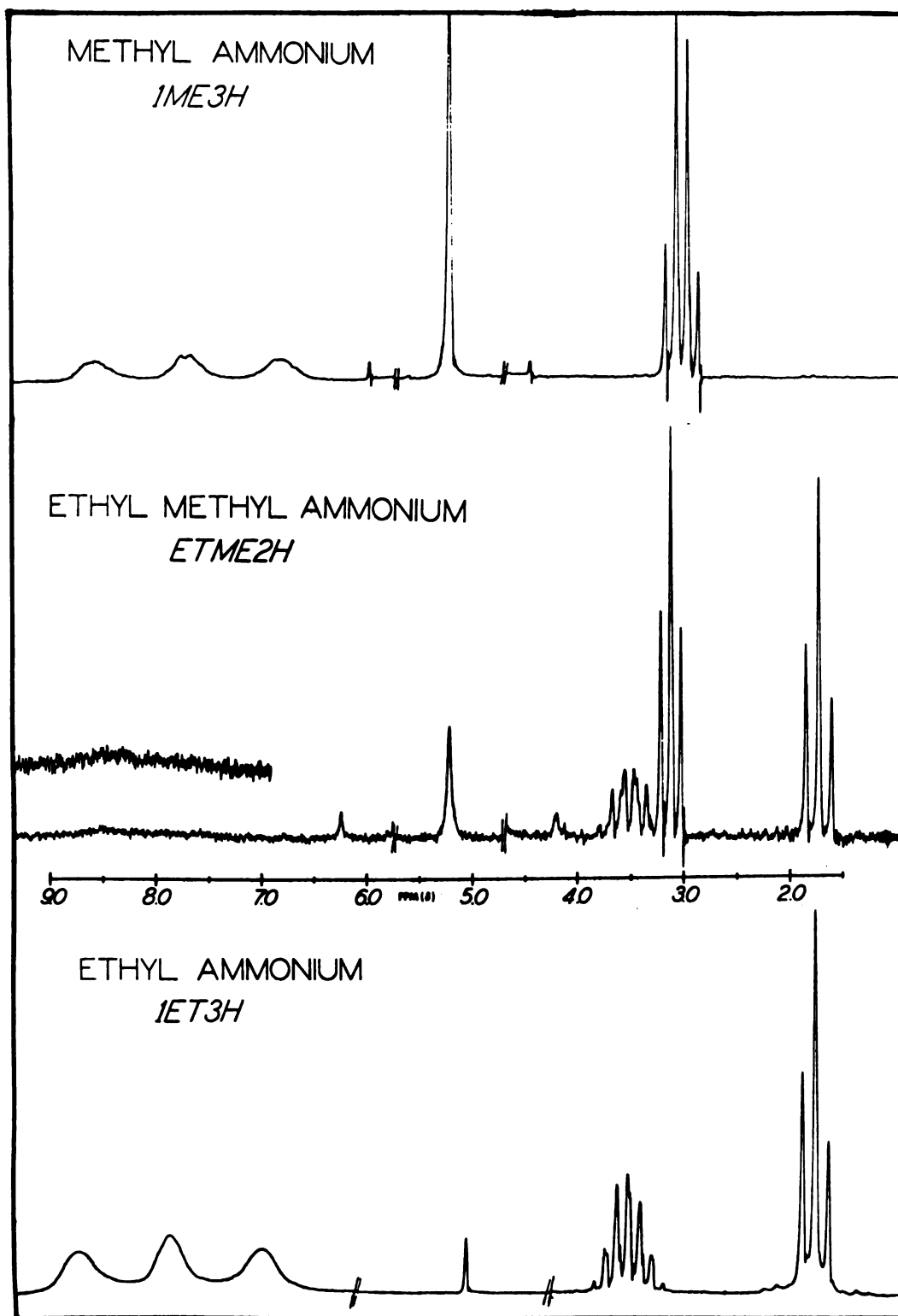


FIGURE 5. COMPLETE PROTON RESONANCE SPECTRA OF A FEW ALKYLAMMONIUM CHLORIDES IN AQUEOUS SOLUTION.

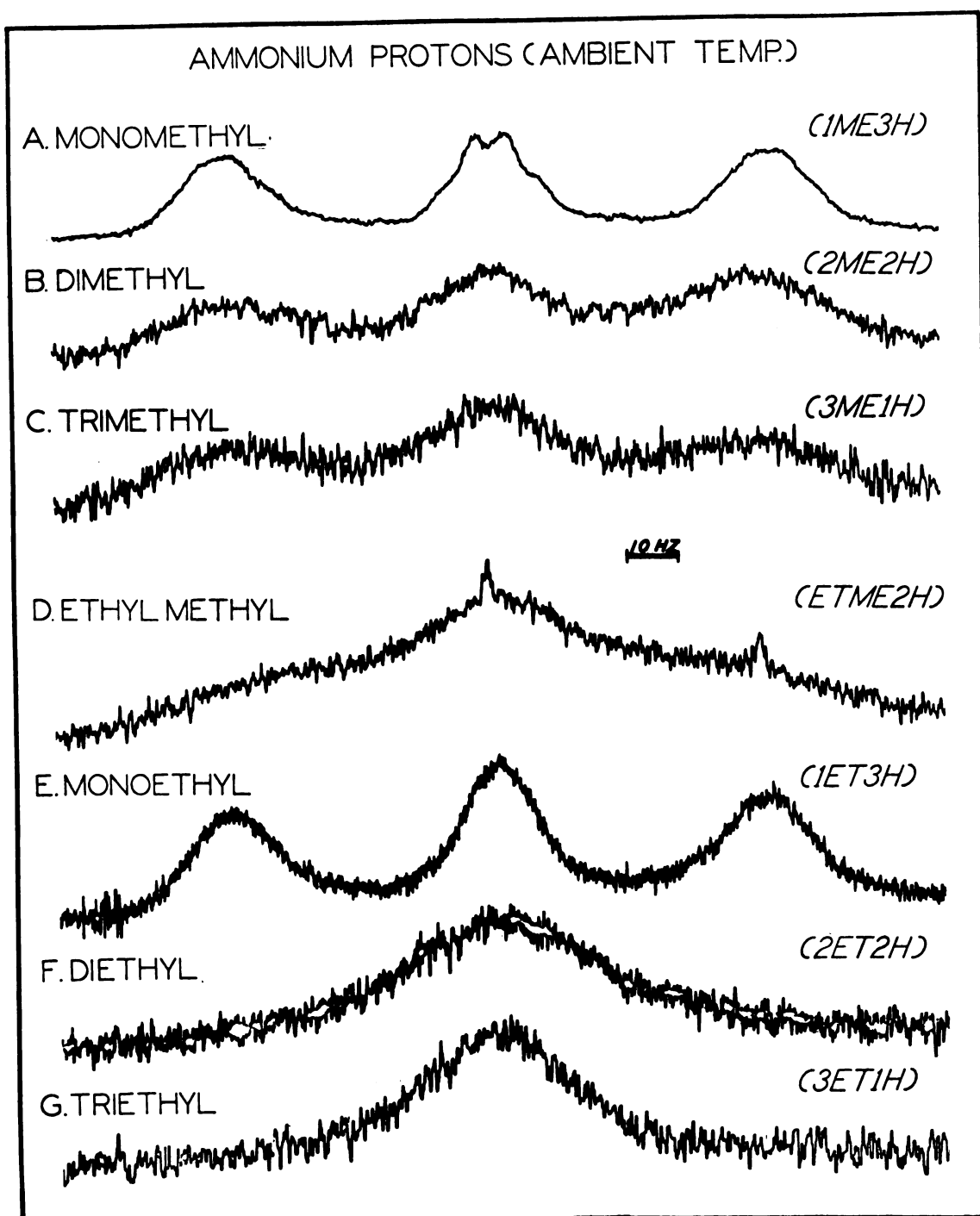


FIGURE 6. NH PROTON SPECTRA FOR A SERIES OF ALKYLAMMONIUM SALTS.

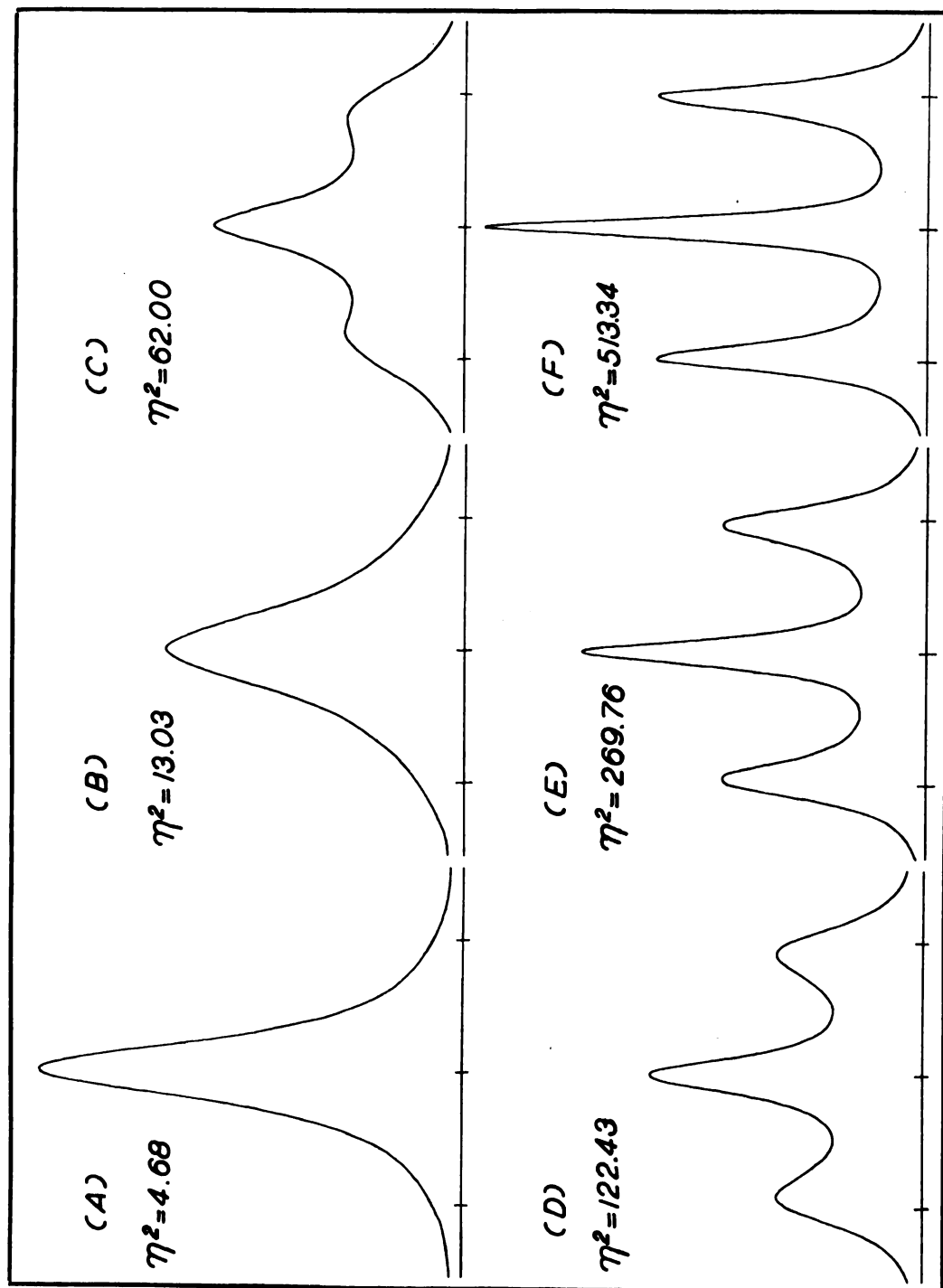


FIGURE 7. NH LINESHAPES CALCULATED FOR VARIOUS VALUES OF  $\eta^2=10\pi J\tau_1$   
FROM POPE'S EQUATION ( REF. 9 )

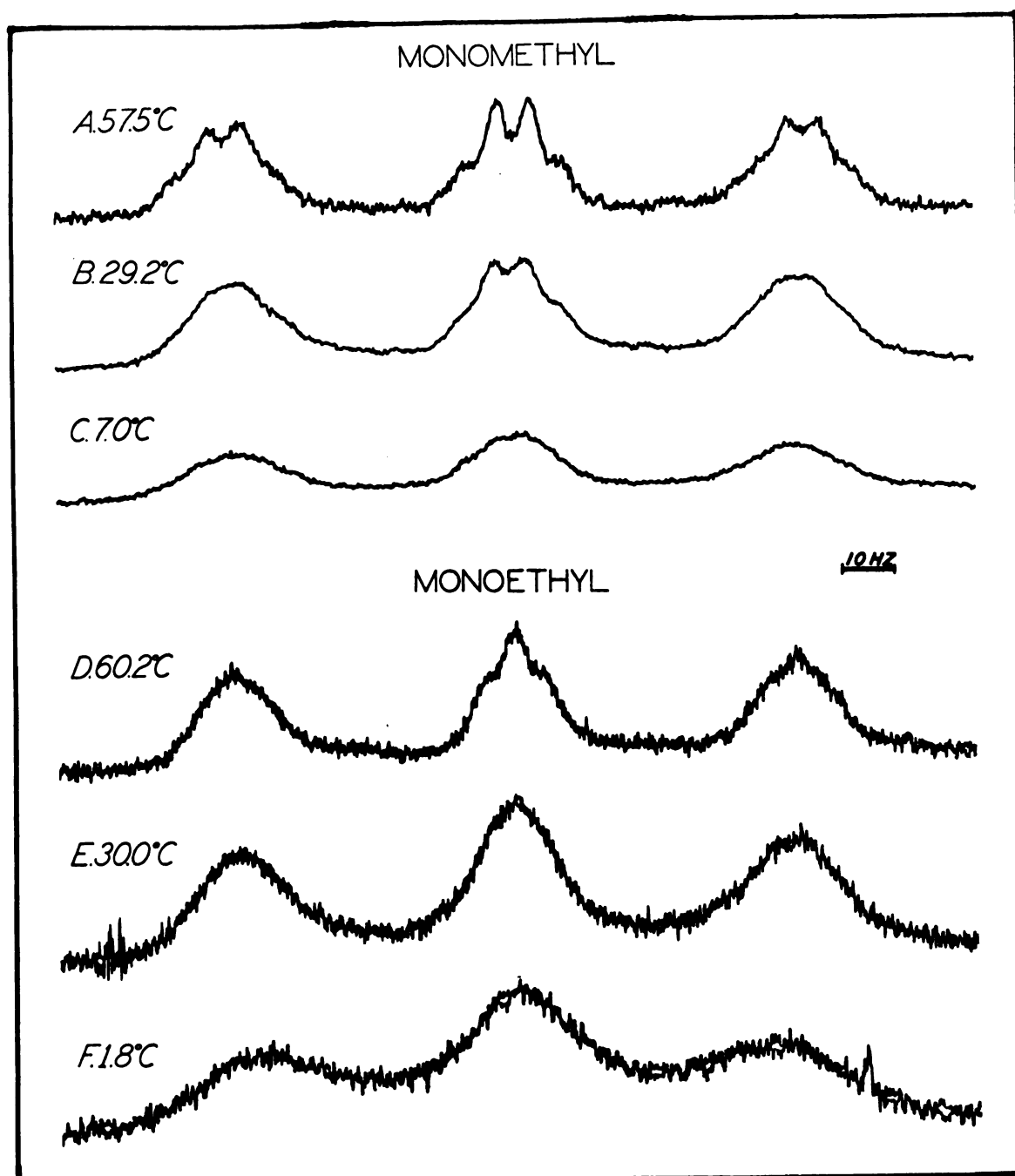


FIGURE 8. EFFECT OF TEMPERATURE ON THE NH RESONANCE OF MONOMETHYLAMMONIUM AND MONOETHYLAMMONIUM IONS.

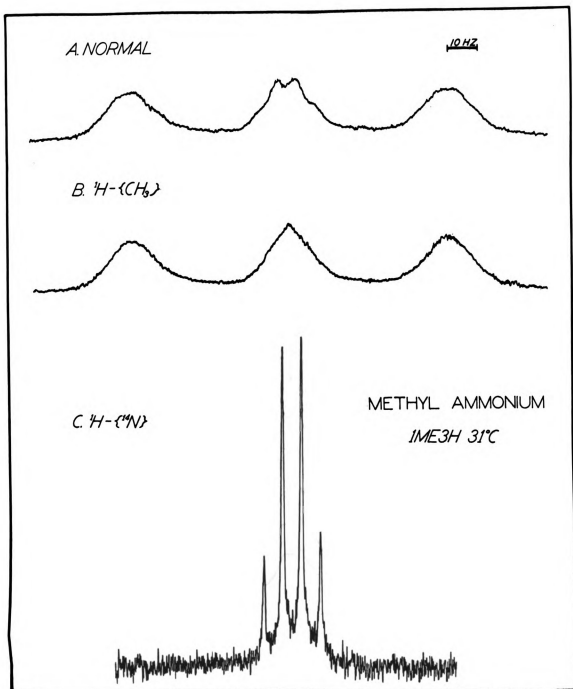


FIGURE 9. NH RESONANCE OF MONOMETHYLAMMONIUM ION SHOWING (A) SINGLE RESONANCE SPECTRUM (B) METHYL PROTON DECOUPLING AND (C) NITROGEN DECOUPLING.

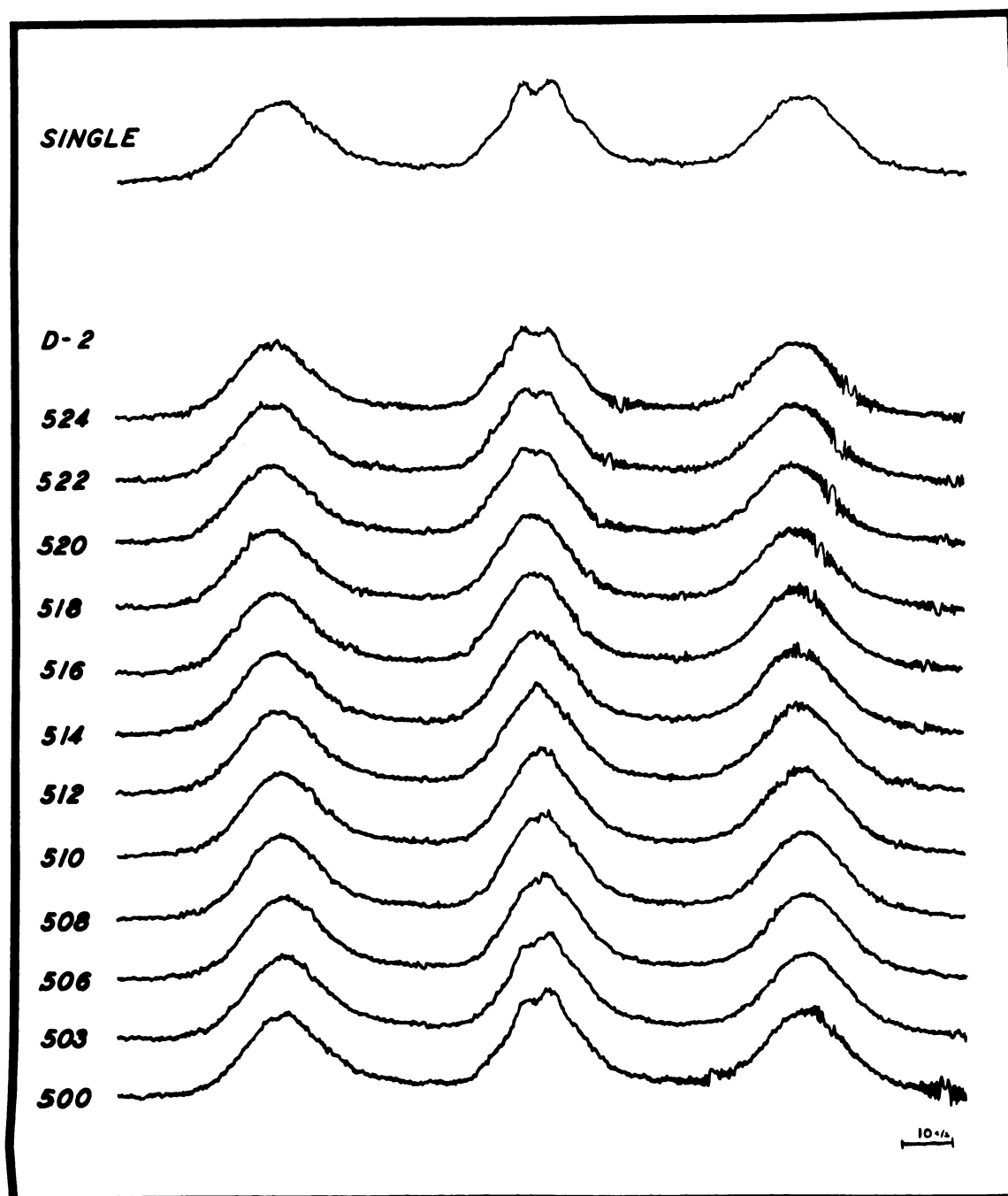


FIGURE 10. NH RESONANCE OF MONOMETHYLAMMONIUM ION SHOWING VARIATION WITH THE FREQUENCY USED TO DECOUPLE THE ALKYL PROTONS.

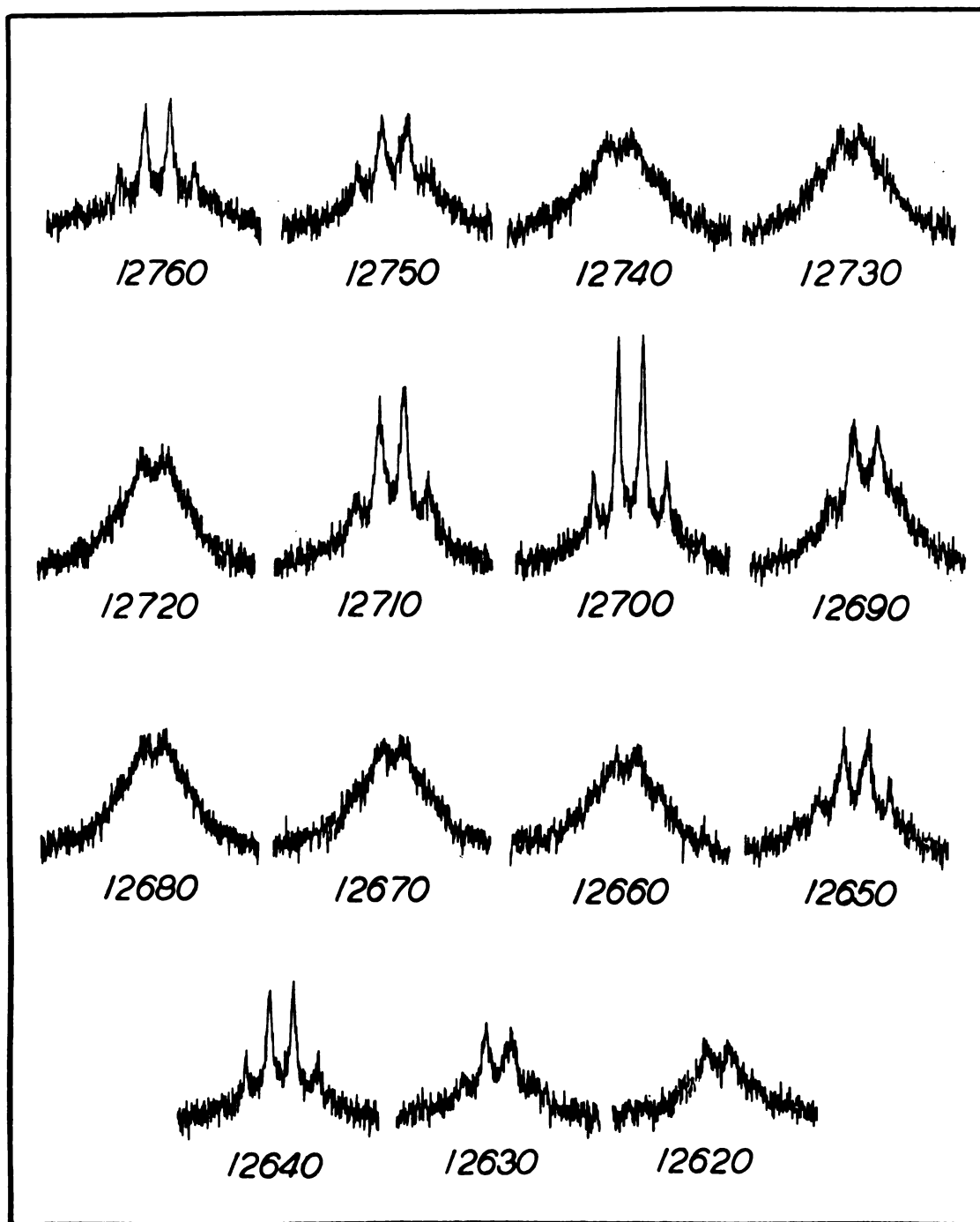


FIGURE 11. NH RESONANCE OF MONOMETHYLAMMONIUM ION SHOWING VARIATION WITH THE FREQUENCY USED TO DECOUPLE NITROGEN.

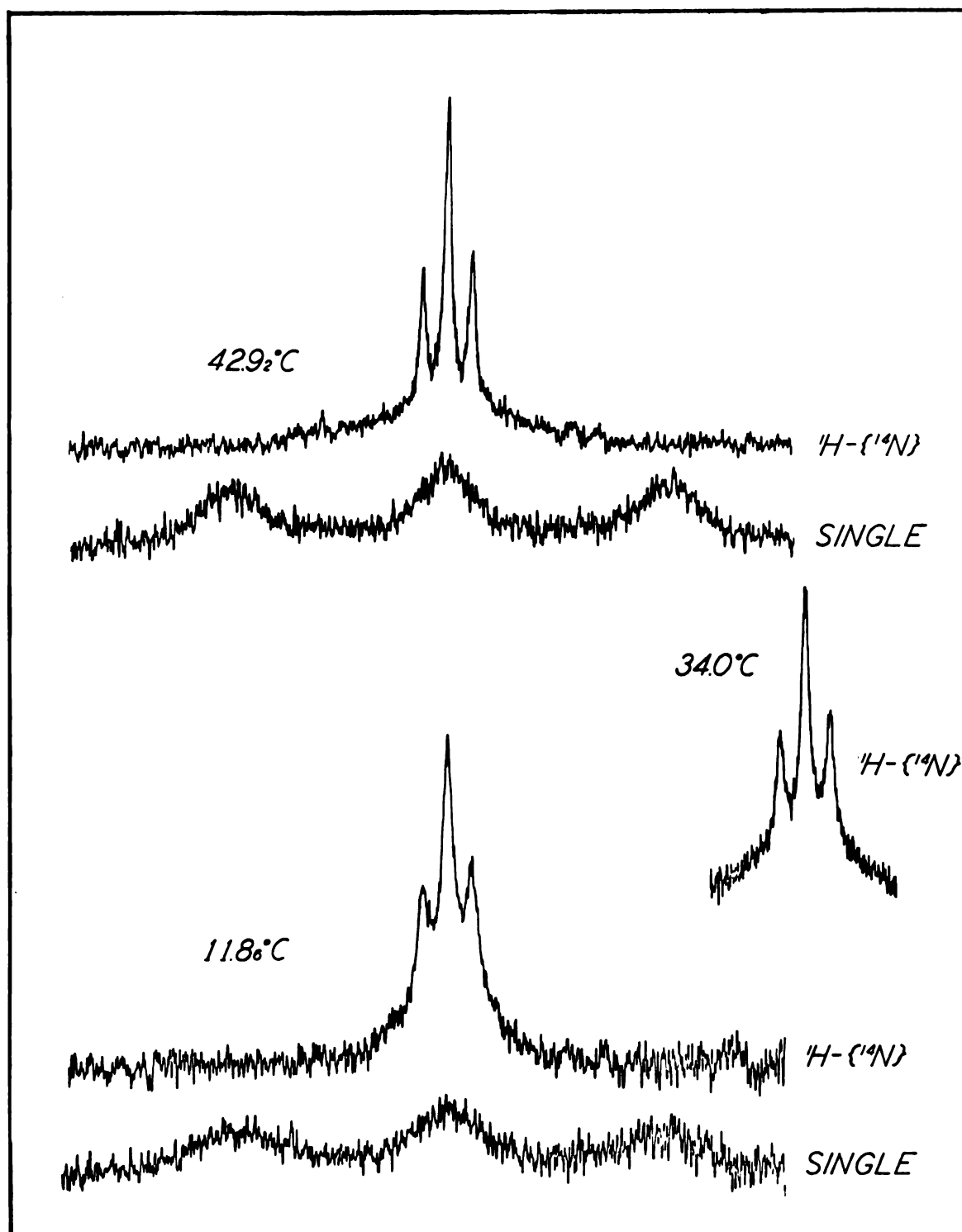


FIGURE 12. VARIABLE TEMPERATURE STUDY OF NH PROTON RESONANCE OF MONOETHYLAMMONIUM ION WHILE DECOUPLING NITROGEN.

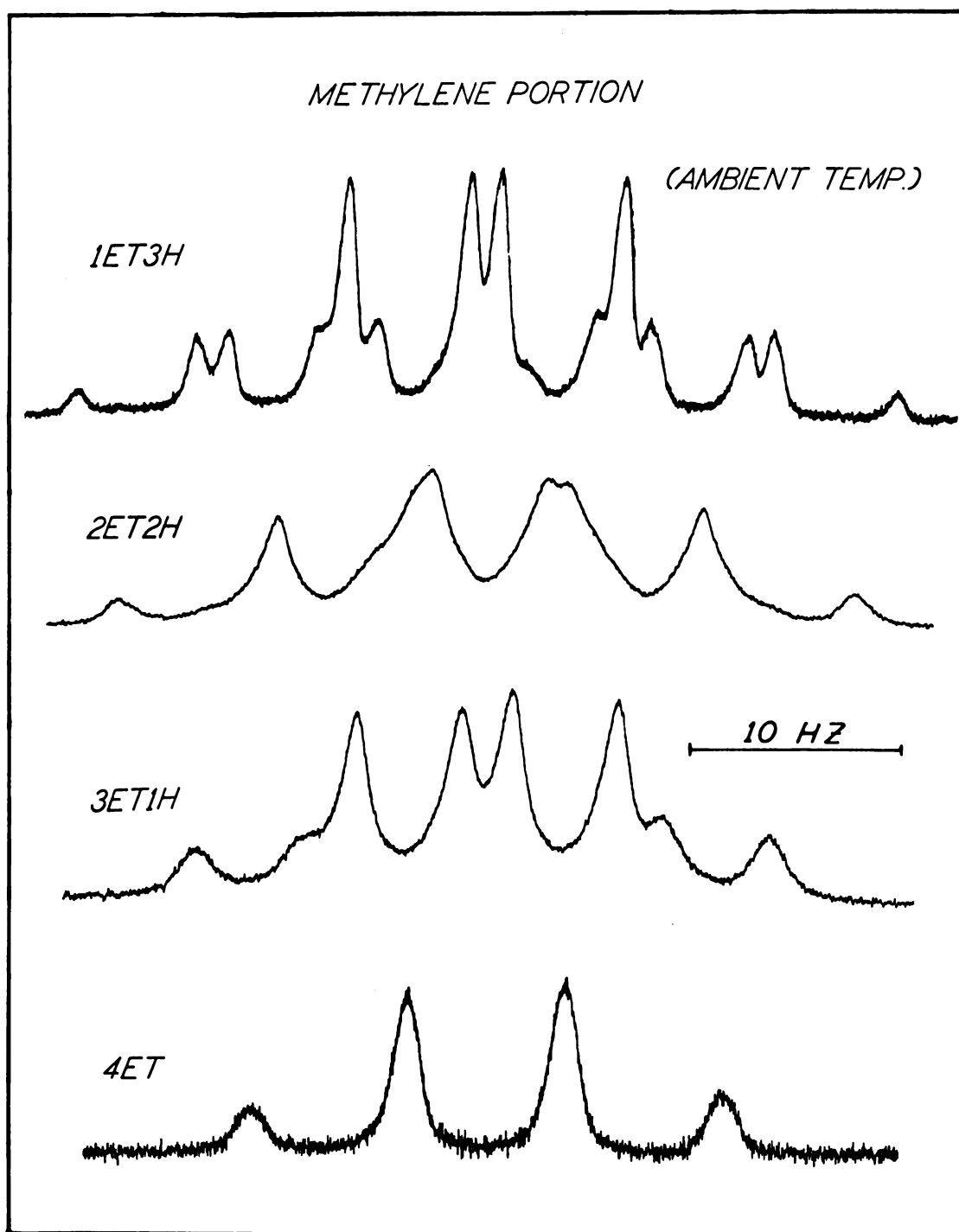


FIGURE 13. DETAIL OF THE METHYLENE PROTON SPECTRUM OF THE SERIES OF ETHYLAMMONIUM IONS SHOWING THE LINE BROADENING.

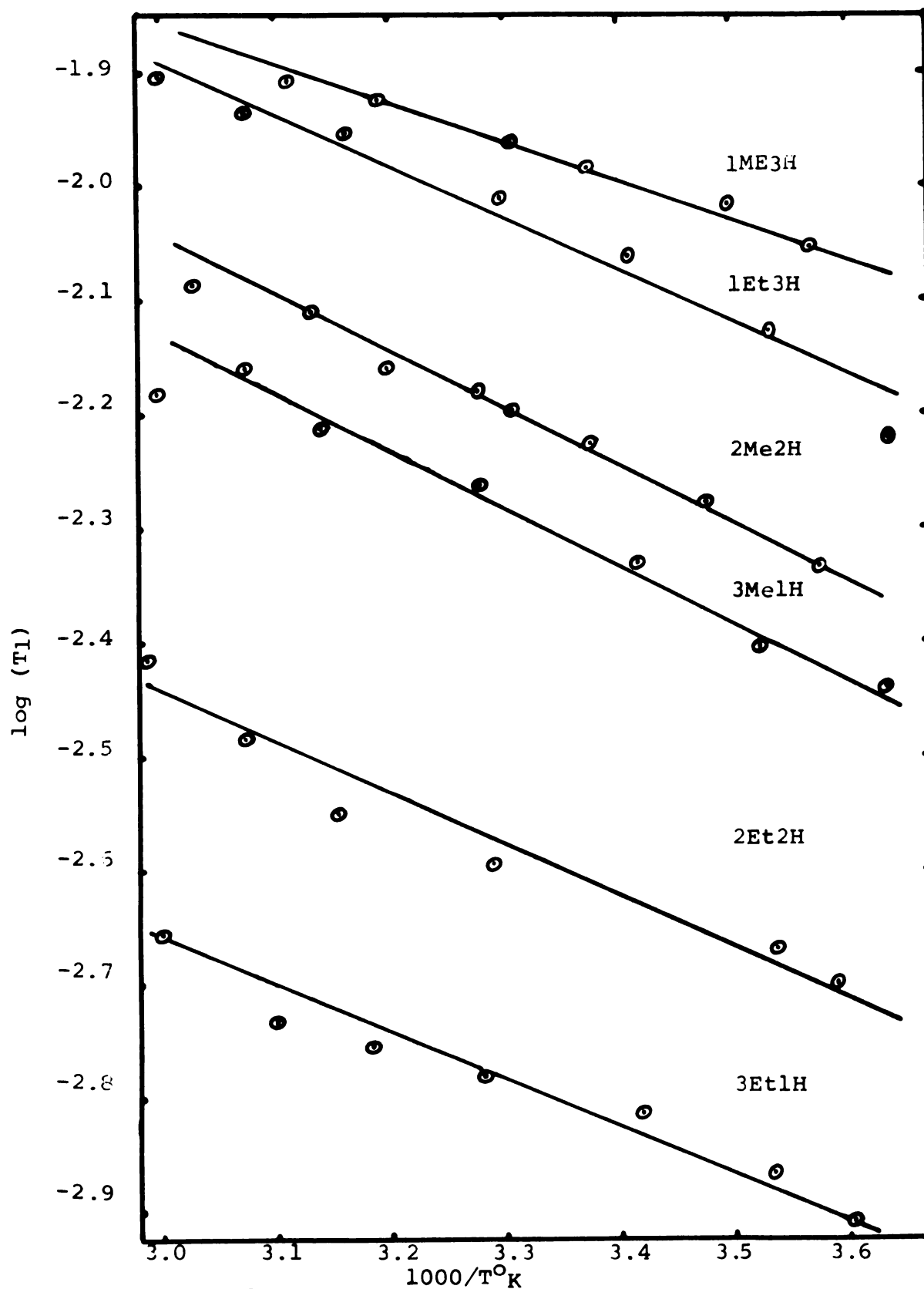


Figure 14.  $^{14}\text{N}$ . spin-lattice relaxation times vs. reciprocal of absolute temperature for the alkyl-ammonium salts

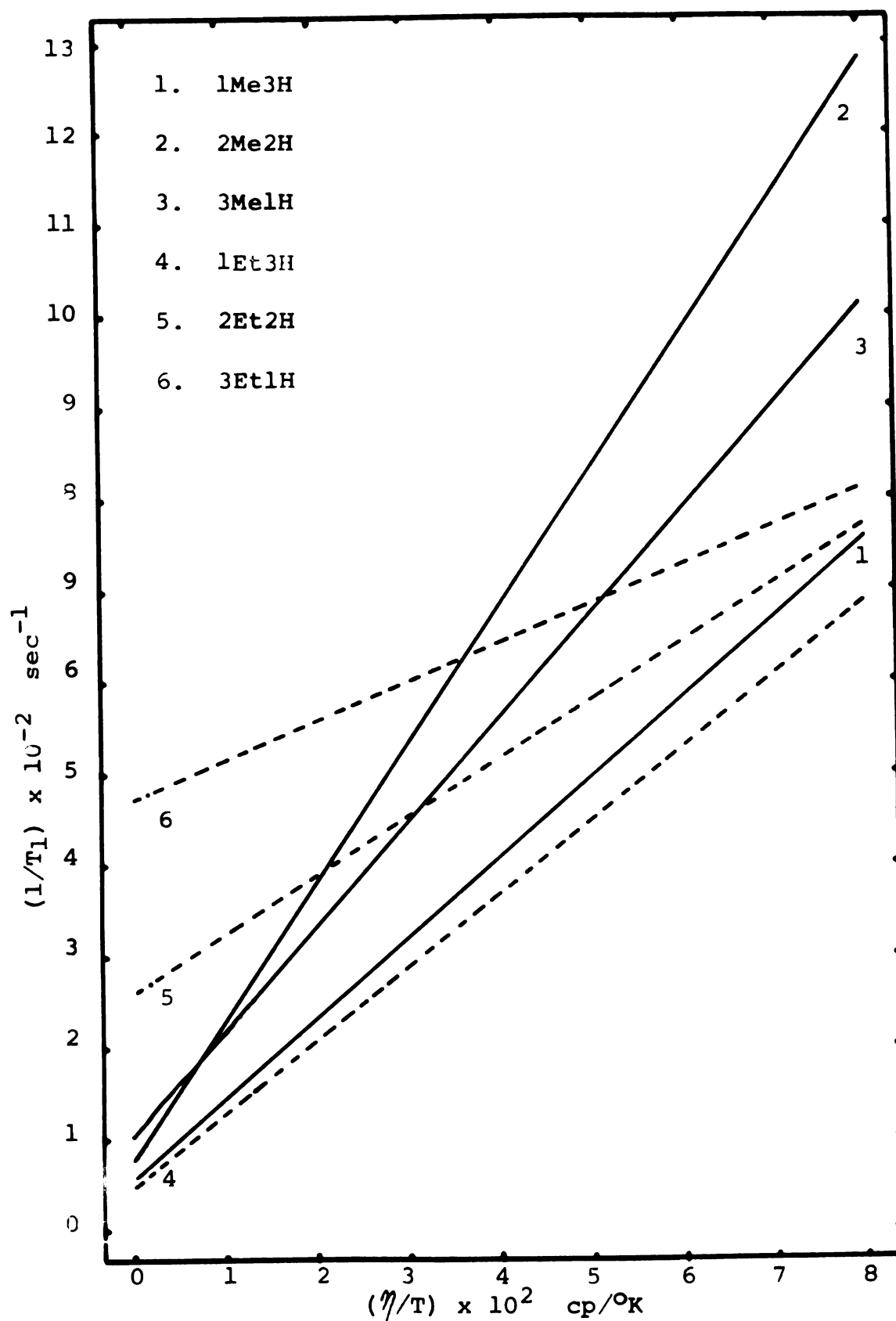


Figure 15.  $^{14}\text{N}$  relaxation rates vs. viscosity/temperature for the alkylammonium salts.

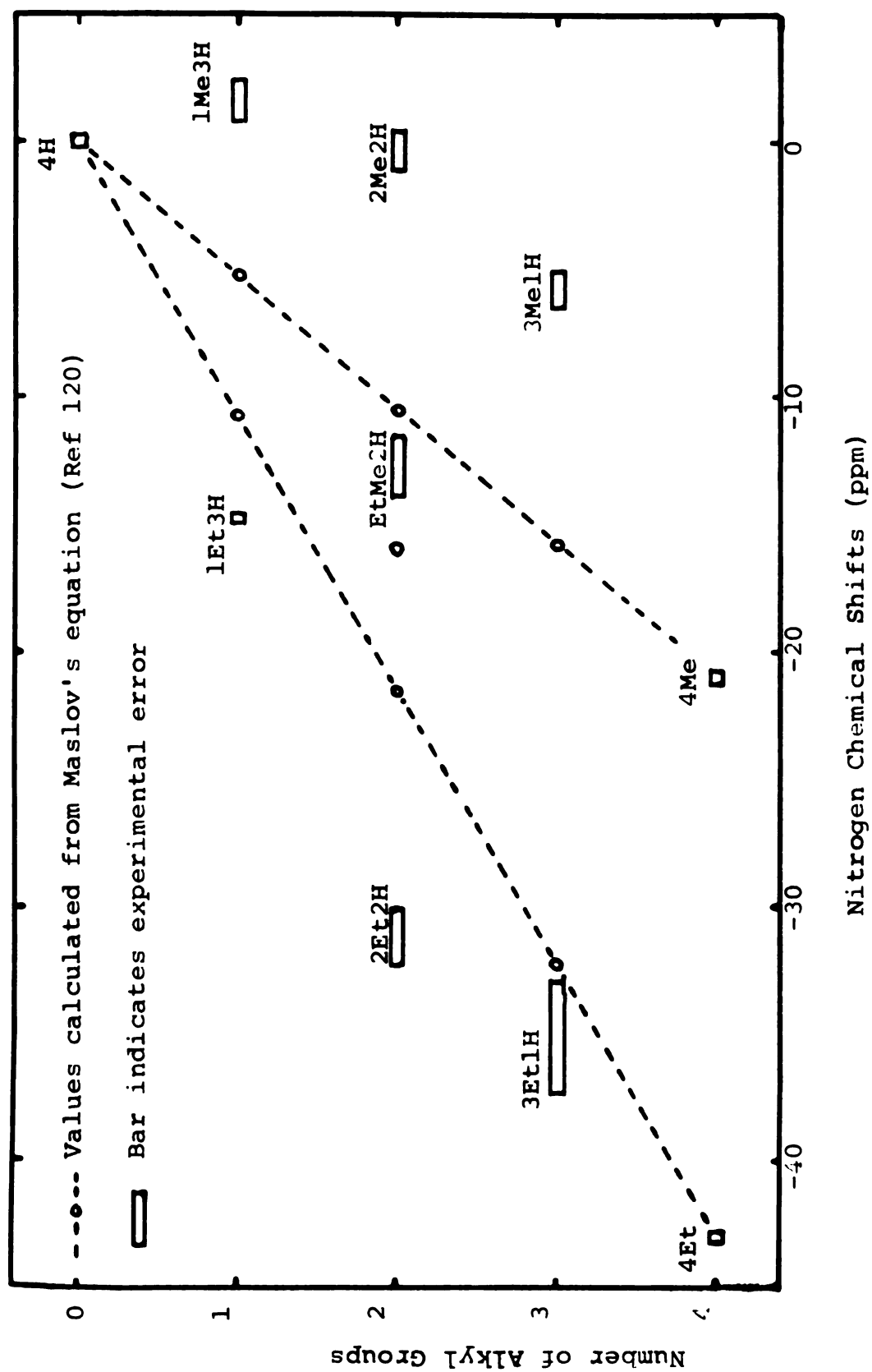


Figure 16. Calculated and experimental nitrogen chemical shifts for alkylammonium salts.

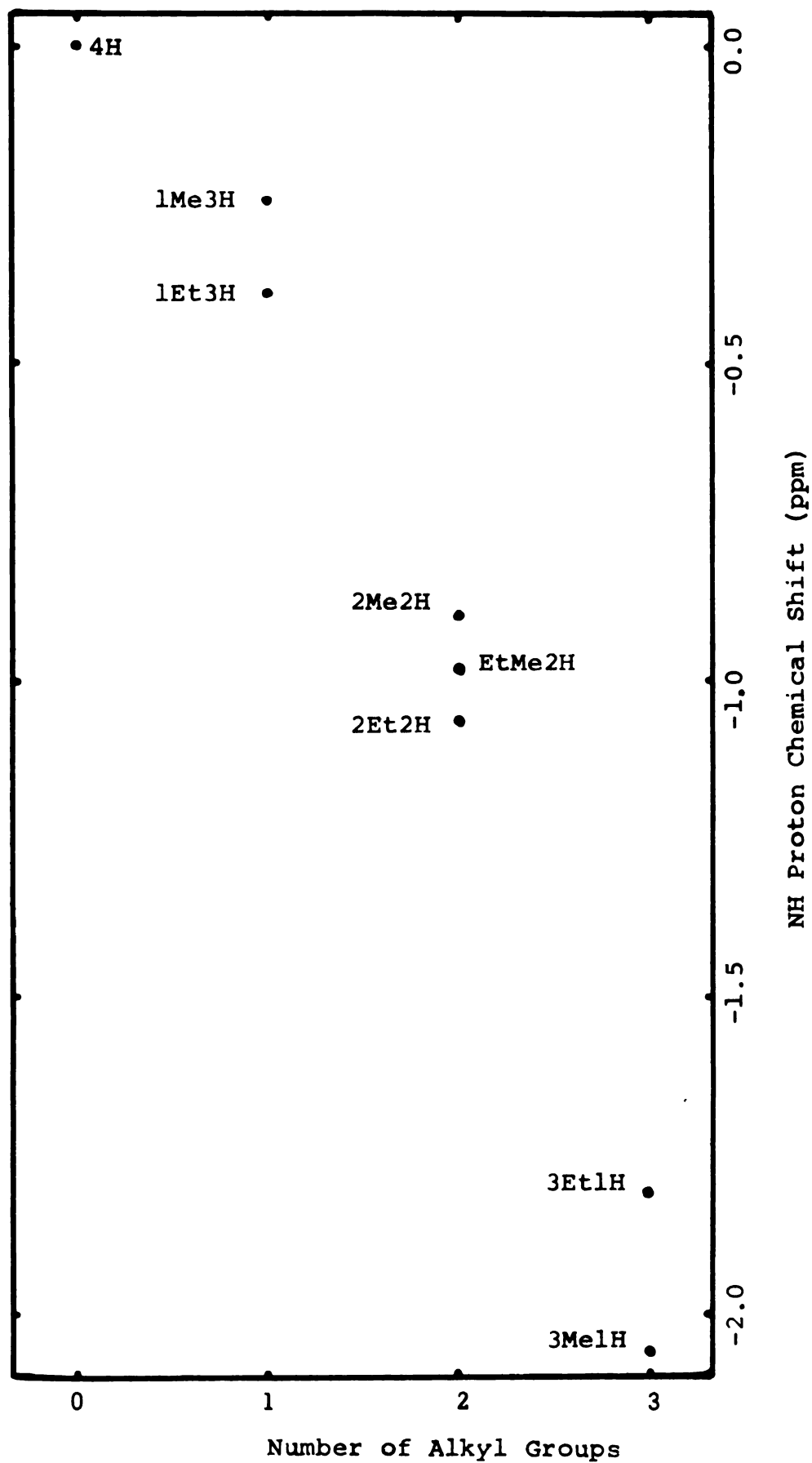


Figure 17. NH Proton chemical shifts for the alkylammonium salts.

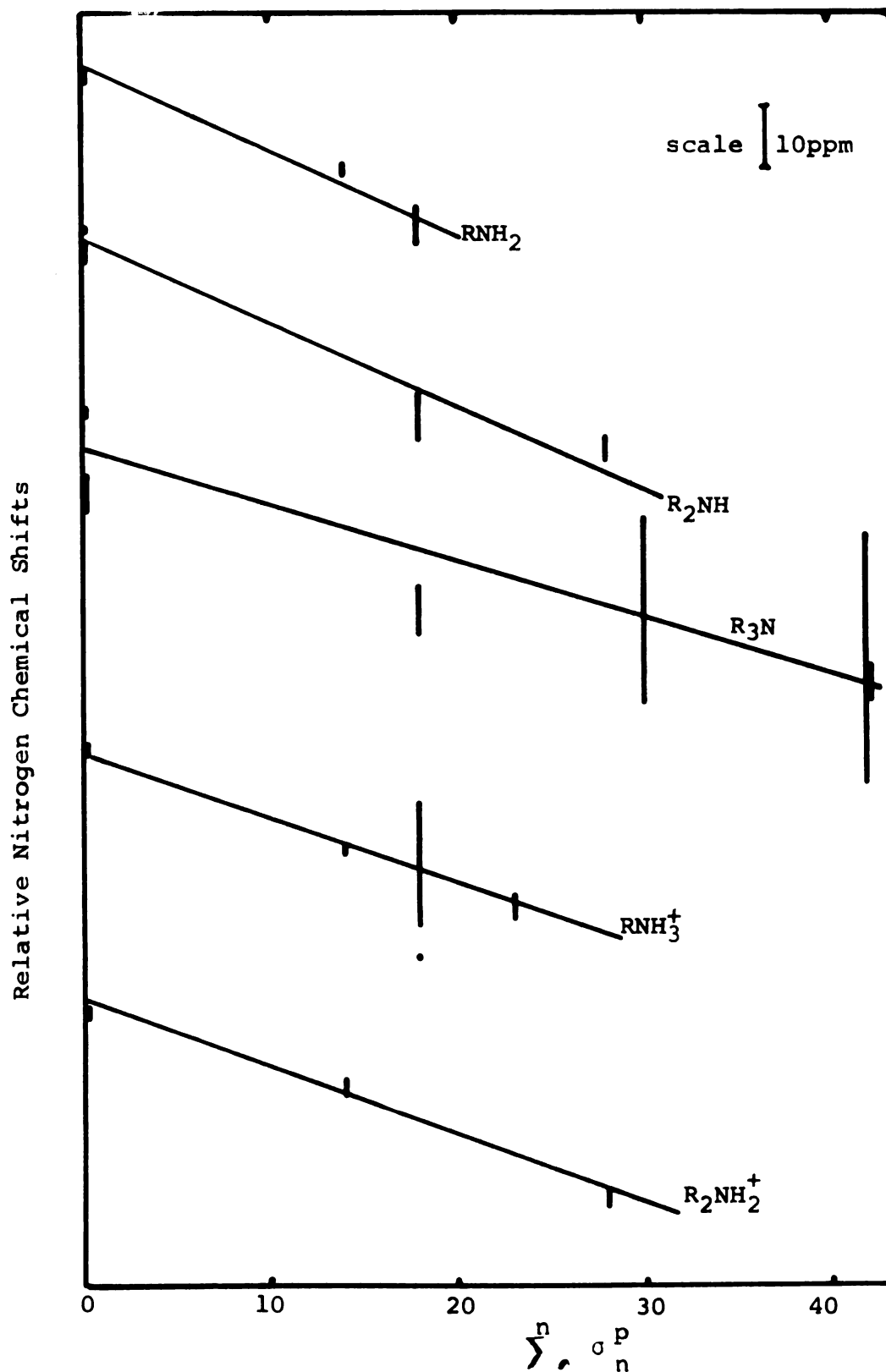


Figure 18. Nitrogen chemical shifts vs.  $\sigma^P$  values (Grim) for amines and substituted ammonium ions. The chemical shifts are relative within each series.

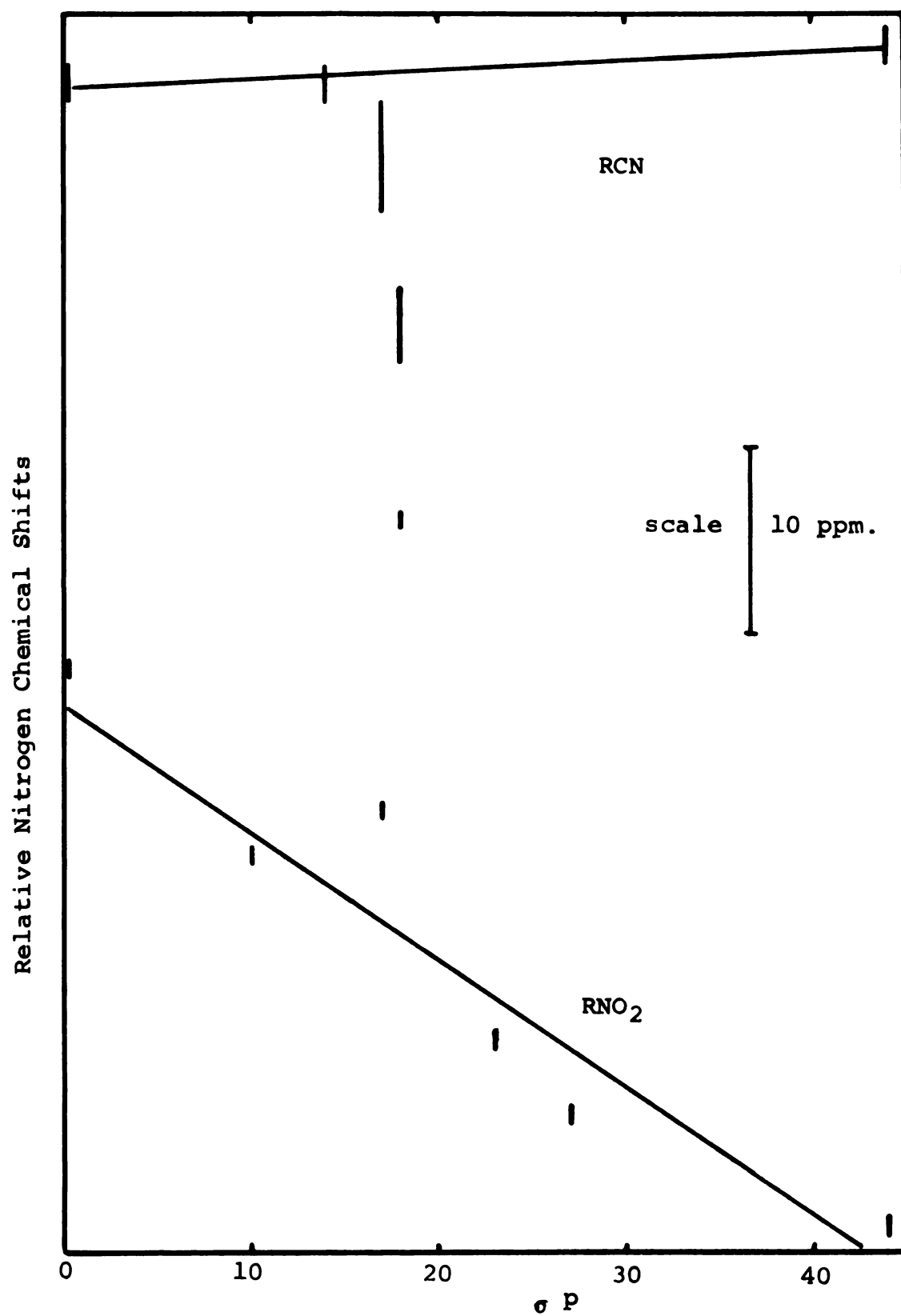


Figure 19. Relative nitrogen chemical shifts and  $\sigma P$  values for nitriles and nitro-compounds.

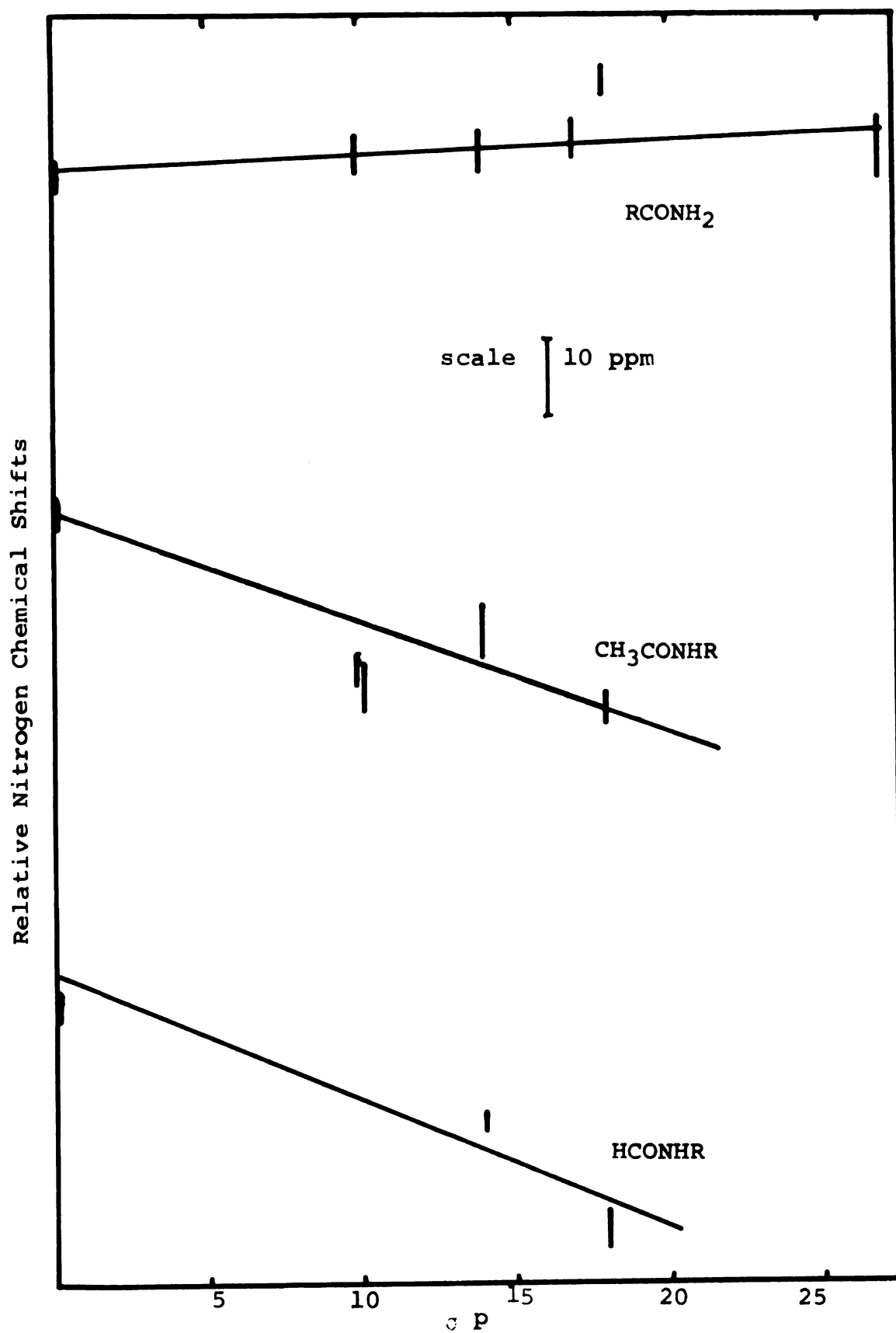


Figure 20. Relative nitrogen chemical shifts and  $\sigma P$  values for amides.

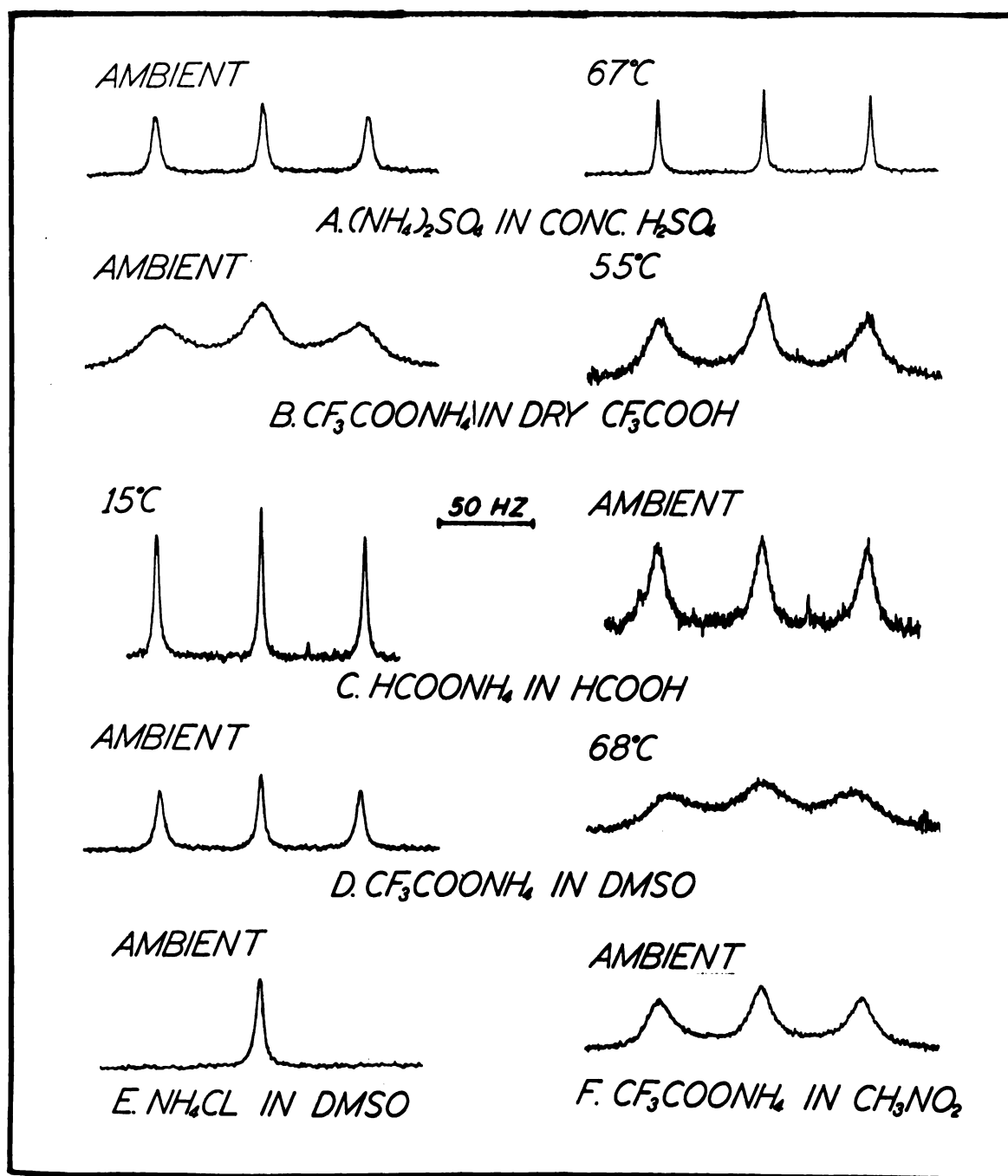


FIGURE 21. PROTON NMR LINESHAPES FOR AMMONIUM SALTS IN VARIOUS SOLVENTS AT SELECTED TEMPERATURES.

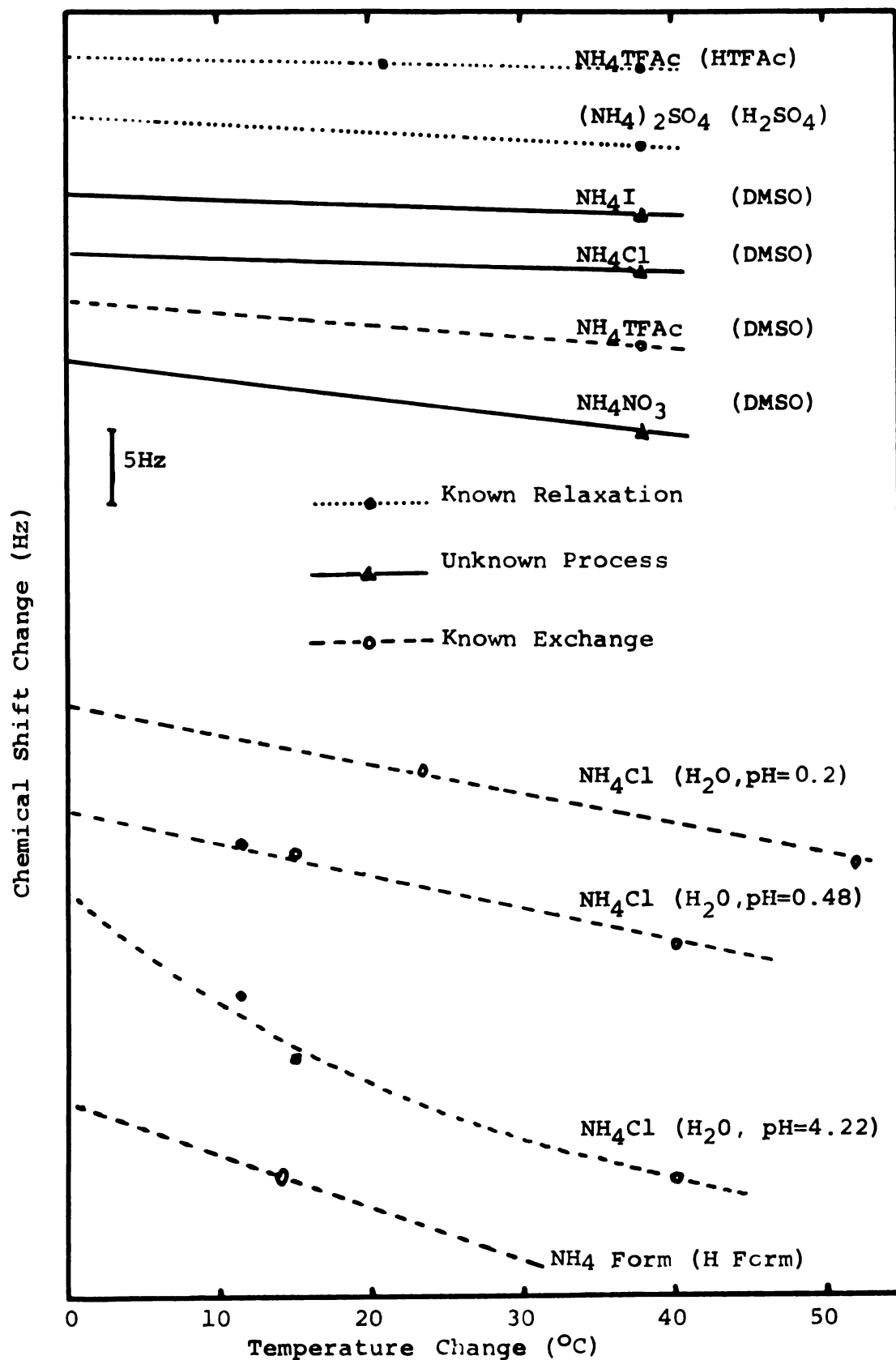


Figure 22. Change of NH proton chemical shift with temperature for ammonium salts in several different solvents.

### B. Data Analysis by Digital Computer

In order to obtain a least-squares fit of the calculated spectrum with the experimental spectrum, estimated values for the nitrogen spin-lattice relaxation time ( $T_{1N}$ ) and the proton-nitrogen coupling constant ( $J_{PN}$ ) had to be supplied as input data. This was done by making a visual match of the experimental ammonium-proton spectrum (for optimum alkyl-group proton decoupling) with a set of theoretically calculated spectra.

Program QUADRELX (APPENDIX A) generates a set of spectra for NH protons according to Pople's equation (9) for assigned values of  $\eta^2$  (ETASQ), where  $\eta = 10\pi T_1 J$ . The areas from a set of such curves (a set of ETASQ values) are all normalized to the largest area and are plotted out for the same ordinate units and abscissa units. A set of such curves are shown in Figure 7, and the corresponding values of relaxation times for the two nitrogen-proton coupling constants are given in Table 10.

Table 10.  $^{14}\text{N}$  relaxation times for various J values.

$\eta^2 = (10\pi T_1 J)^2$ =ETASQ	$T_1(^{14}\text{N}) = \text{TW}\emptyset\text{N}$ $^1\text{J}(^1\text{H}-^{14}\text{H})=\text{CUPJ}=50.0$	$T_1(^{14}\text{N}) = \text{TW}\emptyset\text{N}$ $^1\text{J}(^1\text{H}-^{14}\text{N})=\text{CUPJ}=55.0$
513.34	$14.42 \times 10^{-3}$	$13.11 \times 10^{-3}$
269.76	10.46	9.506
122.43	7.044	6.404
62.00	5.013	4.557
13.03	2.298	2.089
4.68	1.377	1.252

An extensive set of curves such as these was then used to visually match with the experimental alkyl-proton decoupled ammonium-proton spectrum. From this visual fit, ETASQ was obtained and a relaxation time ( $\text{TW}\emptyset\text{N}$ ) calculated from it and the experimentally found (or estimated)  $^1\text{J}(^1\text{H}-^{14}\text{N})$ , called CUPJ.  $\text{TW}\emptyset\text{N}$  and CUPJ obtained in this manner were used as initial values for the least-squares fitting of the experimental spectrum using program NMR FIT8 (APPENDIX B). The experimental spectrum is fed in as a set of frequency, intensity (X, Y) pairs. These values were obtained from the experimental alkyl-ammonium-proton spectrum by the following procedure. First, the spectrum

with optimum alkyl proton decoupling was chosen; thus, it represented only the NH line shape for which Pople's equation was written (9). Second, a baseline was drawn between the two flat portions on each side of the spectrum and, in cases where the right-hand side started to drift upward (due to the broad "wing" from the solvent water at 60 MHz), the baseline was made to follow this curvature. Next, the center of the lineshape was located and a vertical line drawn to intersect both baseline and curve. Using this centerline as a base, vertical lines were drawn at every 2 Hz interval for 80 Hz above and below the centerline giving a total of 81 frequency values (X) running from 0 to 160 Hz with 80 Hz as the center. Initially, only forty-three values were used but the fits were not as good. Now the intensity, intersection of vertical line with baseline and curve, was measured with a ruler to the nearest 1/4mm. In order to insure a symmetrical shape and to reduce measuring errors, corresponding intensities on each side of the center were averaged, e.g., Y at 0 was averaged with Y at 160, Y at 50 was averaged with Y at 110, etc. The spectrum thus digitized was then punched on IBM data cards. In addition to TWØN and CUPJ mentioned above, the baseline (BSLN) and center (CEN) were input values.

The program then incremented ~~TWON~~, CUPJ and BSLN to give the best fit of experimental and theoretical spectra. Normally, 26 loops of the set of three parameters was sufficient to give a good fit. Further loops through NMR FIT8 gave changes in the fourth and fifth digits of the incremented parameters and little or no decrease in the sum of the squares of the differences between experimental and calculated values (SO). The output parameters sought were ~~TWON~~ and CUPJ. The values of these for the best fits are listed in Table 11 (Section C). Programs QUADRELX and NMR FIT8 were run on a Control Data Corporation, Model 3600, Digital Computer.

In addition to the above computer programs, the IBM QUIKTRAN library program LINFIT was used to get linear least-square fits to viscosity data (Table 15). From the slope and intercept of the plot of  $\log$  against  $1/T$  for each compound viscosities were calculated at each temperature for which the relaxation times were known. These results are presented in Table 16.

### C. Data

Table 11. Results of computer least-squares fitting of ammonium proton lineshapes.

Temp. °C	$1J(^1H-^{14}N)$ Hz	$T_1 \times 10^3$ sec.	Temp. °C	$1J(^1H-^{14}N)$ Hz	$T_1 \times 10^3$ sec.
Monomethylammonium (1ME3H)					
6.98°C	54.67 Hz	8.856 sec.	40.19°C	54.48 Hz	11 90 sec
12.73	54.38	9.662	48.17	54.77	12 36
23.12	54.74	10.38	57.48	54.65	11 67
29.18	54.48	10.96			
			ave:	54.59 ± 0.13	
Dimethylammonium (2Me2H)					
6.44	53.10	4.628	31.70	54.86	6 654
14.52	54.44	5.275	39.35	55.39	6.937
23.12	54.97	5.953	45.96	55.68	7.772
29.13	55.36	6.364	56.98	55.92	8 210
			ave:	54.96 ± 0.62	
Trimethylammonium (3Me1H)					
2.06	55.13	3.626	45.03	56.34	6.133
10.64	55.19	3.938	52.06	56.10	6.946
19.54	54.73	4.681	60.86	54.98	6 572
31.70	55.71	5.479			
			ave:	55.45 ± 0.51	

Table 11 (cont'd.)

Temp. °C	$^1J(^1H-^{14}N)$ Hz	$T_1 \times 10^3$ sec	Temp. °C	$^1J(^1H-^{14}N)$ Hz	$T_1 \times 10^3$ sec
Monoethylammonium (1Et3H)					
1.79 °C	53.27 Hz	6.043 sec	42.91 °C	53.72 Hz	11.15 sec
9.86	53.13	7.474	52.24	54.00	11.67
20.08	53.70	8.695	60.20	53.82	12.49
29.98	53.62	9.756			
			ave:	53.61 $\pm$ 0.23	
Diethylammonium (2Et2H)					
5.34	47.12	1.997	43.88	52.41	2.824
9.53	46.67	2.151	52.14	53.46	3.284
30.71	49.62	2.543	61.39	52.44	3.853
			ave:	50.29 $\pm$ 2.48	
Triethylammonium (3Et1H)					
4.37	42.38	1.236	40.95	47.28	1.759
9.75	43.22	1.359	49.40	60.64	1.854
18.46	45.62	1.536	60.00	65.86	2.209
31.59	49.12	1.667			
			ave:	50.59 $\pm$ 7.24	

Table 12. Variation of  $^{14}\text{N}$  relaxation time with temperature for substituted ammonium ions.

$t^{\circ}\text{C}$	$T^{\circ}\text{K}$	$1000/T^{\circ}\text{K}^{-1}$	$\log T_1 (^{14}\text{N})$	$1000 \times T_1 (^{14}\text{N})$ sec
<b>1Me3H</b>				
6.98°C.	280.18°K	3.569°K <sup>-1</sup>	-2.05276	8.856 sec.
12.73	285.93	3.497	-2.01493	9.662
23.12	296.32	3.375	-1.98359	10.385
29.13	302.38	3.307	-1.96035	10.956
40.19	313.39	3.191	-1.92431	11.904
48.17	321.37	3.112	-1.90798	12.36
57.48	330.68	3.024	-1.93293	11.67
<b>2Me2H</b>				
6.44	279.64	3.576	-2.33461	4.628
14.52	287.72	3.476	-2.27778	5.275
23.12	296.32	3.375	-2.22526	5.953
29.18	302.38	3.307	-2.19627	6.364
31.70	304.90	3.280	-2.17692	6.654
39.35	312.55	3.199	-2.15883	6.937
45.96	319.16	3.133	-2.10947	7.772
56.98	330.18	3.029	-2.08566	8.210

Table 12 (cont'd.)

t °C	T °K	1000/T °K <sup>-1</sup>	log T <sub>1</sub> ( <sup>14</sup> N)	1000xT <sub>1</sub> ( <sup>14</sup> N) sec
3Me1H				
2.06°C.	275.26°K	3.633°K <sup>-1</sup>	-2.44057	3.626 sec.
10.64	283.84	3.523	-2.40472	3.938
19.54	292.74	3.416	-2.32966	4.681
31.70	304.90	3.280	-2.26130	5.479
45.03	318.22	3.142	-2.21233	6.133
52.06	325.26	3.074	-2.15826	6.946
60.86	334.06	2.993	-2.18230	6.572
1Et3H				
1.79	274.99	3.637	-2.21875	6.043
9.86	283.06	3.533	-2.12645	7.474
20.08	293.28	3.410	-2.06073	8.695
29.98	303.18	3.298	-2.01073	9.756
42.91	316.11	3.163	-1.95273	11.15
52.24	325.44	3.073	-1.93293	11.67
60.20	333.40	2.999	-1.90344	12.49

Table 12 (cont'd.)

t°C	T°K	1000/T °K <sup>-1</sup>	log T <sub>1</sub> (°K)	1000xT <sub>1</sub> (°K) sec
2Et2H				
5.34°C.	278.54°K	3.590 °K <sup>-1</sup>	-2.69962	1.997 sec.
9.53	282.73	3.537	-2.66736	2.151
30.71	303.90	3.290	-2.59465	2.543
43.88	317.08	3.154	-2.54914	2.824
52.14	325.34	3.074	-2.48360	3.284
61.39	334.59	2.989	-2.41420	3.853
3Et1H				
4.37	277.57	3.603	-2.90798	1.236
9.75	282.57	3.534	-2.86678	1.359
18.46	291.66	3.429	-2.81361	1.536
31.59	304.79	3.281	-2.77806	1.667
40.59	314.15	3.183	-2.75473	1.759
49.40	322.60	3.100	-2.73189	1.854
60.00	333.20	3.001	-2.65580	2.209

Table 13. Results of least-squares fitting of relaxation time-temperature data.

Compound	Corr. Coeff.	Intercept	Slope	$E_a(T_1)$ kcal
1Me3H	-0.9945	-0.9358	-310.65	1.421 kcal.
2Me2H	-0.9933	-0.6794	-459.88	2.104
3Me1H	-0.9824	-0.7962	-451.71	2.067
1Et3H	-0.9849	-0.4772	-470.09	2.151
2Et2H	-0.9773	-1.1607	-430.09	1.968
3Et1H	-0.9830	-1.5693	-368.51	1.686

Table 14. Results of least-squares fitting of viscosity-temperature data.

Compound	Corr. Coeff.	Intercept	Slope	$\Delta E$ (visc.)
1Me3H	1.0000	-2.3501	722.2	3.304 kcal.
2Me2H	0.9995	-2.2925	757.1	3.464
3Me1H	1.0000	-2.5008	863.0	3.949
1Et3H	0.9993	-2.5512	858.2	3.927
2Et2H	0.9988	-3.2572	1195.3	5.496
3Et1H	0.9995	-4.0020	1485.2	6.796

Table 15. Measured solution viscosities.

Compound	t°C	T°K	(1/T) x 10 <sup>3</sup>	log $\eta$	$\eta$ cp
1Me3H	14.7°C.	287.9°K	3.473	0.15794	1.4386cp
	23.8	297.0	3.367	0.08160	1.2067
	39.0	312.2	3.203	-0.03702	0.9183
2Me2H	14.7	287.9	3.473	0.33937	2.1846
	23.25	296.45	3.373	0.25766	1.8099
	39.0	312.2	3.203	0.13399	1.3614
3Me1H	14.7	287.9	3.473	0.49726	3.1424
	23.5	296.7	3.370	0.40630	2.5486
	39.0	312.2	3.203	0.26394	1.8363
1Et3H	13.3	286.5	3.490	0.44696	2.7987
	23.7	296.9	3.368	0.33407	2.1581
	39.0	312.2	3.203	0.19987	1.5844
2Et2H	14.7	287.9	3.473	0.90077	7.9574
	23.5	296.7	3.370	0.76454	5.8148
	23.5	296.7	3.370	0.76638	5.8396
	39.0	312.2	3.203	0.57546	3.7624
3Et1H	14.7	287.9	3.473	1.16065	14.4759
	23.25	296.45	3.373	1.00052	10.0122
	39.0	312.2	3.203	0.75779	5.7252

Table 16. Spin-lattice relaxation rates and calculated solution viscosities.

Compound	$1000/T$ $^{\circ}\text{K}^{-1}$	$\eta$ cp	$100\eta/T$ cp/ $^{\circ}\text{K}$	$1/T_1$ sec $^{-1}$	$T_1 \times 10^3$ sec
1Me3H	3.569 $^{\circ}\text{K}^{-1}$	1.6879 cp	.6024 cp/ $^{\circ}\text{K}$	112.92 sec $^{-1}$	8.856 sec
	3.497	1.4974	.5237	103.50	9.662
	3.375	1.2225	.4126	96.30	10.385
	3.307	1.0918	.3611	91.27	10.956
	3.191	0.9003	.2872	84.01	11.904
	3.112	0.7894	.2456	80.91	12.36
	3.024	0.6820	.2062	85.69	11.67
	3.576	2.6004	.9299	216.07	4.628
	3.476	2.1844	.7592	189.57	5.275
2Me2H	3.375	1.8317	.6181	167.98	5.953
	3.307	1.6269	.5380	157.13	6.364
	3.280	1.5521	.5090	150.28	6.654
	3.199	1.3477	.4312	144.15	6.937
	3.133	1.2012	.3764	128.67	7.772
	3.029	1.0020	.3035	121.80	8.210
	3.633	4.3107	1.5661	275.78	3.626
	3.523	3.4643	1.2205	253.94	3.938
	3.416	2.8008	.9568	213.63	4.681
3Me1H	3.280	2.1375	.7010	182.52	5.479
	3.142	1.6248	.5106	163.05	6.133
	3.074	1.4195	.4364	143.97	6.946
	2.993	1.2084	.3617	152.16	6.572

Table 16 (cont'd.)

Compound	$1000/T \text{ } ^\circ\text{K}^{-1}$	$\eta_{\text{cp}}$	$100\eta/T \text{ cp}/^\circ\text{K}$	$1/T_1 \text{ sec}^{-1}$	$T_1 \times 10^3 \text{ sec}$
1Et3H	3.637	3.7166 cp	1.3516 cp/ $^\circ\text{K}$	165.48 sec $^{-1}$	6.043 sec
	3.533	3.0260	1.0690	133.80	7.474
	3.410	2.3731	0.8092	115.01	8.695
	3.298	1.9019	0.6273	102.50	9.756
	3.163	1.4566	0.4608	89.69	11.150
	3.073	1.2192	0.3746	85.69	11.670
	2.999	1.0534	0.3160	80.06	12.490
2Et2H	3.590	10.811	3.8814	500.75	1.997
	3.537	9.3438	3.3048	464.90	2.151
	3.290	4.7347	1.5580	393.24	2.543
	3.154	3.2564	1.0270	354.11	2.824
	3.074	2.6128	0.8031	304.51	3.284
	2.989	2.0678	0.6180	259.54	3.853
3Et1H	3.603	22.348	8.0514	809.06	1.236
	3.534	17.651	6.2382	735.84	1.359
	3.429	12.326	4.2261	651.04	1.536
	3.281	7.4302	2.4378	599.88	1.667
	3.183	5.3143	1.6917	568.50	1.759
	3.100	4.0010	1.2402	539.37	1.854
	3.001	2.8519	0.8559	452.69	2.209

Table 17. Results of least-squares fitting of data to the equation  $1/T_1(^{14}\text{N})$  vs.  $\eta/T$ .

Compound	Corr. Coeff.	Intercept	Slope
1Me3H	0.9968	59.306	8758.57
2Me2H	0.9978	75.018	15127.91
3Me1H	0.9902	104.278	11386.93
1Et3H	0.9947	53.636	7922.13
2Et2H	0.9561	260.478	6381.02
3Et1H	0.9738	470.831	4286.60

Table 18. Relaxation rates calculated for three selected values of viscosity/temperature.

$(\eta/T)$	Relaxation Rates $1/T_1 \text{ sec}^{-1}$		
	.002 cp/°K	.040 cp/°K	.080 cp/°K
1Me3H	76.8 $\text{sec}^{-1}$	409.6 $\text{sec}^{-1}$	760.0 $\text{sec}^{-1}$
2Me2H	105.3	680.1	1285.0
3Me1H	127.0	559.8	1015.0
1Et3H	69.5	370.5	687.4
2Et2H	273.2	515.7	771.0
3Et1H	479.4	642.3	813.8

Table 19. Proton coupling constants and chemical shifts for alkylammonium ions.

Temp °C	$^3J(D-L)^a$	$^3J(A-D)$	$\delta(L)$	$\delta(D)$	$\delta(A)$
<u>1Me3H</u>					
6.00	6.26 Hz	---	466.7 Hz	188.88 Hz	---
9.50	6.20	---	466.4	183.63	---
30.35	6.17	---	---	183.94	---
30.35	6.16	---	---	---	---(4M) <sup>b</sup>
40.50	6.14	---	---	---	---
51.70	6.15	---	465.48	186.19	---
<u>2Me2H</u>					
9.90	5.71	---	507.3	189.92	---
34.00	5.68	---	505.7	191.40	---
51.70	5.72	---	505.6	193.51	---
<u>3Me1H</u>					
4.25	5.23	---	---	205.82	---
10.00	5.14	---	576.3	206.00	---
19.75	5.19	---	575.7	207.19	---
31.00	5.18	---	575.1	208.20	---
44.25	5.20	---	575.75	209.87	---
51.50	5.12	---	574.7	210.92	---
58.50	5.01	---	576.6	212.16	---
<u>4Me</u>					
30.35	---	---	---	218.90	---

<sup>a</sup>Where L is the ammonium proton ( $NH^+$ ), D is the alkyl Proton  $\alpha$  to the nitrogen ( $+NCH$ ) and A is the alkyl proton  $\beta$  to the nitrogen ( $+NCCH$ ).

<sup>b</sup>This conc 4M all others 5M.

Table 19 (cont'd)

Temp °C	$^3J(D-L)$	$^3J(A-D)$	$\epsilon(L)$	$\epsilon(D)$	$\epsilon(A)$
<u>EtMe<sub>2</sub>H</u>					
30.35	5.76 Hz <sup>C</sup>	7.31 Hz	509.7 Hz	188.4 <sup>C</sup>	---
---	---	---	---	212.06	103.84 Hz
<u>1Et3H</u>					
0.60	5.93	7.33	476.3	209.2	102.42
9.50	5.92	7.27	475.6	210.2	103.16
20.30	5.91	7.30	475.1	211.3	104.20
31.00	5.98	7.39	475.5	212.2	105.39
34.00	5.90	7.26	474.0	212.6	105.65
41.00	5.88	7.34	474.9	213.8	106.50
51.30	---	---	474.4	---	---
60.00	5.91	7.34	474.3	215.4	107.90
<u>2Et2H</u>					
5.00	---	---	516.9	---	---
9.90	---	7.32	---	210.37	103.49
10.00	---	---	516.3	---	---
19.80	---	---	516.2	---	---
30.35	6.23	7.28	---	211.96	104.93
43.70	---	---	513.7	---	---
51.60	6.19	7.30	514.0	213.61	106.73
60.80	6.14	7.31	514.4	214.47	107.42
<u>3Et1H</u>					
4.00	---	---	561.17	---	---
9.90	4.99	7.26	---	219.48	107.78
10.00	---	---	561.05	---	---

<sup>C</sup>Where D is the Me.

Table 19 (cont'd)

Temp °C	$^3J(D-L)$	$^3J(A-D)$	$\delta(L)$	$\delta(D)$	$\delta(A)$
19.75	---	---	560.34 Hz	---	---
31.00	4.92 Hz	7.32 Hz	---	220.44	106.2
34.00	4.97	7.29	560.16	220.51	106.6
38.75	---	---	558.30	---	---
47.00	---	---	560.90	---	---
57.70	4.92	7.45	560.20	222.39	108.37
<u>4Et</u>					
30.35	---	7.27	---	218.40	98.09

Table 20. Measured nitrogen and proton NH chemical shifts.

Compound	Abbr.	Exper. $\delta(^{14}\text{N})$	Calc. $\delta(^{14}\text{N})$	$\delta(^1\text{HN})$
$\text{NH}_4^+$	4H	$0 \pm 0.23$ ppm		0.00 ppm
$\text{CH}_3\text{NH}_3^+$	1Me3H	$+1.62 \pm 0.81$	-5.2 ppm	-0.246
$(\text{CH}_3)_2\text{NH}_2^+$	2Me2H	$-0.35 \pm 0.81$	-10.5	-0.898
$(\text{CH}_3)_3\text{NH}^+$	3Me1H	$-5.77 \pm 0.69$	-15.75	-2.059
$(\text{CH}_3)_4\text{N}^+$	4Me	$-21.02 \pm 0.23$		
$\text{CH}_3\text{CH}_2\text{NH}_3^+$	1Et3H	$-14.78 \pm 0.23$	-10.75	-0.391
$(\text{CH}_3\text{CH}_2)_2\text{NH}_2^+$	2Et2H	$-31.18 \pm 1.15$	-21.5	-1.060
$(\text{CH}_3\text{CH}_2)_3\text{NH}^+$	3Et1H	$-35.10 \pm 2.31$	-32.25	-1.809
$(\text{CH}_3\text{CH}_2)_4\text{N}^+$	4Et	$-42.96 \pm 0.23$		
$(\text{CH}_3\text{CH}_2)\text{CH}_3\text{NH}_2^+$	EtMe2H	$-12.70 \pm 1.15$	-15.95	-0.978

Table 21. Nitrogen chemical shifts for substituted amines.

Compound	State	$\delta(^{14}\text{N})$	$\sigma^{\text{P}}$	Reference
<u>A. Primary Amines</u>				
$\text{CH}_3\text{NH}_2$	Aq NaOH	$0.0 \pm 1$ ppm	0	(118)
$\text{CH}_3\text{CH}_2\text{CH}_2\text{CH}_2\text{NH}_2$	?	$-39.0 \pm 1$	10	(118)
$\text{CH}_3\text{CH}_2\text{NH}_2$	Aq NaOH	$-15.0 \pm 1$	14	(118)
$\text{C}_6\text{H}_5\text{NH}_2$	$\text{Et}_2\text{O}$	$-24.0 \pm 3$	18	(118)
	Liq.	$-35.0$	18	(119)
$\text{NH}_3$	Liq.	$+23.0 \pm 1$	--	(118)
		$+21.0$	--	(117)
<u>B. Secondary Amines</u>			$\sum_n^n \sigma_n^{\text{P}}$	
$(\text{CH}_3)_2\text{NH}$	Liq.	$+5.1$	0	(117)
	Aq NaOH	$+2.0 \pm 2$	0	(118)
$\text{C}_6\text{H}_5\text{CH}_2\text{NH}_2$	$\text{Et}_2\text{O}$	$-25.0 \pm 4$	18	(118)
$(\text{CH}_3\text{CH}_2)_2\text{NH}$	Aq NaOH	$-30.0 \pm 2$	28	(118)
<u>C. Tertiary Amines</u>				
$(\text{CH}_3)_3\text{N}$	Liq.	$+16.0$	0	(117)
	$\text{Et}_2\text{O}$	$+3.0 \pm 3$	0	(118)
$(\text{CH}_3\text{CH}_2\text{CH}_2\text{CH}_2)_3\text{N}$	$\text{Et}_2\text{O}$	$-16.0 \pm 15$	30	(118)
$\text{C}_6\text{H}_5(\text{CH}_3)_2\text{N}$	$\text{Et}_2\text{O}$	$-16.0 \pm 4$	18	(118)
$(\text{CH}_3\text{CH}_2)_3\text{N}$	Liq.	$-24.0 \pm 20$	42	(118)
	$\text{MeNO}_2$	$-28.0 \pm 3$	42	(112)

Table 22. Nitrogen chemical shifts for substituted ammonium ions.

Compound	State	$\delta(^{14}\text{N})$	$\sigma^{\text{P}}$	Reference
<u>A. Primary Ammonium</u>				
$\text{NH}_4^+$	Aq	$0.00 \pm 1.0$ ppm	--	(117, 118, and 119)
	Aq ( $\text{Cl}^-$ )	$0.00 \pm 0.23$	--	This Work
$\text{CH}_3\text{NH}_2^+$	Aq ( $\text{Cl}^-$ )	$+1.62 \pm 0.81$	0	This Work
$\text{CH}_3\text{CH}_2\text{NH}_2^+$	Aq ( $\text{Cl}^-$ )	$-14.78 \pm 0.23$	14	This Work
$\text{C}_6\text{H}_{11}\text{NH}_2^+$	Aq ( $\text{Cl}^-$ )	$-24.00 \pm 2.$	23	(118)
$\text{C}_6\text{H}_5\text{NH}_2^+$	Aq ( $\text{Cl}^-$ )	$-17.00 \pm 10.$	18	(118)
	Aq ( $\text{Cl}^-$ )	$-32.00$	18	(119)
<u>B. Secondary Ammonium</u>				
$(\text{CH}_3)_2\text{NH}_2^+$	Aq ( $\text{Cl}^-$ )	$-0.35 \pm 0.81$	0	This Work
$(\text{CH}_3\text{CH}_2)\text{CH}_2\text{NH}_2^+$	Aq ( $\text{Cl}^-$ )	$-12.70 \pm 1.15$	14	This Work
$(\text{CH}_3\text{CH}_2)_2\text{NH}_2^+$	Aq ( $\text{Cl}^-$ )	$-31.18 \pm 1.15$	28	This Work
<u>C. Tertiary Ammonium</u>				
$(\text{CH}_3)_3\text{NH}^+$	Aq ( $\text{Cl}^-$ )	$-5.77 \pm 0.69$	0	This Work
$(\text{CH}_3\text{CH}_2)_3\text{NH}^+$	Aq ( $\text{Cl}^-$ )	$-35.10 \pm 2.31$	42	This Work

Table 23. Nitrogen chemical shifts for nitriles and isonitriles.

Compound	$\delta(^{14}\text{N})^a$	$\sigma_P$
<u>A. Nitriles</u>		
$\text{C}_6\text{H}_5\text{-CN}$	$-230. \pm 2.0 \text{ ppm}$	18
$\text{C}_6\text{H}_5\text{CH}_2\text{-CN}$	$-221. \pm 3.$	17
$\text{CH}_3\text{CH}_2\text{-CN}$	$-217. \pm 1.$	14
$\text{CH}_3\text{-CN}$	$-217. \pm 1.$	0
$(\text{CH}_3)_3\text{CCN}$	$-215. \pm 1.$	44
<u>B. Isonitriles</u>		
$\text{CH}_3\text{-NC}$	$-136. \pm 0.5$	0
$\text{CH}_3\text{CH}_2\text{-NC}$	$-151. \pm 0.5$	14

<sup>a</sup> Reference 114.

Table 24. Nitrogen chemical shifts for amides.

Compound	$\delta(^{14}\text{N})^a$	$\sigma_P$
<u>A. Formamides</u>		
$\text{HCONH-CH}_3$	$-89.4 \pm 2.0$ ppm	0
$\text{HCONH-CH}_2\text{CH}_3$	$-104.8 \pm 1.5$	14
$\text{HCONH-C}_6\text{H}_5$	$-118.5 \pm 2.5$	18
<u>B. Acetamides</u>		
$\text{CH}_3\text{CONH-CH}_3$	$-84.8 \pm 2.0$	0
$\text{CH}_3\text{CONH-CH}_2\text{CH}_3$	$-100.2 \pm 3.5$	14
$\text{CH}_3\text{CONH-(CH}_2)_3\text{CH}_3$	$-104.9 \pm 2.0$	10
$\text{CH}_3\text{CONH-(CH}_2)_2\text{CH}_3$	$-106.9 \pm 3.5$	10
$\text{CH}_3\text{CONH-C}_6\text{H}_5$	$-110.2 \pm 2.0$	18
<u>C. Unsubstituted Amides</u>		
$\text{CH}_3\text{-CONH}_2$	$-83.9 \pm 2.0$	0
$\text{CH}_3\text{CH}_2\text{-CONH}_2$	$-80.7 \pm 2.5$	14
$\text{CH}_3(\text{CH}_2)_2\text{-CONH}_2$	$-81.1 \pm 2.5$	10
$(\text{CH}_3)_2\text{CH-CONH}_2$	$-80.7 \pm 3.5$	27
$\text{C}_6\text{H}_5\text{CH}_2\text{-CONH}_2$	$-79.0 \pm 2.5$	17
$\text{C}_6\text{H}_5\text{-CONH}_2$	$-71.4 \pm 2.0$	18

<sup>a</sup> Reference 194.

Table 25. Nitrogen chemical shifts for nitro compounds.

Compound	$\delta(^{14}\text{N})^a$	$\rho^b$
$\text{CH}_3\text{-NO}_2$	$-354.5 \pm 0.5$ ppm	0
$\text{CH}_3(\text{CH}_2)_2\text{-NO}_2$	-364.5	10
$\text{CH}_3(\text{CH}_2)_3\text{-NO}_2$	-364.5	10
$\text{CH}_3(\text{CH}_2)_4\text{-NO}_2$	-364.5	10
$\text{CH}_3(\text{CH}_2)_5\text{-NO}_2$	-364.5	10
$\text{C}_6\text{H}_{11}\text{-NO}_2$	-374.5	23
$(\text{CH}_3)_2\text{CH-NO}_2$	-378.5	27
$(\text{CH}_3)_3\text{C-NO}_2$	-384.5	44
$\text{C}_6\text{H}_5\text{CH}_2\text{-NO}_2$	-362.	17
$\text{C}_6\text{H}_5\text{-NO}_2$	-346.5	18

<sup>a</sup>Reference 125.

Table 26. Measured viscosities for ammonium salts in various solvents.

Solution	Kinematic Viscosities
5.04 M Aqueous $\text{NH}_4\text{Cl}$ at pH = 0.2	0.948 cSt (22°C)
Satd. $\text{NH}_4\text{OOC}\text{CF}_3$ soln in dry $\text{CF}_3\text{COOH}$	7.74 cSt (22°C)
2.5 M $(\text{NH}_4)_2\text{SO}_4$ in conc. $\text{H}_2\text{SO}_4$	44.94 cSt (22°C)

Table 27. Summary of NMR results for ammonium salts in various solvents and at various temperatures.

Temp (°C)	Ref <sup>a</sup> Chem shift	Conc-Salt	Peak Structure, Comments
		<u>100% H<sub>2</sub>SO<sub>4</sub></u>	
		<u>2.5 M (NH<sub>4</sub>)<sub>2</sub>SO<sub>4</sub></u>	
	δ(ext HEMDISIO)		
(Amb) 29	389.81 Hz <sup>a</sup>		Broadened triplet $^1J(^1H-^{14}N)=53.88$ Hz
67	391.6		Sharp triplet $^1J(^1H-^{14}N)=53.97$ Hz
		<u>99<sup>+</sup>% HCOOH</u>	
	δ(COOH)	<u>Satd. HCOONH<sub>4</sub></u>	
15	333.9		Sharp triplet $^1J(^1H-^{14}N)=52.80$ Hz
(Amb) 29	329.0		Broadened triplet $^1J(^1H-^{14}N)=52.93$ Hz
67			NH <sub>4</sub> <sup>+</sup> triplet coalesces with carboxyl proton into one broad combination peak
		<u>Dry CF<sub>3</sub>COOH</u>	
	δ(ext HEMDISIO)	<u>Satd. CF<sub>3</sub>COONH<sub>4</sub></u>	
(Amb) 34	403.2		Coalesced triplet
55	403.6		Sharper than amb. but still coalesced

<sup>a</sup>All chemical shifts in Hz at 60 MHz.

Table 27 (Cont'd)

Temp (°C)	Ref, Chem shift	Conc-Salt	Peak Structure, Comments
		<u>Glacial CH<sub>3</sub>COOH</u>	
Amb	δ(CH <sub>3</sub> of acetic)	Satd. CH <sub>3</sub> COONH <sub>4</sub>	
	463.0	Sat. soln. (1)	Broad Combination peak (NH <sub>4</sub> <sup>+</sup> + COOH)
Amb	500.9	Above soln +	
		equal vol HAC (2)	Broader peak
-15	300.0		Separate new broad peak NH <sub>4</sub> <sup>+</sup> -COOH sharp
Amb	538.9	Pure glacial HAC	Sharp single peak (-COOH) for <sup>1</sup> J( <sup>1</sup> H- <sup>14</sup> N)=52 ± 1 Hz (refs 23 and 24)
		<u>H<sub>2</sub>O</u>	
		5.04 M NH <sub>4</sub> Cl (pH=0.2)	
	δ(ext H <sub>2</sub> SO <sub>4</sub> )		
6.0	248.77 Hz		Triplet, Δν 1/2 = 1.3Hz <sup>1</sup> J( <sup>1</sup> H- <sup>14</sup> N) = 52.37Hz
(Amb)	29.5	244.75	Triplet, Δν 1/2 = 1.5 <sup>1</sup> J( <sup>1</sup> H- <sup>14</sup> N) = 52.20
	58.0	238.42	Triplet, Δν 1/2 = 7.66 <sup>1</sup> J( <sup>1</sup> H- <sup>14</sup> N) = 51.75

Table 27 (Cont'd)

Temp (°C)	Ref, Chem shift	Conc-Salt	Peak Structure, Comments
	$\delta(\text{MeNO}_2)$	<u>Nitromethane</u>	
Amb (34)	148.7 Hz	$\text{CF}_3\text{COONH}_4$	Partially coalesced triplet
Amb		$\text{CH}_3\text{COONH}_4$	Could not observe signal
Amb		$\text{NH}_4\text{Cl}$	Could not observe signal
Amb		$\text{NH}_4\text{NO}_3$	Could not observe signal
		<u>Chloroform-<math>\text{d}_1</math></u>	
		$\text{CF}_3\text{COONH}_4$	Singlet signal seen, 20 scans CAT show broadened line
		$\text{NH}_4\text{Cl}$	Weak singlet seen on CRO, 20 scans CAT show no signal
		$\text{NH}_4\text{NO}_3$	Weak singlet seen on CRO
		$\text{CH}_3\text{COONH}_4$	Could not observe signal on CRO

Table 27 (Cont'd)

Temp (°C)	Ref; Chem shift	Conc-Salt	Peak Structure; Comments
<u>Dimethyl Sulfoxide</u>			
$\delta(\text{CH}_3 \text{ of DMSO})$			
Amb	319.6 Hz	$\text{CH}_3\text{COONH}_4$	Singlet )
Amb	389.2	Above + 3 drops HAC	) reacts with DMSO Sharper line )
Amb	468.9	$\text{CH}_3\text{COOH}$	Very broad
Amb	296.4	$\text{NH}_4\text{Cl}$	Broad singlet ) $\Delta\nu 1/2 = 4.31 \text{ Hz}$
67	295.2		= 4.63
Amb	268.1	$\text{NH}_4\text{I}$	Broad singlet ) $\Delta\nu 1/2 = 4.17$
67	267.1		= 6.21
Amb	272.9	$\text{NH}_4\text{NO}_3$	Broad singlet ) $\Delta\nu 1/2 = 17.44$
67	268.8		= 3.04
Amb	282.3	$\text{CF}_3\text{COONH}_4$	Broadened triplet $^1\text{J}(\text{}^1\text{H}-\text{}^{14}\text{N}) = 50.97 \text{ Hz}$
68	279.2		Coalesced triplet
Amb		$\text{HCOONH}_4$	Could observe several signals; Reacts with DMSO
Amb		$(\text{NH}_4)_2\text{SO}_4$	Could not observe signal.

Table 28. Physical properties of solvents.

Solvent	Dielectric Constant	Dynamic Viscosity (cP)	pKa
Acetic Acid (glacial)	6.22 ( 24°) (c)	1.0396 (30°) (g)	4.76 (25°)
	6.15 ( 20°) (a)	1.222 (20°) (g)	
Chloroform	3.7 (100°) (a)	0.464 (40°) (g)	
	4.8 ( 20°) (a)	0.563 (20°) (g)	
	5.6 (-20°) (a)		
Dimethyl Sulfoxide	45.5 ( 40°) (b)	1.98 (25°) (b)	
	48.9 ( 20°) (b)		
Formic Acid	58.5 ( 16°) (a)	1.784 (20°) (g)	3.75 (25°)
Nitromethane	35.8 ( 30°) (a)	0.620 (25°) (h)	
		0.853 ( 0°) (h)	

Table 28 (Cont'd)

Solvent	Dielectric Constant	Dynamic Viscosity (cP)	pK <sub>a</sub>
Sulfuric Acid	100.0 (25°)	19.15 (25°)	(g)
	120.0 (10°)	26.94 (15°)	(g)      pK <sub>2</sub> = 2.00 (25°)
Trifluoroacetic Acid	39.5 (20°)	0.750 (30°)	(i)      0.25 (j)
	9.21 ( 0°)	0.876 (20°)	(i)
Water	78.54 (25°)	0.8903 (23°)	(f)
	80.37 (20°)	1.002 (20°)	(f)

The letters (a) through (j) refer to reference 223.

## V. DISCUSSION

### A. N-H Lineshapes in the Proton Spectra Of Substituted Ammonium Ions

#### Contributions to Linewidths from Proton Exchange

It is first necessary to show that proton exchange has no significant effect on the lineshapes in the proton spectra of the substituted ammonium ions in strong acid solution. Once this has been established the interpretation of the observed lineshapes in terms of  $^{14}\text{N}$  spin-lattice relaxation will be possible.

A very extensive review of proton exchange kinetics between alkylammonium ions, alkylamines and solvents, was presented in Section IIA. The purpose of that review was to examine the conditions under which proton exchange made a significant contribution to the observed lineshapes in the proton spectra of alkylammonium (or alkylamine) salts. It was pointed out that at low pH values ( $\text{pH} < 1.0$ ) exchange by any mechanism was described as "slow," resulting in little or no observable effect on the NMR spectra of the alkylammonium ions. Another way of viewing this is that the residence time of the proton on the amine nitrogen is long on the NMR time scale for  $\text{pH} < 1.0$ . Indeed, the exchange process is so slow that the technique employed to

study it was to start with deuterated alkylammonium salts (e.g.  $R\text{-ND}_3^+$ ) in acidified water, or alkylammonium salts in acidified deuterium oxide, and observe the change in either the  $\text{NH}^+$  or alkyl multiplet on slowly replacing the ammonium protons with deuterons or vice versa.

This will now be demonstrated in more quantitative terms with two calculations relevant to the systems studied in this thesis. Using the data and information of Grunwald, Loewenstein, and Meiboom (2), we begin by combining their Equations 15 and 16 to yield:

$$\Delta\nu_{\text{ex}} = k_{16}/\pi[\text{H}^+] \quad (39)$$

where  $\Delta\nu_{\text{ex}}$  is the contribution to the half-height width of the  $\text{NH}_3^+$  peak from proton exchange, and  $k_{16}$  is a rate constant defined by their Equation (17). Using their values of  $k_{16}$  at several listed pH values, the contribution of exchange to the width of the central  $\text{NH}^+$  line of aqueous  $\text{lMe}_3\text{H}$  can be calculated. Subtracting these results from their values of observed total linewidths (their Table V), the half-height width of the central  $\text{NH}^+$  line without exchange is obtained and is given in the last column of Table 29.

Table 29. Calculated linewidths\* for central NH proton of aqueous monomethylammonium ion

pH	$\Delta\nu$ 1/2 total	$\Delta\nu$ ex	$\Delta\nu$ 1/2 without exchange
3.12	19.9 Hz	1.3 Hz	18.6 Hz
3.41	21.2	2.6	18.6
4.01	28.5	9.9	18.6

\*Reference 2

Thus, the calculated half-height width of the  $\text{NH}^+$  central line without exchange is 18.6 Hz for 4.47 M lMe3H at  $19 \pm 2^\circ\text{C}$  while we found a value of 18.0 Hz for the corresponding line in the spectrum of a 5.11 M solution of lMe3H at  $\text{pH} \approx 0.5$  and  $30^\circ\text{C}$ .

Our line width is approximately the same as that calculated for no exchange, so no appreciable exchange can be occurring; the small difference of 0.6 Hz may be due to either the difference in temperature, since the lineshapes are a function of temperature, or sample spinning, as Grunwald et al. did not spin their samples.

The exchange broadening may also be calculated from the results of Grunwald, et al. Substituting their values for  $k_{11} = 22.6 \times 10^{-3} \text{ sec}^{-1}\text{M}$  (their Table II) and  $p = 0.6$  (their Table IV) for 4.00 M lMe3H at  $25 \pm 1^\circ\text{C}$ , into their Equation (17) we obtain  $k_{16} = 5.88 \times 10^{-3}$ . For a solution in which  $[\text{H}^+] = 0.108 \text{ M}$  ( $\text{pH} = 0.97$ ) this yields  $\Delta\nu_{\text{ex}} = 0.02$

Hz using Equation (39). Therefore, for our 5.11 M 1Me3H at pH = 0.5 the calculated contribution to the NH<sup>+</sup> lineshape from exchange is negligible at ambient temperature.

Loewenstein and Meiboom (33) point out that the NH<sup>+</sup> lineshapes for 2Me2H and 3Me1H are dependent on the <sup>14</sup>N relaxation rates and that quantitative evaluation of the exchange broadening of these lines is impracticable. Since all of the exchange rate constants decrease for the methyl series, and 3Et1H values are smaller than 3Me1H (36 and 41) it is reasonable to assume that exchange broadening of the NH<sup>+</sup> lines for the ethyl series at pH < 1.0 is also negligible.

Thus, exchange kinetics has a negligible effect on NH<sup>+</sup> lineshapes for solutions with pH < 1.0 at ambient temperatures with nothing said about other temperatures. Conner and Loewenstein, (21) made a variable-temperature NMR study of 1Me3H and 4H in order to obtain the activation energies for the kinetic processes, and showed that there was very little effect on these for 1Me3H but a larger effect for 4H. The significant thing is that they attribute the temperature effect on the NH<sup>+</sup> lineshape to changes in <sup>14</sup>N quadrupole relaxation rates rather than to proton exchange.

For the specific alkylammonium salts studied in this

thesis we feel confident that, at the pH values used, the line shapes are primarily determined by the  $^{14}\text{N}$  spin-lattice relaxation rates. In addition to the calculations given above, our experimental results are in agreement with this assumption. As can be seen in Figure 8, increasing the temperature for solutions of  $1\text{Me}_3\text{H}$  and  $1\text{Et}_3\text{H}$  not only causes the triplets ( $^1\text{J}(^1\text{H}-^{14}\text{N})$ ) in the proton spectra to sharpen, evidence of a  $^{14}\text{N}$  spin-lattice relaxation rate decrease (cf. Section IIB.), it also leads to resolution of the spin coupling with the alkyl protons ( $^3\text{J}(^1\text{H}-^1\text{H})$ ) which appears as fine structure on each of the broad triplet components, evidence that proton exchange in these systems is negligible. Additional evidence for low proton exchange rates can be found in the fact that we observe the multiplet structure of the alkyl hydrogens  $\alpha$  to the ammonium group; these show multiplet structure from coupling with ammonium ion protons. It may be recalled that in all the kinetic studies reviewed in Section IIA exchange causes a collapse of these multiplets. The value of the ammonium proton- $\alpha$  alkyl proton coupling ( $^3\text{J}(\text{HNCH})$ ) for each compound shows a decrease (analogous to collapse) with temperature (Table 9) which could be interpreted as resulting from an increased exchange rate at higher temperatures. However, one must exercise extreme

caution when considering changes in coupling constants as was pointed out in Section IID; there are many things which contribute to spin-spin coupling and thus we may be observing a real change in  $^3J(\underline{\text{HNCH}})$  due to changes in the solute-solvent structure.

In the various studies of proton exchange, changes in the lineshapes rather than only multiplet collapse were considered and all the  $\alpha$  alkyl proton peaks show slight broadening with increasing temperature. Here again, one should not be too ready to attribute this to increased proton exchange since it may be due to unresolved coupling between nitrogen and the protons  $\alpha$  to it ( $^2J(^1\text{H}-^{14}\text{N}) < 0.5$  Hz) as was mentioned in Sections IIB and D. As an example, spectra of the methylene hydrogens of the ethyl groups are presented in Figure 13 where it can be seen that there is broadening for 4Et where no exchange occurs but where coupling with  $^{14}\text{N}$  is possible. Various authors have suggested that the broadening of the  $\alpha$  hydrogen peaks is due to unresolved coupling with  $^{14}\text{N}$  and this does appear likely; it also probably contributes to the broadening of the methyl group resonance (cf. Figure 5) in the Et series and experiments showing this are presented later, Section VB. As yet unexplained is the exceptional broadening for the methylene multiplet of 2Et2H.

### Contributions from $^{14}\text{N}$ Spin-Lattice Relaxation and Viscosity

Having confidence now that the lineshapes for the ammonium ion protons (Figure 6) are governed mostly by  $^{14}\text{N}$  relaxation rates, the relaxation rate data obtained from the computer least-squares fitting of the observed spectra may be discussed. These are shown in Table 1, Section IVC. Considering the values in Table 11, the most striking thing is the variation in  $^1\text{J}(^1\text{H}-^{14}\text{N})$  with temperature. Since the majority of the values (2Me2H, 3Me1H, 2Et2H and 3Et1H) were not observed directly but obtained from the computer analysis we cannot really say whether or not they do vary with temperature. A complete discussion of this point is deferred until after discussion of the relaxation times.

In Figure 6 the gradual collapse of the ammonium triplet may be seen. This results from the changes in the  $^{14}\text{N}$  spin-lattice relaxation times caused by variations in electric field gradient from compound to compound; the changing symmetry around nitrogen gives rise to these different field gradients. The values reported in Table 11 may now be compared with those reviewed in Section IIB, keeping in mind that most of those reported by others were estimates.

Our value for 1Me3H is about one-half the 20 msec

estimated by Grunwald et al. (25). The value of Grunwald et al. (25) seems a little high and ours about what it should be, as it falls in line with those reported by Anderson and Baldeschwieler (88) and by Swift et al. (13) about 15.9 msec for liquid ammonia. As the ammonium ion multiplets for 1Me3H and 1Et3H (Figures 5, 6, 8, and 9) are slightly more collapsed than the proton lineshapes for liquid ammonia of Swift et al. (13) our  $T_1 (^{14}\text{N})$  should be (and is) less than the  $T_1 (^{14}\text{N}) \approx 16$  msec of liquid ammonia. The 3Me1H and 2Et2H lineshapes (Fig. 6) match fairly well the shapes for methylammonium chloride in acetic acid of Grunwald and Price (Figure 2 of (29)), and our values of 5.5 msec and 2.5 msec agree quite well with the  $T_1 (^{14}\text{N})$  values they report. Finally, our value of 1.7 msec for 3Et1H agrees rather well with the estimated value of 2.5 msec reported by Ralph and Grunwald (41) for the same salt under similar conditions. In conclusion then, the values obtained and listed in Table 11 are reasonable.

Taking the logarithm of the  $T_1 (^{14}\text{N})$  values and plotting these versus the reciprocal of the corresponding absolute temperatures, one can obtain activation energies for the relaxation process as was done by Moniz and Gutowsky (66). The pertinent values so obtained are listed in columns three and four of Table 12 and are plotted in

Figure 14. The results of computer least-squares fitting of the  $\log T_1$  ( $^{14}\text{N}$ ) and  $T^{-1}$  values are given in Table 13 together with the correlation coefficients (corr. coeff. = 1.0 means all points fall on a straight line) and relaxation activation energies  $E_a(T_1)$  calculated from:

$$E_a(T_1) = -2.303R (\text{slope}) \quad (40)$$

The values obtained here for the alkyl ammonium ions agree very well with those obtained for other nitrogen compounds and reported by Moniz and Gutowsky (66). Before commenting on these results, we need one more set of data.

It has been shown (Equations 19 and 20 of Section IIB) that there is a direct relationship between the solution viscosities and the correlation times. Ultimately (24) the solution viscosities are related to the spin-lattice relaxation time. For this reason, then, the activation energy for relaxation should be related to the activation energy for viscosity, as this also changes with temperature. Since the change in viscosity with temperature is exponential (216), a plot of  $\log \eta$  versus reciprocal absolute temperature yields a straight line. An activation energy may be calculated from the slope:

$$\Delta E(\text{visc}) = 2.303R (\text{slope}) \quad (41)$$

The values of  $\Delta E$  so obtained are listed in Table 15 and the results of the least-squares fit using the computer

library program LINFIT, together with the activation energies for viscosity,  $\Delta E(\text{visc})$ , are given in Table 14.

It can be recalled from the discussion in Section IIB, that a temperature increase lowers the viscosity and both of these operate to decrease the correlation time as given by Equation (20). The correlation time in turn alters the relaxation rate according to Equation (24). Since both relaxation rate and viscosity are temperature dependent processes and both are related through Equation (24) it is quite logical to expect some relationship between the activation energies for viscosity and relaxation. Comparing Tables 13 and 14 it can be seen that  $\Delta E(\text{visc})$  increases for the series 1Me3H 2Me2H and 1Et3H and so also do relaxation activation energies,  $E_a(T_1)$ . The  $E_a(T_1)$  values for other compounds do not follow the  $\Delta E(\text{visc})$  values and more will be said about this a little later. In general,  $\Delta E(\text{visc})$  is larger than  $E_a(T_1)$  and also the range of  $\Delta E(\text{visc})$  values is much larger than the range of  $E_a(T_1)$  values. These facts were noted by Arnold and Packer (93) who speculated that the effect on the rate process by replacing solvent molecules with ions is less for relaxation than for viscous flow. They assume that both rate processes basically depend on similar molecular motions. This however, may be an erroneous assumption since viscosity is

a bulk property of the system, and includes such things as shear forces in liquids and interactions at the viscometer-solution interface. Relaxation, on the other hand, deals only with the rate of energy exchange between spin system and environment, and here specifically the exchange between cation spin system and solution.

Hertz (217) has reported that the reorientation rate of solvent water is greater than the reorientation rate of ion-coordinated water which, in turn, is equal to or greater than the reorientation rate of the ion. This shows that the properties of the solvent differ with location, and measurements on the solvent will take into account a number of interactions whereas measurements on the ion are quite specific, being restricted to one situation.

It is tempting to try to relate activation energies to the structure in the water but Hertz (94 and 217) points out that this is not always possible. For the alkylammonium ions we have investigated there are a number of reasons why this is unwise. First, as reported in Table 13 the differences are very slight. Second, the nature of these salts is such that there is a varying degree of direct interaction with the water through

hydrogen bonding and slow proton exchange. Third, the relaxation process is dominated by the electric field gradient--quadrupole moment interaction. Fourth, the shapes and structures of these molecules are such that the interaction with the solvation sphere is not uniform. Fifth, a small but definite quantity of acid was added and this definitely affects the water structure to an undetermined extent. Because of all these complications, no attempt was made to correlate the activation energies of Table 13 with changes in either solvent structure or solvent-cation structure. We do know, however, that the structures are changing with temperature and will discuss this later.

Again, considering the results of Tables 13 and 14, there should be an increase in the relaxation activation energies ( $E_a(T_1)$ ), paralleling the increase of  $\Delta E$  (visc) values for the reason given above. Another reason to expect an increase in  $E_a(T_1)$  is the change in field gradients, the NMR spectra of compounds with the more symmetrical electric fields being least sensitive to temperature and those with the more asymmetrical electric fields being most sensitive to temperature. The spectra of the compounds 2Me2H, 2Et2H, and EtMe2H (which we didn't

measure) which have the greatest electric field gradients should be most sensitive to temperature and thus have the largest values of  $E_a(T_1)$ . On the other hand, 4H, 4Me and 4Et (which we couldn't measure by this technique) should be the least affected by temperature and thus have the smallest  $E_a(T_1)$  values.

One possible reason for the fact that the measured  $E_a(T_1)$  does not parallel the measured  $\Delta E$  (visc), is that temperature change actually affects more than just the viscosity alone. For example, it has already been pointed out that the field gradient ( $\partial^2 V / \partial Z^2$ ) may be temperature dependent (63,93,100 and 217). Another possibility is that the constant C of Equation (20) may actually be temperature dependent.

A second possible reason for the disagreement of Tables 13 and 14 is the temperature range studied. Hertz and Zeidler (94) pointed out that for aqueous electrolytes  $E_a(T_1)$  for either water or ions is temperature dependent, behaving differently in various temperature ranges. The temperature change may cause a change in water structure (e.g. formation of ice at temperatures near 0°C) rather than water-ion interaction. For this reason then, they obtained  $E_a(T_1)$  values in the 40-80°C range.

A third limitation is that of the equation (Equation (9)) used to calculate the lineshapes. It was derived for lineshapes determined only by quadrupole relaxation, whereas the systems actually studied have some contributions to lineshape from other processes. In addition, the equation most accurately portrays those lineshapes where the linewidths of the multiplet components are less than the separation between the components, i.e.  $^1J(^1H-^{14}N)$ . We shall expand on the limitations of the equation a little later.

In order to circumvent some of these difficulties and thus allow some meaningful interpretation of the relaxation data, a plot of relaxation rate vs. viscosity/temperature was made. This was accomplished in the following way. From a least-squares fit of  $\log \eta$  vs. reciprocal absolute temperature values, given in Table 15, the slopes and intercepts were obtained for each of the six solutions and are listed in Table 14. Using these parameters, viscosities were then calculated at each temperature for which the relaxation time was obtained (Table 11).

These viscosity values, together with relaxation rates (column five) and viscosity/temperature values (column four) are listed in Table 16. A least-squares fit

was then made of  $1/T_1$  vs.  $\eta/T$  and the slopes and intercepts obtained from it are given in Table 17. Next, in order to have a better visual display, the slopes and intercepts of Table 17 were used to calculate relaxation rates at the three selected  $\eta/T$  values of 0.002, 0.04 and 0.08. The results of these calculations are listed in Table 18 and plotted in Figure 15.

In Section IIB, it was shown that a treatment of this type should yield a straight line of slope  $3/8 (e^2qQ/h)^2C$  and with y-intercept zero. From Figure 15 we see that the y-intercepts are not zero; effects of this type were noted in other systems by Arnold and Packer (93) and by Richards (100) and indicate that something is affecting the relaxation rates which is not being accounted for in Equation (24). Arnold and Packer (93) attribute the non-zero y-intercept as being due to a concentration dependence of the relaxation rates particularly a concentration dependence of the quadrupole coupling constant,  $(e^2qQ/h)^2$ . This is understandable for their systems (ionic salts in a solvent of low dielectric constant), where field gradients are induced by the gegen ion at higher concentrations. Richards found the same thing for aqueous electrolytes and attributes the non-zero intercept to

viscosity-independent line broadening such as vibrational and motional effects. In conclusion, if there were no other effects on the relaxation rates calculated from viscosity-temperature data except those acting through the correlation term, the lines should pass through the origin and the slopes should indicate the relative changes in electric field gradients.

With the foregoing in mind, then, we shall now consider the data for the aqueous alkylammonium chlorides presented in Figure 15. Quite obviously they do not follow the ideal predictions, not only with regard to the intercepts but also the slopes. The disagreement is most pronounced with the ethyl series, whereas the predictions hold rather well for the methyl series. The discrepancies shown in Figure 15 seem to parallel the solution viscosities of Table 15, the greatest discrepancies matching the solutions with the highest viscosities. Keeping this in mind, now, we recall that these relaxation rates are for nitrogen and that they were obtained from proton spectra, therefore, we must consider effects on the proton line-shapes. The ammonium proton lineshape results from two factors. The first, and as we have shown, major factor is the nitrogen relaxation rate, the second factor being

the viscosity. For a viscous solution, the proton lines are broadened, thus all the lineshapes of Figure 6 should have much narrower components, whereas the amount of triplet collapse is still determined by the  $^{14}\text{N}$  relaxation rate. The effect of viscosity for 2Et2H, and 3Et1H, where only a single line is found, would be to cause the  $T_1(^{14}\text{N})$  found to be longer than it should be for large  $\eta/T$  (high viscosity and low temperature). On the other hand, for small  $\eta/T$  (low viscosity and high temperature) the  $T_1(^{14}\text{N})$  obtained is shorter than it should be. The result of this on Figure 15 would be to cause all the points ( $1/T_1$  values) on the left-hand side to drop down (possibly to zero y-intercept) while causing the right-hand points ( $1/T_1$  values) to move up, and thus cause an increase in the slopes of 2Et2H and 3Et1H. In addition, the slopes of Figure 14 would be increased as would the  $E_a(T_1)$  values of Table 13.

There are a few experiments which could be performed to check the importance of viscosity on the lineshape of the NH protons. First, lineshape could be studied as a function of temperature while the effect of the nitrogen is removed by  $^{14}\text{N}$  decoupling. This study is discussed in Section VB. A second method of studying this viscosity effect by removing the broadening of the nitrogen would be to study the same compounds highly enriched with the

non-quadrupolar  $^{15}\text{N}$ . A third method would be to use a model nitrogen compound which has very high symmetry and thus little contribution from  $^{14}\text{N}$  relaxation. Such a compound is an ammonium salt and studies on this are described in Section VC.

### Spin-Spin Coupling Constants

Now we return to the data presented in Table 11, particularly the variation in coupling constants,  $^1\text{J}(^1\text{H}-^{14}\text{N})$ . Since these values were obtained from the computer, the first impulse was to assume that the computer was adjusting these to make a good fit and that they should actually be constant. After considering some of the reported  $^1\text{J}(^1\text{H}-^{14}\text{N})$  and  $^1\text{J}(^1\text{H}-^{15}\text{N})$  values (cf, Tables 5 and 8 of section IID) however, and specifically the reports of Randall and Baldeschwieler (132), Sunners et al. (135) and Dudek, et al. (165), it seemed quite possible that the  $^1\text{J}(^1\text{H}-^{14}\text{N})$  values of Table 11 actually were varying with temperature. In addition, from Tables 5 and 8 it can be seen that there is no single directly determined value which could be used for  $^1\text{J}(^1\text{H}-^{14}\text{N})$  for the alkylammonium ions since there is no agreement among them and also the limits of error are larger than for those obtained from our computer analysis of lineshapes. Also, since the

temperature variation of  $^1J(^1H-^{14}N)$  for a specific compound could not be predicted, the values at specific temperatures could not be obtained. Comparing the average  $^1J(^1H-^{14}N)$  values reported in Table 11 with those of Table 5 we see that the average error of our results is much smaller than the errors in those reported earlier. Clearly, the true  $^1J$  values can only be obtained from  $^{15}N$  enriched compounds where there is no quadrupole interaction.

In order to answer the question as to whether or not  $^1J(^1H-^{14}N)$  values do indeed change with solvent and temperature, ammonium salts were studied in several solvents over a temperature range. The ammonium ion was chosen because it is completely symmetrical and thus has a long  $^{14}N$  relaxation time. The results of this study are presented in Section VC.

If  $^1J(^1H-^{14}N)$  is changing, and from the foregoing we are certain that it does, then the hybridization of the nitrogen is changing, and certainly the other hybridizations must also be changing. In short if  $^1J(^1H-^{14}N)$  coupling is changing then certainly other couplings are changing, for it would not be possible to have one coupling value vary while all the others remain constant. Applying this in reverse we see from Table 19 that the

three-bond couplings through nitrogen ( $^3J(D-L)$ ), which can be accurately measured from the spectra are very definitely changing with temperature; therefore, we can be quite sure that  $^1J(^1H-^{14}N)$ , which cannot always be measured from the spectra, is also changing. This comparison along with Table 5 also tells us that  $^1J(^1H-^{14}N)$  for 2Et2H and 3Et1H do not vary as much as indicated by our computer results.

A further indication that temperature changes are causing variations in the coupling constants is seen by examining columns four, five and six of Table 19. These are lists of the chemical shifts  $\delta(L)$  for the NH protons, the chemical shifts of the protons on the carbon  $\alpha$  to the nitrogen  $\delta(D)$  and the chemical shifts of the protons on the  $\beta$  carbon  $\delta(A)$ . Since the chemical shift of the ammonium-proton  $\delta(L)$  is partially influenced by its interaction with water, its shift to high field with increasing temperature may indicate less hydrogen bonding at higher temperature since this is in the correct direction for such a mechanism (94 104 and 128). The unusual thing is that the temperature effect on the  $\alpha$  alkyl proton chemical shift,  $\delta(D)$ , is greater and in the opposite direction (downfield). This may indicate that the

alkyl group has a stronger interaction with water than does the ammonium group. Alternatively the temperature effect on nitrogen hybridization may be an important factor and act to produce a downfield shift in  $\delta(D)$  along with a downfield shift in  $\delta(L)$ . The latter explanation seems more plausible as  $\delta(D)$  for both 4Me and 4Et, where the hybridization is the same, are nearly the same. The change of hybridization with temperature would then be working in the opposite direction to the change in hydrogen bonding with temperature for  $\delta(L)$ , the net result being a slight upfield shift for the ammonium protons as observed.

#### B. Heteronuclear Decoupling

The  $^1\text{H}\{-^{14}\text{N}\}$  decoupling experiments on the alkyl-ammonium salts were mainly undertaken in order to observe the changes in the proton spectra with effects from  $^{14}\text{N}$  removed. First, the ammonium-proton peaks were observed while decoupling nitrogen in order to study effects other than nitrogen quadrupole interactions, on their lineshapes. Second, the alkyl-proton peaks were observed while decoupling nitrogen to see whether long range  $^1\text{H}\text{-}^{14}\text{N}$  coupling could be detected by this method since

it could not be observed in the single-resonance spectrum. Since the  $^{14}\text{N}$  frequencies for optimum decoupling of the alkylammonium salts and the reference ammonium ion were carefully noted, nitrogen chemical shifts were also obtained.

### N-H Proton Lineshapes

One of the effects we wanted to observe was that of varying temperature on the NH proton lineshape, without interference from  $^{14}\text{N}$  interactions. In the preceding part (Section V A) evidence was given to show that the major factor determining the lineshape of the NH proton resonance for the alkylammonium ions is the  $^{14}\text{N}$  relaxation time which is governed both by viscosity and temperature. Therefore, the object of one  $^1\text{H}\{-^{14}\text{N}\}$  decoupling study was to see how temperature (and viscosity) affected the NH lineshapes since by  $^1\text{H}\{-^{14}\text{N}\}$  decoupling we remove the overwhelming effect of  $^{14}\text{N}$  quadrupolar broadening on these lineshapes and can study the minor effects.

The results of  $^1\text{H}\{-^{14}\text{N}\}$  decoupling variable temperature experiments on the 1Et3H spectrum are shown in Figure 12. These spectra were all run on the same day, during about a 5-hour period, and using the same 4.33 MHz decoupling

power. It can be seen that this was less than needed for complete  $^{14}\text{N}$  decoupling. This experiment answers two major questions. The fact that the linewidths decrease and the resolution of the triplet improves with increasing temperature ( $30^\circ$  range) proves conclusively that viscosity (and no doubt hydrogen bonding) plays a role in determining the lineshapes of the NH protons. Also, the fact that the resolution of the triplet improves with increasing temperature, and thus the lines do not broaden with accompanying coalescence, indicates that proton exchange involving the amino group makes a very minor contribution to the lineshapes. These effects will again be demonstrated on a much simpler system in the following part (Section V C).

Under conditions of complete  $^{14}\text{N}$  decoupling, as shown in C of Figure 9, the linewidths of the ammonium multiplets for each salt are quite narrow. Indeed, eight of the expected ten lines for 3Me1H were observed. This again is further proof that proton residence time on the ammonium group is long and that proton exchange for all six compounds makes a very insignificant contribution to the NH lineshapes, whereas  $^{14}\text{N}$  interaction makes the major contribution. This was illustrated by Ogg and Ray (26)

in the spectra of  $\text{1Me3H}$  enriched with  $^{15}\text{N}$ (65%) and we have shown it again by another method, also specifically for the series of substituted ammonium ions.

#### Long-Range Proton-Nitrogen Spin-Spin Coupling

In the single resonance spectra, no  $^1\text{H}$ - $^{14}\text{N}$  coupling can be observed in the alkyl groups for coupling across two and three bonds. As a result of the electric field asymmetry which produces rapid  $^{14}\text{N}$  relaxation, the multiplets from  $^1\text{H}$ - $^{14}\text{N}$  coupling will be partially or completely collapsed for  $\text{3Me1H}$ ,  $\text{2Et2H}$  and  $\text{3Et1H}$ . As seen in Tables 6, 7 and 8, the  $^2\text{J}(^1\text{H}-^{14}\text{N})$  and  $^3\text{J}(^1\text{H}-^{14}\text{N})$  couplings are already small, and multiplet collapse will make these separations even smaller and consequently more difficult to observe. For these reasons, then, the inability to resolve the two- and three-bond couplings in the single resonance spectra is understandable. It was thus reasoned that the existence of these couplings could be detected by means of  $^1\text{H}$ - $\{^{14}\text{N}\}$  decoupling.

The results of the decoupling experiments indeed show that there is unresolvable spin coupling between  $^{14}\text{N}$  and the protons of the alkyl group in substituted ammonium ions. This was proved by slowly changing the nitrogen

decoupling frequency at low power levels while observing the alkyl signals for noticeable sharpening and growth in peak heights. It was particularly noticeable for the  $-\text{CH}_3$  group of  $1\text{Et}3\text{H}$  and  $2\text{Et}2\text{H}$ , the  $^{14}\text{N}$  frequency for optimum  $-\text{CH}_3$  signal height being the same as that for optimum decoupling of the  $-\text{NH}^+$  group. The effect was slight for  $3\text{Et}1\text{H}$ , where rapid  $^{14}\text{N}$  relaxation has just about washed out any coupling already. For two-bond coupling, there was a slight but detectable intensity increase for the methyls of  $1\text{Me}3\text{H}$  and  $3\text{Me}1\text{H}$ , where coupling is unobservable, and a very definite and sharp effect for  $4\text{Me}$ , where  $^2\text{J}(^1\text{H}-^{14}\text{N})$  is easily observable. No detectable change was found for the methylenes of  $1\text{Et}3\text{H}$ ,  $2\text{Et}2\text{H}$  and  $3\text{Et}1\text{H}$ . Checking  $4\text{Et}$ , where  $^{14}\text{N}$  relaxation is a minimum, no change in the methylene group resonance was observed whereas a very clear and sharp  $^{14}\text{N}$  frequency effect was observed for the methyl resonances.

### Nitrogen Chemical Shifts

With regard to the nitrogen chemical shifts first, a comparison of the values obtained here Table 20, with those published earlier, Table 1, is discussed from the viewpoint of establishing which are more accurate.

Second, a qualitative discussion of the  $^{14}\text{N}$  chemical shift itself is given, to explain the increasing paramagnetic shift (i.e. shift to low field) with increasing alkyl substitution around nitrogen.

It is seen (Table 20) that our value for 4Me agrees very well with those determined independently by Schmidt et al. (117) and by Evans and Richards (118) while all three of us disagree with the older value of Holder and Klein (116). As the work of Holder and Klein was performed in the early days of nuclear magnetic resonance when instrumental equipment and techniques were less sophisticated, there can be little doubt that the value of -21 ppm for 4Me is more accurate, particularly since the latter value was arrived at by three independent laboratories.

Next, the value of the  $^{14}\text{N}$  chemical shift for 4Et is considered, and here again there is excellent agreement between our measurement and that of Evans and Richards (118). It can be seen that although the two differ a little, ours nevertheless falls within the range of error reported by Evans and Richards (118). Thus there is little doubt that the value of -43 ppm for 4Et is an accurate one.

There is some doubt about the older values of nitrogen chemical shifts for members of the methylammonium ion series obtained from the published spectra of Ogg and Ray (68). The present values and their correlation with the degree of alkyl substitution should be more reliable for the following reasons.

First, we employ experimental data for the  $^{14}\text{N}$  chemical shifts in the ethyl series in our argument; these values are much larger and possible experimental errors are therefore minimal. In addition, we know that the value for 4Et is accurate. Thus, we find that the experimental  $^{14}\text{N}$  chemical shifts (Table 20) to low field are in the order



Considering only the effect of alkyl groups on the  $^{14}\text{N}$  chemical shift, it would seem reasonable that the methyl series should follow the same order, and indeed this is what we find, the order being



again arranged according to low field shift. That the effect of the alkyl groups on the  $^{14}\text{N}$  chemical shift is mainly additive is experimentally substantiated as can be shown by arranging the three dialkyl ammonium ions in

order of decreasing low field shift



All of these  $^{14}\text{N}$  chemical shifts (relative to ammonium ion) are clearly illustrated in Figure 16.

Operating on the assumption that the  $^{14}\text{N}$  chemical shifts are largely additive for the alkyl groups, one can use the equation of weighted averages of Maslov (120):

$$\delta_i = \frac{1}{s} \sum_j m_j \epsilon_j$$

where:  $\epsilon_i$  = chemical shift of the unknown molecule  $i$

$\epsilon_j$  = chemical shift of the known molecule  $j$

$m_j$  = number of bonds found in the molecule of type  $j$  which are also present in molecule  $i$

$$s = \sum_j m_j = \text{total number of bonds in molecule } i$$

along with the values  $\delta(4\text{H}) = 0$ ,  $\delta(4\text{Me}) = -21$  and  $\delta(4\text{Et}) =$

$-43$ , which are chosen to give exact agreement, to make an

empirical calculation of the chemical shifts. These

calculated values are tabulated in column 4 of Table 20

and plotted as circles and dotted lines in Figure 16.

Quite obviously, the experimental and calculated values shown in the figure and table do not agree too well.

Although the effect of the alkyl group is additive, it

does not fully account for the observed  $^{14}\text{N}$  chemical

shifts. Thus we must look further in order to explain the differences between the observed values and those given by the additive approximation.

Earlier (Section II C) a number of theories for nitrogen chemical shifts were examined and their limitations in explaining or predicting nitrogen shifts discussed. Here we will apply an empirical method which allows a fairly close approximation to any  $^{14}\text{N}$  shift of covalent compounds, once the chemical shifts for three or four compounds are known.

In general there is a shift to low field on protonation of the ammonia or amine nitrogen because the shielding effect of the lone pair electrons is removed by involving these electrons in bonding. This is shown by the large number of examples in Tables 21 and 22. Perhaps this is a proper place to point out the "bowing" of Figure 16 and offer an explanation. It can be noted that for the methyl series there is an upfield "bow" deviation from the dashed Maslov line, whereas for the ethyl series the opposite is observed, namely, a downfield "bow" deviation from the dashed Maslov line. The explanation for these lies in the observed amine shifts listed in Table 21. All of the methyl amines are at higher field than the

protonated forms, whereas for the ethyl series the nitrogen resonances for free amines are at, or very close to, the values for the protonated forms. Thus, the methyl group exerts a stronger influence on the  $^{14}\text{N}$  shift than does the ethyl group, and the effect is to cause a slight shift to higher field for the protonated form. Further evidence for the greater influence of methyl relative to ethyl is noted in the dialkyl series where  $\text{EtMe}_2\text{H}$  lies closer to  $2\text{Me}_2\text{H}$  than to  $2\text{Et}_2\text{H}$  (Figure 16 and Table 22).

Unlike Hampson and Mathias (194), who reported no correlation of  $^{14}\text{N}$  and  $^1\text{H}$  chemical shifts of amides, we do find a very obvious and significant correlation in the case of alkylammonium ions (cf. Table 20, Figures 16 and 17). This is due to the fact that both the  $^1\text{H}$  and  $^{14}\text{N}$  chemical shifts of the alkylammonium ions are governed by  $\sigma_{\text{D}}$  with  $\sigma_{\text{p}}$  as a slight perturbation. Comparing the  $^1\text{H}$  shifts with the  $^{14}\text{N}$  shifts measured for the same sample preparations there are some obvious differences. The  $^1\text{H}$  shifts, unlike the  $^{14}\text{N}$  shifts, show a distinct movement to low field with increasing alkyl group substitution, in the order



Although the NH proton is in between the nitrogen and

solvent water, its resonance value is determined mainly by the nitrogen to which it is bonded (and indirectly by the alkyl groups acting on nitrogen) and only slightly by the much weaker hydrogen bonding to water. Hydrogen bonding shifts the NH proton resonances to low field while decreasing hydrogen bonding results in shifts to higher fields (94, 104 and 128). Accordingly, one would expect the ammonium ion and the monoalkylammonium ions to hydrogen-bond most, the trialkylammonium ions least, so that if hydrogen bonding were the main factor determining the NH proton shifts, the result would be the direct opposite to that observed. Another possible explanation of the observed NH proton shifts could be proton exchange between amine and water. Variable-temperature  $^1\text{H}$  resonance studies described before (Section V A), however, clearly show that proton exchange is relatively slow and thus unimportant in this regard.

The full explanation of the observed  $^{14}\text{N}$  shifts with alkyl substitution was first put forth by Witanowski et al. (111, 113, 114 and 125), who suggested that inductive effects, either electron-donating (+I) or electron-withdrawing (-I), were important. Here we are mainly concerned with alkyl groups which, as a class, are

electron releasing relative to hydrogen, whatever the cause. The particular order of effectiveness of the various alkyl groups among themselves depends upon whether the dominant factor is inductometric or hyperconjugative (218). We will now show that hyperconjugation explains the  $^{14}\text{N}$  shifts we report for the alkyl ammonium ions as well as a large number of  $^{14}\text{N}$  shifts previously reported by others. In addition, this will allow the estimation of many nitrogen shifts which have not been measured.

Since there is a much larger wealth of shift data for  $^{31}\text{P}$  than for nitrogen, and since a larger number of chemical shift theories have been investigated, it was thought that a study of phosphorus chemical shifts could possibly be an aid in not only explaining the nitrogen shifts, but perhaps in allowing prediction of shifts as yet unmeasured. Of particular interest is the work of Maier (219) on primary phosphines and Grim and co-workers on secondary (220) and tertiary (220 and 221) phosphines and phosphonium salts (222). They obtain a linear relationship between the observed  $^{31}\text{P}$  chemical shifts and the sums of empirically determined paramagnetic shielding values,  $\sum P_n$  (see Table II, ref. 221). From these plots which are relative to the methyl compound as zero,

intercepts and slopes are obtained. The differences between calculated and observed values are on the average  $\pm 1$  ppm. or better and, in the worst cases,  $\pm 2.3$  ppm. This is within the experimental errors in  $^{31}\text{P}$  NMR spectroscopy.

As the order of  $^{14}\text{N}$  shifts for various alkyl nitrogen compounds seemed to follow the effect of hyperconjugation, we thought there might be a correlation between the  $^{14}\text{N}$  shifts observed by us, as well as others, and the  $\sigma^{\text{P}}$  values of Grim (221). The results of the correlation of observed  $^{14}\text{N}$  shift with  $\sigma^{\text{P}}$  or  $\sum_n^{\text{P}}$  are listed in Tables 21, 22, 23, 24 and 25 and plotted in Figures 18, 19 and 20. Although the data are sparse, the correlations appear to hold. In addition to explaining the nitrogen chemical shifts in the amines and ammonium ions, the chemical shifts in the alkyl nitro compounds of Witanowski et al. (125) and the N-substituted formamides and acetamides of Hampson and Mathias (194), are also accounted for

Comparing the results of the correlations for the  $^{14}\text{N}$  chemical shifts with those for  $^{31}\text{P}$  (219-222), it can be seen that the accuracy and precision is much better for the latter. One reason for this is that  $^{31}\text{P}$  chemical

shifts are two to three times larger than nitrogen shifts thus subtler effects such as hyperconjugation will be more apparent in phosphorus resonances than in nitrogen resonances. A second reason, which may be the explanation for the first, is that phosphorus has the possibility of using d orbitals in bonding which nitrogen does not have. A third reason arises from the nuclear properties.  $^{31}\text{P}$  has a natural abundance of 100% and this isotope has a spin of  $1/2$ , so will always yield signals which are quite sharp and lead to only small errors in measurement (about  $\pm 1$  ppm);  $^{14}\text{N}$ , on the other hand, has a natural abundance of 99.6%, a spin of 1, and a quadrupole moment associated with it. As a result, the linewidths of the nitrogen resonances are a function of the electronic structure and will yield a very broad signal when the electric field gradient at nitrogen is very asymmetric. As a result the nitrogen chemical shifts may have a large error associated with them, as is the case for a large number of compounds listed in Tables 21-24. Enrichment with the isotope  $^{15}\text{N}$   $I = 1/2$ , is very expensive and so far very few  $^{15}\text{N}$  shifts have been reported. Unfortunately not enough data for  $^{15}\text{N}$  enriched compounds have been reported to complete the alkyl series discussed above; such data are needed to

p2

ga

T

i

1

9

a

a

a

provide another test of the extent to which hyperconjugation correlates with the nitrogen chemical shifts.

Considering the nitrogen chemical shift data in Tables 21-24, and the graphs of the  $^{14}\text{N}$  shifts vs.  $\sum_n^n \sigma_n^P$ , it can be seen that the best correlations, yielding the largest slopes, are obtained when the electron-releasing group is attached directly to nitrogen (e.g. amines, ammonium salts, nitro compounds, N-substituted amides, and possibly the isonitriles). Furthermore, their slopes are always negative. However, when the electron-releasing group acts through an intervening atom or group, as in the nitriles and the carbonyl carbon-substituted amides, the slopes are very definitely smaller and appear to be positive. Even though the slopes are small, it appears that the effect is present and measurable. Finally, it can be noted that, in almost all compounds, the aromatic ring causes a marked deviation, and this deviation is largest when the ring is attached directly to nitrogen, and somewhat less when acting through methylene as in the benzyl group. This may be an anisotropic shielding effect caused by the  $\pi$ -cloud current, or some resonance form causing perturbations of the nitrogen p-orbitals.

In conclusion, we are suggesting again, as did Bose et al. (119), that nitrogen resonances can be used to demonstrate electron-release through hyperconjugation. However, we feel that the effect is best shown if the functional group is attached directly to nitrogen rather than operating through an aromatic ring as in the compounds they studied. In addition, nitrogen resonance studies appear to afford a more reliable method of observing electron-releasing or electron-withdrawing effects than many other techniques. Thus, measurements of basicity constants,  $pK_b$ , for amines are often complicated by other effects like steric strain, as elucidated by Brown (42):

C. Solvent Effects on Proton  
NMR Spectra of Ammonium Salts

Changes of  $^1J(^1H-^{14}N)$  with Solvent and Temperature

The main stimulus for the work reported in this part was to answer the question as to whether the variations of  $^1J(^1H-^{14}N)$  with temperature, which we found from computer analysis of the complex lineshapes in the NMR spectra of alkylammonium salts, were really significant. The present study of the directly bonded  $^1J(^1H-^{14}N)$

coupling itself constitutes a separate test from the study of the other coupling constant,  $^3J(\underline{HNCH})$  presented before (Section V A).

It was reasoned that the best species for this study would be the ammonium ion ( $4H$ ), since it is completely symmetrical and thus there would be no complicating effects on the spectra from  $^{14}N$  relaxation, provided that proton exchange was minimized. Consulting the literature (Tables 5 and 8 of Section II D), it was learned that there was no agreement on the value of  $^1J(^1H-^{14}N)$  for the ammonium ion. The disagreement could be due to experimental error or it could be real, resulting from the variety of anions and solvents used in the various investigations. Since none of these authors had noted this difference, a re-examination of the spectra of various ammonium salts in a variety of solvents became necessary.

From Table 27 (Section IV C) we see that there is a measurable variation in  $^1J(^1H-^{14}N)$  with anion, solvent and temperature. For convenience, we list the values at ambient temperature in Table 30.

Table 30.  $^1J(^1H-^{14}N)$  for ammonium salts in various solvents.\*

$^1J(^1H-^{14}N)$	Salt	Solvent and Conditions
51.0 Hz	$CF_3COONH_4$	Saturated in dry DMSO
$52.4 \pm 0.3$	$NH_4Cl$	5.04 M in $H_2O$ ; pH = 0.2
52.9	$HCOONH_4$	Saturated in 99+% $HCOOH$
53.9	$(NH_4)_2SO_4$	2.5 M in 100% $H_2SO_4$

\*Data taken from Table 27.

These values may be compared with those reported in Table 5 (Section II D). The first one to consider is the value for the aqueous ammonium ion in highly acidified solution. The values of Meiboom et al. (18) and Anderson et al. (143) are lower than that reported in this work while the value of Emerson et al. (19) is higher. These values are rather old and, as can be seen, our value agrees very well with the more recent measurement of Baldeschwieler (144).

The second value for consideration is that for ammonium ion in sulfuric acid. Our value agrees with that of Fraenkel et al. (145) and both differ from the value for the aqueous ammonium ion. We also measured

$^1J(^1H-^{14}N)$  in 100% sulfuric acid solution to see if there was any change with acid concentration, and there does appear to be a change.

The surprising thing we find is that all these values fall within such a narrow range ( $\sim 3$  Hz) for such vastly different solvents. The point is, though, that there is very definitely a measurable difference in  $^1J(^1H-^{14}N)$  with variation of solvent and, for the same salt-solvent system, with temperature. To explain these variations would involve a more detailed study and is beyond the scope of this investigation.

In the course of this search for variations in the  $^1J(^1H-^{14}N)$  coupling constant of the ammonium ion in various solvents, a number of other interesting effects were noted. A few of these are shown in Figure 21. In order to explain these lineshapes, variations of anion, solvent and temperature were made in a fashion similar to that of Randall et al. (80-82) and of Kintzinger and Lehn (65). Thus, we found that a very simple nitrogen compound, the ammonium salts could illustrate all the effects described in Sections II A and B, whereas other investigators (65, 69, 71, 73, 78 and 79) had employed much more complex nitrogen compounds.

### General Effects on NH Lineshapes

The chief feature used in determining the ammonium salt/solvent interaction is the characteristic shape of the ammonium ion proton signal and the change in that lineshape with temperature. As was pointed out earlier, Roberts (8) was the first to suggest that variation in the NH proton lineshape with temperature could be used as a diagnostic method to distinguish between the effects of proton-nitrogen exchange and  $^{14}\text{N}$  relaxation. He noted that increasing temperature causes faster exchange rates and consequent collapse or coalescence of multiplets and, generally, sharpening of broad singlets (cf. Figure 7, going from F to A) when the NH lineshape is governed by exchange. The opposite behavior is observed when the NH lineshape is governed by  $^{14}\text{N}$  relaxation; increasing temperature then causes sharpening of triplets, the appearance of a triplet from a broad peak or the broadening of a sharp singlet (cf. Figure 7, going from A to F).

In considering a triplet or partially coalesced triplet, the diagnostic temperature test to distinguish between exchange and relaxation is quite clear cut. However, for a single line, observation of changes in line

shape with temperature does not lead to an unequivocal answer. One must therefore probe deeper into such things as the mechanism giving rise to the single line and consider whether the peak is a "pure" NH line or a "composite" NH/solvent line. Experiments relative to this problem will be discussed below.

### Ammonium Ion in Acidic (Protic) Solvents

At the outset we will consider acidic solvents since these were chosen first in order to reduce the effects from proton exchange. A, B and C of Figure 21 show the ammonium ion in three different acids at ambient temperature ( $\sim 30^\circ\text{C}$ ). The spectra are dramatically different. If we consider viscosity changes as a possible explanation for the fact that the formic acid (HForm) ammonium ion resonance (C) is broader than the sulfuric acid ammonium ion resonance (A) or why the trifluoroacetic acid (HTFAc) ammonium peak (B) is coalesced we see that the data do not support the hypothesis. From Tables 26 and 28,  $\eta(\text{H}_2\text{SO}_4) > \eta(\text{HForm}) \geq \eta(\text{HTFAc})$  and on this basis, with Equations (20) and (24), we would predict that

$$1/T_1(\text{H}_2\text{SO}_4) > 1/T_1(\text{HForm}) \gtrsim 1/T_1(\text{HTFAC}) \text{ or} \\ T_1(\text{H}_2\text{SO}_4) < T_1(\text{HForm}) \leq T_1(\text{HTFAC}).$$

This would mean that the formic and trifluoroacetic acids would give approximately the same NH lineshapes and a sharper triplet than observed while the sulfuric acid would lead to a coalesced NH peak. Obviously this is an incorrect interpretation since the observed spectra do not agree with this order. Considering Equation (24) we see that the other term to consider is the field gradient. Thus, the ammonium ion in sulfuric acid must have a completely symmetrical electric field, which is true for a completely ionized salt; this would be expected for a solvent with this large a value of the dielectric constant ( $\epsilon = 100$ ;  $25^\circ$ ). Also judging from the well-resolved triplet observed for ammonium formate, and the partially coalesced triplet for ammonium trifluoroacetate, one would predict that free ions are present in formic acid but that some ion pairing is occurring in trifluoroacetic acid; these predictions are in agreement with the moderately high dielectric constant of formic acid ( $\epsilon = 58.5$ ,  $16^\circ$ ) and the much lower one for trifluoroacetic acid ( $\epsilon = 39.5$ ,  $20^\circ$ ). The origin of the

slight residual broadening in the lines of each spectrum can be clarified by a temperature study. At ambient temperatures the multiplet in sulfuric acid is noticeably broader than that in aqueous ammonium salts ( $\text{pH} = 0.2$ ) and the viscosity data of Table 26, as well as the sharpening of the multiplet in sulfuric acid at  $67^\circ$  (lower viscosity) prove that the broadening is a viscosity effect on the proton lines alone. That the coalescence of the lines in trifluoroacetic acid at ambient temperatures is quadrupolar in origin (*i.e.* from the  $^{14}\text{N}$ ) is shown by the sharpening of the lines with increased temperature ( $55^\circ$ ), as was discussed above. This change in relaxation time with increased temperature results largely from change of correlation time ( $\tau_c$ ) with temperature. As Equation (20) shows, the correlation time is inversely proportional to the temperature and directly proportional to the viscosity. As a result of these proportionalities, increasing temperature itself and the resulting lower viscosity both operate in conjunction to cause a lower correlation time, as was pointed out by Kintzinger and Lehn (65). According to Equation (24) the lower correlation time means a slower relaxation rate and thus longer relaxation time (65, 92 and 93).

Considering now the ammonium formate spectra variable temperature studies show that the broadened peaks at ambient temperature ( $\sim 30^\circ$ ) result from exchange. At  $67^\circ\text{C}$  the ammonium ion triplet is completely merged with the carboxy proton peak to give the usual broad combination peak, whereas at  $15^\circ$  the triplet is much sharper than at ambient temperature.

The remaining acidic solvent studied was glacial acetic acid and here the dominant process appears to be exchange, as has been shown by the extensive studies of Grunwald et al. (23 and 24). Comparing the ammonium ion spectra in acetic and formic acids the major difference represents a difference in exchange rates. Since acetic acid is a weaker acid than formic acid exchange will be a dominant factor over a vast range of temperatures and concentrations for acetic acid solutions. Another factor which helps determine whether the ammonium ion proton peak will be a singlet or triplet in these two solvents is the major difference in dielectric constant. The dielectric constant will also influence the degree of ionization and thus the symmetry of the resulting species. The small dielectric constant for acetic acid promotes

ion association, as has been shown by Grunwald et al. (23 and 29), and the ion pairs produce large field gradients at nitrogen leading to collapse of the ammonium triplet.

#### Ammonium Ion in Non-Acidic (Aprotic) Solvents

In interpreting the lineshape of the ammonium ion in other solvents, it is more often than not important to also consider the gegen ion. In this regard we differ with the viewpoint of Kawazoe et al. (79) who consider the role of the gegen ion as being of minor importance. However, they were considering changes in  $^{14}\text{N}$  relaxation times of substituted quaternary piperidine salts and there the effect of the gegen ion may be reduced. Randall and co-workers (80-82) report no effect of solvent or gegen ion on lineshapes, and hence on  $^{14}\text{N}$  relaxation times, in a series of quaternary alkylamine halides, which in turn was the one exception reported by Kawazoe et al. (79) as showing the effects! Our findings are substantially the same as those of Cocivera (31) who notes that the shape of the NH resonance for methylammonium salts is a function of the solvent and gegen ion. More apropos here, Grunwald and Price (29) report a great difference in lineshape for the ammonium ion in glacial acetic acid depending on whether the anion is acetate or chloride.

The answer as to why some workers report such solvent-counter ion effects whereas other workers debate the existence of such effects, can be given by examination of Equation (24). For all the cases mentioned above, there should be little difference in the correlation times,  $\tau_c$ , and thus we must focus on the quadrupole coupling constant,  $(eQ/h)(\partial^2 V/\partial Z^2)$ . Since we are talking about  $^{14}\text{N}$  in all these compounds,  $(eQ/h)$  is constant and thus it is the field gradient which must be examined. As was pointed out above (Section IIB), the effect of the electronic environment on the field gradient is short ranged, being a function of  $(r_i)^{-3}$ , the distance between the  $i$ 'th electron and the nucleus (9 and 57). Thus as this distance grows large there will be a smaller influence on the  $^{14}\text{N}$  nucleus and hence a smaller influence on the relaxation time. For this reason, then, Kawazoe (79) and Randall (80-82) saw little or no effect from solvent and anion on lineshape, since their molecules were too large, the distances  $r_i$  large, and consequently the influence on  $T_1(^{14}\text{N})$  small. Also, for this reason, the effects were more obvious to Cocivera (31), Grunwald and Price (29) and ourselves. This is the main point here, and provides the main reason why the ammonium ion is such a good probe of solvent-solute

interactions.

Another factor worth considering is the  $^1\text{H}$ - $^{14}\text{N}$  coupling constant since, for coupling over a single bond the values range from 44 to 70 Hz (Table 5), whereas the coupling across two and three bonds is only 0.2 to 5.0 Hz (Tables 4 and 7). Therefore, observation of changes for a proton one bond away give an advantage of from 8 to 120 over changes observable for protons two and three bonds distant.

Bearing these things in mind, we now consider the ammonium salts in other specific solvents. In chloroform the very low dielectric constant dictates that any salt will be associated into ion pairs or higher aggregates. It is not surprising, therefore, that the trifluoroacetic acid salt (the only salt soluble enough for us to observe an ammonium proton signal) gives a rather sharp singlet because of the field gradient produced by the associated trifluoroacetate ion.

Nitromethane has about the same dielectric constant as trifluoroacetic acid and, as ion-pairing was given as the explanation for the coalesced ammonium ion peaks of ammonium trifluoroacetate in trifluoroacetic acid, it is quite reasonable to expect that ion-pairing will also occur in

nitromethane. Quite unexpectedly, ammonium trifluoroacetate in nitromethane (Figure 21F) shows a triplet less collapsed at ambient temperatures than that shown by the same salt in trifluoroacetic acid (Figure 21B). From this, one can infer that there is only a slight field gradient around the ammonium ion and most likely the structure consists of the polar nitro groups pointing toward the ammonium ion, the two oxygens of a nitro group appearing to the ammonium ion as being very similar to the two oxygens of the trifluoroacetate.

Dimethylsulfoxide (DMSO) has a dielectric constant slightly higher than nitromethane and trifluoroacetic acid and slightly lower than formic acid. Indeed, conductivity measurements show (101) that in concentrations greater than  $10^{-2}M$  ion pairing predominates. From the concentrations we used, we would expect ion-pairing to be important and this is supported by the fact that the chemical shift of the ammonium ion is a function of its anion (Table 27). The shifting of the NH resonances for methylammonium salts was noted by Cocivera (31) to be dependent on the anion in the solvent *t*-butyl alcohol ( $\epsilon=12.47$ ;  $25^{\circ}$ ) where ion pairs exist.

The easiest ammonium salt-DMSO interaction to explain

is that with ammonium trifluoroacetate, which shows a clear well-defined triplet at ambient temperature. On raising the temperature about  $38^{\circ}$ , this triplet coalesces (Figure 21D), thus indicating that for the trifluoroacetate salt proton exchange between the ammonium ion and solvent is of great importance. As to why a triplet is observed for the trifluoroacetate and not for the other salts the same explanation given for trifluoroacetate in nitromethane may be used, namely, the solvent plus the trifluoroacetate ion form an aggregate with the ammonium ion which has high symmetry. The nitrogen nucleus then sees a highly symmetrical structure, the ammonium hydrogens interacting in the same manner with all oxygens whether they belong to the trifluoroacetate or DMSO. Comparing the triplet structure for the same salt, ammonium trifluoroacetate, in the three solvents-trifluoroacetic acid, nitromethane, and dimethylsulfoxide (Figure 21B, D, and F)-one can easily see that the  $^{14}\text{N}$  relaxation time is longest for the DMSO. As pointed out above, the structure for DMSO-ammonium ion is very similar to that of trifluoroacetate-ammonium ion (in the ion pair) and, since DMSO has only one oxygen, one might speculate that the ammonium ion comes into contact with just one oxygen of the trifluoroacetate.

The two halide and nitrate salts in DMSO present an example of the "single-line" problem. Indeed, here it is a dilemma, as the ammonium halide peaks broaden while the ammonium nitrate peaks sharpen with increasing temperature. The fact that each of these single lines have different half-height widths and different chemical shifts means that the gegen ion has an influence on their shapes. Therefore, this in part explains the singlet rather than triplet lineshape; the gegen ion being very different from the DMSO of the solvent shell gives rise to large field gradients causing short relaxation times.

Since the line width changes were perplexing, it was thought that a consideration of the chemical shifts with temperature for these salts in DMSO compared with the known changes of relaxation times or exchange rates with temperature could clarify the situation. From the kinetic work (Section IIA) there is ample evidence that there is a large chemical shift change of the NH resonance, or of the combination band, with change in exchange rates and/or temperature. The changes in temperature with magnitude of change in chemical shift (irrespective of the direction of shift) are listed in Table 31. A plot of these values is shown in Figure 22, the first point for each

Table 31. Change of NH proton chemical shift with temperature.<sup>a</sup>

System	$\Delta t$ ( $^{\circ}\text{C}$ )	$ \Delta \nu $	System	$\Delta t$ ( $^{\circ}\text{C}$ )	$ \Delta \nu $
$(\text{NH}_4)_2\text{SO}_4$ ( $\text{H}_2\text{SO}_4$ )	38	1.8 Hz	5.04M aq $\text{NH}_4\text{Cl}$	23.5	4.0Hz
$\text{NH}_4\text{Form}$ ( $\text{HForm}$ )	14	4.9	(pH = 0.2)	52.0	10 35
$\text{NH}_4\text{TFac}$ ( $\text{HTFac}$ )	21	0.4	4.99M aq $\text{NH}_4\text{Cl}$	11.5	1.9
	38	0.72	(pH = 0.48)	15.0	2.5
				40.2	8.7
$\text{NH}_4\text{Cl}$ (DMSO)	38	1.2			
$\text{NH}_4\text{I}$ (DMSO)	38	1.0	4.99M aq $\text{NH}_4\text{Cl}$	11.5	6.8
$\text{NH}_4\text{NO}_3$ (DMSO)	38	4.7	(pH = 4.32)	15.0	11.2
$\text{NH}_4\text{TFac}$ (DMSO)	38	3.1		40.2	19.0

<sup>a</sup>Data taken from Table 27. The change in shift  $|\Delta \nu|$ , is observed for the change in temperature  $\Delta T$ .

salt-solvent combination being chosen as a zero and all other points for the same system being relative to it. In essence, we have a comparison of the slopes of the plots of chemical shift vs. temperature.

From Figure 22, there is a very obvious correlation between relative chemical shift and temperature, a much larger change being noted for an exchange process than for a quadrupole relaxation process. Incidentally, it should be pointed out that from the slopes of the plots of Figure

22, one might expect that the activation energy for exchange occurring in formic acid should be larger than for comparable processes in water ( $\text{pH} \leq 0.48$ ) while it should be smaller for ammonium trifluoroacetate in DMSO.

It can now be said with more certainty that the change in the line shape of the peaks for ammonium nitrate in DMSO is due to an appreciably rapid exchange process because first the line sharpens up with increased temperature which is characteristic of a kinetic process and second the change in chemical shift with temperature falls in between values for known exchange processes. The same two considerations clearly identify the changes in the spectra of the ammonium halides in DMSO with temperature as being governed by a quadrupolar relaxation process. First the broadening with increased temperature and second the relative change of chemical shift with increased temperature falls in the range of values for known relaxation processes. The other two ammonium salts investigated in DMSO the formate and acetate reacted with DMSO at ambient temperature expelling gaseous ammonia.

Considering the behavior of all the ammonium salts in DMSO and the reasons for some being mainly relaxation controlled and others being mainly controlled by exchange

processes, and still others reacting chemically, we can only be intrigued and leave this for further study. One thing is certain, however, and that is that the particular process occurring in DMSO is controlled by the gegen ion.

a  
a  
t  
a  
t  
a  
t

1

## VI. SUMMARY

The NMR spectra of the mono-, di-, and trimethyl- and mono-, di-, and triethyl-substituted ammonium chlorides have been studied in aqueous solution at low pH ( $<1.0$ ). It has been shown that the proton lineshape of the NH proton portion of the alkyl ammonium ion NMR spectrum is governed by the nitrogen relaxation rate which is a function of the electric field gradient at the nitrogen atom and varies from compound to compound. In addition, it has been shown that the relaxation process is a function of temperature, and activation energies for the process were obtained.

Attempts to obtain proton NH lineshapes for 2,2,2-trifluoroethylamine and benzylamine failed because of their low solubility in water at pH  $< 1.0$ .

The nitrogen spin-lattice relaxation times were obtained by least-squares fitting of observed proton lineshapes to computed curves. It has been shown that this technique works well when the restrictions on the theoretical equation are observed but yields less reliable results otherwise. The theoretical equation is restricted to ammonium proton lineshapes which are governed only by nitrogen relaxation rates and for which the separation between multiplets is greater than the half-height width of each individual component. It has been

found that when triplet structure from  $^1J(^1H-^{14}N)$  coupling could be observed satisfactory values of  $T_1$  and  $^1J$  could be obtained. For cases where these conditions were met, it was found that the activation energy for relaxation paralleled the activation energy for viscous flow. As a result, the nitrogen relaxation rates are largely a function of solution viscosity.

Quite unexpectedly, the  $^1J(^1H-^{14}N)$  coupling was found to vary with temperature, as were other proton-proton coupling constants for the same compounds. Studies of the  $^1J(^1H-^{14}N)$  coupling constants for the ammonium ion in various solvents showed that indeed this varies with solvent, and with temperature for the same ammonium salt-solvent system. From this it was concluded that the variation of  $^1J(^1H-^{14}N)$  for the alkylammonium chlorides with temperature is real and probably results from changes in water structure or from water-alkylammonium ion interactions.

A 4.33 MHz (resonance frequency for  $^{14}N$ ) transmitter coil was wound and then mounted on a Dewar jacket which surrounded a 60 MHz (resonance frequency for  $^1H$ ) receiver coil. This design permitted nitrogen decoupling at high RF power while observing the proton spectrum at a temperature controlled by passing heated or cooled dry air

over the sample.

Nitrogen decoupling experiments have been used to show that the proton NH lineshapes for the alkylammonium ions are controlled almost entirely by the nitrogen relaxation rates and that spin-spin coupling of these NH protons with the alkyl protons is present, although it cannot always be observed. Variable temperature nitrogen decoupling experiments showed that part of the NH proton linewidths is a result of viscosity effects and thus viscosity partially contributes to the NH lineshapes in the single resonance spectra. Since the theoretical equation used does not take into account viscosity broadening it will not hold exactly; the resulting errors should not be too serious for the monomethyl-, dimethyl-, and monoethyl-ammonium ions but may be quite serious for the trimethyl-, diethyl-, and triethylammonium ions.

It has been proved by nitrogen decoupling experiments that there is indeed coupling between the NH nitrogen and the alkyl protons of substituted ammonium ions although it cannot be resolved in the single-resonance spectra but appears as broadening of the alkyl-group proton multiplets.

Accurate measurements of the nitrogen chemical shifts in the methylammonium ions show that many of the values

reported in the literature are erroneous. It has also been shown that the nitrogen chemical shifts for alkylammonium ions are accounted for by hyperconjugation with the alkyl hydrogens.

Studies of the proton NMR spectra of simple ammonium salts in various solvents have shown that a number of complications such as ion pairing arise which cause difficulties with interpretation of the NH lineshapes.

## VII. RECOMMENDATIONS

This study has shown that there is a variation with temperature of the  $^{14}\text{N}$  spin-lattice relaxation times for mono-, di-, and trimethyl and mono-, di-, and triethylammonium chlorides in aqueous solution at low pH. It has also shown that since the  $^{14}\text{N}$  relaxation times were obtained from proton steady-state NMR lineshapes, there are contributions to these NH lineshapes from viscosity effects and from spin-spin coupling with the alkyl protons. In certain cases, these produce violations of the restrictions on the theoretical equation used to obtain the  $^{14}\text{N}$  spin-lattice relaxation times. These difficulties and complications could be circumvented by use of the spin-echo method, pulsing the nitrogen resonance frequency. By this method, more accurate  $^{14}\text{N}$  relaxation times would be obtained and hence more reliable activation energies for reorientation of alkylammonium ions.

These studies have also indicated that there is a trend in the single-bond nitrogen-proton coupling constants with number and type of alkyl group on nitrogen. In order

to study this in detail, it is recommended that compounds enriched with  $^{15}\text{N}$  be utilized, because the nitrogen-proton couplings could then be measured accurately. In addition, since all nitrogen-proton couplings will be observable (i.e., both NH protons and alkyl protons), the relative signs for nitrogen-proton coupling across one, two and three bonds could be obtained from double resonance experiments.

## **BIBLIOGRAPHY**

## BIBLIOGRAPHY

1. E. Grunwald, A. Loewenstein, and S. Meiboom, J. Chem. Phys., 25, 382 (1956).
2. E. Grunwald, A. Loewenstein, and S. Meiboom, ibid., 27, 630 (1957).
3. R. A. Ogg, J. Chem. Phys., 22, 560 (1954).
4. R. A. Ogg, Faraday Soc., Discussion 17, 215 (1954).
5. H. S. Gutowsky and A. Saika, J. Chem. Phys., 21, 1688 (1953).
6. H. S. Gutowsky and S. Fujiwara, J. Chem. Phys., 22, 1782 (1954).
7. R. A. Ogg and J. D. Ray, J. Chem. Phys., 26, 1515 (1957).
8. J. D. Roberts, J. Amer. Chem. Soc., 78, 4495 (1956).
9. J. A. Pople, Mol. Phys., 1, 168 (1958).
10. T. Birchall and W. L. Jolly, J. Amer. Chem. Soc., 87, 3007 (1965).
11. T. Birchall and W. L. Jolly, ibid., 88, 5439 (1966).
12. M. Alei and A. E. Florin, J. Phys. Chem., 72, 550 (1968).
13. T. J. Swift and S. B. Marks, and W. G. Sayre, J. Chem. Phys., 44, 2797 (1966).
14. T. J. Swift and D. R. Clutter, Abstracts, 154th National Meeting of the American Chemical Society, Chicago, Ill., Sept. 1967, No. V5.
15. D. R. Clutter and T. J. Swift, J. Amer. Chem. Soc., 90, 601 (1968).

16. J. G. Powles and J. H. Strange, Discussions Faraday Soc., 34, 30 (1962).
17. H. M. McConnell and D. D. Thompson, J. Chem. Phys., 26, 958 (1957).
18. S. Meiboom, A. Loewenstein, and S. Alexander, J. Chem. Phys., 29, 969 (1958).
19. M. T. Emerson, E. Grunwald, R. A. Kromhout, J. Chem. Phys., 33, 547 (1960).
20. M. T. Emerson, E. Grunwald, M. L. Kaplan, and R. A. Kromhout, J. Amer. Chem. Soc., 82, 6307 (1960).
21. T. M. Conner and A. Loewenstein, J. Amer. Chem. Soc., 83, 560 (1961).
22. E. Grunwald and A. Y. Ku, J. Amer. Chem. Soc., 90, 29 (1968).
23. E. Grunwald and E. Price, J. Amer. Chem. Soc., 86, 2970 (1964).
24. E. Grunwald and M. Cocivera, Discussions Faraday Soc., 39 105 (1965).
25. E. Grunwald, A. Loewenstein, and S. Meiboom, J. Chem. Phys., 27, 641 (1957).
26. R. A. Ogg and J. D. Ray, J. Chem. Phys., 26, 1340 (1957).
27. E. Grunwald, P. J. Karabatsos, R. A. Kromhout, and E. L. Purlee, J. Chem. Phys., 33, 556 (1960).
28. I. M. Kolthoff and S. Bruckenstein, J. Amer. Chem. Soc., 78, 1 (1956).
29. E. Grunwald and E. Price, J. Amer. Chem. Soc., 86, 2965 (1964).
30. M. Cocivera and E. Grunwald, J. Amer. Chem. Soc., 87, 2070 (1965).
31. M. Cocivera, ibid., 88, 672 (1966).
32. M. Cocivera, ibid., 88, 677 (1966).

33. A. Loewenstein and S. Meiboom, J. Chem. Phys., 27, 1067 (1957).
34. E. Grunwald, J. Phys. Chem., 67, 2208 (1963).
35. E. Grunwald, J. Phys. Chem., 67, 2211 (1963).
36. E. Grunwald and E. K. Ralph, J. Amer. Chem. Soc., 89, 4405 (1967).
37. R. J. Day and C. N. Reilley, J. Phys. Chem., 71, 1588 (1967).
38. G. Fraenkel and Y. Asahi, J. Phys. Chem., 71, 1706 (1967).
39. Z. Luz and S. Meiboom, J. Chem. Phys., 39, 366 (1963).
40. E. Grunwald, J. Phys. Chem., 71, 1846 (1967).
41. E. K. Ralph and E. Grunwald, J. Amer. Chem. Soc., 89, 2963 (1967).
42. H. C. Brown, J. Chem. Soc., 1248 (1956).
43. C. G. Swain, J. T. McKnight, M. M. Labes, and V. P. Kreiter, J. Amer. Chem. Soc., 76, 4243 (1954).
44. C. G. Swain, R. F. W. Bader, Tetrahedron, 10, 182 (1960).
45. C. G. Swain, R. F. W. Bader and E. R. Thornton, ibid., 10, 200 (1960).
46. M. Steinblatt, J. Amer. Chem. Soc., 87, 672 (1965).
47. M. Steinblatt, ibid., 88, 2123 (1966).
48. E. Grunwald and M. S. Puar, J. Amer. Chem. Soc., 89, 6842 (1967).
49. J. L. Sudmeier and G. Occupati, J. Amer. Chem. Soc., 90, 154 (1968).
50. G. E. Pake, Amer. J. Phys., 18, 438, 473 (1950).
51. E. R. Andrew, "Nuclear Magnetic Resonance," Cambridge University Press, New York, N. Y. (1955).

52. H. Sillescu, "Nuclear Magnetic Resonance," Springer-Verlag, New York, N.Y. (1966), p. 97.
53. F. Bloch, Phys. Rev., 70, 460 (1946).
54. N. Bloembergen, E. M. Purcell, and R. V. Pound, Phys. Rev., 73, 679 (1948).
55. N. Bloembergen, "Nuclear Magnetic Relaxation," W. A. Benjamin, Inc., New York (1961).
56. R. Kubo and K. Tomita, J. Phys. Soc. Jap., 9, 888 (1954).
57. See Appendix 3 of Reference 51.
58. A. Abragam, "The Principles of Nuclear Magnetism," Oxford University Press, New York (1961).
59. R. K. Wangsness and F. Bloch, Phys. Rev., 89, 728 (1953).
60. C. P. Slichter, "Principles of Magnetic Resonance," Harper and Row, Evanston (1963).
61. C. Sandorfy, "Electronic Spectra and Quantum Chemistry," Prentice-Hall, Englewood Cliffs, N.J. (1964).
62. D. H. Evans and R. E. Richards, Mol. Phys., 7, 515 (1964).
63. M. St. J. Arnold and K. J. Packer, Mol. Phys., 14, 241 (1968).
64. M. K. Kemp, J. M. Pochan, and W. H. Flygare, J. Phys. Chem., 71, 765 (1967).
65. J. P. Kintzinger and J. M. Lehn, Mol. Phys., 14, 133 (1968).
66. W. B. Moniz and H. S. Gutowsky, J. Chem. Phys., 38, 1155 (1963).

67. W. Gordy, Discussions Faraday Soc., 19, 14 (1955).
68. R. A. Ogg and J. D. Ray, J. Chem. Phys., 26, 1339 (1957).
69. G. V. D. Tiers and F. A. Bovey, J. Phys. Chem., 63, 302 (1959).
70. H. G. Hertz and W. Spalthoff, Zeit Elektrochem, 63, 1096 (1959).
71. J. M. Anderson, J. D. Baldeschwieler, D. C. Dittmer, and W. D. Phillips, J. Chem. Phys., 38, 1260 (1963).
72. E. Bullock, D. G. Tuck, and E. J. Woodhouse, ibid., 38, 2318 (1963).
73. J. M. Lehn and M. F. Neumann, ibid., 43, 1421 (1965).
74. M. F. Neumann and J. M. Lehn, Mol. Phys., 7, 197 (1963-64).
75. P. G. Gassman and D. C. Heckert, J. Org. Chem., 30, 2859 (1965).
76. J. M. Lehn and R. Seher, Chem. Commun., 847 (1966).
77. J. M. Lehn, Bull. Soc. Chim. France, 2141 (1966).
78. J. F. Biellmann and H. Callot, ibid., 397 (1967).
79. Y. Kawozoe, M. Tsuda and M. Ohnishi, Chem. Pharm. Bull. (Tokyo), 15, 214 (1967).
80. A. G. Massey, E. W. Randall, and D. Shaw, Spectrochim. Acta 20, 379 (1964).
81. A. G. Massey, E. W. Randall, and D. Shaw, ibid., 21, 263 (1965).
82. R. J. Chuck, A. G. Massey, E. W. Randall, and D. Shaw in "N.M.R. in Chemistry," Biagio Pesce, ed., Academic Press, New York, N.Y., 1966, p. 189.

83. J. Bacon, R. J. Gillespie, and J. W. Quail, *Can J Chem.*, 41, 3063 (1963).
84. M. Suzuki and R. Kubo, *Mol Phys.*, 7, 201 (1964).
85. I. D. Kuntz, P. von R. Schleyer, and A. Allerhand, *J. Chem. Phys.*, 35, 1533 (1961).
86. A. H. Lamberton, I. O. Sutherland, J. E. Thorpe, and H. M. Yusuf, *J. Chem. Soc. (B)*, 6 (1968).
87. P. Hampson and A. Mathias, unpublished results.
88. J. M. Anderson and J. D. Baldeschwieler, *J. Chem. Phys.*, 40, 3241 (1964).
89. N. Boden, J. Deck, E. Gore, and H. S. Gutowsky, *J. Chem. Phys.*, 45, 3875 (1966).
90. J. Deck, N. Boden, E. Gore, and H. S. Gutowsky, 8th Experimental N.M.R. Conference, Mellon Institute, Pittsburgh, Pa., March 1967.
91. T. H. Cannon and R. E. Richards, *Trans Faraday Soc.*, 62, 1378 (1966).
92. M. St. J. Arnold and K. J. Packer, *Mol. Phys.*, 10, 141 (1966).
93. M. St. J. Arnold and K. J. Packer, *ibid.*, 14, 249 (1968).
94. H. G. Hertz and M. D. Zeider, *Ber. Bunsenges. Phys Chem.*, 68, 821 (1964).
95. G. Bonera and A. Rigamonti, *J. Chem. Phys.*, 42, 175 (1965).
96. G. Boden, H. S. Gutowsky, J. R. Hansen, and T. C. Farrar, *J. Chem. Phys.*, 46, 2849 (1967).
97. R. Freeman, R. R. Ernst, and W. A. Anderson, *ibid.*, 46, 1125 (1967).

98. C. H. Townes and A. L. Schawlow, "Microwave Spectroscopy," McGraw-Hill Book Co., Inc., New York, N.Y., (1955).
99. T. P. Das and E. L. Hahn, "Nuclear Quadrupole Resonance Spectroscopy," in Solid State Physics, F. Seitz and D. Turnbull, Ed., Academic Press Inc., New York, N.Y. (1958).
100. R. Richards, presented in part at the 9th Experimental N.M.R. Conference, Pittsburgh, Pa., March 1968.
101. J. M. Crawford and R. P. H. Gasser, Trans. Faraday Soc., 63, 2758 (1967).
102. H. G. Hertz, Ber. Bunsenges. Phys. Chem., 67, 311 (1963).
103. M. Eisenstadt and H. L. Friedman, J. Chem. Phys., 46, 2182 (1967).
104. H. G. Hertz, Ber. Bunsenges. Phys. Chem., 68, 907 (1964).
105. H. S. Frank and W. Y. Wen, Discussions Faraday Soc., 24, 133 (1957).
106. K. W. Bunzl, J. Phys. Chem., 71, 1358 (1967).
107. W. G. Proctor and F. C. Yu, Phys. Rev., 77, 717 (1950).
108. W. G. Proctor and F. C. Yu, ibid., 81, 20 (1951).
109. P. Hampson and A. Mathias, Mol. Phys., 13, 361 (1967).
110. C. F. Poranski and W. B. Moniz, J. Phys. Chem., 71, 1142 (1967).
111. M. Witanowski and L. Stefaniak, J. Chem. Soc. (B), 1061 (1967).

112. M. Witanowski and H. Januszewski, ibid., 1062 (1967).
113. M. Witanowski, L. Stefaniak and G. A. Webb, ibid., 1065 (1967).
114. M. Witanowski, Tetrahedron, 23, 4299 (1967)
115. L. O. Anderson and J. Mason, Chem. Commun., 99 (1968).
116. B. E. Holder and M. P. Klein, J. Chem. Phys., 23, 1956 (1955).
117. B. M. Schmidt, L. C. Brown and D. Williams, J. Mol. Spectry., 2, 539 (1958).
118. D. Herbison Evans and R. E. Richards, Mol. Phys., 8, 19 (1964).
119. M. Bose, N. Das, and N. Chatterjee, J. Mol. Spectry., 18, 32 (1965).
120. P. G. Maslov, J. Phys. Chem., 72, 1414 (1968).
121. Chapt. 4 of Reference 60.
122. A. Saika and C. P. Slichter, J. Chem. Phys., 22, 26 (1954).
123. J. B. Lambert and J. D. Roberts, J. Amer. Chem. Soc., 87, 4087 (1965).
124. J. E. Kent and E. L. Wagner, J. Chem. Phys., 44, 3530 (1966).
125. M. Witanowski, T. Urbanski, and L. Stefaniak, J. Amer. Chem. Soc., 86, 2569 (1964).
126. pp. 143-146 of Reference 51.
127. p. 102 of Reference 60.
128. J. A. Pople, W. G. Schneider and H. J. Bernstein, "High-resolution Nuclear Magnetic Resonance," McGraw-Hill Book Company, Inc., New York (1959)

129. J. W. Emsley, J. Feeney and L. H. Sutcliffe, "High-Resolution Nuclear Magnetic Resonance Spectroscopy," Pergamon Press, New York (1965)
130. J. A. Pople and D. P. Santry, Mol. Phys., 8, 1 (1964).
131. M. Freifelder, R. W. Mattoon and R. Kriese, J. Phys. Chem., 69, 3645 (1965).
132. E. W. Randall and J. D. Baldeschwieler, J. Mol. Spectry., 8, 365 (1962).
133. J. Hedberg, J. A. Weil, G. A. Janusonis, and J. K. Anderson, J. Chem. Phys., 41, 1033 (1964).
134. M. Freifelder, R. W. Mattoon and R. Kriese, Can. J. Chem., 45, 21 (1967).
135. B. Sunners, L. H. Piette, and W. G. Schneider, ibid., 38, 681 (1960).
136. P. T. Narasimhan and M. T. Rogers, J. Chem. Phys., 31, 1430 (1959).
137. P. T. Narasimhan and M. T. Rogers, J. Amer. Chem. Soc., 82, 34 (1960).
138. P. T. Narasimhan and M. T. Rogers, J. Chem. Phys., 33, 727 (1960).
139. B. R. McGarvey and G. Slomp, ibid., 30, 1586 (1959).
140. P. T. Narasimhan and M. T. Rogers, J. Amer. Chem. Soc., 82, 5983 (1960).
141. J. V. Acrivos, J. Chem. Phys., 36, 1097 (1962).
142. T. Birchall and W. L. Jolly, J. Amer. Chem. Soc., 87, 3007 (1965).
143. L. W. Anderson, F. M. Pipkin and J. C. Baird, Phys Rev., 116, 87 (1959).

144. J. D. Baldeschwieler, J. Chem. Phys. , 36, 152 (1962).
145. G. Fraenkel, Y. Asahi, H. B. Hernandez and R. Bernheim, ibid., 44, 4647 (1966).
146. G. Kotowycz, T. Schaefer and E. Bock, Can. J. Chem. , 42, 2541 (1964).
147. I. C. Smith and W. G. Schneider, Can. J. Chem. , 39, 1158 (1961).
148. Y. Kato, M. Miura and A. Saika, Mol. Phys. , 13, 491 (1967).
149. W. McFarlane, J. Chem. Soc. A, 1660 (1967).
150. J. P. Maher, ibid., A,1855 (1966).
151. A. J. R. Bourn and E. W. Randall, J. Mol. Spectry., 13, 29 (1964).
152. M. Ohtsuru and K. Tori, Chem. Commun., 20, 750 (1966).
153. A. Loewenstein and Y. Margalit, J. Phys. Chem., 69, 4152 (1965).
154. A. J. R. Bourn, D. G. Gillies and E. W. Randall in "N. M. R. in Chemistry," Biagio Pesce, ed., Academic Press, New York, N. Y. (1966) p. 277.
155. Y. Terui, K. Aono and K. Tori, J. Amer. Chem. Soc., 90, 1069 (1968).
156. R. A. Bernheim and H. B. Hernandez, J. Chem. Phys., 40, 3446 (1964).
157. G. Binsch, J. B. Lambert, B. W. Roberts and J. D. Roberts, J. Amer. Chem. Soc., 86, 5564 (1964).
158. E. W. Randall, B. J. Ellner and J. J. Zuckerman, J. Amer. Chem. Soc., 88, 622 (1966).
159. E. W. Randall and J. J. Zuckerman, Chem. Commun., 732 (1966).
160. W. McFarlane, Mol. Phys., 10, 603 (1966).

161. H. Hogeveen, *Rec. Trav. Chim.*, 86, 1288 (1967).
162. A. J. R. Bourn and E. W. Randall, *Mol. Phys.*, 8, 567 (1964).
163. M. T. Rogers and L. A. LaPlanche, *J. Phys. Chem.*, 69, 3648 (1965).
164. A. K. Bose and I. Kugajevsky, *Tetrahedron*, 23, 1489 (1967).
165. G. O. Dudek and E. P. Dudek, *J. Amer. Chem. Soc.*, 86, 4283 (1964).
166. B. W. Roberts, J. B. Lambert and J. D. Roberts, *ibid.*, 87, 5439 (1965).
167. J. P. Kintzinger and J. M. Lehn, *Chem. Commun.*, 660 (1967).
168. D. Crepaux and J. M. Lehn, *Mol. Phys.*, 14, 547 (1968).
169. J. A. Happe and M. Morales, *J. Amer. Chem. Soc.*, 88, 2077 (1966).
170. K. Tori, M. Ohtsuru, K. Aono, Y. Kawazoe and M. Ohnishi, *J. Amer. Chem. Soc.*, 89, 2765 (1967).
171. M. T. Miles, R. B. Bradley and E. D. Becker, *Science*, 142, 1569 (1963).
172. Y. Kawazoe, M. Ohnishi and N. Kataoka, *Chem. Pharm. Bull. (Tokyo)*, 13, 396 (1965).
173. J. B. Lambert, B. W. Roberts, G. Binsch and J. D. Roberts, "N. M. R. in Chemistry," Biagio Pesce, ed., Academic Press, New York, N. Y., 1966, p. 269.
174. R. A. Hoffman and Sture Forsen in "Progress in N. M. R. Spectroscopy," Vol. 1, J. W. Emsley, J. Feeney and L. H. Sutcliffe, ed., Pergamon Press, New York, N. Y., 1966, Chapt. 2.
175. V. J. Kowalewski, D. G. de Kowalewski and E. C. Ferra, *J. Mol. Spectry.*, 20, 203 (1966).

176. E. B. Baker, J. Chem. Phys., 37, 911 (1962).
177. E. B. Baker, L. W. Burd and G. N. Root, Rev. Sci. Instr., 34, 243 (1963).
178. R. A. Hoffman, B. Gestblom, S. Forsen, J. Chem. Phys., 40, 3734 (1964).
179. J. D. Baldeschwieler and E. W. Randall, Chem. Rev., 63 81 (1963).
180. K. F. Kuhlmann and J. D. Baldeschwieler, J. Chem. Phys., 43, 572 (1965).
181. F. A. L. Anet and A. J. R. Bourn, J. Amer. Chem. Soc., 87, 5250 (1965).
182. John D. Baldeschwieler, private communication.
183. E. B. Baker, J. Chem. Phys., 45, 609 (1966).
184. S. L. Gordon and J. D. Baldeschwieler, ibid., 41, 571 (1964).
185. R. S. Milner and D. W. Turner, Chem. Commun., 31 (1965).
186. R. Freeman, J. Chem. Phys., 43, 3087 (1965).
187. L. H. Piette, J. D. Ray and R. A. Ogg, J. Mol. Spectry., 2, 66 (1958).
188. H. Kamei, Bull. Chem. Soc. (Japan), 38, 1212 (1965).
189. J. B. Merry and J. H. Goldstein, J. Amer. Chem. Soc., 88, 5560 (1960).
190. S. Castellano, C. Sun and R. Kostelnik, J. Chem. Phys., 46, 327 (1967).
191. J. D. Baldeschwieler and E. W. Randall, Proc. Chem. Soc. (London), 303 (1961).
192. See Page 105 of Ref. 179.
193. J. A. Glasel, L. M. Jackman and D. W. Turner, Proc. Chem. Soc. (London), 426 (1961).

194. P. Hampson and A. Mathias, *Mol. Phys.*, 11, 541 (1966).
195. J. M. Anderson, *J. Chem. Educ.*, 42, 363 (1965).
196. E. F. Friedman and H. S. Gutowsky, *J. Chem. Phys.*, 45, 3158 (1966).
197. I. M. Heilbron, "Dictionary of Organic Chemistry," 4th ed., Oxford University Press, New York (1965).
198. A. F. McKay and G. R. Vavasour, *Can. J. Chem.*, 32, 639 (1954).
199. E. R. Bissell and M. Finger, *J. Org. Chem.*, 24, 1256 (1959).
200. M. S. Raasch, *ibid.*, 27, 1406 (1962).
201. G. A. Clarke and S. Sadler, *Chem. Anal.*, 50 76 (1961).
202. Varian Associates, Analytical Instrument Division, Palo Alto, California 94303.
203. (a) R. Freeman, "Technical Information Bulletin," Varian Associates, Analytical Instrument Division (Summer 1965); (b) R. Freeman and D. H. Whiffen, *Proc. Phys. Sec. (London)*, 79, 794 (1962); (c) R. Freeman and W. A. Anderson, *J. Chem. Phys.*, 37, 2053 (1962); (d) R. Ernst and H. Primas, *Discussions Faraday Soc.*, 34, 43 (1962); (e) J. H. Noggle, *Rev. Sci. Inst.*, 35, 1166 (1964); and (f) D. D. Elleman, S. Manatt and C. D. Pearce, *J. Chem. Phys.*, 42, 650 (1965).
204. W. C. T. Tung, Ph.D. Thesis, Michigan State University, East Lansing, Mich., 1968.
205. (a) A. L. Van Geet, *Anal. Chem.* 40, 2227 (1968); (b) D. N. Glew, H. D. Mak, J. S. McIntyre and N. S. Rath, *ibid.*, 38, 1964 (1966); and (c) R. Duerst and A. Merbach, *Rev. Sci. Instr.*, 36, 1896 (1965).
206. N. M. R. Specialities, Inc., 145 Greensburg Rd., New Kensington, Pa.
207. (a) J. N. Shoolery and J. D. Roberts, *Rev. Sci.*

- Instr., 28, 61 (1957); (b) J. C. Woodbrey, Ph.D. Thesis, Michigan State University, East Lansing, Mich., 1960; (c) W. C. Lawrence, Rev. Sci. Instr., 35, 752 (1964); (d) D. S. Schreiber, ibid., 35, 1582 (1964); (e) P. R. Shafer, 2nd Experimental N. M. R. Conference, Mellon Institute, Pittsburgh, Pa., February, 1961.
208. F. E. Terman, "Radio Engineering," McGraw-Hill Book Company, New York, N. Y. (1947).
  209. "The Radio Amateur's Handbook," The American Radio Relay League, Incorporated, Neuwington, Conn. (1965).
  210. M. Soutif and R. Gabillard in "Nuclear Paramagnetic Resonance," P. Grivet, ed., National Center of Scientific Research, Paris, 1955, Chapt. 5.
  211. Paul Yajko and Thomas Hill of N. M. R. Specialties, private communication.
  212. J. B. Stothers and J. R. Robinson, Can. J. Chem., 42, 967 (1964).
  213. Cannon Instrument Company, P. O. Box 16, State College, Pa. 16801
  214. Standard Electric Time Company, Springfield, Mass.
  215. Precision Scientific Company, Chicago, Illinois.
  216. W. J. Moore, "Physical Chemistry," Prentice-Hall, Inc., Englewood Cliffs, N. J., 3rd ed. (1964) p. 723.
  217. H. G. Hertz in "Progress in N. M. R. Spectroscopy," Vol. 3, J. W. Emsley, J. Feeney and L. H. Sutcliffe, ed., Pergamon Press, N. Y., 1967, Chapt. 5.
  218. E. E. Royals, "Advanced Organic Chemistry," Prentice-Hall, Inc., Englewood Cliffs, N. J. (1954) pp. 71-6.
  219. L. Maier, Helv. Chim. Acta, 49, 1718 (1966).
  220. S. O. Grim and W. McFarlane, Nature, 208, 995 (1965).
  221. S. O. Grim, W. McFarlane and E. F. Davidoff, J. Org. Chem., 32, 781 (1967).

222. S. O. Grim, W. McFarlane, E. F. Davidoff and T. J. Marks, J. Phys. Chem., 70, 581 (1966).
223. (a) "Table of Dielectric Constants of Pure Liquids," Circular 514, National Bureau of Standards, Washington, D. C. (1951); (b) Chemical Products Division, Crown Zellerbach Corporation, Camas, Washington 98607; (c) W. Dannhauser and L. Bahe, J. Chem. Phys., 40, 3038 (1964); (d) H. H. Sisler, "Chemistry of Non-Aqueous Solvents," Reinhold Publishing Corporation, New York (1965); (e) F. E. Harris and C. T. O'Konski, J. Amer. Chem. Soc., 75, 4317 (1954); (f) A. Korosi and B. M. Fabuss, Anal. Chem., 40, 157 (1968); (g) "Handbook of Chemistry," N. A. Lange, ed., Handbook Publishers Incorporated, Sandusky, Ohio, 9th ed. (1956); (h) "Handbook of Chemistry and Physics," R. C. Weast, ed., The Chemical Rubber Co., Cleveland, Ohio, 48th ed. (1967); (i) J. Timmermans, "Physico-Chemical Constants of Pure Organic Compounds," Elsevier Publishing Co., Incorporated, New York (1950); (j) G. C. Hood, O. Redlich and C. A. Reilly, J. Chem. Phys., 23, 2229 (1955).
224. J. D. Rynbrandt, M. S. Thesis, Michigan State University, East Lansing, Michigan, 1966.

## **APPENDICES**

## APPENDIX

### A. Program QUADRELX

This program simply calculates a set of spectra of nuclei of spin  $1/2$  coupled to a nucleus of spin  $1$ , according to Equation (3.5) of Pople (9). An example of such a set of spectra is given in Figure 7 (cf. Section IV A). It is necessary to have a set of these spectra so that one can get a value of  $T_1(^{14}\text{N})$ , knowing or estimating  $^1J(^1\text{H}-^{14}\text{N})$ , for a first approximation in the least squares fitting of calculated and experimental NH lineshapes using program NMR FIT8.

The input information which must be supplied is first NUMB, the total number of spectra (i.e. the number of ETASQ values to be supplied) and N, the total number of points on the individual spectrum (e.g. 55). Second, the values of ETASQ, where  $\text{ETASQ} = \eta^2 = 10\pi T_1(^{14}\text{N})^1J(^1\text{H}-^{14}\text{N})$ , are assigned for each spectrum desired; for example, six were used in Figure 7.

The program functions by incrementing the X variable and calculating the corresponding  $F(X)$  for each ETASQ. It then approximates the areas under each curve by the

trapezoid method, searches for the largest area and scales up all other spectra to this area. Finally, it calculates a scale for the ordinate (each printout line is the abscissa) and prints out each spectrum with computer output page (Note, this does not use the CAL COMP plotter).

The computer output consists of three parts.

First, the spectrum number (JETA), assigned value of  $\eta^2$  (ETASQ), and the frequencies and calculated intensities. The second part of the output is a listing of the areas calculated for the spectra. Finally, each spectrum is printed out as an array with each calculated intensity point shown as an asterisk.

A listing of Program QUADRELX follows.

12/07/66

## PROGRAM QUADRELX

```

C      J. A. POPLER, J. MOL. PHYSICS, 1, P168(1958)
C      STG(JETA,I,1) = X = FREQUENCY VARIABLE
C      STG(JETA,I,2) = F(X) = INTENSITY
C      JETA = NUMBER OF THE CURVE. I = A POINT ON CURVE JETA
C
COMMON STG(10,200,2), KP(101), N, NUMB, STEP, SUM(20), XINCR
READ(60,1) NUMB,N
1  FORMAT(15,15)
   XWON = (-1.5000*(N+1))/(N-1)
   XINCR = 3.0000/(N-1)
   DO 15 JETA = 1, NUMB
     READ (60,4) ETASQ
4    FORMAT(F14,2)
     PRINT 6, JETA, ETASQ
6    FORMAT(*1*,10X,*DATA BEFORE AREA NORMALIZATION FOR CURVE*13,5X,*ET
   CA SQUARED IS *F6.2)
     DO 15 I = 1, N
       STG(JETA,I,1) = XWON + I*XINCR
       STG(JETA,I,2) = (45.*ETASQ*(5.*STG(JETA,I,1)**2+1.))/(225.*STG(JE
CTA,I,1)**2*ETASQ*(34.*STG(JETA,I,1)**4-2.*STG(JETA,I,1)**2+4.)+(E
CTASQ**2)*(STG(JETA,I,1)**6-2.*STG(JETA,I,1)**4+STG(JETA,I,1)**2))
       PRINT 14, I, STG(JETA,I,1), STG(JETA,I,2)
14    FORMAT (3X,*I = *13,5X,*X = *E12,5.5X,*F(X) = *E15.8)
15    CONTINUE
     CALL AREAS
     BIGAREA = 00.000
     DO 19 JETA = 1, NUMB, 1
       IF(SUM(JETA).GT.BIGAREA) BIGAREA = SUM(JETA)
19    CONTINUE
     DO 24 JETA = 1, NUMB
       SKALFACT = BIGAREA/SUM(JETA)
       DO 24 I = 1, N
         STG(JETA,I,2) = (STG(JETA,I,2))*SKALFACT
24    CONTINUE
     B = 00.00 $ S = 00.00
     DO 29 JETA = 1, NUMB
       DO 29 I = 1, N
         IF (STG(JETA,I,2).GT.0) B = STG(JETA,I,2)
29    CONTINUE
     STEP=(B-S)*.01
     DO 34 JETA = 1, NUMB
       CALL GRAPH(JETA)
       WRITE(61,33) JETA
33    FORMAT(*-,12X,*GRAPH NUMBER*14)
34    CONTINUE
END

```

.20

12/07/66

## SUBROUTINE AREAS

```

C
C THIS SUBROUTINE CALCULATES AREA UNDER CURVES
C BY THE TRAPAZOID APPROXIMATION
C
COMMON STG(10,200,2), KP(101), N, NUMH, STEP, SUM(20), XINCR
DO 304 JETA = 1, NUMH
SUM(JETA) = 0000.0000
CALC = (STG(JETA,1,2) + STG(JETA,N,2))/2.0
INL = N - 1
DO 301 I = 2, INL
CALC = CALC + STG(JETA,I,2)
301 CONTINUE
SUM(JETA) = CALC*XINCR
PRINT 303, JETA, SUM(JETA), XINCR
303 FORMAT (2X, *AREA OF CURVE*13, * IS *E15.0, 5X, *XINCR IN SUBROUTINE I
        (S *E15.0)
304 CONTINUE
END

```

.3B

12/67/66

```

SUBROUTINE GRAPH(JETA)
C
C   PARAMETERS USED FOR STG AND F.
C   COLUMN ONE OF STG CONTAINS THE X-VARIABLE.
C   COLUMN TWO OF STG CONTAINS F(X).
C   I IS THE NUMBER OF POINTS TO BE PLOTTED.
C   I IS TO BE 1000 OR LESS.
C
COMMON STG(10,200,2), KP(101), N, NUMB, STEP, SUM(20), XINCR
DATA(KH=1H*), (KI=1H*), (KM=1H*)
IC=1
DO 102 I=2,100
102  KP(I)=KM
    KP(1)=KI $ KP(IC)=KI $ KP(101)=KI
    PRINT 200, (KP(I), I=1,101)
200  FORMAT(*1*,6X,*X*,18X,*F(X)*,8X,101A1)
    DO 104 I=1,N
    DO 103 J=1,101
103  KP(J)=KH
    KP(1)=KI $ KP(IC)=KI $ KP(101)=KI
    IL = (STG(JETA,1,2))/STEP + 1.5
    KP(IL)=KI
104  PRINT 201, STG(JETA,1,1), STG(JETA,1,2), (KP(K), K=1,101)
201  FORMAT(1X,E12.5,2X,E15.8,3X,101A1)
    DO 105 I=2,100
105  KP(I)=KM
    KP(1)=KI $ KP(IC)=KI $ KP(101)=KI
    PRINT 202, (KP(K), K=1,101)
202  FORMAT(33X,101A1)
END

```

1,0,5000

### B. Program NMR FITS

This program matches the calculated NH proton spectrum with the experimental NH portion of the alkyl-ammonium ion spectrum. Equation (3.5) of Pople (9) is used to calculate the NH spectrum and subroutines written by J. D. Rynbrandt (224) are used to adjust the calculated lineshape to match the experimental lineshape by means of least-squares fitting.

The input information is quite critical in terms of saving computer time and it is therefore discussed in detail.

The first set of input data is very straight forward. K is the number of experimental NH spectra to be fitted. Because of the computer time involved, it is recommended that K be three or less. CUPJ is an estimate of  $^1J(^1H-^{14}N)$  and must be expressed in the same units as CEN and X(I). TWON is an estimate of  $T_1(^{14}N)$  expressed in units of seconds. The correction for measured baseline error, BSLN, should be between 0.1 and 1.0 mm, the same units as Y(1). The center of the multiplet, CEN, is expressed in the same units as CUPJ and X(I), and for this version (number 8) it was not incremented. Finally, N is the number of X(I), Y(I) (or frequency, intensity) pairs from the experimental spectrum, eighty-one pairs were

found to be adequate.

Another set of input data, which follows later but which is also quite straight forward is the  $X(I)$ ,  $Y(I)$  pairs and the  $C(J)$  values. Again, it is emphasized that these values must have the same units as certain other variables. The reason why  $X(I)$ , the frequency value, and  $CUPJ$  may be expressed in units of length is that this program converts them to non-dimensional units as explained by Pople (9).  $C(J)$ , the increment to each of the variables,  $CUPJ$ ,  $TWON$  and  $BSLN$ , will be adjusted by the program but the initial values for the start should be one percent of the respective variable.

The third set of input data are somewhat difficult to approximate on the first run of fit of experimental and calculated NH spectrum. Once a fit has been run through the program, successive fits of the same experimental spectrum then use the last values of  $B$ ,  $BO$ , and  $SO$  as input. To start the iterations through the various loops the value of  $B$  was chosen between fifty and two thousand, and  $BO$  is twenty-five percent of the value for  $B$ .  $SO$ , the sum of the squares of the difference between calculated and experimental intensities is chosen between forty and eight hundred.  $TRYS$  is the maximum iterative steps for each variable ( $CUPJ$ ,  $TWON$ , and  $BSLN$ ) per cycle through

SUBROUTINE SIZE and was between one and twenty-five.

The program increments and adjusts CUPJ, TWØN and BSLN to make the best fit of the calculated spectrum to the experimental spectrum. Details of how the fitting subroutines work can be found in the thesis of J. D. Rynbrandt (224).

As output from the computer, of course, the last values of TWØN, CUPJ and BSLN are given. The last values of B and SO are also given. In addition, there is printed out a table, which contains the X(I) and Y(I) values read in, the calculated Y(I) values, the Y(I) plus the baseline, BSLN, and the difference between Y(I) experimental and Y(I) calculated plus the baseline.

A listing of Program NMR FIT8 follows.

08/17/67

```

PROGRAM NMR FIT8
COMMON X(200),Y(200),YC(200),YD(200),C(4),P(4),B,SO,TRYS,N,J,TR,
CBO,REC, CMPD, DATE, YF(200), K ,YER
READ 10, K
10  FORMAT ( I10)
DO 30 JDATA = 1, K
READ 1, CUPJ, TWON, BSLN, CEN, N, REC, CMPD, DATE
1  FORMAT (4E10.3, I10,3A8)
READ 12, B, SO, TRYS
12  FORMAT (3E10.3, F10.2 )
READ 14, ( C(J), J = 1, 4 )
14  FORMAT ( 4E10.3 )
P(1) = CUPJ  S  P(2) = TWON  S  P(3) = BSLN  S  P(4) = CEN
READ 2,(Y(I),Y(I),I = 1,N)
2  FORMAT (8F10.4)
PRINT 4, CMPD, REC, DATE
4  FORMAT (*1*, 15X, *DATA OF SPECTRUM *2A8,3X,*DATE RUN *A8)
DO 19 MB = 1,13
DO 19 J = 1,3
CALL ADJ
19  CONTINUE
DO 20 I = 1,N
YF(I) = YC(I) + P(3)
20  CONTINUE
YER = Y(5) - YF(5) - YD(5)
CALL DRAW
30  CONTINUE
END

```

06/17/67

```

SUBROUTINE ADJ
C
C THIS SUBROUTINE ADJUSTS THE PARAMETER P(J) AND THE INCRIMENT C(J) C
C
COMMON X(200),Y(200),YC(200),YD(200),C(4),P(4),B,SO,TRYS,N,J,TR,
CBO,REC,CHPD,DATE,YF(200),K,YER
PRINT 202
202 FORMAT(*C*,2X,*CN*5X,*CONST*7X,*ADJ*9X,*INT*10X,*SQ*6X,*TR*3X,*TRI
CALS*/)
      TRIALS = 0.0
      T = 999999.9
      V = 1.0 + C(J)
      DO 208 N1 = 1,2
203 CONTINUE
      CALL SIZE
      TO = T
      T = SO
      TRIALS = TRIALS + 1.0
      IF (TRIALS = TRYS) 205,209,209
205 CONTINUE
      IF (J.EQ.3) 215,216
215 GBL = ABSF(P(3))
      IF (GBL.LT.0.0001) P(3) = +P(3)*10.0
216 IF (T = TO) 206,207,207
206 CONTINUE
      P(J) = P(J)*V
      GO TO 203
207 CONTINUE
      C(J) = -C(J)
      V = 1.0 + C(J)
      P(J) = P(J)*V
208 CONTINUE
209 C(J) = C(J)*TRIALS/10.0
      PRINT 211, J, P(J), C(J), B, SO, 1H, TRIALS
211 FORMAT (15,4E12.4, 2F5.0,5X,*STMT 211*)
      END

```

08/17/67

## SUBROUTINE SIZE

```

C
C THIS SUBROUTINE ADJUSTS THE INTENSITY BY MEANS OF THE SCALE FACTOR C
C B, THE MULTIPLICATIVE PARAMETER A, AND THE INCREMENT TO A, W C
C
COMMON X(200),Y(200),YC(200),YD(200),C(4),P(4),B,SO,TRYS,N,J,TR,
CRO,REC,CMFD,DATE,YF(200),K,YER
CUPJ = P(1) $ TWON = P(2) $ BSLN = P(3) $ CEN = P(4)
S = 0.0
W = 0.025*(B -80)/ABS(B -80)
BO = B
DO 311 I = 1,N
YC(I) = 0.0 $ YD(I) = 0.0
ETASQ = (31.415927*TWON+CUPJ)**2
EXSQ = ((Y(I) - CEN)/CUPJ)**2
CAL = (45.*ETASQ*(5.*EXSQ+1.))/(225.*EXSQ+ETASQ*(34.*EXSQ**2,-2.*E
CXSQ+4.)+(ETASQ**2.)*(EXSQ**3,-2.*EXSQ**2.+EXSQ))
310 YC(I) = CAL*B
YD(I) = Y(I) - YC(I) - BSLN
SQ = YD(I)*YD(I)
311 S = S+SQ
TR = 0.0
DO 318 N2 = 1,7
A = 1.0 + W
315 CONTINUE
B = B*A
SO = S
S = 0.0
TR = TR+1.0
DO 316 I = 1,N
YC(I) = A*YC(I)
YD(I) = Y(I) - YC(I) - BSLN
SQ = YD(I)*YD(I)
316 S = S+SQ
IF (S - SO ) 315,317,317
317 CONTINUE
W = -W*0.25
318 CONTINUE
END

```

08/17/67

## SUBROUTINE DRAW

```

C
COMMON X(200),Y(200),YC(200),YD(200),C(4),P(4),B,SO,TRYS,N,J,IR,
CBO,REC, CMPD, DATE, YF(200), K ,YER
PRINT 401, CMPD, REC, DATE
401  FORMAT (*1-,15X,*FINAL VALUES LST FIT FOR *240,3X,*RUN ON *A5)
PRINT 402, P(2), P(1), P(4), P(3)
402  FORMAT(*0+,3X,*TWOX =*E12.5,* J COUP =*E12.5,* CENTER =*E12.5,
C* BASELINE =*E12.5)
PRINT 405, B, SO, N, YER
405  FORMAT(*0+,3X,*B =*E12.5,4X,*SO =*E12.5,3X,*N =*14,3X,*Y ERROR =*E
C7.4)
PRINT 407
407  FORMAT(*0+,2X,*1+,6X,*X(1)+,8X,*Y(1)+,8X,*YC(1)+,8X,*YF(1)+,8X,*YD
C(1)+/)
PRINT 409,(1,X(1),Y(1),YC(1),YF(1),YD(1), 1 = 1,4)
409  FORMAT (14,2X,F10.4,2X,F10.4,2X,F10.4,2X,F10.4,2X,F10.4)
END
N,1,1000

```



MICHIGAN STATE UNIVERSITY LIBRARIES



3 1293 03143 1780